mRNA export in *Arabidopsis*: molecular and genetic analysis of TREX components

DISSERTATION ZUR ERLANGUNG DES DOKTORGRADES

DER NATURWISSENSCHAFTEN (DR. RER. NAT.)

DER FAKULTÄT FÜR BIOLOGIE UND VORKLINISCHE MEDIZIN

DER UNIVERSITÄT REGENSBURG

vorgelegt von

Hans-Friedrich Ehrnsberger

aus

Regensburg

im Jahr 2019

Der Promotionsgesuch wurde eingereicht am:

14.11.2019

Die Arbeit wurde angeleitet von:

Prof. Dr. Klaus D Grasser

Unterschrift:

Hans-Friedrich Ehrnsberger

Contents

List of figures

List of tables

Abbreviations

(v/v)	Volume per volume
(w/v)	Weight per volume
aa	Amino acid
ACT2	Actin 2
ALY	Ally of AML-1 and LEF1
ANOVA	Analysis of variance
AP-MS	Affinity purification coupled to mass spectrometry
bp	base pair
CBB	Coomassie brilliant blue
CBC	Cap binding complex
CBP20	Cap binding protein 20
CBP80	Cap binding protein 80
cDNA	complementary DNA
CDS	Coding sequence
CHTOP	Chromatin target of PRMT1
CIP29	Cytokine-induced protein of PRMT1
CLSM	Confocal laser scanning microscopy
Col-0	Columbia-0
CTD	C-terminal domain
DAPI	4’,6-Diamidin-2-phenylindol
DAS	Days after stratification
DDX39	DEAD box polypeptide 39
DNA	Deoxyribonucleic acid
dNTP	Deoxynucleoside triphosphate
DTT	Di-thiotreitol
E. coli	Escherichia coli
EDTA	Ethylene diamine tetraacetic acid
eGFP	enhanced green fluorescent protein
FACT	Facilitates chromatin transcription
FG-NUPs	Phenylalanine–glycine repeat containing nucleoporin
FRET	Förster resonance energy transfer
GAP	Glycerinaldehyde-3-phosphate dehydrogenase
gDNA	Genomic DNA
GFP	Green florescent protein
GK	Gabi-Kat

GO	Gene ontology
hnRNP	Heterogenous nuclear ribonucleoprotein
HPR1	Hyper recombinant 1
HYG	Hygromycin B
Kan	Kanamycin
kDa	kilo Dalton
LB	Left border or Luria Bertani
LD	Long day
LRR	Leucine rich repeat
LUZP4	Leucine zipper protein 4
MEX67	Messenger RNA export factor of 67 kDa molecular weight
miRNA	MicroRNA
MOS11	Modifier of SNC1, 11
mRNA	Messenger RNA
mRNP	Messenger ribonucleoprotein
MS	Murashige-Skoog or mass spectrometry
MTR2	mRNA transport defective 2
N. benthamiana	Nicotiana benthamiana
N/C ratio	ratio nuclear/cytosol signal intensity
NAB2	Nuclear polyadenylated RNA-binding 2
NASC	Nottingham Arabidopsis stock centre
NES	Nuclear export signal
NLS	Nuclear localization signal
NPC	Nuclear pore complex
NPL3	Nuclear protein localization 3
NTF2L	Nuclear transport factor-2
NTR	Nuclear transport receptor
NUPs	Nucleoporin protein
NXF1	Nuclear RNA export factor 1
NXT1	NTF2-related export protein 1
o/n	Over night
OD600	Optical density measured at 600 nm
PAGE	Polyacrylamide gel electrophoresis
PCR	Polymerase chain reaction
PMSF	Phenylmethylsulphonyl fluoride
PP2AA	Serine/threonine-protein phosphatase 2A
qRT-PCR	Quantitative reverse transcription-polymerase chain reaction

RB	Right border
RBD	RNA binding domain
RFP	Red fluorescent protein
RNA	Ribonucleic acid
RNAPII	RNA polymerase II
ROI	Region of interest
Rpm	Rounds per minute
RRM	RNA recognition motif
S. cerevisiae	Saccharomyces cerevisiae
SAIL	Syngenta Arabidopsis Insertion Library
SBP	Streptavidin binding peptide
SDS-PAGE	Sodium dodecyl sulphate polyacrylamide gel electrophoresis
Ser2	Serine 2 phosphorylated CTD
Ser5	Serine 5 phosphorylated CTD
SG Tag	consisting of SBP and 2x Protein G domains
snRNA	Small nuclear RNA
SR	Serine rich
SUB2	Suppressor of Brr1-1, 2
tasiRNA	Trans-acting siRNA
T-DNA	Transfer DNA
ter	Terminator
TEV	Tobacco Etch Virus protease
TEX1	Trex component 1
THO	A suppressor of the transcriptional defects of HPR1 mutants by overexpression
THP1	THO2/HPR1 phenotype 1
TREX	Transcription and export complex
TREX-2	Transcription and export complex 2
UAP56	U2AF65 associated protein
UBA	Ubiquitin associated domain
UIEF	UAP56-Interacting Export Factor
UIF	UAP56-interacting factor
UTR	Untranslated region
WT	Wild type
Y2H	Yeast-two-Hybrid
YRA1	Yeast RNA annealing protein 1

Summary

In *Arabidopsis,* orthologs of the human mRNA export adaptors ALY and UIF are diversified with the genome encoding four ALY family members and two UIF-like factors. In this study four ALY and two UIEF proteins were characterised as mRNA export factors and seven candidates that co-purified with ALY and UIEF proteins in affinity purification experiments were further analysed as possible mRNA export receptors.

ALY and UIEF proteins directly interacted with the TREX subunit UAP56 demonstrating that ALY and UIEF proteins are recruited to TREX by an interaction with the RNA helicase UAP56. Plants lacking all four ALY proteins were severely affected in plant growth and development accompanied by a general mRNA export defect demonstrating that ALY proteins function as mRNA export factors. *uief* single and double mutant plants displayed defects in plant growth and development and showed a moderate mRNA export block. Since plants lacking four ALY and two UIEF proteins displayed more pronounced plant growth and development defects and showed a stronger mRNA export block than *4xaly* plants, also the UIEF proteins could be described as mRNA export factors. The observation that *aly* single and double mutant plants exhibited no obvious phenotype but *4xaly* displayed a pleiotropic phenotype indicated that ALY proteins can function redundantly. Mutants lacking three ALY proteins displayed different phenotypes that could be clearly distinguished from wildtype and *4xaly* plants what demonstrated that besides functional redundancy different ALYs also have specific functions. RNA sequencing of nuclei and whole cells showed that *4xaly* is a general mRNA export mutant and additional transcriptomic analysis of *aly* and *uief* mutants demonstrated that ALY proteins regulate the mRNA export of a variety of transcripts. The influence of UIEF proteins on mRNA export on the other hand is limited to only a subset of transcripts. Transcriptomic analysis and export assays of *3xaly* mutant plants further revealed that the different phenotypes of *3xaly* and *4xaly* mutant plants are rather caused by defects in mRNA export of specific transcripts or subsets of transcripts than by differences in a bulk mRNA export block.

Proteomic analysis of proteins co-purifying with the four ALY and two UIEF export factors identified seven candidates that share some features with the human heterodimeric export receptor. Fusion proteins of the seven candidates were detected in the cytoplasm of cells and an enriched signal could be detected around the nuclear envelope when candidate fusion proteins were expressed in tobacco leaf cells. Plants lacking several receptor candidates did not show mRNA export defects indicating that plant mRNA receptors could be highly diversified, but additional studies are needed to characterize the seven mRNA receptor candidates.

1. Introduction

1.1 From mRNA biogenesis to mRNA export in three defining steps

A key feature of eukaryotic cells is that the site where genetic information is stored - the nucleus - is spatially separated from the site where this information is translated into proteins - the cytoplasm -. Thus, a mechanism to transfer this information to the site of protein biosynthesis is necessary. In all eukaryotes the information encoding the molecular components of life is stored in DNA. DNA itself is tightly packed into chromatin and a double-membrane nuclear envelope separates this nuclear information from the cytoplasmic translation of proteins. To overcome this barrier, nuclear pore complexes (NPC) are embedded into the nuclear envelope that allow the exchange of molecules between nucleus and cytoplasm. Metabolites, ions and small molecules (< approximately 40 kDa) can passively diffuse through NPCs whereas the translocation of larger molecules needs to be facilitated by an active transport mediated by nuclear transport receptors (NTRs, Ribbeck and Görlich, 2001; Kabachinski and Schwartz, 2015). mRNAs are the molecules that encode the information that in the cytoplasm is translated into proteins. These mRNAs are transcribed from DNA within the nucleus by the RNA-Polymerase II (RNAPII). The key protein complex for nucleocytoplasmic mRNA export is the conserved TREX complex (TRanscription and EXport). It co-transcriptionally assembles onto nascent mRNAs (Figure 1A), hands mRNAs over to a heterodimeric mRNA export receptor (Figure 1B) which guides export-competent messenger ribonucleoproteins (mRNPs) through NPCs (Figure 1C, Walsh et al., 2010; Heath et al., 2016).

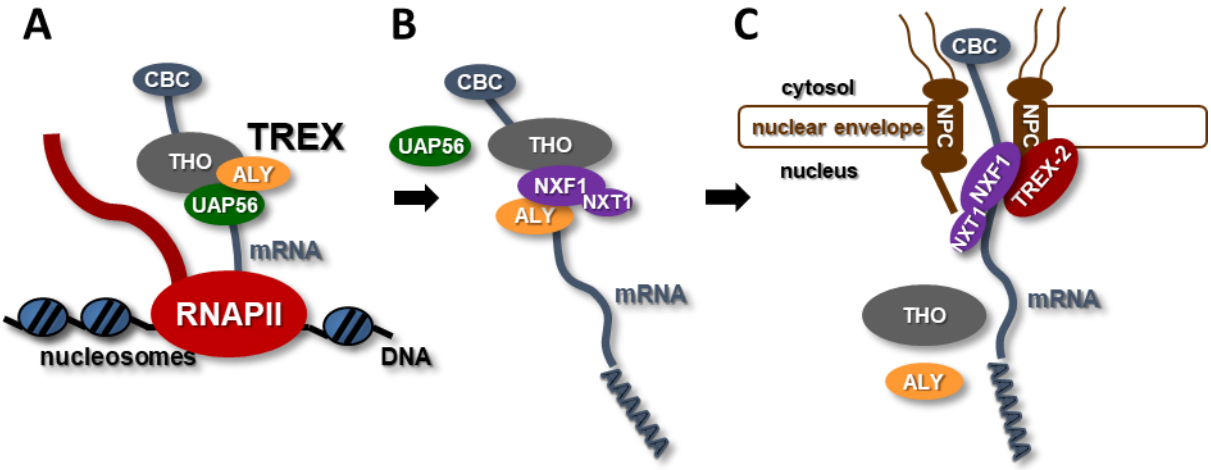

Figure 1. Key steps from mRNA biogenesis to mRNA export in metazoans. (A) mRNAs are produced in the nuclei by RNAPII using DNA as a template. Co-transcriptionally the TREX complex composed of the core THO complex, the RNA helicase UAP56 and export adaptors represented by ALY is loaded onto nascent mRNAs. (B) Processed mRNAs are released from the DNA template and both export adaptors and THO complex mediate contact of the heterodimeric export receptor NXF1/NXT1 with mRNAs resulting in export competent mRNPs while UAP56 is stripped of mRNAs. (C) Export competent mRNPs travel to the nuclear pores and both THO complex and export adaptors are removed within the nucleus from mRNPs whereas NXF1 mediates translocation through NPCs by direct interaction with TREX2 and nucleoporins and both NXF1 and NXT1 travel along mRNAs through NPCs (Walsh et al., 2010, Heath et al., 2016).

1.2 TREX as the key regulator of mRNA export

TREX is the key regulator that contributes to transcription and initiates mRNA export (Sträßer et al., 2002). TREX structure and function is conserved from yeast to humans containing a core THO complex consisting of THOC1, 2, 3, 5, 6, 7 (Tho2, Hpr1, Mft1, and Thp2 in yeast) to which the RNA helicase UAP56 (Sub2 in yeast) as well as RNA export adaptors and co-adaptors are bound (Heath et al., 2016). The key mRNA export adaptor is ALY (ALYREF, Yra1 in yeast, Stutz et al. 2000; Strässer and Hurt, 2000; Rodrigues et al., 2001), though some shuttling SR proteins (Huang et al., 2003) besides several other proteins also function as mRNA export adaptors in human cells (Heath et al., 2016).

Even though TREX is conserved, studies also revealed differences regarding composition of TREX and the mechanisms how TREX is loaded onto mRNAs in yeast and higher eukaryotes. In yeast for instance there are no orthologues of the mammalian TREX components CHTOP, POLDIP3 and ZC3H11A whereas two orthologous genes of the single human *ALY* gene exist in yeast (Heath et al., 2016). A certain divergence between yeast and higher eukaryotes is also seen since only THOC1, THOC2 and THOC3 of the THO complex have orthologues in both yeast and higher eukaryotes while the THO complex subunits THOC5, THOC6, THOC7 and Mtf2 and Thp2 are restricted to either higher eukaryotes or yeast (Sträßer et al., 2002; Rehwinkel et al., 2004; Heath et al., 2016).

1.3 Loading of TREX onto mRNAs

TREX is loaded onto mRNAs throughout different stages of mRNA biosynthesis. Yeast TREX is mainly recruited by the transcription machinery whereas metazoan TREX primarily associates with mRNAs in a splicing dependent manner (Luo and Reed, 1999; Moore and Proudfoot, 2009; Heath et al., 2016). Early assembly of TREX subunits in metazoans can also be mediated by an active RNAPII through adaptor proteins that bind the carboxy-terminal domain (CTD) of the large subunit of RNA Pol II. SPT6, which works alongside FACT to remodel nucleosomes during transcription, can initiate this first assembly by directly binding to RNAPII CTD. SPT6 recruits IWS1 that in turn directly interacts with ALY to bring the export machinery to actively transcribed genes (Bortvin and Winston, 1996; Orphanides et al., 1999; Yoh et al., 2007). Another mechanism how TREX can be indirectly recruited is shared by yeast and higher eukaryotes and involves the PRP19 (Prp19 in yeast) complex, which functions in splicing, transcription and transcription-coupled DNA damage repair (Heath et al., 2016).

The yeast TREX complex is primarily recruited via a direct interaction with the CTD of RNAPII and subsequently loading onto nascent mRNAs (Figure 2A). This binding relies on the Ser2/Ser5 phosphorylation of RNAP II CTD that insures TREX recruitment to actively

transcribed genes only. Since Ser2 phosphorylation of RNAP II CTD is increases in a 5' to 3' direction, accompanied by an increased loading of RNAPII with TREX, a sufficient recruitment of TREX also to longer genes is ensured (Figure 2B, Meinel et al., 2013; Heath et al., 2016).

In higher eukaryotes, loading of TREX onto mRNAs is strongly interconnected with the three steps of mRNA processing. Before an mRNA can be exported out of the nucleus it needs to be capped at the 5' end, introns have to be removed by the spliceosome and a 3' poly(A) tail must be added by the 3' processing machinery.

In a first step of mRNA processing, a 7-methylguanosine cap is added to the 5' end of nascent transcripts followed by the recruitment of the heterodimeric cap binding complex (CBC) consisting of the two subunits CBP80 and CBP20 (NCBP1 NCBP2) what increases the stability of pre-mRNAs (Moore and Proudfoot, 2009).

In a second crucial step in the build-up of an export competent mRNP, intronic sequences, present between exon coding sequences of transcripts, are removed by the spliceosome through a complex series of reactions that function to join the 3' end and 5' end of neighbouring exons. After the splicing reaction is finished, an exon junction complex (EJC) is deposited close to the joint exons, 20–24 nucleotides upstream from the 5' end of the splice junction, that serves as a platform for interaction with several other components of the gene expression pathway (Fica and Nagai, 2017; Stewart, 2019).

Before transcripts are released from the DNA template, in a last step of mRNA processing poly(A) tails (~250 nt in higher eukaryotes, ~60 nt in yeast) are added to the 3' end of transcripts by complexes that mediate cleavage in the 3'-UTR, poly(A) addition and regulation of 3' end processing (Stewart 2019).

Over the last years it emerged that factors that are involved in all three steps of mRNA processing contribute to TREX loading onto mRNAs in metazoans. Earlier, contradictory results were obtained leading to two long-standing views that TREX is either recruited in an CBC dependent manner via an interaction with CBP80, consistent with the idea that messenger mRNPs are exported 5' end first, (Cheng et al., 2006; Chi et al., 2013) or mainly by the EJC that is deposited after splicing (Le Hir, 2001; Singh et al., 2012). In recent years it was shown that ALY associates with mRNAs in a CBC and EJC-dependent manner, likely in a way where CBC acts as a transient landing platform for ALY which is then transferred to exon-exon junctions along the RNA located upstream of the EJC (Figure 2C, Gromadzka et al., 2016; Shi et al., 2017; Viphakone et al., 2019).

Additionally, over the last years accumulating evidence emerged that there is a link between polyadenylation and mRNA export. In yeast it could be shown that Yra1 interacts with the 3' processing factor Pcf11 (Johnson et al., 2009). In metazoans an association of TREX complex

subunit THOC5 with several 3' processing factors as well as a binding of ALY to the 3' machinery components PABPN1 and CstF64 was shown (Katahira et al., 2013; Tran et al., 2014; Shi et al., 2017).

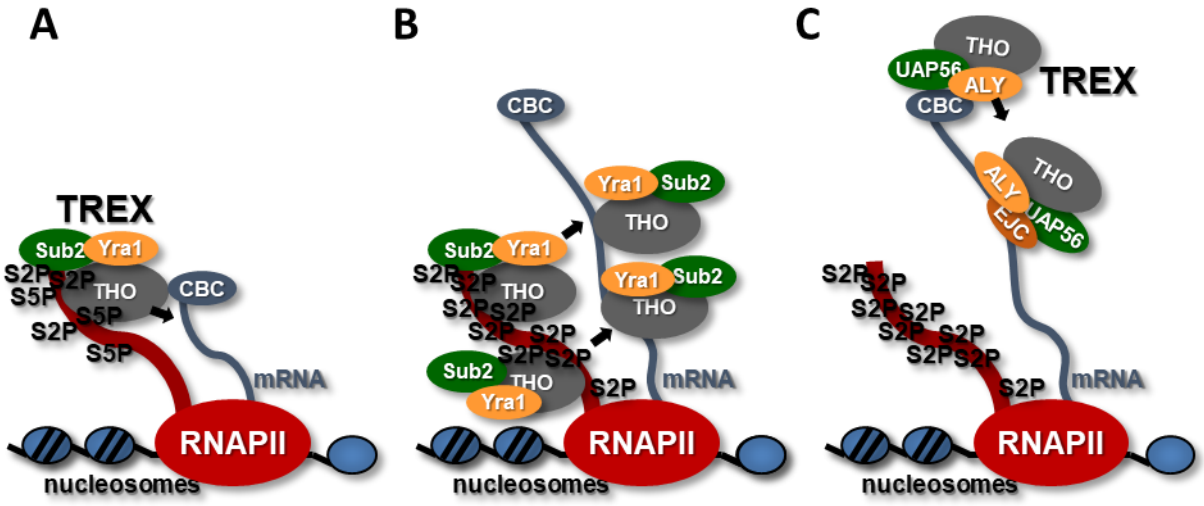

Figure 2. Main mechanisms of TREX loading onto nascent mRNAs in yeast and metazoans. (A) In yeast, TREX is initially recruited to the transcription machinery by interaction of THO with serine 2-serine 5 (S2/S5) diphosphorylated CTD of RNAPII. (B) Throughout transcription, occupancy of TREX increases from the 5' to the 3' end of the gene in accordance with the CTD S2 phosphorylation pattern allowing a sufficient TREX loading also for longer genes (Meinel et al., 2013). (C) In metazoans TREX is recruited in a CBC and EJC-dependent manner likely in a way where CBC acts as a transient landing platform for ALY which is then transferred to exon-exon junctions along the RNA located upstream of the EJC (Viphakone et al., 2019).

1.4 TREX and the nuclear quality control of mRNAs by the exosome

After transcripts are released from the template DNA and before they are exported to the cytoplasm, quality controls make sure that only properly processed transcripts are exported to the site of protein biosynthesis. The major nuclear RNA surveillance machine that degrades most types of RNA is the highly conserved 3'–5' exo- and endo-nucleolytic RNA exosome, whose function strongly depends on the RNA helicase MTR4 (Kilchert et al., 2016). Recent studies indicated that in human cells sorting of mRNAs for export or degradation by the exosome is regulated by a competition of export adaptor ALY and exosome associated factors MTR4 or ZFC3H1 for binding with transcripts on both 5' and 3' ends (Figure 3, Silla et al., 2018; Fan et al., 2017; Fan et al., 2018).

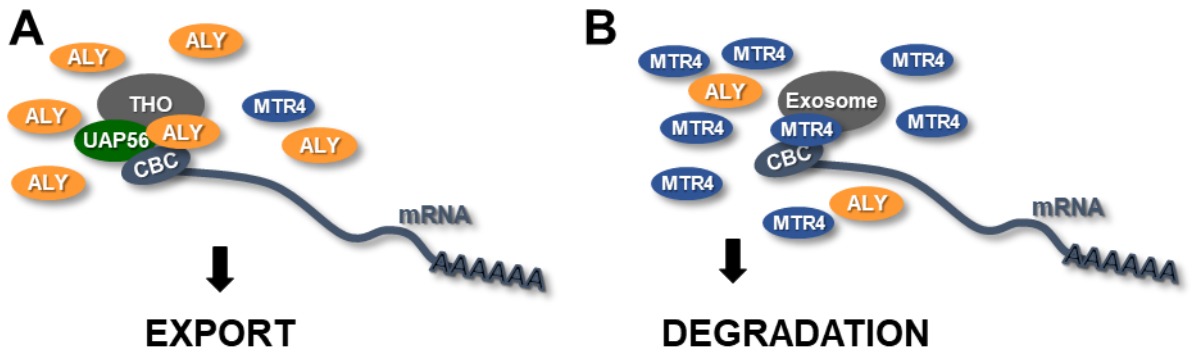

Figure 3. mRNAs are sorted for export or degradation by a competition of ALY and exosome associated factor MTR4. (A) ALY outcompetes MTR4 for association with the CBC complex on properly processed transcripts resulting in loading of TREX onto mRNAs and subsequent export of the mRNA. (B) When exosome associated factor MTR4 outcompetes ALY for binding onto the CBC, the exosome is recruited and mRNAs are degraded (Fan et., al 2017)..

1.5 TREX mediates the handover of mRNAs to export receptors

A key function of TREX in the process of mRNA export lies in the transfer of mRNAs to the heterodimeric export receptor NXF1/NXT1 (TAP/P15, Mex67/Mtr2 in yeast) which is conserved in yeast and humans and which mediates the passage through the NPCs to the cytosol. While the smaller NXT1/Mtr2 proteins are composed of a single NTF2-like (NTF2L) domain in yeast and humans, the bigger NXF1/Mex67 proteins also share a similar modular domain organization. NXF1 and Mex67 consist of an RNA-recognition motif (RRM) domain followed by a leucine-rich repeat (LRR domain), an NTF2L domain and a C-terminal ubiquitin-associated domain (UBA) domain. NXF1 additionally displays an N-terminal RNA-binding domain (RBD, Figure 4, Viphakone et al., 2012; Stewart, 2019). Compact heterodimerization is mediated by an interaction of the two NTF2L domains opposing each other across the convex faces of their β-sheets (Valkov et al., 2012).

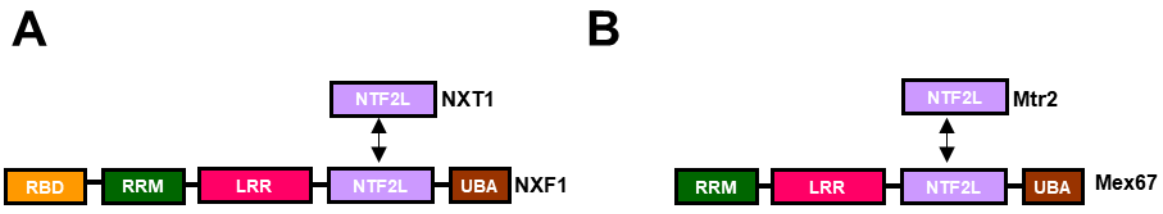

Figure 4. Composition of the human and yeast heterodimeric export receptor. (A) The human export receptor is composed of a bigger NXF1 and the smaller NXT1 subunit. While NXT1 is built of a single NTF2L domain, NXT1 comprises an N-terminal RBD, an RRM, a LRR domain, NTF2L domain and a C-terminal UBA-fold motif. The yeast counterpart is composed of a bigger Mex67 and the smaller Mtr2 subunit. Accordingly Mtr2 is built of a single NTF2L domain while Mex67 comprises an N-terminal RRM, a LRR domain, NTF2L domain and a C-terminal UBA-fold motif. Compact heterodimerization is in both organisms mediated by an interaction of the two NTF2L domains (Stewart, 2019).

The NTF2L and UBA domains are responsible for binding to nucleoporins (Nups) that harbour Phe and Gly-rich repeats (FG-Nups) at the NPC what mediates the passage to the cytosol. Both *in vitro* and *in vivo* studies also revealed that NXF1/NXT1 and Mex67/Mtr2 bind RNA (Segref et al., 1997; Liker, 2000; Strässer et al., 2000; Katahira et al., 2002; Wiegand et al., 2002; Valkov et al., 2012; Katahira, 2015). Since this binding of NXF1/NXT1 and Mex67/Mtr2 to RNA is only weak and nonspecific, additional factors are needed to enhance the export receptors binding to mRNA. Factors that mediate this binding of export receptor to mRNA are called export adaptors and in both, yeast and human cells, a series of these export adaptors were characterized (Katahira, 2015; Heath et al., 2016). In human cells besides the major export adaptor ALY, the TREX complex component THOC5 and the TREX associated adaptors CHTOP, LUZP4 and UIF as well as the serine-arginine (SR) rich proteins 9G8 and SRp20 were characterized as mRNA export adaptors (Rodrigues et al., 2001; Hautbergue et al., 2009; Katahira et al., 2009; Chang et al., 2013; Viphakone et al., 2015; Katahira, 2015). These studies also revealed that in human cells adaptors show some functional redundancy since only a simultaneous knockout of ALY and CHTOP, LUZP4 or UIF leads to a severe mRNA export block.

In yeast on the other hand, the number of export adaptors is reduced compared to the situation in human cells. Yra1, the ALY orthologue, is an essential factor that acts as the major mRNA export adaptor by directly binding to the N-terminal domain of Mex67 through its arginine- and glycine-rich region. Additionally Mex67/Mtr2 can be recruited to mRNAs by the adaptor proteins Npl3 and Nab2 (Katahira, 2015).

In metazoans, ALY binds both mRNA and NXF1 via the same arginine-rich region and binding of ALY to NXF1 triggers the transfer of the mRNA to NXF1/NXT1. Arginine methylations of ALY were found to be crucial for this handover process (Hautbergue et al., 2008; Hung et al., 2010). In the course of this process a concerted action of ALY and THO complex is necessary to enhance the mRNA binding affinity of NXF1/NXT1. In a non-RNA bound state, an intramolecular interaction between the N-terminal RBD domain and NTF2L domain of NXF1 results in an autoinhibition of the export receptor (Figure 5A). Simultaneous binding of ALY to the N-terminal part of NXF1 and THOC5 to the NTF2L domain induces a conformational change relieving the autoinhibition and exposing the RNA binding activity of the export receptor (Figure 5B, Viphakone et al., 2012).

Besides activating NXF1/NXT1, it is also speculated that TREX might initiate a conformational change of mRNAs that facilitates binding to the export receptor. It is hypothesized that the DEAD-box helicase UAP56 hydrolyses ATP resulting in remodelling of the exported mRNA to which NXF1/NXT1 binds with a higher affinity (Stewart, 2019).

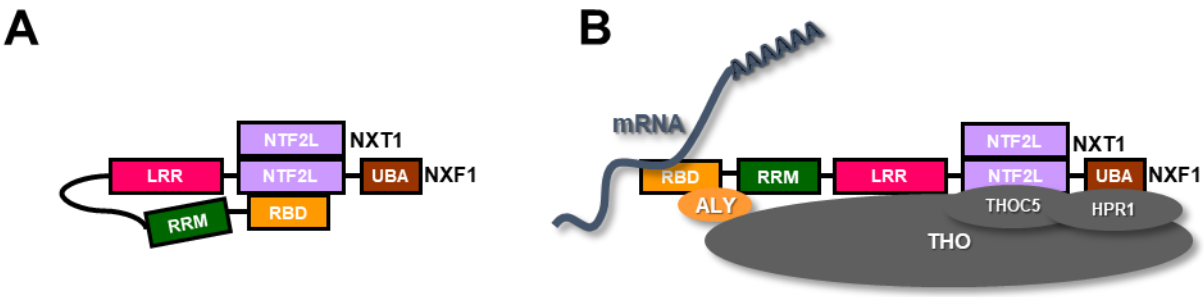

Figure 5. Mechanism how TREX enhances the mRNA binding affinity of human NXF1/NXT1. (A) In a non-RNA bound state, an intramolecular interaction between the N-terminal RBD domain and NTF2L domain of NXF1 results in an autoinhibition of the export receptor, preventing the binding of the RBD domain to mRNA. (B) Simultaneous binding of ALY to the N-terminal part of NXF1 and the THO subunit THOC5 to the NTF2L domain induces a conformational change and an opening up of NXF1 exposing the RNA binding site of RBD (Viphakone et al., 2012).

Not much is known about the type of secondary structure that is preferentially bound by NXF1/NXT1, but observations in simple retroviruses give some indication of how an NXF1/NXT1-mRNA binding might be mediated. Simian type-D retroviruses exploit the host NXF1/NXT1 machinery to export their unspliced genomic RNA comprising an ~130-nt viral constitutive transport element (CTE). This CTE has a 2-fold symmetric motif with both lobes predicted to form distinctive L-shaped stem loops that can bind an NXF1:NXT1 platform without the need of export adaptors, suggesting that similar RNA secondary structures might be generated by nuclear DEAD- box helicases to facilitate NXF1:NXT1 binding (Grüter et al., 1998; Teplova et al., 2011; Aibara et al., 2015; Stewart, 2019).

1.6 NXF1/NXT1 mediates the passage through the NPC

Export competent mRNPs travel to the nuclear envelope and are guided by NXF1/NXT1 through the NPC to the cytosol. Since mRNPs are not actively transported within the cell but rely on passive diffusion to reach their destination, the ‘gene gating’ hypothesis was proposed more than 30 years ago (Blobel, 1985). This model suggests that active genes that are located in close proximity to NPCs would preferentially export their mRNAs into the cytoplasm whereas nowadays the emerging paradigm is that active genes are attached to NPCs through interactions with Nups and transcription factors (Ben-Yishay et al., 2016).

In mammalians, the nuclear travel of released and export competent mRNPs to the NPC is probably the rate-limiting step in the nucleocytoplasmic transport pathway. Experiments demonstrated that mRNA travel can last for several minutes (~ 5-50 min) whereas a small-sized nucleus in yeast allows a faster journey to the NPC suggesting that in yeast the rate-limiting step is situated at the NPC (Mor et al., 2010; Saroufim et al., 2015; Ben-Yishay et al., 2016).

Arrived at the NPC, mRNPs come in contact with TREX-2, a complex that is anchored to the nuclear pore basket on the nucleoplasmic side of the NPC. TREX-2 links TREX transcription with nuclear mRNA export, mediated by an interaction of export receptor and TREX-2 before the translocation through the huge NPC is initiated (Figure 7A, Chinnusamy et al., 2008; Fischer et al., 2004; Wickramasinghe et al., 2010; Wickramasinghe et al., 2014; Dimitrova et al., 2015; Okamura et al., 2015).

NPCs have molecular masses of approximately 60 MDa in yeast and 120 MDa in humans and are built from several (8–64) copies of around 30 different Nups (Beck and Hurt, 2017). Even though the overall NPC structure, which integrates about 500–1000 Nups, and function is conserved, recent studies revealed that human and yeast NPC composition and architecture are quite different (Beck and Hurt, 2017; Kim et al., 2018; Rajoo et al., 2018; Shav-Tal and Tripathi, 2018). The principle structure of NPCs includes the elements inner pore ring, nuclear ring, cytoplasmic ring, nuclear basket and cytoplasmic filaments (Figure 6A). Nups that build the NPCs can be basically categorized into scaffold Nups, that serve architectural roles, and FG-Nups, which carry FG rich repeats and interact with the nucleocytoplasmic transport machinery (Beck and Hurt, 2017). Most Nups are organized into stable subcomplexes that comprise strongly interacting Nups and different amounts of these conserved building blocks in yeast and humans cause the diversity in composition and architecture in these organisms (Figure 6B, Shav-Tal and Tripathi, 2018).

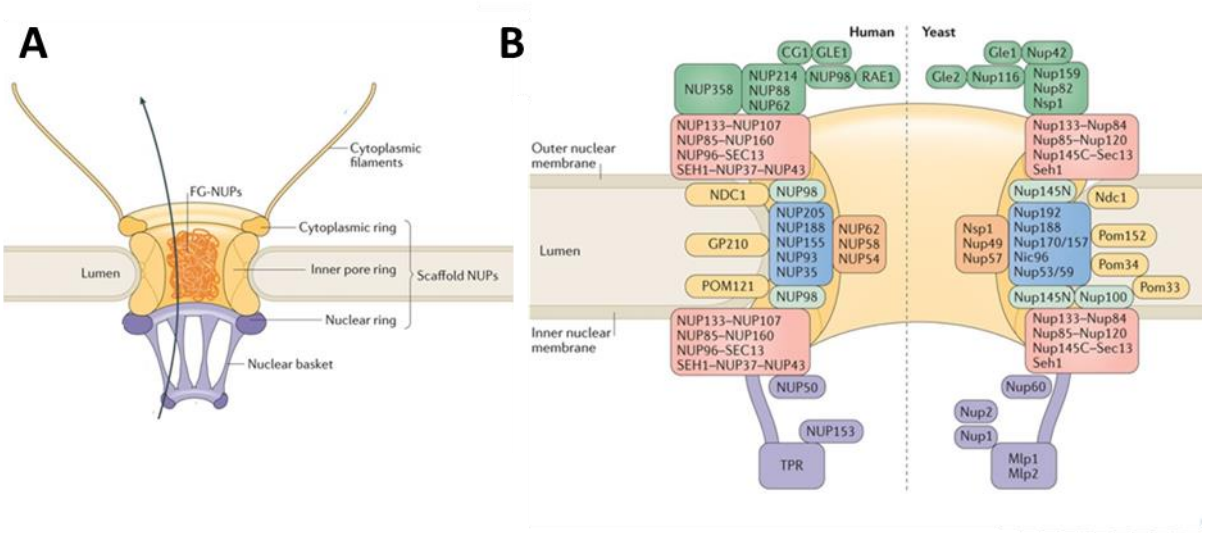

Figure 6. Composition of the NPC. (A) The NPC is embedded into the nuclear envelope and is composed of the key structural elements cytoplasmic ring, the inner pore ring and the nuclear ring, as well as peripheral elements such as the nuclear basket and the cytoplasmic filaments. The central channel of the NPC is lined by FG-Nups that facilitate mRNP translocation from the nucleus to the cytosol as indicated. (B) NPCs are conserved in yeast and humans and Nups are organized into subcomplexes. Y-complexes are shown in red; the inner ring complex in blue; the transmembrane Nups in yellow; the NUP62 complex in orange; cytoplasmic complexes in green; and nuclear basket complexes in purple. Modified from Beck and Hurt 2017.

The central channel of the NPC forms the passage for a possible bi-directional nucleo-cytoplasmic transport and is lined with FG-Nups from the NUP62 complex consisting of NUP62 (Nsp1 in yeast), NUP58 (Nup49 in yeast) and NUP54 (Nup57 in yeast) as well as NUP98 (Nup145N in yeast, Figure 6B, Beck and Hurt, 2017). Even though it is well established that FG repeats bind to NTRs and enable a passage of cargos through the NPC, the underlying mechanism how mRNPs pass the NPCs is not clear (Aitchison et al., 1996; Damelin and Silver, 2000; Allen et al., 2001; Katahira et al., 2002; Beck and Hurt, 2017). Several models have been proposed to explain how FG-Nups facilitate a cargo specific translocation through the NPC. These models have in common, that FG-Nups are assumed to generate a disordered meshwork which attract cargos, thereby mediating their passage through the central channel (Rout et al., 2003; Aitchison and Rout, 2012; Hülsmann et al., 2012; Schmidt and Görlich, 2016; Beck and Hurt, 2017). The time frames measured for the transport of an mRNP through the NPC range from ~180 ms for β-actin mRNA to ~500 ms for dystrophin mRNA and although both fast and slow (>800 ms) transport rates are measured for a single mRNA type mRNP, translocation occurs about 15-fold faster than diffusion through the nucleus (Grünwald and Singer, 2010; Mor et al., 2010; Adams and Wente, 2013; Ben-Yishay et al., 2016). Interestingly, the efficiency of mRNP translocations seems to be rather low, since only a small portion (15–36%) of mammalian mRNAs that start the export process or interact with an NPC end the process successfully and are released into the cytoplasm (Grünwald and Singer, 2010; Siebrasse et al., 2012; Ma et al., 2013; Ben-Yishay et al., 2016).

Directionality of the translocation and release at the cytoplasmic site of the NPC is dependent on the ATP/ADP cycling of the highly conserved RNA-dependent DEAD-box helicase Dbp5 (DBP5 or DDX19 in mammalians) that is located at the cytoplasmic fibrils of the NPC (Folkmann et al., 2011; Adams and Wente, 2013). The ATPase activity of Dbp5 is activated by binding to the Nup Gle1 and its co-activator inositol hexakisphosphate (IP_6). An activated ATP/Dbp5/Gle1-IP_6 complex then binds to the emerging mRNP what stimulates both the release of Gle1-IP_6 and the ATP hydrolysis event (Figure 7B). The change from ATP to ADP in turn triggers a conformational change that drives a remodelling process of the mRNP and that causes the release of the mRNA from Dbp5 and also probably from the export receptor (Figure 7C, Lund and Guthrie, 2005; Weirich et al., 2006; Folkmann et al., 2011; Hodge et al., 2011; Adams and Wente, 2013; Stewart, 2019).

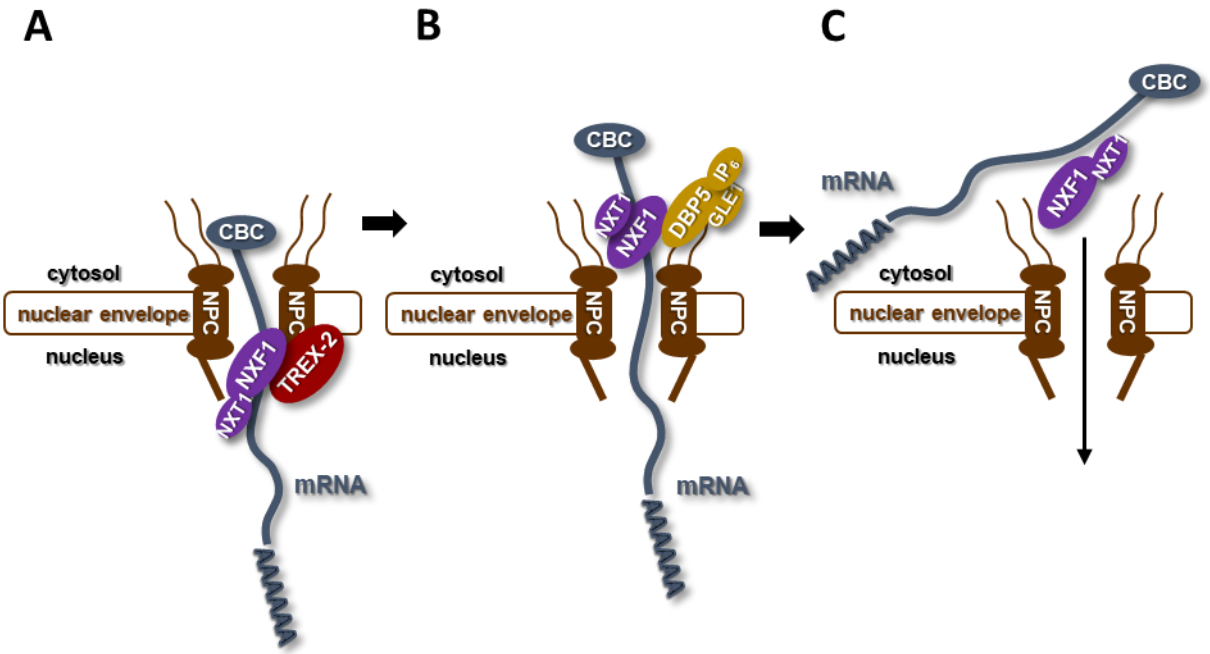

Figure 7. The translocation of mRNPs through the NPC. (A) At the NPC translocation of mRNPs is initiated by an interaction of NXF1 with both TREX-2 that sits at the nuclear site of the NPC and FG-Nups of the NPC. (B) Directionality of the translocation and release at the cytoplasmic site of the NPC is dependent on the RNA helicase DBP5 that is located at the cytoplasmic fibrils of the NPC and that is activated by GLE1 and its co-activator IP_6.(C) DBP5 mediated remodeling of the mRNA releases the mRNA into the cytosol and probably also causes the release of NXF1/NXT1 that then is recycled back into the nucleus (Okamura et al., 2015).

1.7 mRNA export in plants – key complexes are conserved

In yeast and humans, the key players and mechanisms of mRNA export are well characterized, whereas comparatively little is known about mRNA export in plants (Gaouar and Germain, 2013). Studies revealed that the key complexes of mRNA export TREX, TREX-2 and NPC are conserved, although differences regarding composition/structure of these complexes can be observed in plants (Table 1). Whether the mechanisms underlying mRNA export are also conserved from yeast to plants is poorly understood (Lu et al., 2010; Tamura et al., 2010; Yelina et al., 2010; Meier et al., 2017; Sørensen et al., 2017; Pfab et al., 2018). For the last defining NPC translocation step of mRNA export on the other hand, plants may have evolved a distinct solution, since no orthologues of the well conserved heterodimeric export receptor NXF1/NXT1 (Mex67/Mtr2) can be identified (Ehrnsberger et al., 2019a).

Table 1. ***Arabidopsis*** **mRNA export factors compared with those of yeast and mammals (Ehrnsberger et al., 2019a).**

Export factor	Arabidopsis	AGI	Yeast	Mammals
THO complex	HPR1 (THO1, EMU)	AT5G09860	Hpr1	THOC1 (HPR1)
	THO2	AT1G24706	Tho2	THOC2
	TEX1 (THO3)	AT5G56130	Tex1	THOC3 (TEX1)
	THO5A	AT5G42920		THOC5
	THO5B	AT1G45233		
	THO6 (DWA1)	AT2G19430		THOC6
	THO7A	AT3G02950		THOC7
	THO7B	AT5G16790		
			Thp2, Mft1	
DEAD-box helicase	UAP56A	AT5G11170	Sub2	UAP56 (DDX39B)
	UAP56B	AT5G11200		URH49 (DDX39A)
UAP56-associated	MOS11	AT5G02770	Tho1	CIP29 (SARNP)
	ALY1	AT5G59950	Yra1	ALY (REF,THOC4)
	ALY2	AT1G02530		
	ALY3	AT1G66260		
	ALY4	AT5G37720		
	UIEF1	AT4G10970		UIF
	UIEF2	AT4G23910		
	n.d.		n.d.	CHTOP
	n.d.		n.d.	LUZP4
mRNA export receptor	n.d.		Mex67	NXF1 (TAP)
			Mtr2	NXT1 (p15)
TREX-2 complex	SAC3A	AT2G39340		
	SAC3B	AT3G06290		
	SAC3C	AT3G54380		
	CEN1	AT3G50360	Cdc31	CETN2
	CEN2	AT4G37010		CETN3
	THP1	AT2G19560	Thp1	PCID2
	DSS1	AT5G45010	Sem1	DSS1
	ENY2	AT3G27100	Sus1	ENY2
Cytosolic RNA helicase	LOS4	AT3G53110	Dbp5	DBP5
	GLE1	AT1G13120	Gle1	GLE1

1.8 TREX in plants

Affinity purifications in combination with mass spectrometry (AP-MS) revealed that the *Arabidopsis* TREX complex consists of a THO core complex, ALY proteins, UAP56 and MOS11 (Yelina et al., 2010; Sørensen et al., 2017).

Arabidopsis THO rather resembles the hexameric mammalian THO complex than the pentameric yeast THO complex since it consists of the subunits HPR1, THO2, TEX1, THO5A, THO5B, THO6, THO7A and THO7B with THO5 and THO7 each occur in two isoforms. *Arabidopsis* mutant plants that lack specific THO subunits are differentially affected regarding plant growth and development ranging from almost not affected *tho6* mutant plants (Furumizu et al., 2010), to mildly affected *tex1* and *hpr1* mutant plants (Jauvion et al., 2010; Pan et al., 2012; Xu et al., 2015; Sørensen et al., 2017) and very severely affected *tho2* mutant plants (Furumizu et al., 2010; Jauvion et al., 2010; Yelina et al., 2010; Francisco-Mangilet et al., 2015). Whole-mount in situ hybridisation using fluorescently labelled oligo(dT) probes (WISH) demonstrated an nuclear enrichment of polyadenylated mRNAs in *hpr1* and *tex1* mutant plants and thereby demonstrated a contribution of THO to mRNA export (Pan et al., 2012; Xu et al.,

2015; Sørensen et al., 2017). Apart from being involved in mRNA export, *Arabidopsis* THO also regulates small RNAs since levels of siRNAs or miRNAs are reduced in *hpr1*, *tho2*, and *tex1* plants (Furumizu et al., 2010; Jauvion et al., 2010; Yelina et al., 2010; Francisco-Mangilet et al., 2015).

The Arabidopsis genome encodes four ALY proteins (ALY1-ALY4) that were identified as interactors of the tomato bushy stunt virus protein (Uhrig et al., 2004). It could be shown that ALY proteins exhibit differential sub-nuclear localization and that they interact with the RNA helicase UAP56. However, if ALY proteins share similar functions in the process of mRNA export with their human or yeast counterparts and if there are functional differences between the four ALY proteins needs further analysis (Uhrig et al., 2004; Canto et al., 2006; Sørensen, 2016) .

In *Arabidopsis*, an identical UAP56 protein is coded by two neighbouring genes and biochemical characterisation revealed that UAP56 preferentially binds ssRNA, has an ATP-dependent RNA-helicase activity and that it interacts *in vivo* and *in vitro* with MOS11 and ALY proteins. This indicates that plant UAP56 has a similar function regarding mRNA export like the orthologues in yeast and humans by recruiting the export machinery to mRNAs (Kammel et al., 2013; Sørensen et al., 2017).

MOS11, the last component of plant TREX is an orthologue of metazoan CIP29/ SARNP and yeast Tho1. A contribution of MOS11 to mRNA export was shown by WISH, but the molecular function of MOS11 remains to be elucidated (Germain et al., 2010).

1.9 mRNA export in plants beyond TREX

The export receptor mediating the last step of mRNA export as well as if there is a putative interplay between export adaptors and receptors like described in other eukaryotes is not known in plants (Ehrnsberger et al., 2019a).

A proteomic study revealed the components of plant NPC and showed that Nup subcomplexes and classes are well conserved throughout eukaryotes although several Nups are missing or have been replaced by plant-specific proteins (Tamura et al., 2010; Meier et al., 2017). Several studies showed that different Nups are required for mRNA export and downregulation of these Nups results in pleiotropic phenotypes (Parry, 2015; Meier et al., 2017). At the cytoplasmic site of NPCs, a similar mechanism of releasing the mRNPs into the cytosol like described in other organisms can be supposed, since LOS4, the orthologue of human DBP5, together with GLE1 and its co-activator IP_6 are required also in plants for mRNA export (Lee et al., 2015).

The biological relevance of mRNA export is shown as the loss of different subunits of THO, TREX, TREX-2 and NPC results in impaired growth and development and at least in some of these mutants a direct correlation between phenotype and altered mRNA export can be assumed (Ehrnsberger et al., 2019a). For other proteins supposed to be important for mRNA export, like the four orthologues of the human export adaptor ALY, it is not known if the downregulation of these genes affects plant growth and development and if these factors also contribute to mRNA export in plants. The influence of mRNA export on a broad range of biological mechanisms is furthermore demonstrated as mRNA transport contributes to the regulation of plant immunity (Staiger et al., 2013), plant stress responses (Chinnusamy et al., 2008) and circadian clock (Romanowski and Yanovsky, 2015).

1.10 Aims of the project

Characterization of mRNA export factors

In *Arabidopsis* four orthologues of the human mRNA adaptor ALY are described as part of TREX, but it is not known if the loss of these factors affects plant growth and development and if these factors contribute to mRNA export. Since *aly* single and double mutant plants do not show an obvious phenotype, a homozygous mutant line lacking all four Arabidopsis *ALY* proteins (*4xaly*) will be generated and phenotypically analysed. To further characterize the ALY proteins as mRNA export factors, a possible recruitment of ALY proteins to TREX by UAP56 will be investigated by analysing potential protein-protein interactions between ALY proteins and UAP56 using FRET experiments. A potential contribution of ALY proteins to mRNA export will be tested by WISH, comparing Col-0 and *4xaly* plants. To analyse what mRNAs are targeted by ALY proteins for mRNA export an RNAseq approach will be applied to identify transcripts that are enriched in *4xaly* nuclei compared to Col-0 nuclei.

Another question that will be addressed is, why in plants four *ALYs* evolved and if there might be some functional differences between the four ALY proteins. Four different triple mutant plant lines, each lacking three ALYs but producing a functional fourth ALY, will be generated and phenotypically analysed. Possible functional differences between AYL proteins will be additionally investigated by genome-wide transcript profiling of plants from the four triple mutant lines compared to Col-0 and *4xaly* plants.

In humans, several factors act redundantly as mRNA export adaptors whereas in yeast the ALY orthologue is an essential factor. In *Arabidosis* two orthologues (UIEF1 and UIEF2) of the additional human export adaptor UIF can be identified and it will be tested if these factors act as mRNA export factors in *Arabidopsis*. Since *2xuief* double mutant plants display only a mild phenotype, plants lacking four ALY and two UIEF proteins (*4xaly 2xuief*) will be phenotypically

analysed to see if these plants are more severely affected in plant growth and development than *4xaly* plants. A possible recruitment of UIEF proteins to TREX by UAP56 will be investigated by analysing potential protein-protein interactions between UIEF proteins and UAP56 using FRET experiments and a potential contribution of UIEF proteins to mRNA export will be tested by WISH comparing Col-0, *2xuief, 4xaly* and *4xaly 2xuief* plants. Additionally, genome-wide transcript profiling in Col-0, *2xuief, 4xaly* and *4xaly 2xuief* plants will be applied to identify transcripts that potentially use ALY and/or UIEF proteins as export factors.

Identification of mRNA export receptor(s)

In plants it is not known what factor(s) act as export receptor(s). In human cells the mRNA handover process to a heterodimeric export receptor is initiated by a direct protein-protein interaction of export adaptors and the export receptor NXF1. To identify possible plant mRNA export receptor candidates, a proteomic approach after affinity purification using ALY and UIEF export factors as bait proteins will be applied and co-purifying proteins will be screened for similarities regarding protein domain structure to the human NXF1/NXT1 export receptor. Reciprocal tagging of export receptor candidates will be used to verify the obtained results. Subcellular localization of export receptor candidate-GFP fusion proteins will be analysed and a possible co-localization with the NPC marker NUP54-tagRFP will be investigated. A reverse genetics approach using T-DNA insertion mutants and the phenotypic characterization of receptor candidate mutant plants will give insights about the function of these factors and a possible contribution of export receptor candidates to mRNA export will be tested by WISH in export receptor mutant plants compared to Col-0.

2. Results

2.1 Analysis of ALY proteins as potential mRNA export factors

2.1.1 Arabidopsis ALY proteins share common motifs with human ALY

In Arabidopsis, four orthologues of the human mRNA export adaptor ALY are described (Uhrig et al., 2004). A comparison of the amino acid sequences of the four *Arabidopsis* ALY proteins with the sequence of the human ALY protein reveals that ALY1/2 and ALY3/4 show ~44% and ~38% amino acid sequence identity with human ALY respectively (Pfaff et al., 2018, Figure 8). Within the four *Arabidopsis* proteins a high degree of similarity between ALY1 and ALY2 (54% amino acid sequence identity) as well as ALY3 and ALY4 (70% amino acid sequence identity) can be observed, whereas the amino acid sequence identity between ALY1/2 versus ALY3/4 is clearly lower (less than 42%). The alignment additionally reveals, that a central RRM as well as an N-and C-terminal UAP-binding motif (UBM), which in humans mediates the interaction of ALY with UAP56 and its paralog DDX39, are conserved (Luo et al., 2001; Golovanov et al., 2006).

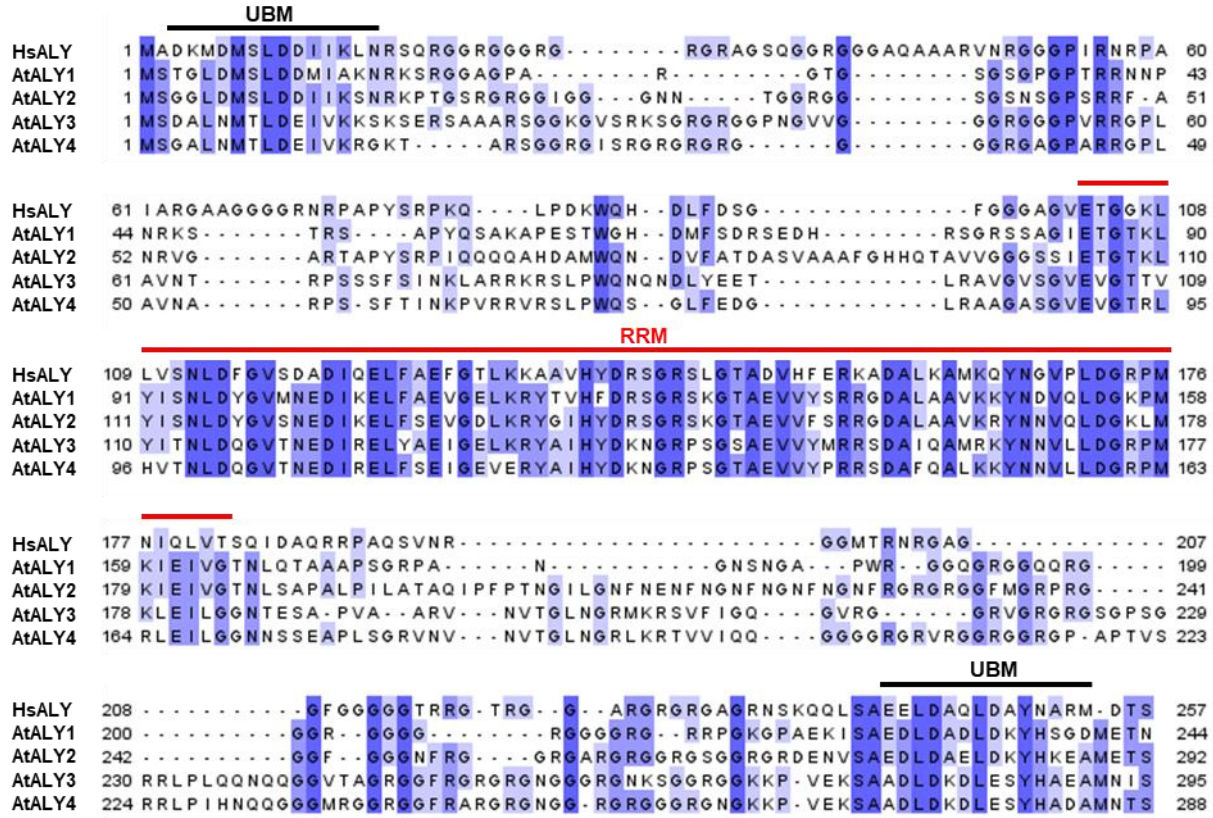

Figure 8. The amino acid sequence of the four ALY proteins is conserved. The human ALY sequence was aligned to the sequences from the four *Arabidopsis* ALY proteins. The predicted N-terminal (SLDD/E) and C-terminal (LDxxLD) UAP56 binding motifs are highlighted in black and a central RRM is highlighted in red (Gromadzka *et.al*, 2016). Multiple sequence alignment was generated using Clustal Omega (Sievers et., 2011) and the conservation of amino acid residues is highlighted in blue using JalView (Waterhouse et., al 2009). .

2.1.2. ALY1 and ALY3 directly interact with UAP56 in plant cells

In yeast and metazoans, it was shown that the export adaptor ALY (Yra1 in yeast) is recruited to the TREX complex by an interaction with UAP56 (Sub2 in yeast, Luo et al., 2001; Sträßer and Hurt, 2001; Preker et al., 2002). Plant ALY proteins were shown to directly interact with UAP56 in yeast cells, indicating a similar mechanism of ALY recruitment (Kammel et al., 2013; Sørensen, 2016).

To verify an ALY- UAP56 interaction in plant cells, a FRET approach was pursued. As all four *Arabidopsis* ALY proteins share an N- and C- terminal UBM and ALY1/ALY2 as well as ALY3/ALY4 share high sequence identity, ALY1 and ALY3 were selected as representatives to test a possible direct protein-protein interaction between ALY1/ALY3 and UAP56. *ALY1* and *ALY3* fused to *eGFP* were both co-expressed with *UAP56* fused to mCherry as donor/acceptor pairs in *Nicotiana benthamiana* leaf cells and a possible direct protein-protein interaction was measured by Förster resonance energy transfer (FRET).

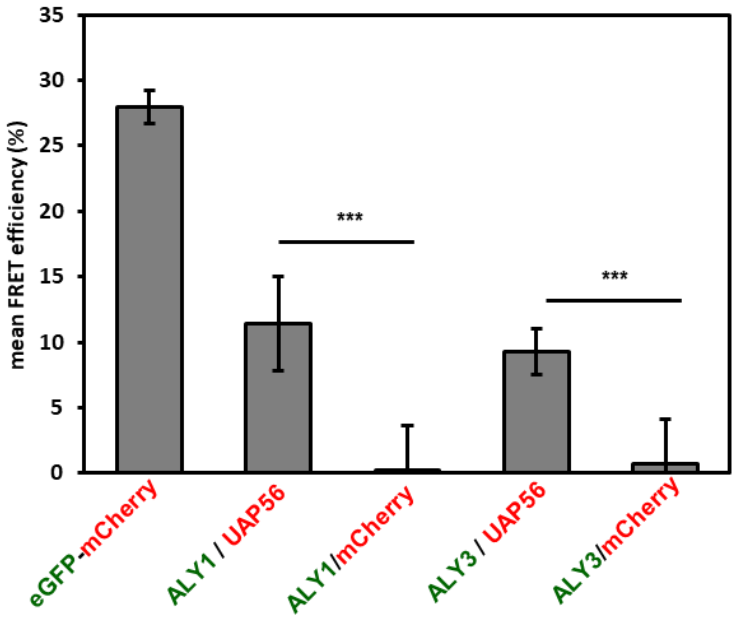

Figure 9. ALY1 and ALY3 directly interact with UAP56 in FRET experiments. FRET efficiencies were measured in *N. benthamiana* leaf cells co-expressing a donor (eGFP, ALY1-eGFP, ALY3-eGFP, green) and an acceptor (mCherry, UAP-mCherry, red). FRET efficiencies measured in cells expressing an eGFP-mCherry fusion protein served as a positive control wheras FRET efficiencies measured in cells co-expressing AL1-eGFP or ALY3-eGFP and unfused mCherry served as a negative control. Mean FRET efficiencies were measured in 8 nuclei for each donor/acceptor pair. ***, Statistically significant difference assessed by Student's t test ($P < 0.001$).

Both ALY1-eGFP and ALY3-eGFP directly interacted with UAP56-mCherry with mean FRET efficiencies of 11.4% (ALY1) and 9.3% (ALY3), whereas mean FRET efficiencies in leaf cells co-expressing ALY1-eGFP or ALY3-eGFP and unfused mCherry showed background levels

(0.2% for ALY1-eGFP/unfused mCherry and 0.7% for ALY3-eGFP/unfused mCherry). As a positive control a mean FRET efficiency of 27.9% was measured in leaf cells expressing an eGFP-mCherry fusion protein (Figure 9).

2.1.3. Plants lacking all four ALY proteins show severe growth defects

To characterize the four ALY proteins as potential export factors, the four T-DNA insertion lines *aly1-1*, *aly2-1*, *aly3-1* and *aly4-1* were previously characterized on a molecular basis and homozygous single mutant plants as well as the corresponding *aly1 aly2* and *aly3 aly4* double mutant plants were phenotypically analysed (Sørensen, 2016).

As these plants are only mildly affected in growth and development and show no or only a moderate mRNA export block, the double mutant plants *aly1 aly2* and *aly3 aly4* were crossed and a homozygous quadruple mutant (*aly1 aly2 aly3 aly4)* was identified in the next generations by genotyping, that in the following is referred to as *4xaly.*

Compared to single and double mutant plants, *4xaly* plants were severely affected regarding plant growth and development (Figure 10). In early stages of plant development (8 DAS), *4xaly* plants showed reduced growth of the primary root and elongated hypocotyls compared to Col-0 (Figure 10 C,J,K). *4xaly* plants also started bolting later and had less leaves and a smaller rosette at this stage (Figure 10 A,F,G,H). Later in plant development, *4xaly* plants showed a reduced plant height and less primary inflorescences (Figure 10 B,I). Apart from defects in plant growth and development, *4xaly* plants also displayed an altered flower morphology and reproductive defects. About 25% of flowers showed an abnormal number of petals (ranging from 3 to 7) and plants displayed a clearly reduced seed set (Figure 10 D,E).

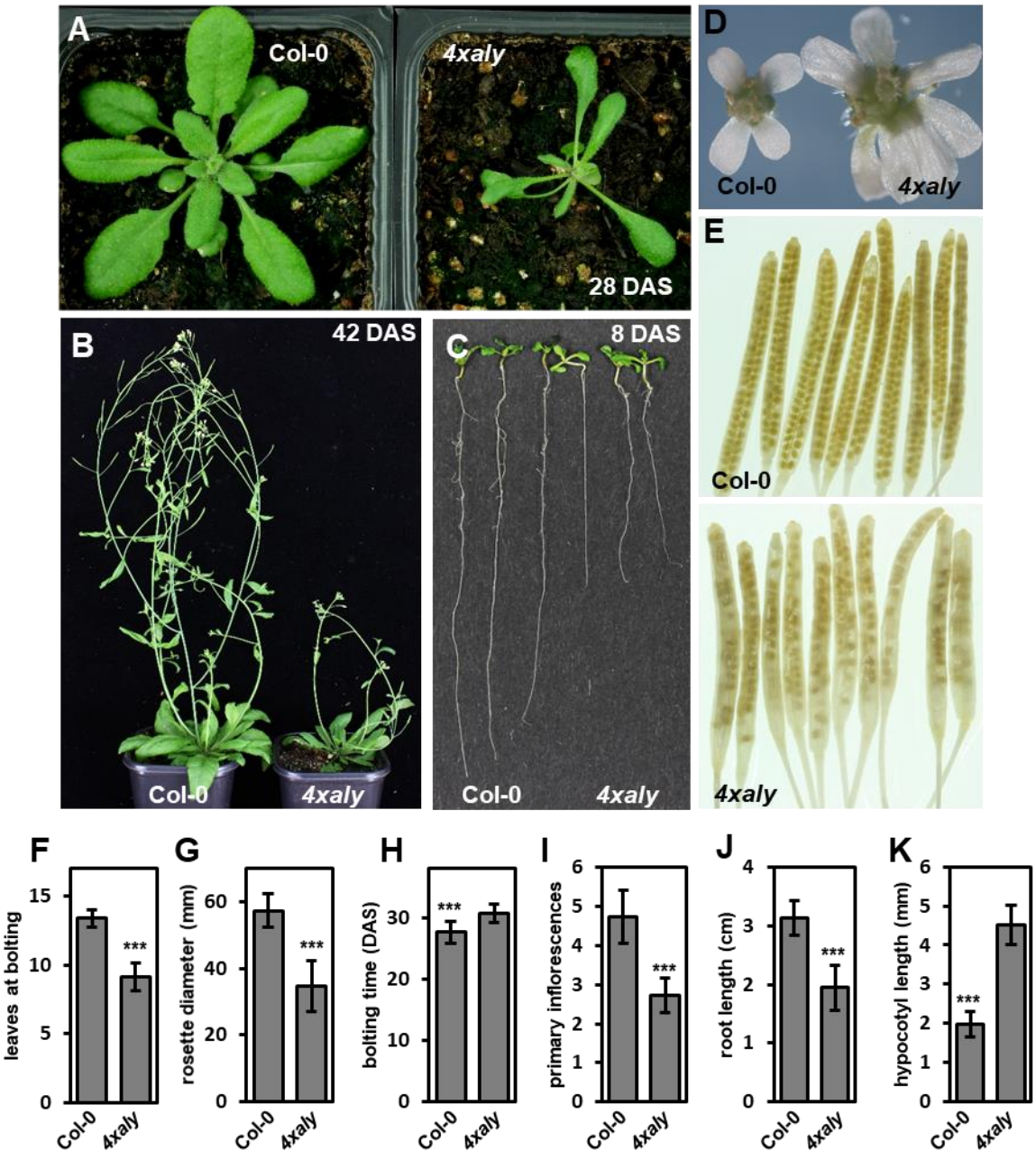

Figure 10. ***4xaly* plants are severely affected regarding plant growth and development.** Phenotype of *4xaly* plants compared to Col-0 at 28 DAS (A) and 42 DAS (B). 4xaly plants show reduced root length and longer hypocotyls at 8 DAS (C). *4xaly* plants show altered flower morphology with up to 7 petals (D) and a reduced seed set (E). (F-K) Phenotypic analysis for (F) leaves at bolting, (G) rosette diameter at bolting, (H) bolting time, (I) primary inflorescences 42 DAS, (J) root length 8 DAS and (K) hypocotyl length 8 DAS. Error bars indicate SD of 15 plants (F,G,H,I) and 30 plants (C,F). Data sets marked with asterisks are significantly different ($P < 0.001$) as assessed by Student´s t test.

2.1.4. *4xaly* plants show bulk mRNA export block

To test if the loss of all four ALY proteins results in a general mRNA export block, whole-mount in situ hybridization (WISH) with a fluorescently labelled 48-nucleotide oligo(dT) probe was performed in roots from 6 DAS seedlings (Figure 11). With this method polyadenylated RNAs can be visualized and a strong nuclear signal compared to the cytosolic signal indicates a general defect in mRNA export demonstrated by an enrichment of polyadenylated mRNAs in the nucleus (Gong et al., 2005).

The TREX-2 complex mutant *thp1* served as a positive control, as the loss of THP1 leads to a severe general mRNA export block (Lu et al., 2010). Fluorescence signals in nuclei and surrounding cytosols were visualized after WISH by confocal laser scanning microscopy (CLSM) and nuclear and cytosolic signal intensities in 58 or more nuclei per genotype were measured (Figure 11 B). A statistically significant higher average nucleus/cytosol signal ratio in both *4xaly* and *thp1* was calculated compared to Col-0 showing a general mRNA block in both mutant genotypes with a more pronounced export defect detected in *thp1* compared to *4xaly* (Figure 11 C).

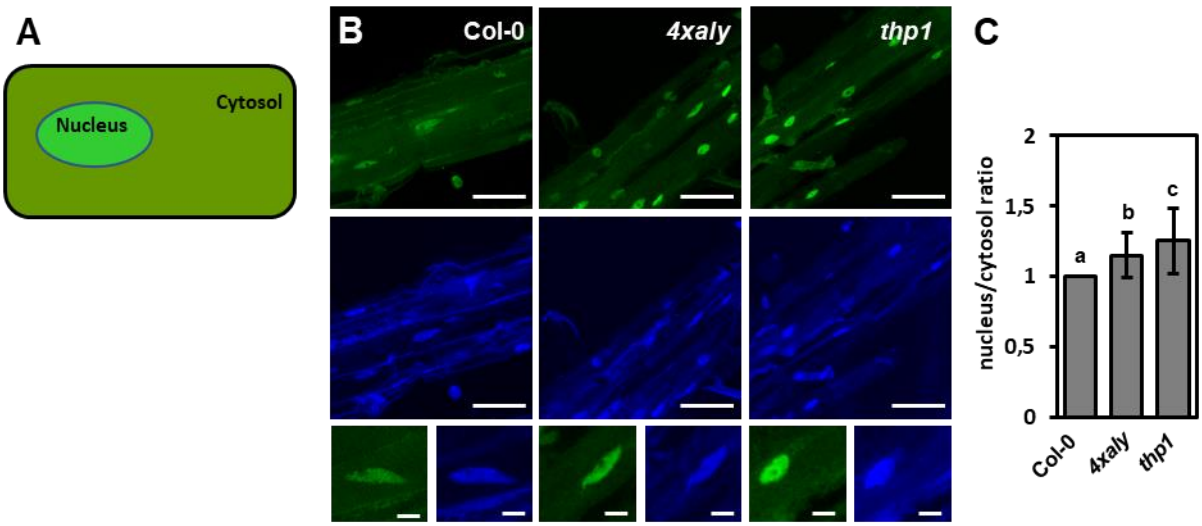

Figure 11. *4xaly* plants show bulk mRNA export block. To identify mRNA export defects, whole-mount in situ hybridization (WISH) with a fluorescently labeled 48-nucleotide oligo(dT) probe was performed in roots from 6 DAS seedlings and the signal ratio of nucleus/cytosol was determined (A). (B) CLSM images from representative sections from roots of Col-0, *4xaly* and *thp1* plants with Alexa Fluor 488 oligo (dT) signal in green and DAPI signal in blue. Bars = 60 µm (top rows) and 10 µm (bottom row). (C) Average nuclear/cytosol signal ratio of 59 or more nuclei per genotype in Col-0, *4xaly* and *thp1*. The ratios are shown relative to Col-0 (ratio of 1), with error bars indicating SD. Data sets marked with different letters are significantly different as assessed by a multicomparison Tukey's test ($P < 0.01$) after one-way analysis of variance.

2.1.5. Identification of mRNAs retained in the nucleus in *4xaly*

WISH showed that a variety of transcripts are retained in the nucleus when all four *ALY* genes are mutated. To identify these transcripts, the obvious method would be to separate nuclei from the cytoplasm in Col-0 and *4xaly* plants and by RNAseq identify transcripts that are enriched in *4xaly* nuclei compared to Col-0 nuclei relative to the amount of the respective transcript in the cytosol.

In plants, cells are surrounded by a quite robust cell wall what causes problems separating nuclei and cytosol. The mechanic force that is necessary to open plant cells can cause a partly disruption of nuclei resulting in a cytosolic fraction that is often not free from nuclear elements. Hence a different approach of sequencing nuclear mRNAs and comparing the transcript level to the transcript level of the cytosolic fraction was chosen. Plant material from aerial parts of 14 DAS old seedlings of Col-0 and *4xaly* plants was separated into a smaller (0.05 gram) and a bigger portion (0.4 gram, Figure 12).

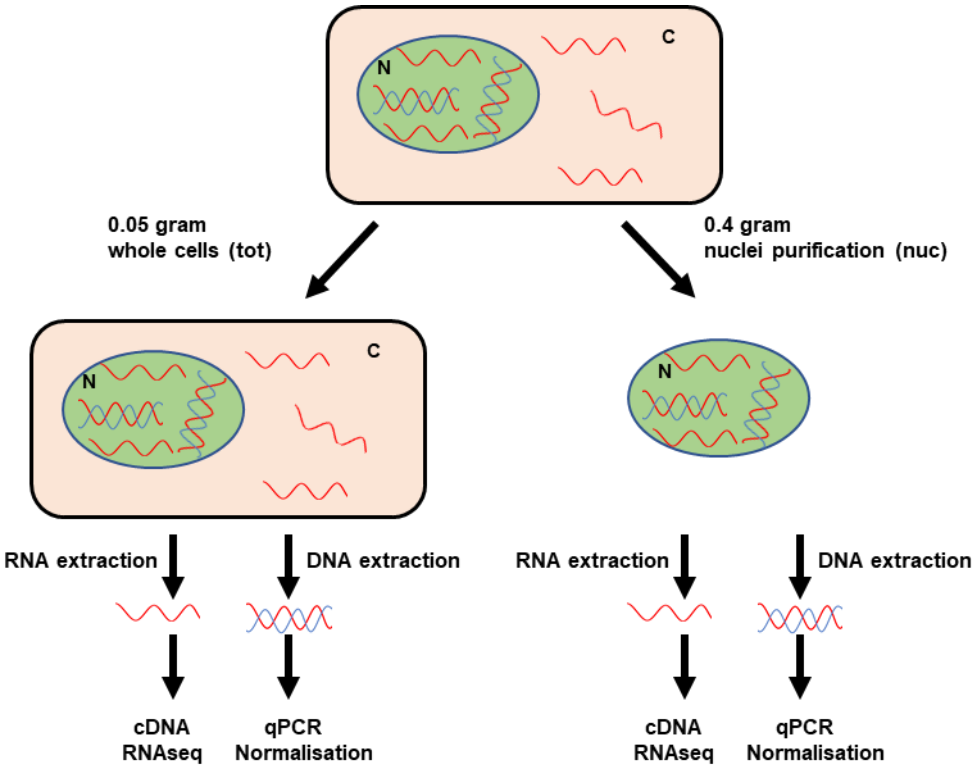

Figure 12. Work flow of RNAseq experiment sequencing transcripts of total cells and nuclei in *4xaly* and Col-0 plants . Plant material from 14 DAS old seedlings of Col-0 and *4xaly* plants was divided into a smaller portion of 0.05 grams and a bigger portion of 0.4 grams. The smaller portion was used to extract RNA and DNA from whole cells (tot), whereas RNA and DNA was extracted from isolated nuclei (nuc) that were purified from the bigger portion of plant material. The isolated RNA was translated into cDNA and cDNA was used for deep sequencing. The isolated genomic DNA was used as a template for qPCR to normalize the amount of total cells and nuclei in *4xaly* and Col-0 used for RNAseq.

The smaller portion was used to extract RNA from whole cells (nuclei + cytosol) whereas from the bigger portion nuclei were isolated and subsequently RNA was extracted (Figure 12). In the following, RNAs from whole cells (total, tot) and nuclei (nuc) were sequenced and the transcript level tot. vs. nuc. was calculated in Col-0 and *4xaly*.

To ensure that the same ratio of total cells to nuclei was compared in Col-0 and *4xaly,* a normalization step was included. Along RNA extraction from whole cells and nuclei, genomic DNA was extracted (Figure 12). By amplification of three single copy genes (*SSRP1, TEX1 and MOS11*) from these genomic DNAs by qPCR the input amount of cells and nuclei could be determined (Supplement S8). The transcript levels determined by RNAseq were then in the course of the RNAseq data analysis normalized to the number of cells or nuclei used to extract RNA.

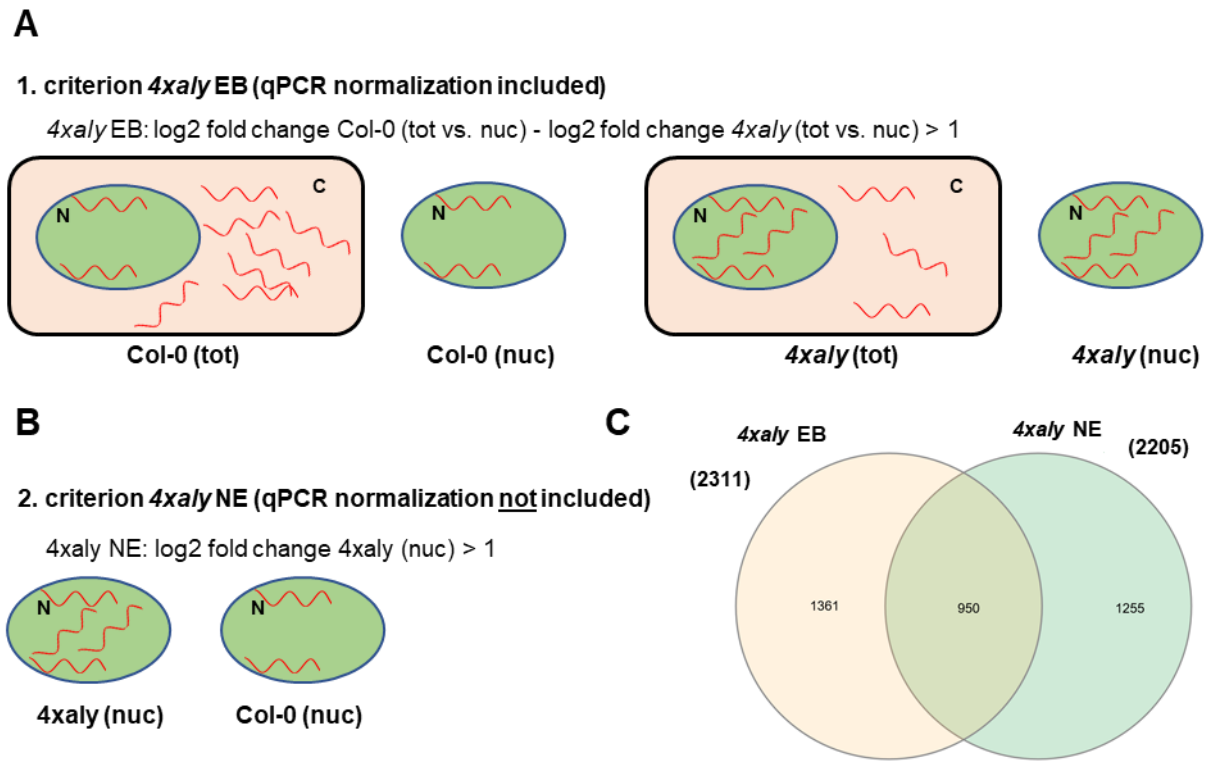

Figure 13. Criteria that were applied to identify reliable candidates that are enriched in *4xaly* nuclei and by that use the ALY mRNA export pathway. (A) First, candidates were selected that have more total (tot) transcripts relative to nuclear (nuc) transcripts in Col-0 compared to *4xaly* and a threshold of log2 fold change Col-0 (tot vs. nuc) - log2 fold change 4xaly (tot vs. nuc) > 1 was set to select the candidates. Candidates are referred to as 4xaly Export Blocked. (B) Additionally, candidates should be enriched in *4xaly* compared to Col-0 regardless of the amount of nuclei used for RNA extraction with a threshold of log2 fold change *4xaly* (nuc) > 1. Candidates are referred to as *4xaly* Nuclear Enriched. (C) 2311 candidates fulfilled criterion 1 (A), 2205 candidates fulfilled criterion 2 (B) and 950 candidates fulfilled both criteria and were considered as the most reliable candidates that were used for further analysis.

By RNAseq 29328 transcripts were detected in at least one of the four sequenced fractions (Col-0 (tot), Col-0 (nuc), *4xaly* (tot) and *4xaly* (nuc), Figure 14 A). To identify mRNAs that were retained in *4xaly* nuclei and by that use a putative ALY dependent mRNA export pathway, the relative quantities of total transcripts compared to nuclear transcripts were calculated in Col-0 (tot vs. nuc) and *4xaly* (tot vs. nuc). Candidates were considered to be affected by an *4xaly* export block when log2 fold change Col-0 (tot vs. nuc) - log2 fold change *4xaly* (tot vs. nuc) > 1. In the following these candidates will be referred to as *4xaly* export blocked (*4xaly* EB, Figure 13 A). In total 2311 transcripts met this criterion (Figure 13 C, 14 B).

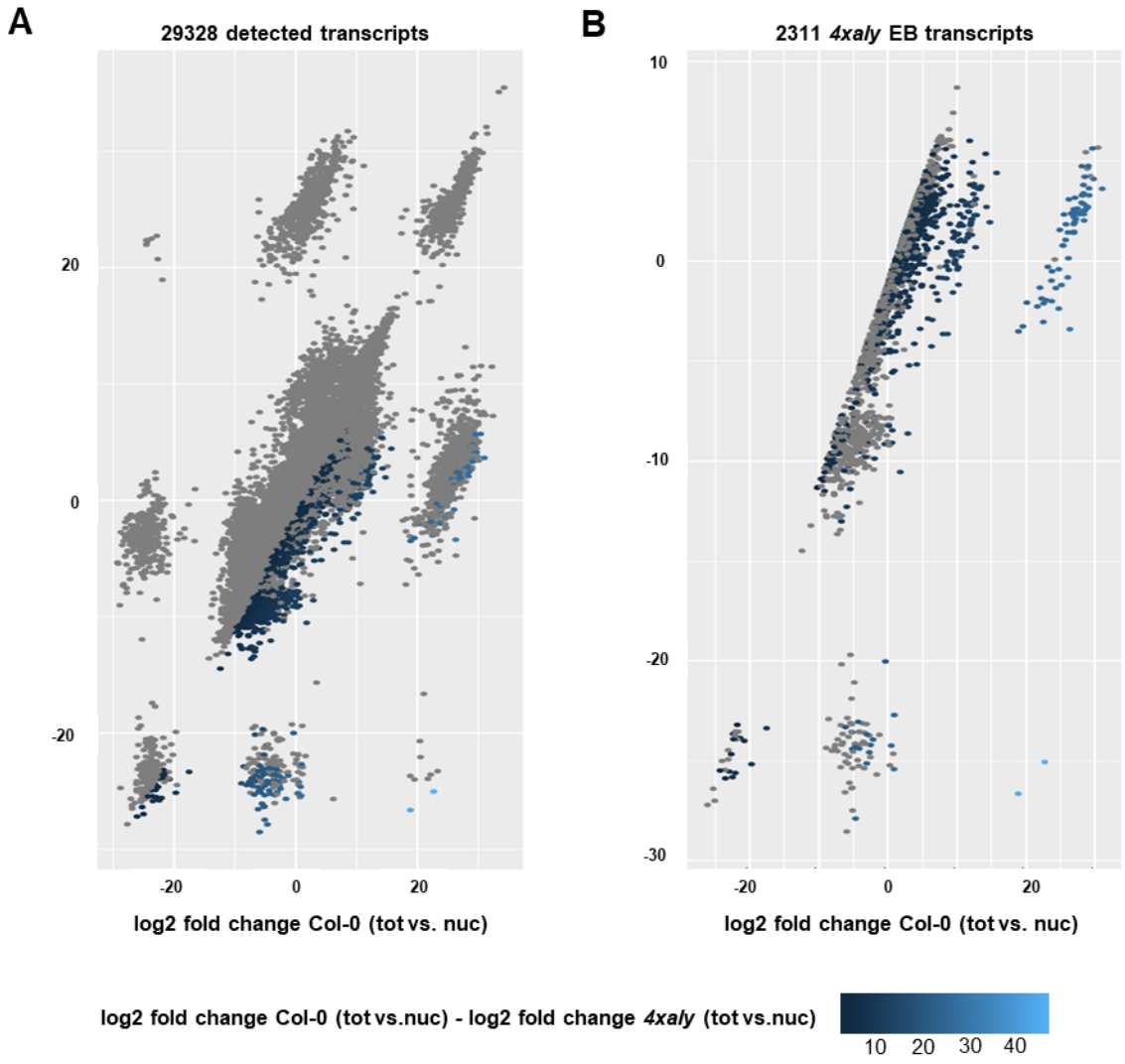

Figure 14. Scatterplots of transcripts identified by RNAseq in total cells and nuclei of Col-0 and *4xaly* plants. (A) 29328 transcripts detected in total and/or nuclear fraction of Col-0 and *4xaly* plants. Transcripts are plotted against their log2 fold change of the transcript level total vs. nuclear in Col-0 (x-axis) and *4xaly* (y-axis). Blue dots highlight 2311 *4xaly* EB transcripts with a log2 fold change Col-0 (tot vs. nuc) - log2 fold change 4xaly (tot vs. nuc) > 1. (B) 2311 *4xaly* EB transcripts highlighted in (A) with blue dots now highlighting 950 *4xaly* EB and *4xaly* NE transcripts that additionally show a log2 fold change 4xaly (nuc) >1, adding a second criterium to screen for most reliable candidate transcripts that are enriched in *4xaly* nuclei.

To obtain even more reliable candidates, a second criterion was applied (Figure 13 B). In addition to *4xaly* EB, which was calculated after normalization to the amount of cells or nuclei

used for RNA extraction, candidate mRNAs were considered as being targets of the ALY export pathway when being enriched in *4xaly* nuclei compared to Col-0 nuclei with a log2 fold change *4xaly* (nuc) > 1 regardless of the number of cells or nuclei used for RNA extraction. In the following these candidates will be referred to as *4xaly* nuclear enriched (*4xaly* NE).

In total 950 mRNAs were both *4xaly* EB and *4xaly* NE and by that were considered reliable candidates to be exported by an ALY mRNA export mechanism (Figure 13 C, 14 B). To validate the results obtained by RNAseq, qRT-PCR was performed on six candidates that were selected from the 950 most reliable candidates (Figure 15 A). Only transcripts detected in all four fractions were considered putative candidate transcripts. Transcripts absent in at least one fraction were excluded from the analyses. To verify the RNAseq data, the relative quantities of the six candidate mRNAs in nuclei compared to whole cells was determined in *4xaly* and Col-0 and the ratio of *4xaly*/Col-0 was built (Figure 15 B).

A

AGI	DESCRIPTION	*4xaly* EB	*4xaly* NE
		log2 fold change	log2 fold change
AT1G73480	Alpha/beta-Hydrolases superfamily protein	3.39	1.65
AT2G43010	Transcription factor	1.81	1.22
AT5G46110	Triose phosphate/phosphate translocator TPT	2.4	1.58
AT4G24350	Phosphorylase superfamily protein	2.03	2.07
AT1G25400	Transmembrane protein	1.12	1.09
AT2G29310	NAD(P)-binding Rossmann-fold superfamily protein	1.98	1.03

B

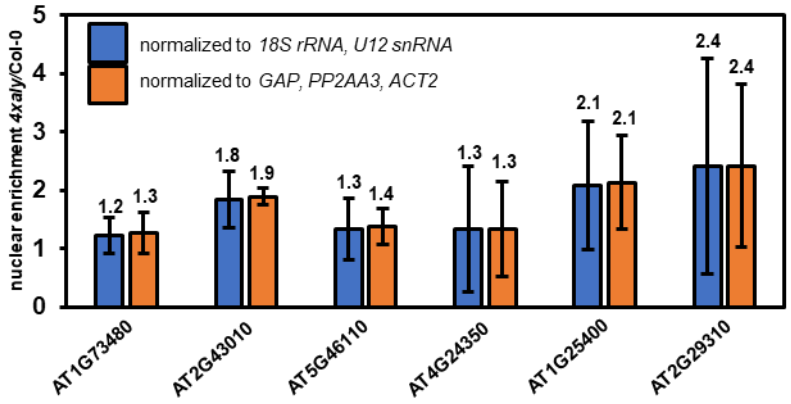

Figure 15. Validation of the enrichment of six candidate transcripts in *4xaly* nuclei compared to Col-0 nuclei by qRT-PCR. (A) Six candidate genes were selected from 950 most reliable candidates for validation of the RNAseq results that fulfil the two criteria *4xaly* EB and *4xaly* NE. (B) The relative expression of six candidate genes in nuclei compared to total cells was determined in *4xaly* and Col-0 and the ratio of *4xaly*/Col-0 was built. This ratio is displayed above the columns whereby a value > 1 indicates an enrichment of the transcript in *4xaly* nuclei compared to Col-0.nuclei relative to the quantity of the respective transcript in whole cells. The relative quantity of the candidate mRNAs in nuclei and total cells was normalized in one approach to the relative quantity of *18S rRNA* and *U12 snRNA* in nuclei and whole cells (blue) and in one approach to the relative quantity of the mRNAs *GAP*, *PP2AA3* and *ACTIN2* in nuclei and whole cells (orange).

Since WISH demonstrated that *4xaly* is an mRNA export mutant, it is not excluded that also reference mRNAs, that are widely used to normalize the relative quantities of transcripts may

not be properly exported in an export block mutant, what could falsify the results obtained by qRT-PCR. Thus, in a first approach the relative quantities of the two non-mRNA reference transcripts *18S rRNA* and *U12 snRNA,* that are exported out of the nucleus by a different mechanism, were used to normalize the relative quantities of the candidate transcripts in whole cells and nuclei. In a second approach, the three widely used reference genes *GAP*, *PP2AA3* and *ACTIN2,* whose transcripts should not be retained in the nucleus in *4xaly* according to the RNAseq data, were used for normalization.

Figure 15 B shows, that both ways to normalize the relative quantities of the candidate transcripts lead to almost identical results, demonstrating the reliability of the obtained results. For all six tested candidates in *4xaly* more transcripts were retained in the nucleus compared to whole cells than in Col-0 resulting in a value > 1. For the candidates AT2G43010, AT1G25400 and AT2G29310 mRNAs were almost 2-fold or more then 2-fold enriched in *4xaly* nuclei compared to Col-0 nuclei. For the other three candidates a clear, but less strong enrichment in *4xaly* nuclei was detected.

2.1.6. *3xaly* plants are differently affected in plant growth and development

It could be shown that *4xaly* is an mRNA export mutant and ALY proteins function as export factors. Since *aly* single and double mutant plants are only mildly affected on a phenotypic level, while the quadruple *4xaly* mutant is severely affected, a key question that is not answered is if ALY proteins preferentially bind different subsets of transcripts and by that affect plant growth and development in various ways. This was addressed by phenotypic analysis of four versions of triple mutant plants, each expressing one of the ALY proteins and lacking the other three ALY proteins. In the following these four triple mutant plant lines are referred to as *3xalyALY1*, *3xalyALY2*, *3xalyALY3* and *3xalyALY4* that are homozygous for either the wild type *ALY1*, *ALY2*, *ALY3* or *ALY4* gene and homozygous for the remaining three *aly* mutant alleles (*3xaly*).

Interestingly, these triple mutant plants were clearly differently affected in plant growth and development. Plants expressing wild type *ALY1* showed similar but still distinct phenotypic alterations compared to *4xaly* plants. The triple mutants *3xalyALY2*, *3xalyALY3* and *3xalyALY4* on the other hand looked more like the wild type but displayed still distinct phenotypic alterations compared to Col-0 plants (Figure 16). *3xalyALY1* plants started bolting later compared to Col-0, albeit not as late as *4xaly* plants, whereas the other triple mutants showed a clear early bolting phenotype with *3xalyALY3* and *3xalyALY4* plants bolting earlier then *3xalyALY2* plants (Figure 16 A,E). A difference in the phenotypes of *3xalyALY1* on the one hand and the other triple mutants on the other hand was further visible 28 DAS with *3xalyALY1* plants, like *4xaly*, having a smaller rosette whereas the rosettes from *3xalyALY2* and

3xalyALY3 plants had similar sizes like Col-0 plants. *3xalyALY4* plants had bigger rosettes compared to *3xalyALY1* or *4xaly* albeit smaller than Col-0, *3xalyALY3* or *3xalyALY4* plants (Figure 16 A,F). The delayed development of *4xaly* and *3xalyALY1* plants could also be observed 42 DAS with both mutants showing a reduced plant height whereas the other triple mutant plants showed a similar plant height like Col-0 (Figure 16 B,G).

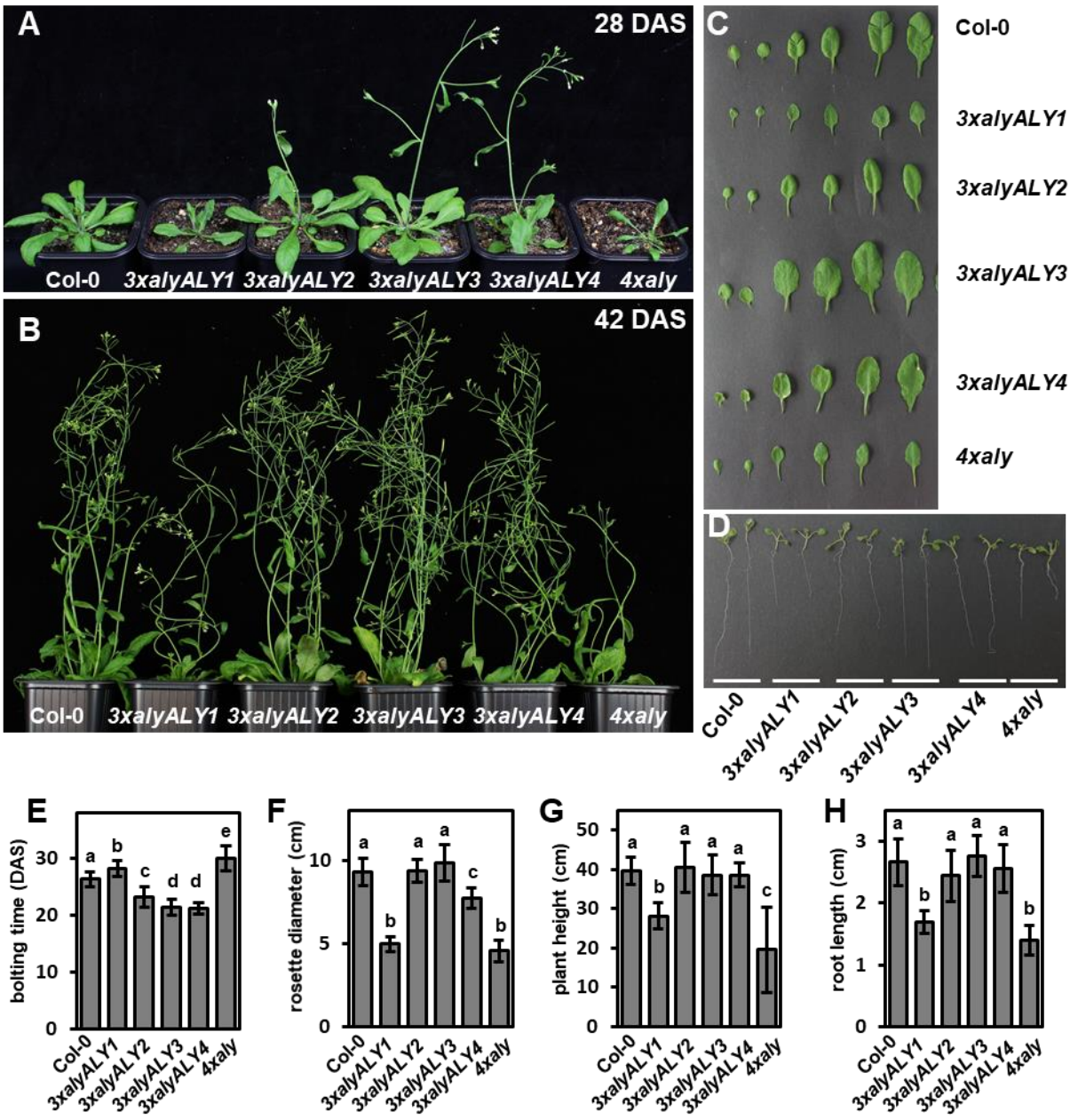

Figure 16. ***3xaly*** **plants are differently affected in plant growth and development.** Phenotype of *3xaly* plants compared to Col-0 and *4xaly* at 28 DAS (A) and 42 DAS (B). (C) Leaf morphology of true leaves 3-8 of *3xaly* plants compared to Col-0 and *4xaly* plants 28 DAS. (D) Root length 8 DAS of *3xaly* plants compared to Col-0 and *4xaly*. (E-H) Phenotypic analysis for (E) bolting time, (F) rosette diameter 28 DAS, (G) plant height 42 DAS and (H) root length 8 DAS. Error bars indicate SD of 15 plants. Data sets marked with different letters are significantly different as assessed by a multicomparison Tukey's test ($P < 0.05$) after one-way analysis of variance.

The observation that the severe phenotype of the *4xaly* plant is mainly caused by mutations in *ALY2*, *ALY3* and *ALY4* was further supported by the leaf morphology in the different mutants (Figure 16 C). Leaves that arise very early in plant development (true leaves 3-8) were smaller and more arrow-shaped in *3xalyALY1* and *4xaly* compared to Col-0, *3xalyALY2*, *3xalyALY4* and especially to *3xalyALY3.* Severe defects in plant growth and development could not only be detected in the aerial parts of *3xalyALY1* and *4xaly* mutant plants but also in roots. 8 DAS a reduced root growth could be monitored in these two mutants whereas the root length of *3xalyALY2*, *3xalyALY3* and *3xalyALY4* mutant plants was not altered compared to Col-0 (Figure 16 D,H).

2.1.7. *3xaly* plants show a general mRNA export block

Since the different *3xaly* mutants were differently affected regarding plant growth and development and all *3xaly* mutants showed a distinct phenotype from *4xaly,* in the following it was analysed if these differences could be explained by differences in a bulk mRNA export block.

To analyse the subcellular distribution of mRNAs in the four different *3xaly* mutants compared to *4xaly*, whole-mount in situ hybridization with a fluorescently labelled 48-nucleotide oligo(dT) was performed like described in figure 11. Interestingly, in all triple mutant plant lines an mRNA export block similar to the block in *4xaly* could be detected (Figure 17 B).

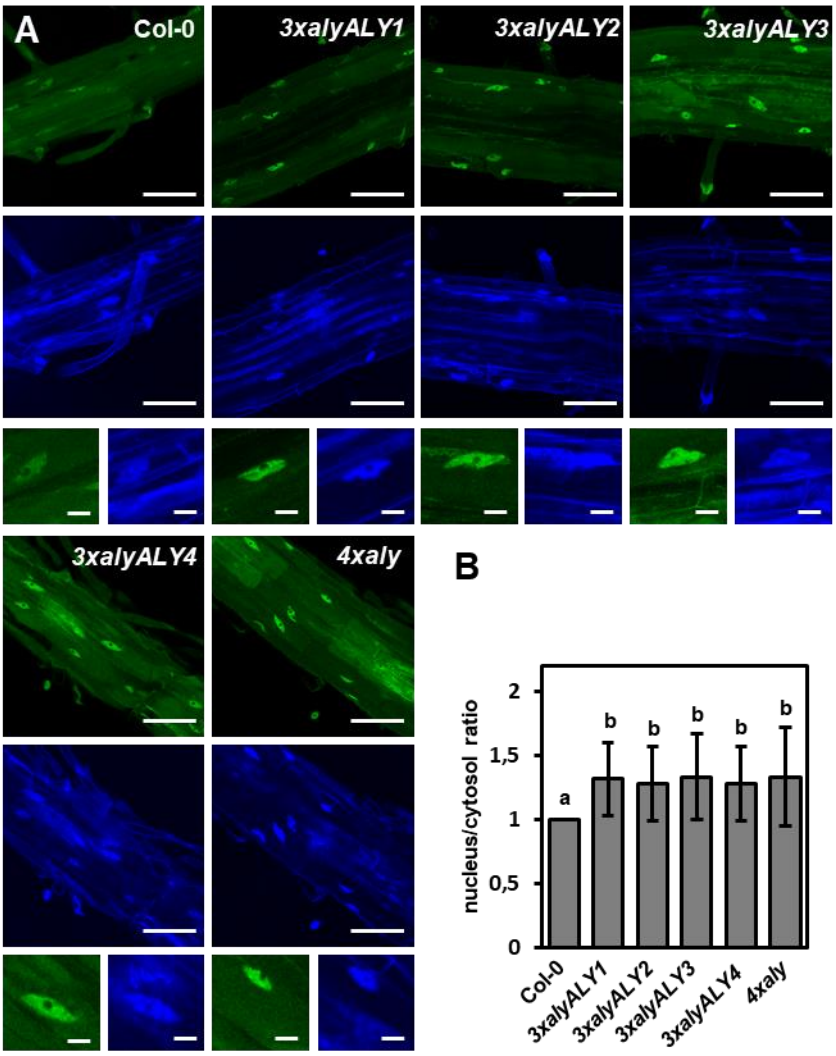

Figure 17. All *3xaly* mutants show a bulk mRNA export block. (A) CLSM images from representative sections from roots of Col-0, *3xalyALY1*, *3xalyALY2*, *3xalyALY3, 3xalyALY4* and *4xaly* plants after WISH with the Alexa Fluor 488 oligo (dT) signal in green and DAPI signal in blue. Bars = 60 µm (top rows) and 10 µm (bottom row). (B) Average nuclear/cytosol signal ratio of 38 or more nuclei per genotype. The ratios are shown relative to Col-0 (ratio of 1), with error bars indicating SD. Data sets marked with different letters are significantly different as assessed by a multicomparison Tukey's test ($P < 0.001$) after one-way analysis of variance.

2.1.8. Transcript profiling in *3xaly* mutants

WISH experiments displayed in chapter 2.1.7 indicated that differences in *3xaly* mutant phenotypes are rather caused by export defects affecting different subsets of transcripts than by differences in a bulk mRNA block. To address the question if different ALY proteins might regulate the export of different mRNAs, transcript profiling in the four different *3xaly* mutants as well as in *4xaly* compared to Col-0 was performed. RNAs were extracted from aerial parts of 10 DAS seedlings and for each genotype RNAs from four biological replicates were sequenced.

It was assumed, that in an export block mutant, transcripts that are not properly exported out of the nucleus should be degraded over time when sequestered in the nucleus, leading to in

total less transcripts within the cell compared to Col-0. Genes downregulated in *4xaly* were compared with candidate genes that give rise to transcripts that were found to be affected by an mRNA export block in *4xaly* (chapter 2.1.5). Transcript profiling revealed 1306 mRNAs transcribed from 1085 gene loci that were reduced in *4xaly* compared to Col-0 with a log2 fold change < -1 (Figure 18, 19). A minor overlap could be determined when these candidates were compared to the candidates detected by RNAseq of total cells and nuclei to be affected by an mRNA export block in *4xaly*. When the 1085 *4xaly* downregulated genes were compared with the 3342 candidate genes that give rise to 3565 transcripts that were identified by cell fractioning to be *4xaly* EB or *4xaly* NE (Figure 13), 220 candidates were identified by both sequencing approaches (Figure 18 A). When the 964 *4xaly* EB and *4xaly* NE most reliable candidates (Figure 13 C) were compared with the 1085 *4xaly* downregulated genes, 70 candidates were detected by both sequencing approaches (Figure 18 B, Supplement S10). GO term analysis of the 1085 *4xaly* downregulated genes and the 964 *4xaly* EB and *4xaly* NE genes additionally revealed similar molecular functions of those candidates. More than 75% of the candidates (*4xaly* downregulated, 4xaly EB and *4xaly* NE) display either binding properties or catalytic activities (Supplement S9).

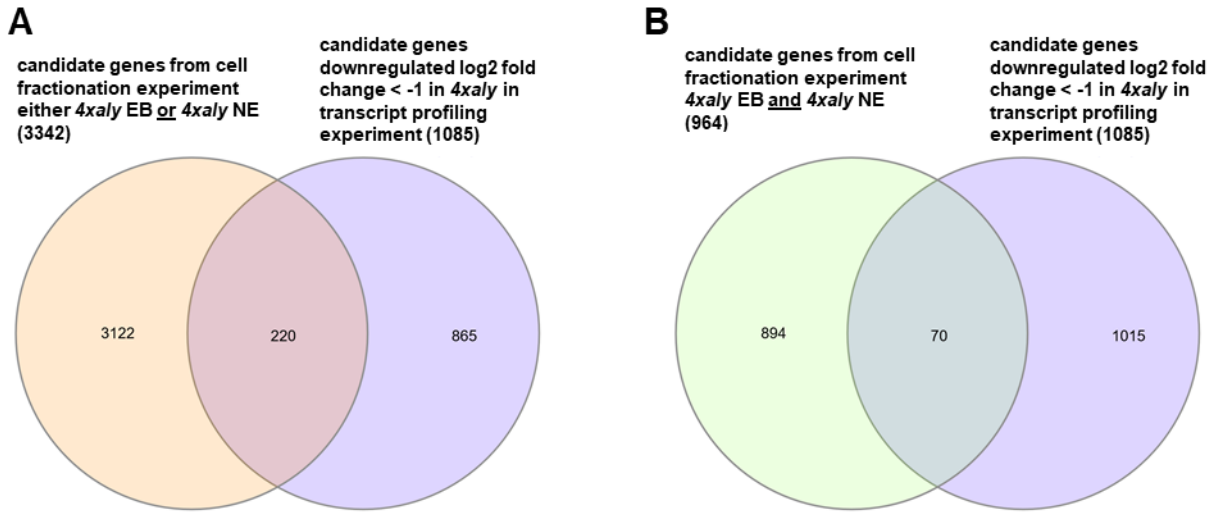

Figure 18. Overlap of candidates identified in the cell fractioning experiment as being enriched in *4xaly* nuclei and candidates with a reduced transcript level in *4xaly* compared to Col-0 identified by transcript profiling. (A) Overlap of 3342 candidate genes that give rise to 3565 transcripts that were identified in the cell fractioning experiment as *4xaly* EB or *4xaly* NE and 1085 candidate genes identified by transcript profiling that give rise to 1306 mRNAs with a reduced transcript level in *4xaly* compared to Col-0 with log2 fold change < -1. (B) Overlap of 964 candidate genes that give rise to 950 transcripts that were identified in the cell fractioning experiment as *4xaly* EB and *4xaly* NE and 1085 candidate genes identified by transcript profiling that give rise to1306 mRNAs with a reduced transcript level in *4xaly* compared to Col-0 with log2 fold change < -1.

In the following it will be assumed that a general downregulation in *3xaly* and *4xaly* mutants is mainly caused by a defect in mRNA export.

When comparing genes that were downregulated in the four *3xaly* mutants and *4xaly,* the biggest misregulation could be observed in *4xaly*. By transcript profiling 1306 transcripts corresponding to 1085 genes showed reduced transcript levels with a log2 fold change < -1 in the *4xaly* quadruple mutant (Figure 19 B). For the *3xaly* mutants a similar downregulation in *3xalyALY1*, *3xalyALY2* and *3xalyALY3* could be observed, with 686, 663 and 687 genes downregulated in the respective mutants that give rise to 788, 736 and 793 transcripts that were reduced in those genotypes (Figure 19 B). The least differences regarding relative transcript levels could be observed in *3xalyALY4* with only 315 genes being downregulated and 378 mRNAs that were reduced compared to Col-0.

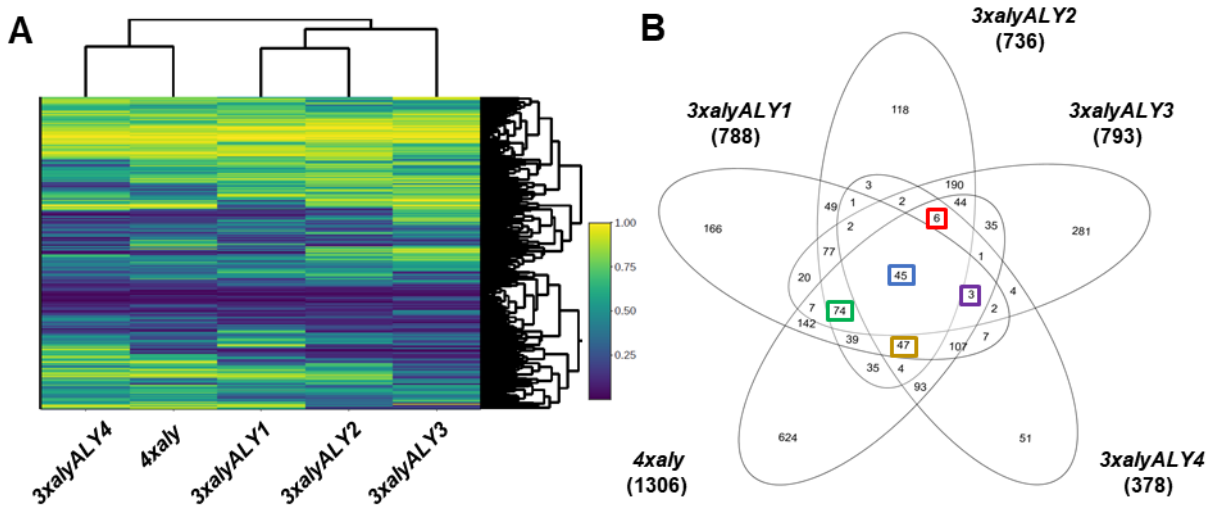

Figure 19. RNAseq of *3xaly* and *4xaly* mutants . (A) Gene expression in four *3xaly* mutants and *4xaly* detected by RNAseq and visualized as a heatmap. Genes downregulated are depicted in blue with dark blue indicating the strongest downregulation whereas yellow shows upregulated genes. Hierarchical clustering of expressed genes is shown on the right and hierarchical clustering of genotypes is shown above the heatmap. (B) Venn diagram of genes reduced > 2-fold in the five genotypes with transcripts highlighted in blue representing mRNAs that are reduced in all genotypes, in red mRNAs that are reduced in all genotypes but *3xalyALY1,* in purple mRNAs that are reduced in all genotypes but *3xalyALY2,* in brown mRNAs that are reduced in all genotypes but *3xalyALY3* and in green mRNAs that are reduced in all genotypes but *3xalyALY4*.

2.1.9. Subsets of transcripts are potentially exported by single ALY factors

When comparing the transcripts that were reduced in the different *3xaly* mutants with those reduced in *4xaly,* a variety of mRNAs are shared in those genotypes. The biggest overlap could be observed in *3xalyALY4* with ~ 83% of *3xalyALY4* downregulated mRNAs also being downregulated in *4xaly* (Figure 19 B). The highest correlation between the triple mutant *3xalyALY4* and *4xaly* was also identified when analysing changes in transcript levels of all detected transcripts demonstrated by a clustering of these two genotypes in a heatmap (Figure 19 A) The biggest differences on the other hand could be observed in *3xalyALY2* and

3xalyALY3 that both shared around 40% of reduced transcripts with *4xaly* whereas ~ 60% of mRNAs reduced in *3xalyALY1* were also reduced in *4xaly* (Figure 19 B).

In the following candidate mRNAs were bioinformatically identified that are potentially specifically exported by one of the four ALY proteins. To identify these transcripts, it was assumed that the transcript level of an mRNA that is specifically exported by one ALY factor (i) was reduced in *4xaly*, (ii) was reduced in three *3xaly* mutants but (iii) was not altered in the *3xaly* mutant that produces the wild type ALY that should export the respective transcript. In figure 19 B transcripts are highlighted that were reduced with a log2 fold change < -1 in *4xaly* and three *3xaly* mutants but not in a fourth *3xaly* mutant with i) 6 transcripts that were not reduced in *3xalyALY1* (red), ii) 3 transcripts that were not reduced in *3xalyALY2* (purple), iii) 47 transcripts that were not reduced in *3xalyALY3* (brown) and iv) 74 transcripts that were not reduced in *3xalyALY4* (green). Among those transcripts, in all four *3xaly* mutant genotypes mRNAs originating from the respective wildtype *ALY* genes were detected, confirming the integrity of the plant material used for sequencing.

In addition to mRNAs that potentially utilize an ALY specific mRNA export pathway, transcript levels of mRNAs that were reduced in all *3xaly* mutants and *4xaly* are of special interest because the export of these candidates depends on a concerted action of more than one ALY protein because a possible redundant function between ALY proteins is not sufficient to allow a proper mRNA export in the *3xaly* mutants. In total 45 transcripts were identified to be reduced with log2 fold change < -1 in all five *aly* mutant genotypes (Figure 19 B)

In table 2 candidates are listed that were used to validate RNAseq data by qRT-PCR with i) two candidate genes highlighted in blue that give rise to transcripts that were reduced in all five *aly* mutant genotypes, ii) two candidate genes highlighted in red that give rise to transcripts that are potentially specifically exported by ALY1, iii) one candidate gene highlighted in purple that gives rise to a transcript that is potentially specifically exported by ALY2, iv) two candidate genes highlighted in brown that give rise to transcripts that are potentially specifically exported by ALY3 and v) two candidate genes highlighted in green that give rise to transcripts that are potentially specifically exported by ALY4.

Table 2. Transcript levels of candidates reduced in *4xaly* and reduced in different *3xaly* mutants according to RNAseq and qRT-PCR. Candidate genes were selected from groups of genes highlighted in Figure 19 with transcript levels of two genes highlighted in blue being reduced in all genotypes according to RNAseq, transcript levels of two genes highlighted in red being reduced in all genotypes but *3xalyALY1*, transcript level of one gene highlighted in purple being reduced in all genotypes but *3xalyALY2*, transcript levels of two genes highlighted in brown being reduced in all genotypes but *3xalyALY3* and two genes highlighted in green downregulated in all genotypes but *3xalyALY4*.

AGI	*3xalyALY1*		*3xalyALY2*		*3xalyAly3*		*3xalyALY4*		*4xaly*	
	Fold change		Fold change		Fold change		Fold change		Fold change	
	RNAseq	qPCR	RNAseq	qPCR	RNAseq	qPCR	RNAseq	qPCR	RNAseq	qPCR
AT5G48490	-6.92	-4.08	-6.06	-3.31	-12.21	-9.16	-3.61	-3.26	-4.06	-2.76
AT1G66100	-8.17	-7.64	-3.43	-2.71	-2.60	-2.18	-3.58	-3.06	-13.93	-13.11
AT2G21650	-1.04	1.12	-1.65	-1.74	-2.09	-2.17	-1.68	-2.15	-2.99	-3.28
AT5G03350	1.43	1.41	-3.41	-3.95	-3.78	-4.98	-2.38	-2.92	-2.48	-2.85
AT3G28740	-1.96	-1.36	1.08	1.46	-1.38	-1.26	-1.58	-1.31	-3.27	-2.82
AT3G48360	-3.89	-3.76	-2.04	-1.96	1.01	1.05	-3.01	-3.39	-4.99	-6.32
AT2G05540	-6.54	-7.48	-2.51	-2.63	1.13	-1.03	-9.85	-9.91	-13.73	-14.68
AT3G22740	-2.68	-2.22	-3.53	-3.84	-3.68	-3.60	1.05	-1.28	-4.38	-4.36
AT4G20820	-5.17	-3.56	-5.70	-4.78	-6.36	-6.64	1.00	1.09	-3.27	-3.22

In general, the reduced transcript levels in the different *aly* mutants determined by RNA profiling could be verified by qRT-PCR. For the candidate gene AT5G48490 a comparatively stronger reduction in the transcript level was detected by qRT-PCR in some genotypes but for all other candidates a similar downregulation was identified by RNAseq and qRT-PCR (Table 2). The high correlation of RNAseq and qRT-PCR results is for instance demonstrated for the two candidates AT1G66100 and AT2G055404 that were strongly downregulated in *4xaly* according to the RNAseq experiment with a fold change of -13.93 and -13.74 and similar reduced transcript levels were also detected by qRT-PCR with fold changes of -13.11 and -14.68 respectively (Table 2).

qRT-PCR demonstrated, that transcripts derived from the gene loci AT5G48490 and AT1G66100 are candidates that potentially need the interplay of two or more ALY factors to be properly exported out of the nucleus, since in all four analysed *3xaly* mutants as well as in *4xaly* transcript levels were significantly reduced with a fold change < -2 (Figure 20 A, Table 2).

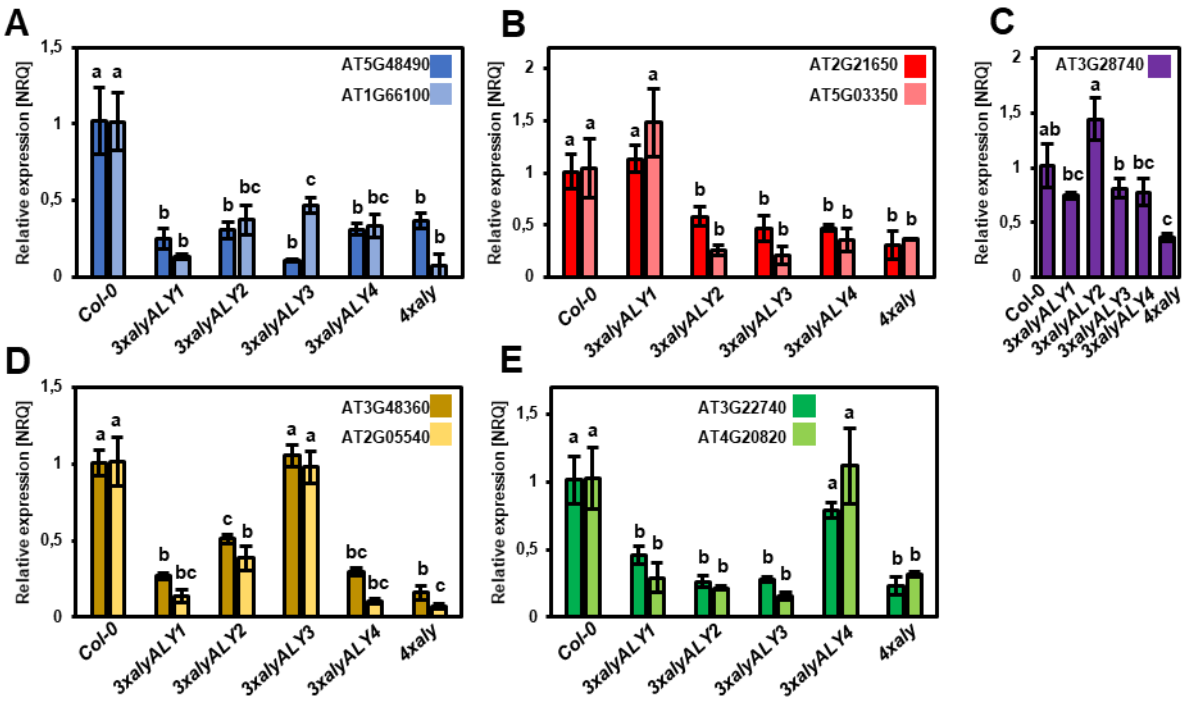

Figure 20. Validation of RNAseq results by qRT-PCR in *3xaly* and *4xaly* mutants. Relative expression of candidate genes listed in table 2 was determined in the four *3xaly* mutants and *4xaly* relative to Col-0 using three biological and two technical replicates. The normalized relative quantities (NRQ) and the normalized relative standard errors are shown. The NRQ was determined by normalization to the NRQs of *GAP*, *PP2AA3* and *ACTIN2* mRNA. (A) shows candidates with reduced transcript levels in all genotypes according to RNAseq, (B) candidates with reduced transcript levels in all genotypes but *3xalyALY1*, (C) a candidate with reduced transcript level in all genotypes but *3xalyALY2*, (D) candidates with reduced transcript levels in all genotypes but *3xalyALY3* and (E) candidates with reduced transcript levels in all genotypes but *3xalyALY4*. Differences in NRQ among genotypes is indicated by different letters as assessed by a multicomparison Tukey's test ($P < 0.05$) after one-way analysis of variance.

RNAseq and qRT-PCR experiments showed that mRNAs derived from AT5G03350 were not downregulated in *3xalyALY1* but downregulated in all the other mutants. (Figure 20 B). Additionally, AT2G21650 derived mRNAs display a similar pattern, even though this candidate did not fulfil the very stringent criterium that according to the RNAseq transcript levels should be reduced by < -2-fold in all the respective mutants (Table 2). Since for both candidate genes qRT-PCR showed a statistically significant lower transcript level in all the downregulated mutants compared to Col- (Figure 20 B), both AT5G03350 and AT2G21550 are candidates that potentially utilize ALY1 as the only mRNA export factor.

Only a limited number of candidates were not downregulated in *3xalyALY2* but downregulated in the other mutants (Figure 19B). The two candidates (the third is *ALY2*) obtained when correlating all reduced transcripts with a log2 fold change < -1 (Figure 19 B) are also downregulated -1.65 and -1.72-fold in *3xalyALY2.* AT3G28740 is the only candidate that was analysed by qRT-PCR and it only fulfilled a less stringent criterion, a log2 fold change > 0.5 between the *3xaly* mutant that shows no altered transcript level and the three *3xaly* mutants and *4xaly* that display reduced transcript levels for the respective mRNA (Table 2). qRT-PCR

could support the RNAseq result, since a significant difference in the transcript levels between *3xalyALY2* and the other *aly* mutants was determined. (Figure 20 C).

Several candidate mRNAs were detected by RNA profiling not to be downregulated in *3xalyALY3* or *3xalyALY4* but downregulated in the other mutants. Transcript levels of 47 and 74 transcripts, that were reduced by log2 fold change < -1 in all other mutants, were not misregulated respectively (Figure 19 B). In both genotypes two candidates were analysed by qRT-PCR and RNAseq data could be verified (Figure 20 D,E, Table 2). For all four tested candidate transcripts no change in the transcript level could be observed in *3xalyALY3* or *3xalyALY4,* whereas a significant downregulation was detected in all other mutants.

2.1.10. *4xaly* phenotype can be complemented by expression of transgenic ALY3 protein

As transcript profiling depicted in chapter 2.1.9 revealed that transcripts potentially utilize ALY specific mRNA export pathways, we will analyse in future experiments if different ALY proteins directly bind in *vivo* to specific mRNAs or subsets of transcripts. Therefore, tagged ALY fusion proteins expressed in transgenic plant or cell lines will be immunoprecipitated after crosslinking to RNAs to identify mRNAs that directly bind different ALYs. To test if these ALY fusion proteins are functional, it was investigated whether the expression of an *ALY* transgene in *4xaly* background can complement the severe *4xaly* phenotype. For the complementation experiments ALY3 fusion proteins were selected, as *3xalyALY3* mutant plants show a clear distinguishable phenotype compared to *4xaly* mutant plants displayed by a very early bolting phenotype and an overall more wildtype-like habitus (Figure 16). Since SG-tagged fusion proteins expressed in *Arabidopsis* cell suspension culture are widely used for affinity purifications in plant cells (Van Leene et al., 2008), a respective *ALY3-SG* transgene was integrated into the genome of *4xaly* plants by *A. tumefaciens* mediated transformation (Figure 21 A). Three independent lines homozygous for the inserted transgene were selected on MS plates supplemented with hygromycin and the presence of the transgene was verified by PCR (Figure 21 B). The expression of ALY3-SG fusion proteins could complement the *4xaly* phenotype, as plants of the three different independent lines bolted around the same time as *3xalyALY3* plants and by that clearly earlier than *4xaly* plants (Figure 21 C,D). The early bolting phenotype in the three independent transgenic lines was further illustrated by plant heights of more than 7 cm 28 DAS what resembles *3xalyALY3* while *4xaly* plants did not start bolting at 28 DAS (Figure 21 C,F). Besides the early bolting phenotype, the complementation in the three transgenic lines was also evident from a bigger rosette size in the three transgenic lines at 28 DAS and an overall phenotype that clearly resembled *3xalyALY3* plants but not *4xaly* plants (Figure 21. C,E). Line #4.8 showed some small differences compared to *3xalyALY3* with a less

pronounced early bolting phenotype displayed by a later bolting time and a reduced plant height 28 DAS as well as a bigger rosette 28 DAS, but the overall plant phenotype clearly resembled *3xalyALY3* and not 4xaly plants.

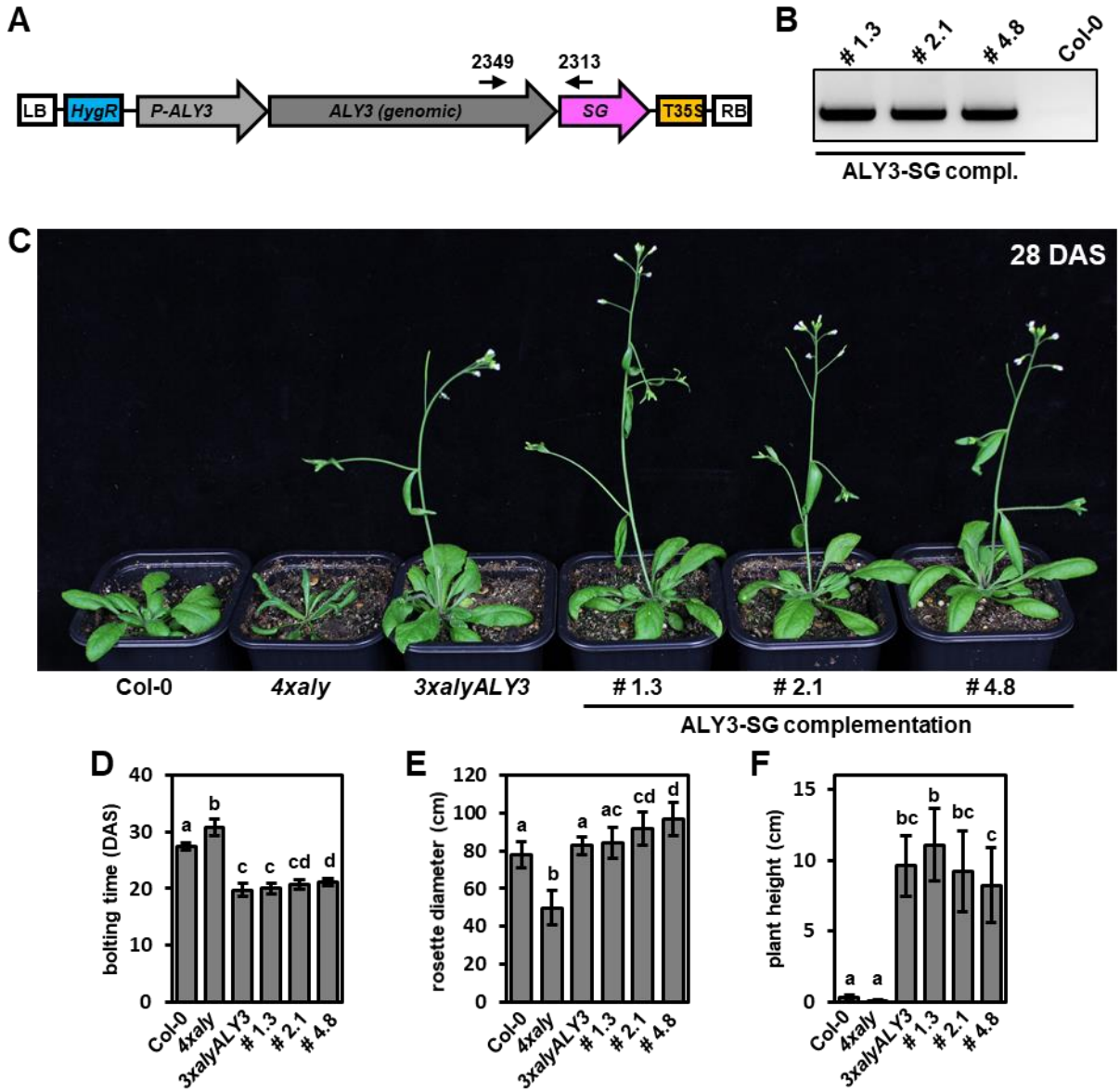

Figure 21. Expression of *ALY3-SG* can complement the *4xaly* phenotype. (A) Schematic illustration of the transgene inserted into the genome of *4xaly* to complement the phenotype. The expression of genomic *ALY3* was driven by the endogenous *ALY3* promotor. Primers used for genotyping (B) are indicated by black arrows. White boxes = left and right border, blue box = resistance marker hygromycin, light grey arrow = *ALY3* promotor, dark grey arrow = genomic *ALY3*, pink arrow = *SG* tag, yellow box = 35S termination UTR. Three independent lines (# 1.3, # 2.1, #, 4.8) homozygous for the inserted transgene were selected on MS plates supplemented with hygromycin and genotyped (B). (C) Phenotype of a representative plant of the three independent lines # 1.3, # 2.1, #, 4.8 compared to Col-0, *4xaly* and *3xalyALY3* 28 DAS. (D-E) Phenotypic analysis for (D) bolting time, (E) rosette diameter 28 DAS and (F), plant height 28 DAS. Error bars indicate SD of 15 plants. Data sets marked with different letters are significantly different as assessed by a multicomparison Tukey's test ($P < 0.05$) after one-way analysis of variance.

In recent years the iCLIP (individual-nucleotide resolution cross-linking and immunoprecipitation) method was successfully introduced for the use in plants (Meyer et al., 2017). Since the protocol developed by Meyer *et al*. uses the 'GFP-trap' (Chromotek) to specifically immunoprecipitate GFP-fused RNA binding proteins after UV crosslinking, it was also tested if ALY3-eGFP, after insertion of the respective transgene into the genome of *4xaly* by *A. tumefaciens* mediated transformation, could complement the *4xaly* phenotype (Figure 22 A). Three independent lines homozygous for the inserted transgene were selected on MS plates supplemented with hygromycin and the presence of the transgene was verified by PCR (Figure 22 B). The outcome of this complementation experiments was similar to the outcome of the above-mentioned experiments using ALY3-SG to complement the *4xaly* phenotype (Figure 21). Plants of three independent lines homozygous for the inserted transgene bolted around the same time as *3xalyALY3* and clearly earlier than *4xaly* plants showing that ALY3-eGFP could complement the phenotype of *4xaly* (Figure 22 C,D). The complementation could also be observed 28 DAS were plants of the three transgenic lines displayed similar rosette sizes and plant heights like *3xalyALY3* plants and overall clearly resembled the phenotype of *3xalyALY3* plants and not *4xaly* plants (Figure 22. C,E,F). Line #5.10 and #7.9 displayed some small differences compared to *3xalyALY3* with plants from line #5.10 bolted later and plants from line #7.9 were taller 28 DAS but the overall plant phenotype in these lines clearly resembled *3xalyALY3* and not *4xaly* plants.

In summary complementation experiments demonstrated that ALY-SG and ALY-eGFP fusion proteins are functional and future RNA immunoprecipitation experiments will show if transcripts use putative ALY specific mRNA export pathways.

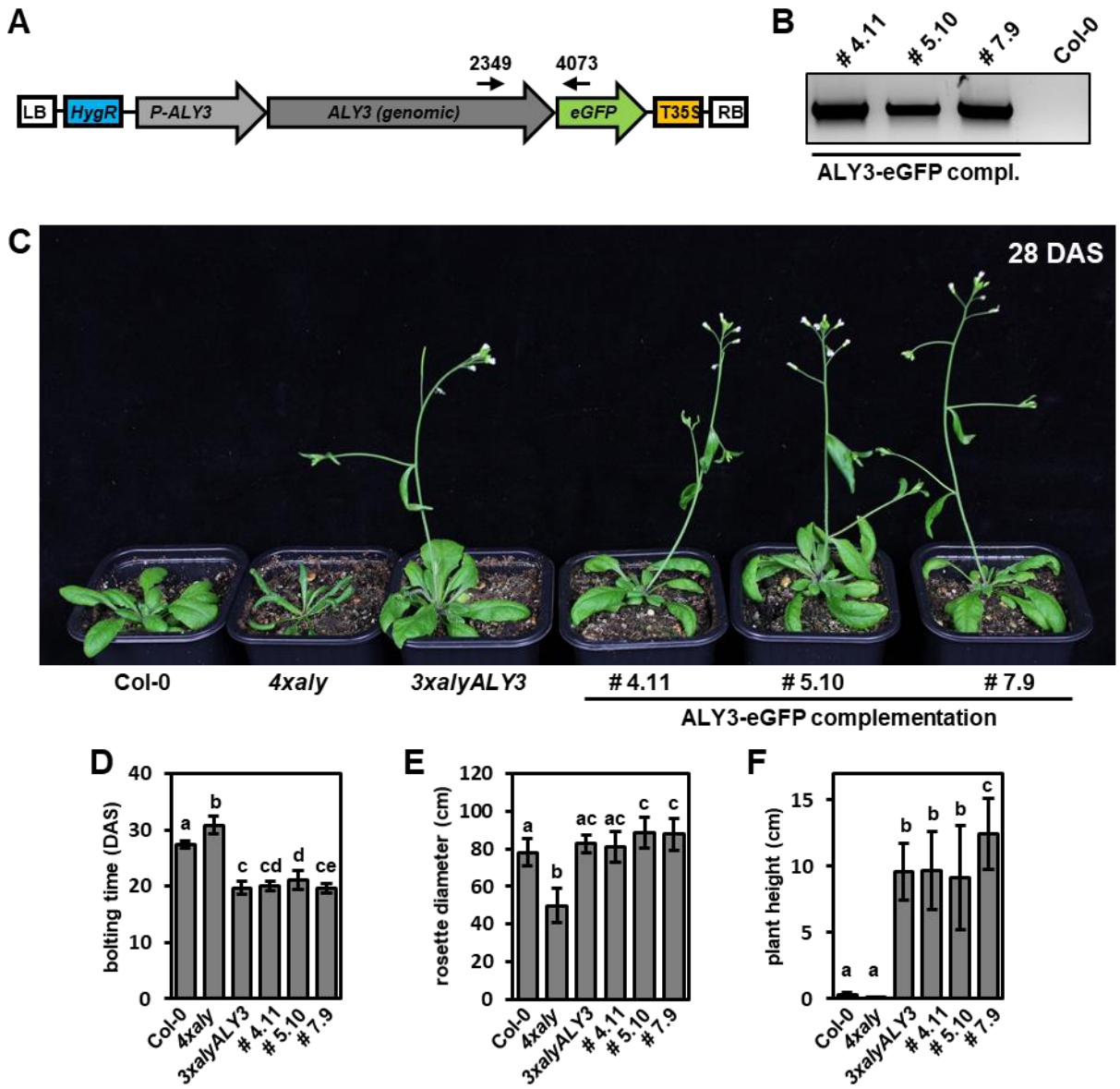

Figure 22. Expression of *ALY3-eGFP* can complement the *4xaly* phenotype. (A) Schematic illustration of the transgene inserted into the genome of *4xaly* to complement the phenotype. The expression of genomic *ALY3* was driven by the endogenous *ALY3* promotor. Primers used for genotyping (B) are indicated by black arrows. White boxes = left and right border, blue box = resistance marker hygromycin, light grey arrow = *ALY3* promotor, dark grey arrow = genomic *ALY3,* green arrow = *eGFP* tag, yellow box = 35S termination UTR. Three independent lines (# 4.11, # 5.10, #, 7.9) homozygous for the inserted transgene were selected on MS plates supplemented with hygromycin and genotyped (B). (C) Phenotype of a representative plant of the three independent lines # 4.11, # 5.10, #, 7.9 compared to Col-0, *4xaly* and *3xalyALY3* 28 DAS. (D-E) Phenotypic analysis for (D) bolting time, (E) rosette diameter 28 DAS and (F), plant height 28 DAS. Error bars indicate SD of 15 plants. Data sets marked with different letters are significantly different as assessed by a multicomparison Tukey's test ($P < 0.05$) after one-way analysis of variance.

2.2 Analysis of UIEF proteins as potential mRNA export factors

2.2.1. Two *Arabidopsis* proteins show sequence similarities to the human mRNA export factor UIF

By WISH it could be shown that ALY proteins act as export factors (Figure 11) and FRET experiments showed that they are recruited to the TREX complex by an interaction with the RNA helicase UAP56 (Figure 9). The severe phenotype displayed by *4xaly* plants further demonstrated that ALY proteins play a crucial role in mRNA export but on the other hand it showed, that apart from the ALY proteins other proteins can function as export factors regulating mRNA export sufficiently in the absence of the four ALY proteins so that plants can survive. This resembles more the situation in human cells, where over the last years several export factors were identified that can act redundantly, whereas in yeast the knockout of the *ALY* orthologue *Yra1* is lethal (Strässer and Hurt, 2000; Heath et al., 2016). Bioinformatical analysis of the *Arabidopsis* database (https://www.arabidopsis.org) using the BLAST algorithm revealed two proteins that both share around 18% amino acid identity with the human mRNA export adaptor UIF. As the term “UIF” is used in *Arabidopsis* for an unrelated protein, the two identified proteins were termed UIEF1 and UIEF2 (UAP56-INTERACTING EXPORT FACTOR1/2). The predicted amino acid sequences of UIEF1 (24.5 kD) and UIEF2 (22.3 kD) are 48.4% identical and both UIEF1 and UIEF2 share a putative N-terminal UAP56 binding motive (Ehrnsberger et al., 2019b, Figure 23).

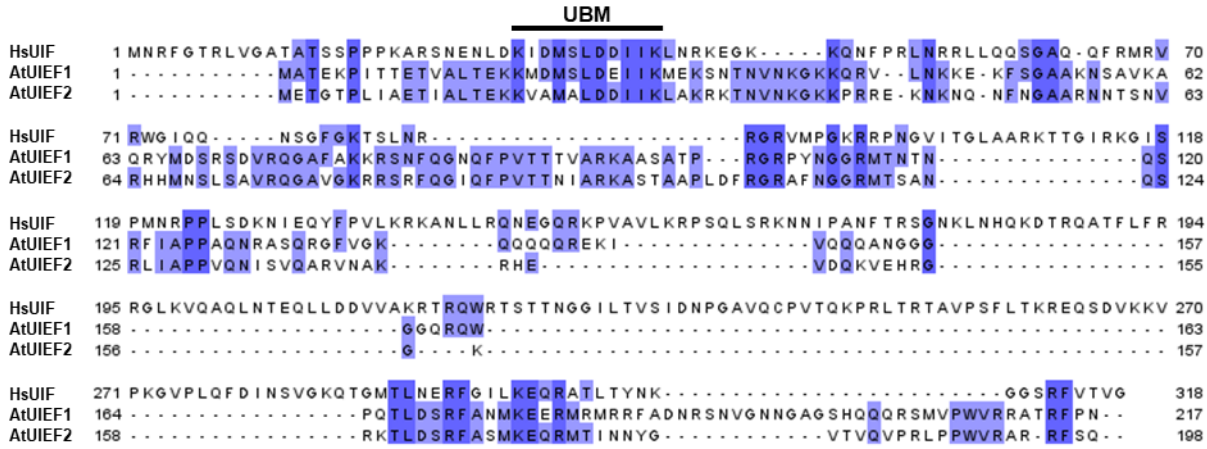

Figure 23. Two *Arabidopsis* proteins show aa sequence similarities to the human export adaptor UIF. The human UIF sequence was aligned to the sequences from the two *Arabidopsis* UIEF proteins. The predicted conserved N-terminal UAP56 binding motif is highlighted in black. Multiple sequence alignment was generated using Clustal Omega (Sievers et., 2011) and the conservation of amino acid residues is highlighted in blue using JalView (Waterhouse et., al 2009).

2.2.2. UIEF1 and UIEF2 directly interact with UAP56 in plant cells

To characterize the two UIEF proteins as possible export factors, it was first tested if both proteins are recruited to the mRNA export machinery by a direct protein-protein interaction with the RNA helicase UAP56, like demonstrated for the ALY proteins ALY1 and ALY3 (Figure 9). To investigate the protein-protein interactions of UIEFs and UAP56, *UIEFs* fused to *eGFP* were co-expressed with *UAP56* fused to *mCherry* as donor/acceptor pairs in *N. benthamiana* leaf cells and a possible direct protein-protein interaction was measured by Förster resonance energy transfer (FRET). Both UIEF1-eGFP and UIEF2-eGFP directly interacted with UAP56-mCherry demonstrated by mean FRET efficiencies of 8.5% (UIEF1) and 8.2% (UIEF2) whereas mean FRET efficiencies in leaf cells co-expressing UIEF1-eGFP or UIEF2-eGFP and unfused mCherry showed background levels (0.7% for UIEF1-eGFP/unfused mCherry and 0.3% for UIEF2-eGFP/unfused mCherry, Figure 24 B).

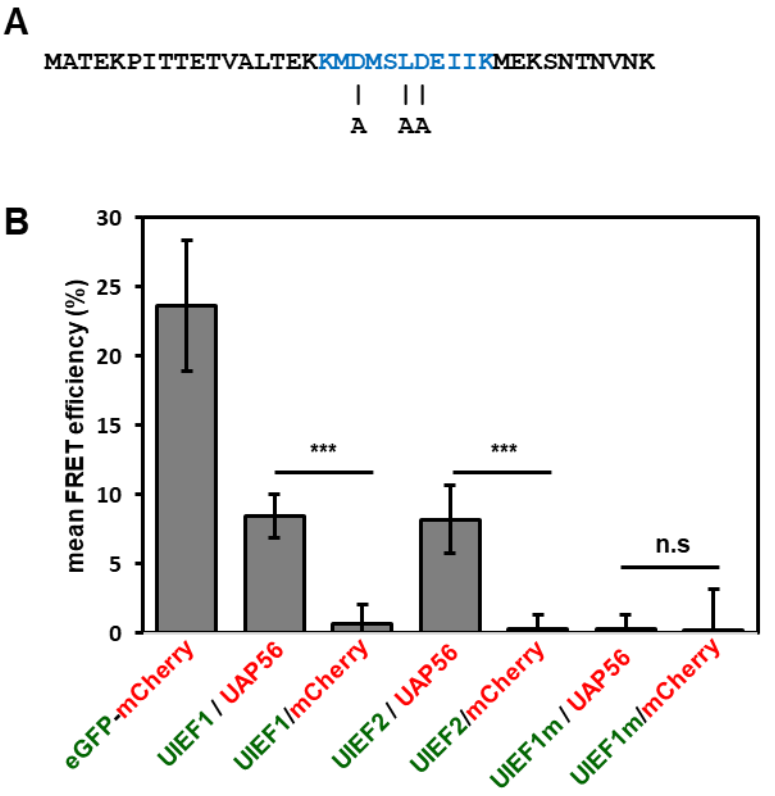

Figure 24. UIEF1 and UIEF2 directly interact with UAP56 through contact with the UBM in FRET experiments. (A) Three conserved amino acid residues of the UBM of UIEF1 were mutated to alanine to generate the mutated UIEF1m version. (B) FRET efficiencies were measured in *N. benthamiana* leaf cells co-expressing a donor (eGFP, UIEF1-eGFP, UIEF2-eGFP, UIEF1m-eGFP green) and an acceptor (mCherry, UAP-mCherry, red). FRET efficiencies measured in cells expressing an eGFP-mCherry fusion protein served as a positive control whereas FRET efficiencies measured in cells co-expressing UIEF1-eGFP, UIEF2-eGFP or UIEFm-eGFP and unfused mCherry served as a negative control. Mean FRET efficiencies were measured in 8 nuclei for each donor/acceptor pair. ***, Statistically significant difference assessed by Student's t test ($P < 0.001$).

Additionally, it was tested if the N-terminal UBM mediates the interaction with UAP56 by also analysing the interaction of UAP56 and an UIEF1 version (UIEF1m) where three conserved amino acid residues of the UBA motif were mutated (Figure 24 A). An UBA mediated direct protein-protein interaction of UIEF1 and UAP56 could be demonstrated as FRET efficiencies showed only background levels when the mutated version *UIEF1m-eGFP* was co-expressed with *UAP56-mCherry* (Figure 24 B). As a positive control a mean FRET efficiency of 23.7% was measured in leaf cells expressing an eGFP-mCherry fusion protein (Figure 24 B).

2.2.3. UIEF1 and UIEF2 are nuclear proteins

In yeast and metazoans, export adaptors are nuclear proteins that are stripped off mRNAs after recruiting the mRNA export receptor and before export competent mRNPs travel through the NPC to the cytosol (Stewart, 2010). To investigate the localization of UIEF1 and UIEF2 proteins within plant cells, roots of transgenic plants (Pfaff, 2017) expressing *UIEF1* and *UIEF2* fused to *GFP* under control of the endogenous promotor in the respective mutant background, were analysed by CLSM. Both UIEF1-GFP and UIEF2-GFP fusion proteins could be detected in all root cells and the GFP signal was restricted to nuclei, showing that both UIEFs are nuclear proteins (Ehrnsberger et al., 2019b, Figure 25).

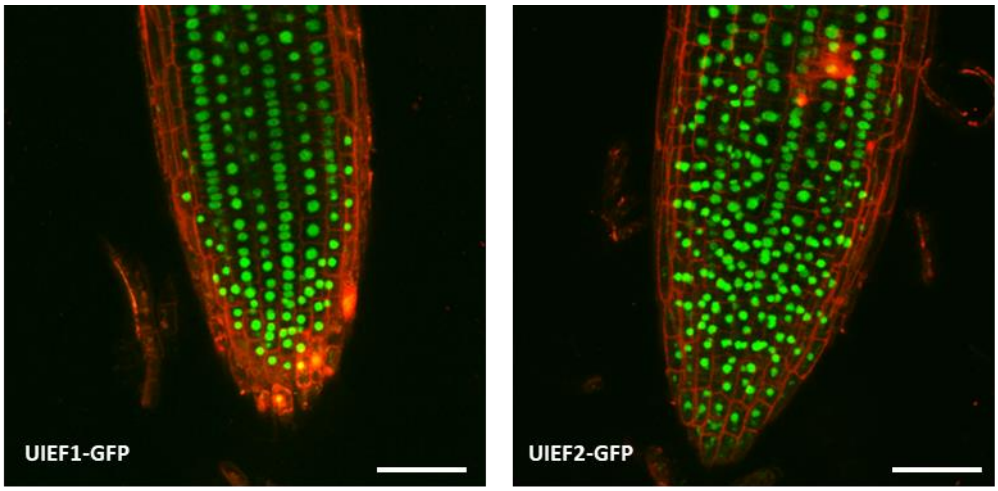

Figure 25. UIEF1 and UIEF2 are nuclear proteins. Root tips from 8 DAS transgenic plants expressing UIEF1-GFP or UIEF2-GFP in the respective mutant background analysed by CLSM. A green nuclear UIEF signal can be detected in all root cells while cell walls were stained with propidium iodide (red). Size bars = 50 µm

2.2.4.*4xaly 2xuief* plants display more pronounced plant growth and development defects than *4xaly* plants

To analyse the role of UIEF proteins during plant growth and development, *uief* T-DNA insertion mutant plants (Supplement S11) were phenotypically analysed und a potential defect in bulk mRNA export was examined by WISH. Homozygous *uief* single and double mutant plants displayed smaller rosettes at bolting (Figure 26 A,E; Supplement S13) and a reduced plant height 42 DAS (Figure 26 A,E; Supplement S13). Since *2xuief* plants do not show a strong phenotype, *4xaly* and *2xuief* plants were crossed and a homozygous mutant plant was identified in the next generations lacking all four ALY and the two UIEF proteins, that in the following is referred to as *4xaly 2xuief* (Hachani, 2018). In addition to the phenotypical alterations of *uief* single and double mutant plants strong evidence for the involvement of UIEF proteins in mRNA export can be considered when these sextuple mutant plants display more pronounced plant growth and development defects than *4xaly* mutant plants.

To analyse if *4xaly 2xuief* plants display more pronounced plant growth and development defects, Col-0, *2xuief*, *4xaly* and *4xaly 2xuief* plants were phenotypically analysed (Figure 26). An additive effect of *aly* and *uief* mutations on plant growth and development could be observed at 28 DAS since at this developmental stage *4xaly 2xuief* plants showed a reduced average rosette size compared to *4xaly* (Figure 26 A,E). Also later in plant development at 42 DAS, *4xaly 2xuief* plants were smaller compared to *4xaly* mutant plants although this difference was not significant (Figure 26 B,F). Other traits like root length 8 DAS or bolting time were not different in *4xaly 2xuief* and *4xaly* (Figure D,G).

To investigate if *uief* mutations cause mRNA export defects, mRNA export assays were performed.

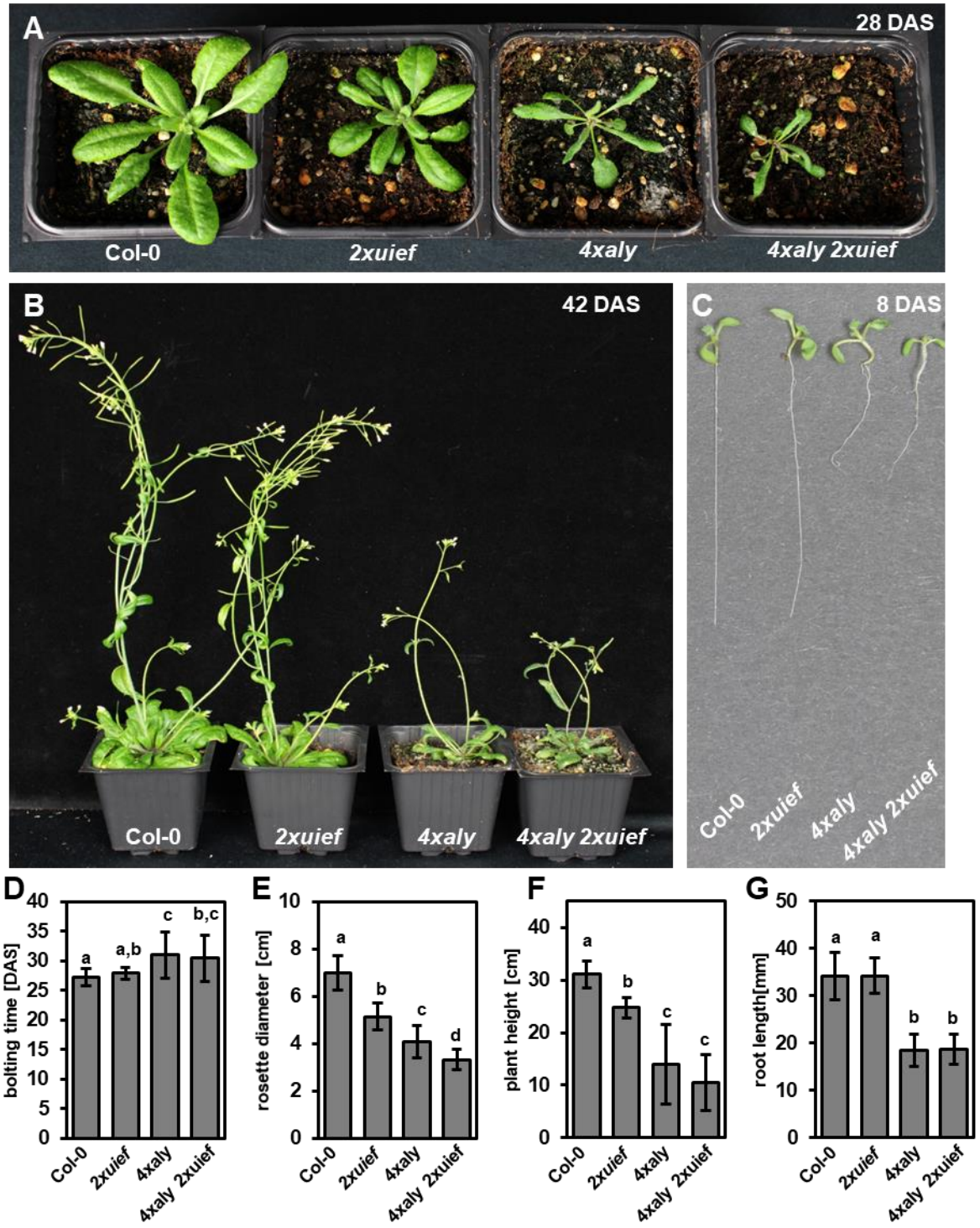

Figure 26. ***4xaly 2xuief*** **plants display more pronounced plant growth and development defects than** ***4xaly*** **plants.** Phenotype of *2xuief, 4xaly* and *4xaly 2xuief* plants compared to Col-0 at 28 DAS (A) and 42 DAS (B) *4xaly 2xuief* plants show no altered root length at 8 DAS compared to *4xaly* (C). (D-G) Phenotypic analysis for (D) bolting time, (E) rosette diameter at bolting, (F) plant height 42 DAS and (G) root length 8 DAS. Error bars indicate SD of 15 plants Data sets marked with different letters are significantly different as assessed by a multicomparison Tukey's test ($P < 0.05$) after one-way analysis of variance.

2.2.5. *4xaly 2xuief* plants show stronger mRNA export block than *4xaly* plants

WISH mRNA export assays like described in figure 11 performed in *uief* single and double mutant plants showed that mutations of *uief1* and/or *uief2* results in a moderate, but still significant mRNA export block (Supplement S12). Additionally, WISH in Col-0, *2xuief*, *4xaly* and *4xaly 2xuief* roots showed an additive effect of *aly* and *uief* mutations on bulk mRNA export (Figure 27). In all mutant lines an mRNA export block was detected with the highest nuclear/cytosol signal ratio measured in *4xaly 2xuief* and the lowest nuclear/cytosol signal ratio measured in *2xuief,* showing that the strength of the mRNA export defect is increasing from *2xuief* < *4xaly* < *4xaly 2xuief* (Figure 27 B).

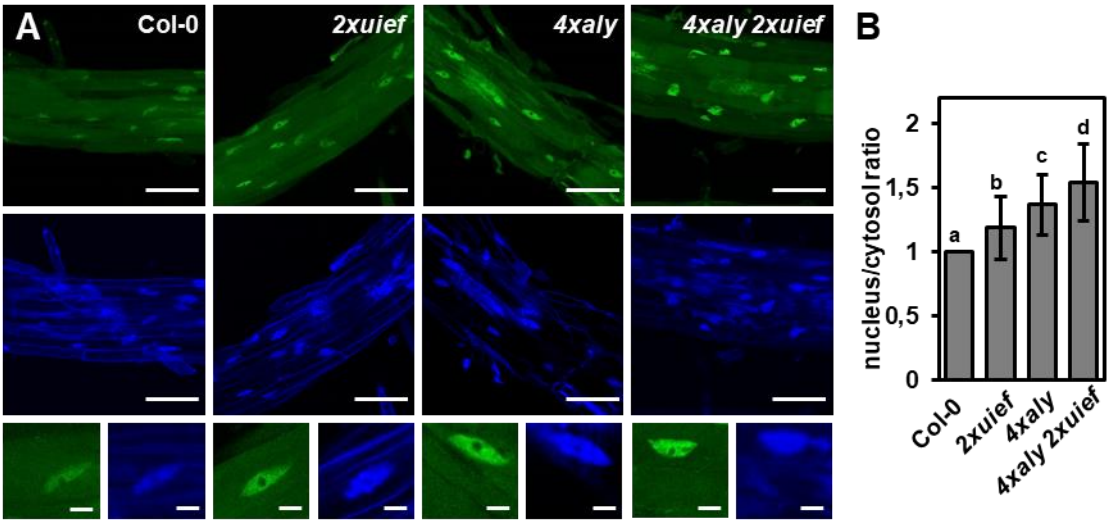

Figure 27. ***4xaly 2xuief*** **plants show strongest mRNA export block.** (A) CLSM images from representative sections from roots of Col-0, *2xuief, 4xaly* and *4xuief 2xaly* plants after WISH with the Alexa Fluor 488 oligo (dT) signal in green and DAPI signal in blue. Bars = 60 µm (top rows) and 10 µm (bottom row). (B) Average nuclear/cytosol signal ratio of 50 or more nuclei per genotype. The ratios are shown relative to Col-0 (ratio of 1), with error bars indicating SD. Data sets marked with different letters are significantly different as assessed by a multicomparison Tukey's test ($P < 0.001$) after one-way analysis of variance.

In summary the interaction of UIEF proteins and UAP56, the nuclear localization of UIEF proteins and the phenotypic analysis and mRNA export assays performed on *uief* single and double mutants strongly indicated that UIEF proteins are involved in mRNA export. Since a generated sextuple mutant lacking all four ALY and the two UIEF proteins showed more pronounced plant growth and development defects and a stronger mRNA export block than *4xaly* it could be shown that UIEF proteins act as mRNA export factors. Indirectly these experiments also showed, that the situation in plants resembles the situation in human cells where several export adaptors can act redundantly (Heath et al., 2016) since *4xaly 2xuief* mutant plants are still viable, although they are severely affected in plant growth and development and show a strong mRNA export block.

2.2.6. Identification of ALY and UIEF export targets

In the previous chapters it was described that in *Arabidopsis* four ALY proteins and two UIEF proteins act as mRNA export factors. In human cells it could be shown that ALY and UIF proteins act redundantly, since only a knockdown of both factors causes a bulk mRNA export block (Hautbergue et al., 2009). In the following it was tested by transcript profiling if there are transcripts that potentially are exported by ALY and UIF proteins. Additionally, RNAseq should reveal candidates that potentially are specifically exported by ALY or UIEF proteins.

RNAs from *2xuief* and *4xaly 2xuief* plants were extracted and sequenced in the course of the transcript profiling experiment comparing the transcriptomes of four different *3xaly* mutants and *4xaly* (Figure 19). *2xuief, 4xaly* and *4xaly 2xuief* plants were grown simultaneously, RNAs were extracted simultaneously and sequencing was performed at the same run making a comparative analysis of *2xuief*, *4xaly* and *4xaly 2xuief* transcriptomes possible.

Like described in chapter 2.1.8 it was assumed that a reduced transcript level in the three export mutants is mainly caused by an mRNA export defect with the same threshold of log2 fold change < -1 set to describe candidates that were not properly exported in the respective mutant. In general, a similar misregulation in *4xaly 2xuief* and *4xaly* could be observed with 1053 genes that give rise to 1263 transcripts being downregulated with a log2 fold change < -1 in *4xaly 2xuief* (Figure 28 B). About 70% of transcripts that were reduced in *4xaly 2xuief* were also reduced in *4xaly.* In *2xuief* on the other hand the misregulation of genes was by far less distinct since only 585 genes that give rise to 637 transcripts were downregulated (Figure 28 B).

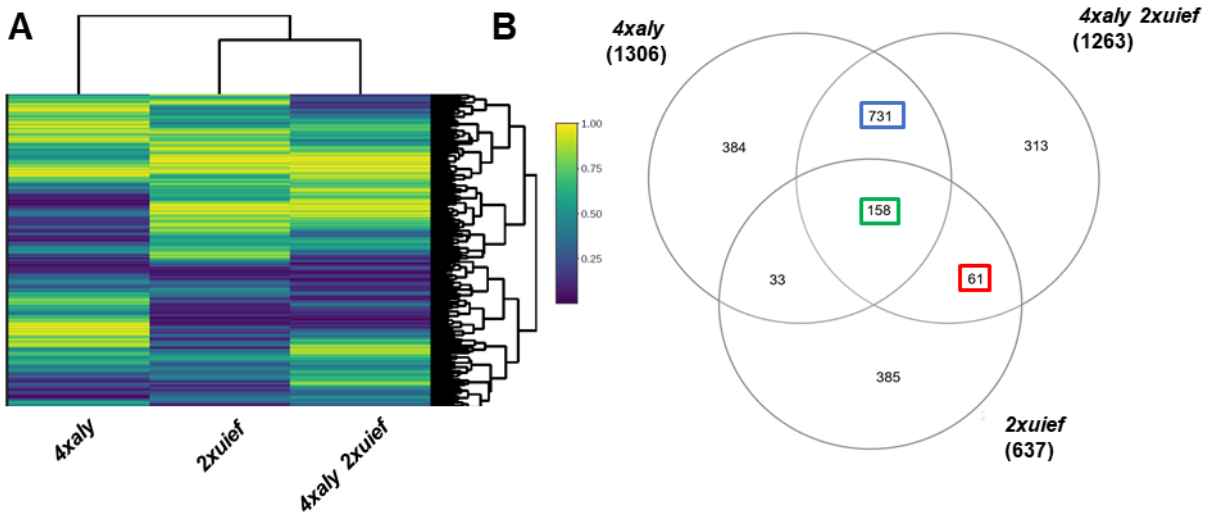

Figure 28. RNAseq of *2xuief*, *4xaly* and *4xaly 2xuief* mutant plants. (A) Gene expression in *2xuief*, *4xaly and 4xaly 2xuief* mutant plants detected by RNAseq and visualized as a heatmap. Genes downregulated are depicted in blue with dark blue indicating the strongest downregulation whereas yellow shows upregulated genes. Hierarchical clustering of expressed genes is shown on the right and hierarchical clustering of genotypes is shown above the heatmap. (B) Venn diagram of genes downregulated > 2-fold in the three genotypes with genes highlighted in blue representing genes that are downregulated in *4xaly* and *4xaly 2xuief*, in red genes that are downregulated in *4xaly 2xuief* and *2xuief* and in green genes that are downregulated in all genotypes.

To identity candidates that potentially are exported by ALY proteins and not by UIEF proteins, transcripts were selected that were not misregulated in *2xuief* but downregulated in *4xaly* and *4xaly 2xuief*. In total 731 mRNAs highlighted in blue in figure 32 B could be grouped into this category showing that the loss of all four ALY proteins results in a potential defective export of a variety of transcripts.

In a second group, candidates were included that could be specifically exported by UIEF proteins indicated by a downregulation in *2xuief* and *4xaly 2xuief* whereas transcript levels in *4xaly* were not reduced to this extend (log2 fold change > -1). Compared to the candidates potentially exported by ALY proteins, this group of transcripts is rather small with only 61 mRNAs fulfilling the criteria.

In a last group that was further analysed, candidates were pooled that potentially are exported by both ALY and UIEF proteins. In total, transcript levels of 158 mRNAs were reduced in all three mutant plant lines and candidates were selected for qRT-PCR analysis that showed the strongest downregulation in *4xaly 2xuief* (Figure 28 B). The strongest reduction in transcript levels in *4xaly 2xuief* would point to some functional redundancy between ALY and UIEF proteins.

For every group two candidates were selected to validate the RNAseq results by qRT-PCR with i) two candidate genes highlighted in blue in table 3 that give rise to transcripts that should be exported by ALY proteins only, ii) two candidate genes highlighted in red that give rise to transcripts that should be exported by UIEF proteins only and iii) two candidate genes

highlighted in green that give rise to transcripts that should be exported by ALY and UIEF proteins. For the second group comprising the candidates that potentially are specifically exported by UIEF proteins, only suboptimal candidates that were also reduced in *4xaly* according to the RNAseq results (-1.36-fold change and -1.26-fold change) could be selected, because the great majority of the 61 candidates were also downregulated to some extent in *4xaly.*

Table 3. Candidate genes differentially downregulated in *2xuief*, *4xaly* and *4xaly 2xuief* mutants used to verify RNAseq data by qRT-PCR. Candidate genes were selected from groups of genes highlighted in Figure 28 B with two genes highlighted in blue downregulated in the *aly* mutants *4xaly* and *4xaly 2xuief* genotypes according to RNAseq, two genes highlighted in red downregulated in the *uief* mutants *2xuief* and *4xaly 2xuief* and two genes highlighted in green downregulated in all mutant genotypes.

AGI	*2xuief*		*4xaxly*		*4xaly 2xuief*	
	Fold change		Fold change		Fold change	
	RNAseq	qPCR	RNAseq	qPCR	RNAseq	qPCR
AT2G29310	-1.26	-1.14	-3.10	-2.59	-3.14	-2.56
AT1G60140	1.17	1.33	-2.91	-2.36	-2.38	-2.04
AT3G06145	-2.75	-1.96	-1.36	-1.39	-2.04	-1.80
AT2G44910	-3.46	-4.74	-1.26	-2.22	-2.20	-3.49
AT4G04840	-2.75	-2.10	-3.73	-3.82	-5.35	-3.97
AT5G51720	-2.95	-3.65	-8.22	-9.43	-11.39	-11.09

qRT-PCR confirmed the downregulation of transcripts when all four ALY proteins are lost. The two candidates AT2G29310 and AT1G60140 were downregulated in *4xaly* and *4xaly 2xuief* with fold changes < -2 in RNAseq and qRT-PCR experiments whereas transcript levels were not reduced in *2xuief* (Figure 29 A, Table 3).

For candidates that were only downregulated when plants lack the two UIEF proteins on the other hand, qRT-PCR could not unequivocally confirm that there are transcripts that potentially are specifically exported by UIEF export factors. Like mentioned above, candidates used for qRT-PCR validation were also downregulated in *4aly* to some extent and qRT-PCR revealed that the downregulation in *4xaly* is even higher (Table 3). Even though transcript levels of the candidates AT3G06145 and AT2G44910 were stronger reduced in *2xuief* and *4xaly 2xuief* compared to *4xaly,* no statistical differences were obtained between these genotypes (Figure 29 B.

qRT-PCR on the candidates AT4G04840 and AT5G51720 showed that there are transcripts whose functional mRNA export potentially depends on UIEF and ALY proteins (Figure 29 C). Both candidates were downregulated in all mutant genotypes with a stronger downregulation

in *4xaly* and *4xaly 2xuief* compared to *2xuief*. RNAseq results showed for AT4G04840 and AT5G51720 a downregulation of -3.72-fold and -8.22-fold in *4xaly* and a downregulation of -5.35-fold and -11.39-fold in *4xaly 2xuief* indicating an additive effect of *uif* and *aly* mutations. This additive effect pointing to some partial redundancy between UIEF and ALY proteins was detected by qRT-PCR only to a small extent. Almost no differences in the downregulation of AT4G04840 between *4xaly* and *4xaly 2xuief* were detected and for AT5G51720 the transcript level was reduced -9.43-fold in 4xaly and -11.09-fold in *4xaly 2xuief*, but this difference was not significant (Figure 29 C).

Transcriptome profiling of *2xuief*, *4xaly* and *4xaly 2xuief* demonstrated that the concerted knockdown of four *ALY* export factors has a stronger effect on transcript levels as the concerted knockdown of two *UIEF* export factors. The experiments further demonstrated that there is a variety of transcripts that are downregulated when all ALY proteins are missing and that there is a group of transcripts that is downregulated when ALY and/or UIEF factors are lost.

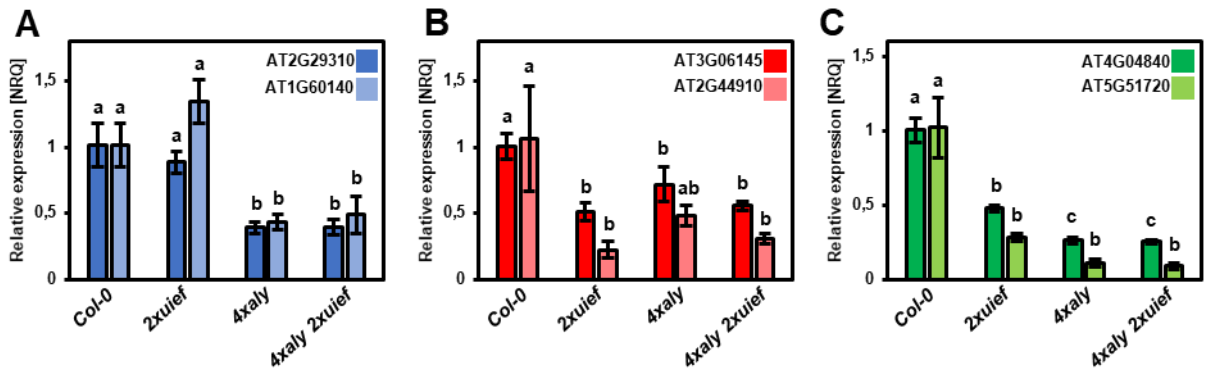

Figure 29. Validation of RNAseq data by qRT-PCR in *2xuief*, *4xaly* and *4xaly 2xuief* mutants. Relative expression of genes listed in table 3 was determined in *2xuief*, *4xaly* and *4xaly 2xuief* mutants relative to Col-0 using three biological and two technical replicates. The normalized relative quantities (NRQ) and the normalized relative standard errors are shown. The NRQ was determined by normalization to the NRQs of *GAP*, *PP2AA3* and *ACTIN2* mRNA. (A) shows genes downregulated in the *aly* mutants *4xaly* and *4xaly 2xuief* according to RNAseq, (B) genes downregulated in the *uief* mutants *2xuief* and *4xaly 2xuief* and (C) genes downregulated in all mutants. Differences in NRQ among genotypes is indicated by different letters as assessed by a multicomparison Tukey's test ($P < 0.05$) after one-way analysis of variance.

2.3. Identification and characterization of *Arabidopsis* mRNA export receptor candidates

2.3.1. Export factors interact with proteins that share features of the human mRNA export receptor NXF1

In human cells, ALY and UIF proteins are export adaptors that bind to the heterodimeric export receptor NXF1/NXT1 and thereby enhance the RNA binding affinity of NXF1/NXT1. (Hautbergue et al., 2009; Viphakone et al., 2012). The final step of mRNA export is initiated by NXF1/NXT1 guiding mRNAs to and through the NPC (Stewart, 2010). In plants no proteins with similarities to the main export receptor subunit NXF1 or its orthologues from other organisms can be identified (Pendle et al., 2005) so it is not clear what factor(s) mediate the translocation through the NPC in plants. In this study four ALY proteins and two UIEF proteins were described as export factors that share characteristics with their human counterparts. Thus, if the basic mechanism of mRNA export is conserved, ALY and/or UIEF proteins are most likely also involved in recruiting the plant mRNA export receptor(s). Therefore, a global screen for possible interaction partners of the four Arabidopsis ALYs and two Arabidopsis UIEF proteins was performed by using the combination of affinity purification and mass spectrometry (AP-MS, Pfab et al 2017).

To screen for possible plant mRNA receptor candidates, the six identified export factors were expressed in PSB-D *Arabidopsis* cell suspension cultures under control of the 35S promotor and C-terminally fused to a SG tag consisting of a streptavidin binding protein, a TEV cleavage site and two domains Protein G (Figure 30 A). In a one-step affinity purification (AP) procedure protein G of the tagged bait proteins bound to IgGs coupled to magnetic beads and by that direct interaction partners (blue) and indirect interaction partners (yellow) could be co-purified with the bait proteins (Figure 30 B). To exclude that an interaction is mediated by DNA or RNA binding, cell extracts were treated with the endonuclease benzonase that degrades all forms of DNA and RNA. Bait proteins and co-purified interactors were further subjected to SDS-PAGE, stained with Coomassie Blue (Figure 30 C) and after in-gel trypsin digest interactors were analysed by mass spectrometry (MS). All AP-MS experiments were performed in three replicates and proteins were considered being true interactors when they were identified in two out of three affinity purifications with a MASCOT score (measure for reliability of the detection) ≥ 80. Proteins identified two out of three times in the negative unfused SG control with a MASCOT score higher than 80 were considered being unspecific interactors and were removed from the true interactor list. Additionally, co-purified proteins were compared with a list of nonspecific interactors (Van Leene et al., 2015) that were identified in 543 TAP experiments from PSB-D cells using 115 different bait proteins. The list of all true interactors in the six affinity purification experiments is depicted in Supplement S14.

When analysing cells expressing the export factors ALY1, ALY2 or UIEF1 fused to SG, reproducibly more bait proteins and more putative interactors were co-purified compared to cells expressing ALY3-SG, ALY4-SG and UIEF2-SG, visible by the staining of more bands with higher intensities (Figure 30 C). In the negative control besides the unfused SG protein few proteins were visible by SDS-PAGE. These observations could be confirmed my mass spectrometry that revealed 99 true interactors for ALY1-SG, 118 for ALY2-SG, 97 for UIF1-SG, 85 for ALY3-SG, 42 for ALY4-SG and 71 for UIEF2-SG.

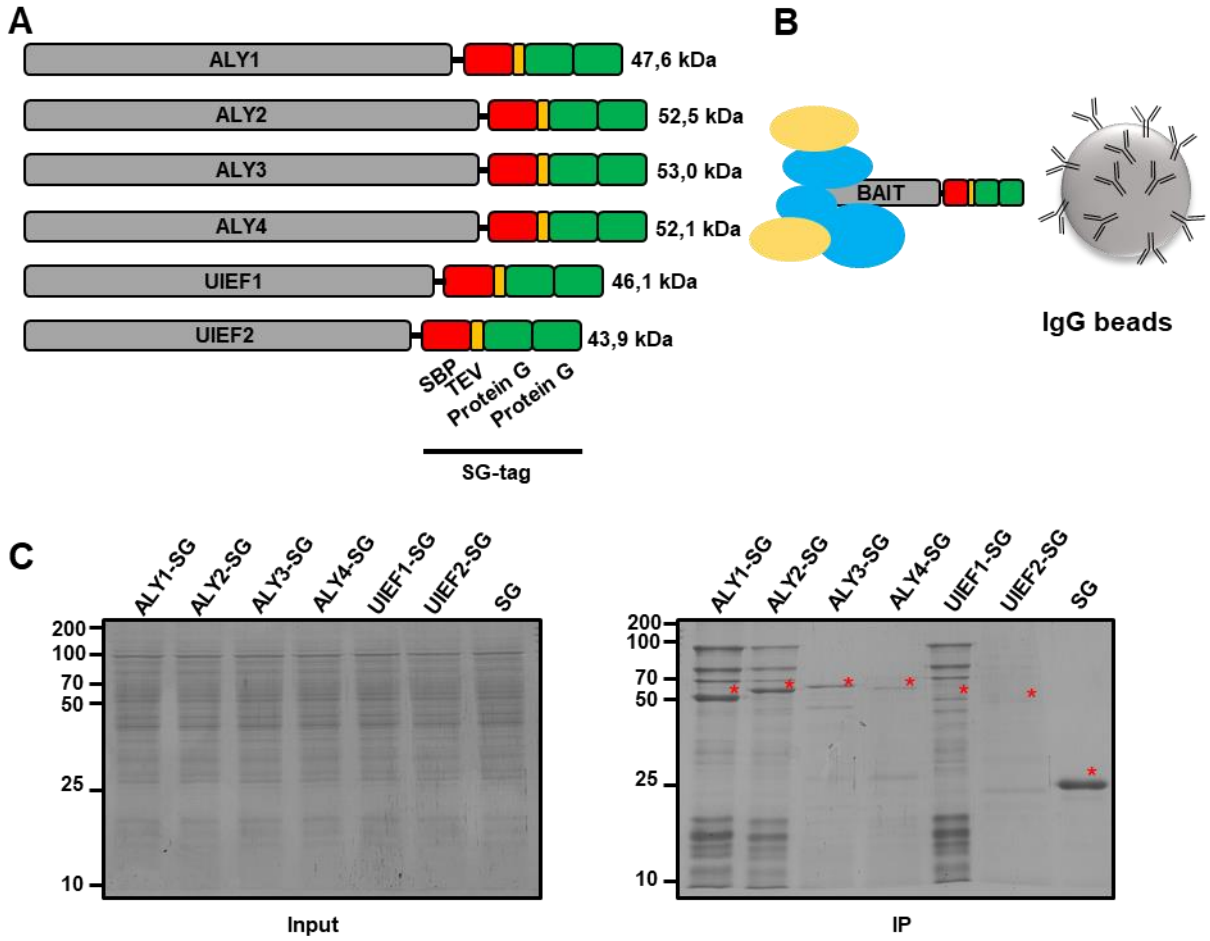

Figure 30. AP-MS analysis to screen for interactors of plant mRNA export factors. (A) Four ALY and two UIEF proteins were expressed in *Arabidopsis* cell suspension culture C-terminally fused to a SG tag composed of a streptavidin binding protein (SBP), a TEV cleavage site and two domains Protein G. Predicted molecular weights were calculated by ExPaSy pI/Mw tool. (B) Affinity purification by binding of Protein G domains of the SG tag to IgG coupled to magnetic beads. Direct interactors of the bait protein are depicted in blue and indirect interactors in yellow. (C) Proteins were separated by SDS-PAGE and stained by Coomassie Blue. Left panel shows input used for affinity purification of the cell suspension lines transformed with the six export factor-SG transgenes driven by a 35S promotor and the cell suspension line that was transformed with unfused SG driven by a 35S promotor that served as a negative control. Right panel shows co-purifying proteins after affinity purification with red asterisks marking the respective SG-tagged bait protein. Molecular weights are depicted in kDa.

When analysing the co-purified proteins of the six export factors identified by MS, it was focused on the one hand if factors of the TREX complex co-purified with the six export factors

and on the other hand it was screened for proteins that share features with the heterodimeric mRNA export receptor NXF1/NXT1 (Mex67/Mtr2) that is conserved in other eukaryotes.

The analysis of the AP-MS results revealed potential interactions between different export factors but no other TREX subunits could be co-purified in any of the six AP-MS experiments, indicating that ALY and UIEF export factors are not stably linked to the other TREX subunits (Table 4). The export factors ALY1, ALY2 and ALY4 were also detected two out of three times in the unfused SG negative control with average MASCOT scores of 131, 185 and 158 respectively, what causes problems in the interpretation of the results. Even though several detected co-purifications between export factors are potentially unspecific, some of these factors may be true interactors. A specific co-purification can be assumed between UIEF1 and ALY3 since both proteins were not detected in the free SG negative control and ALY3 was detected with a high average MASCOT score of 857 in all three UIEF1-SG experiments. Additionally, a specific co-purification between ALY3 and the other three ALY proteins can be assumed since ALY3 was detected in all nine ALY1-SG, ALY2-SG and ALY4-SG AP-MS experiments.

Table 4. Seven candidates with a characteristic NTF2L domain co-purify with export factors. (A) Six ALY and UIEF export factors fused to a SG tag were used as bait proteins for co-IP experiments. Besides an interaction among the export factors an interaction with seven candidates (NXF1-NXF7) that comprise a characteristic NTF2L domain was detected. The numbers indicate the respective MASCOT score of the identified interactor and how many times the interactor was identified in three independent experiments. A protein was only considered to be a true interactor when identified in at least in two out of three experiments. In the last row interactors and corresponding MASCOT score are listed that were identified in the unfused SG negative control.

AGI	Protein	ALY1-SG	ALY2-SG	ALY3-SG	ALY4-SG	UIEF1-SG	UIEF2-SG	SG
AT5G59950	ALY1	2269/ 3	429/ 3	145/ 3		476/ 2	182/ 2	131/ 2
AT5G02530	ALY2	320/ 2	1337/ 3	214/ 3	277/ 3			185/ 2
AT1G66260	ALY3	499/ 3	463/ 3	2749/ 3	177/ 3	420/ 3		
AT5G37720	ALY4	910/ 3	893/ 3	956/ 3	1995/ 3	857/ 3	361/ 2	158/ 2
AT4G10970	UIEF1	120/ 2	87/ 2			1448/ 3		
AT4G23910	UIEF2						1335/ 3	
AT5G43960	NXF1			1491/ 2				
AT5G60980	NXF2	2497/ 3	2963/ 3	636/ 3	398/ 3	2711/ 3	395/ 3	137/ 2
AT3G25150	NXF3	1121/ 3	1346/ 3			1388/ 3		
AT5G48650	NXF4	1124/ 3	1867/ 3	472/ 3	157/ 3	1218/ 3		97/ 2
AT1G69250	NXF5	1153/ 3	1293/ 3	248/ 2		1531/ 3		
AT1G13730	NXF6	2840/ 3	2584/ 3			3307/ 3	147/ 2	
AT2G03640	NXF7	359/ 3	447/ 3			380/ 3		167/ 3

Searching for *Arabidopsis* mRNA export receptor candidates, the AP-MS results revealed seven proteins that form a subgroup of the 19 NTF2L proteins listed in the database (www.uniprot.org, figure 31). All seven proteins display besides an NTF2L domain a C-terminal predicted RRM motif. In other eukaryotes, the big subunit of the heterodimeric mRNA export receptor (NXF1 in metazoans, Mex67 in yeast) is composed of an N-terminal region mediating contact with mRNAs (RRM in yeast, RBD and RRM in metazoans), an LRR domain, an NTF2L domain and a C-terminal UBA domain (Heath et al., 2016). Since all seven identified

candidates share the two domains RRM and NTF2L with the metazoan NXF1, it was hypothesised that they might also have similar functions and in the following these seven proteins are referred to as NXF1-NXF7. A similar problem like seen when analysing putative interactions of different export factors arises, since the three export receptor candidates NXF2, NXF4 and NXF7 were also detected in the unfused SG negative control, making it difficult to draw conclusions when these factors were detected by MS. But compared to the potential unspecific interactions between some export factors, a detection of especially NXF2 and NXF4 in several AP-MS experiments with very high MASCOT scores compared to the MASCOT scores of the detection in the negative control is a strong indication that the co-purifications between export factors and both NXF2 and NXF4 are potentially specific (Table 4). NXF2 for instance was detected in all ALY1-SG, ALY2-SG and UIEF1-SG AP-MS experiments with average MASCOT scores of 2497, 2963 and 2711 respectively, what displays more than an 18-fold higher MASCOT score than the detection in the negative control. Accordingly, NXF4 was detected in all ALY1-SG, ALY2-SG and UIEF1-SG AP-MS experiments with an average MASCOT score more than 11-fold higher than in the negative control. Other NXF candidates that were not detected in the negative control co-purified with different export factors. NXF1 was detected only in the ALY3-SG experiment, NXF3 in ALY1-SG, ALY2-SG and UIEF1-SG, NXF5 in ALY1-SG, ALY2-SG, ALY3-SG and UIEF1-SG and NXF6 in ALY1-SG, ALY2-SG, UIEF1-SG and UIEF2-SG.

AP-MS experiments revealed that seven mRNA export receptor candidates co-purified with ALY and UIEF export factors. In the following the influence of the seven candidates on plant growth and development was investigated by a reverse genetic approach analysing *nxf* knockout plants. It was further studied where NXF proteins are located within plant cells and whether the loss of NXF factors causes defects in mRNA export.

2.3.2. Plant NXF1-like candidates share characteristic NTF2-like domain

The seven mRNA export receptor candidates that co-purified with different mRNA export factors share an N-terminal NTF2L domain that is characteristic for both subunits of the human heterodimeric export receptor NXF1/NXT1 and that mediates the contact between these two proteins (Valkov et al., 2012). Additionally, the seven identified candidates share a predicted RNA recognition motif and display several RG and RGG motifs at their C-terminal ends that potentially mediate contact to mRNAs.

The seven identified candidates are part of a group of 19 *Arabidopsis* proteins containing a NTF2L domain. Three proteins of this group are small proteins of ~ 15 kDa that comprise an NTF2L domain only and by that resemble the small subunit of the export receptor NXT1 (Mtr2 in yeast, Figure 31). Besides the seven identified candidates, At3G07250 is the only additional

RRM containing NTF2L protein with three predicted C-terminal RRMs. All other NTF2L containing proteins comprise one or two NTF2L domains but are otherwise heterogenous in domain composition.

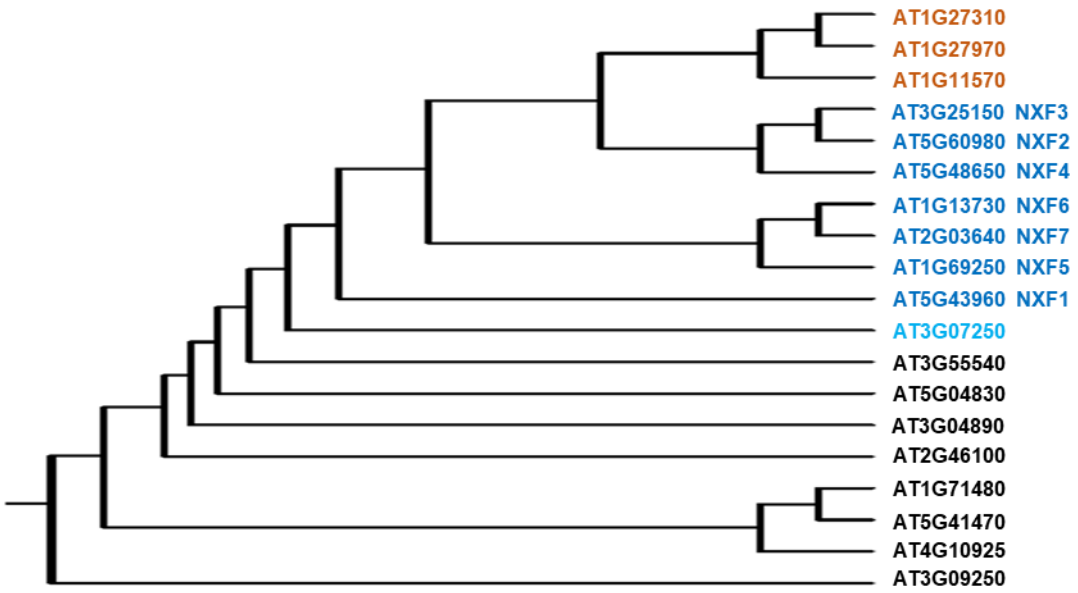

Figure 31. In *Arabidopsis* 19 proteins contain NTF2L domains. In *Arabidopsis* 8 proteins highlighted in blue display an NTF2L domain and RRM motifs with the seven candidates identified by AP-MS highlighted in dark blue. Additionally 11 proteins display an NTF2L domain but no RRMs with three proteins consisting of an NTF2L domain only highlighted in brown. Tree was generated using Clustal Omega (Sievers et., 2011).

Within the NXF candidates, NXF2, NXF3 and NXF4 can be grouped according to sequence similarities as well as NXF5, NXF6 and NXF7, whereas NXF1 has less similarities to the other candidates (Figure 31).

The sequence alignment of the seven NXF candidates illustrates the conserved N-terminal NTF2L domain and the RRM that is conserved in all candidates towards the C-terminus (Figure 32). Besides these two conserved regions, in all seven proteins RG and RGG motifs, that are known to mediate the binding of proteins to RNA (Thandapani et al., 2013), can be found at the C-terminal regions of the proteins. The most RG and RGG motifs are found in NXF1 and NXF2 with NXF1 comprising 6 RG and 3 RGG motifs and NXF2 comprising 3 RG and 7 RGG motifs. NXF5 on the other hand is the candidate with the least predicted RNA binding ability with only one RG motif being detected.

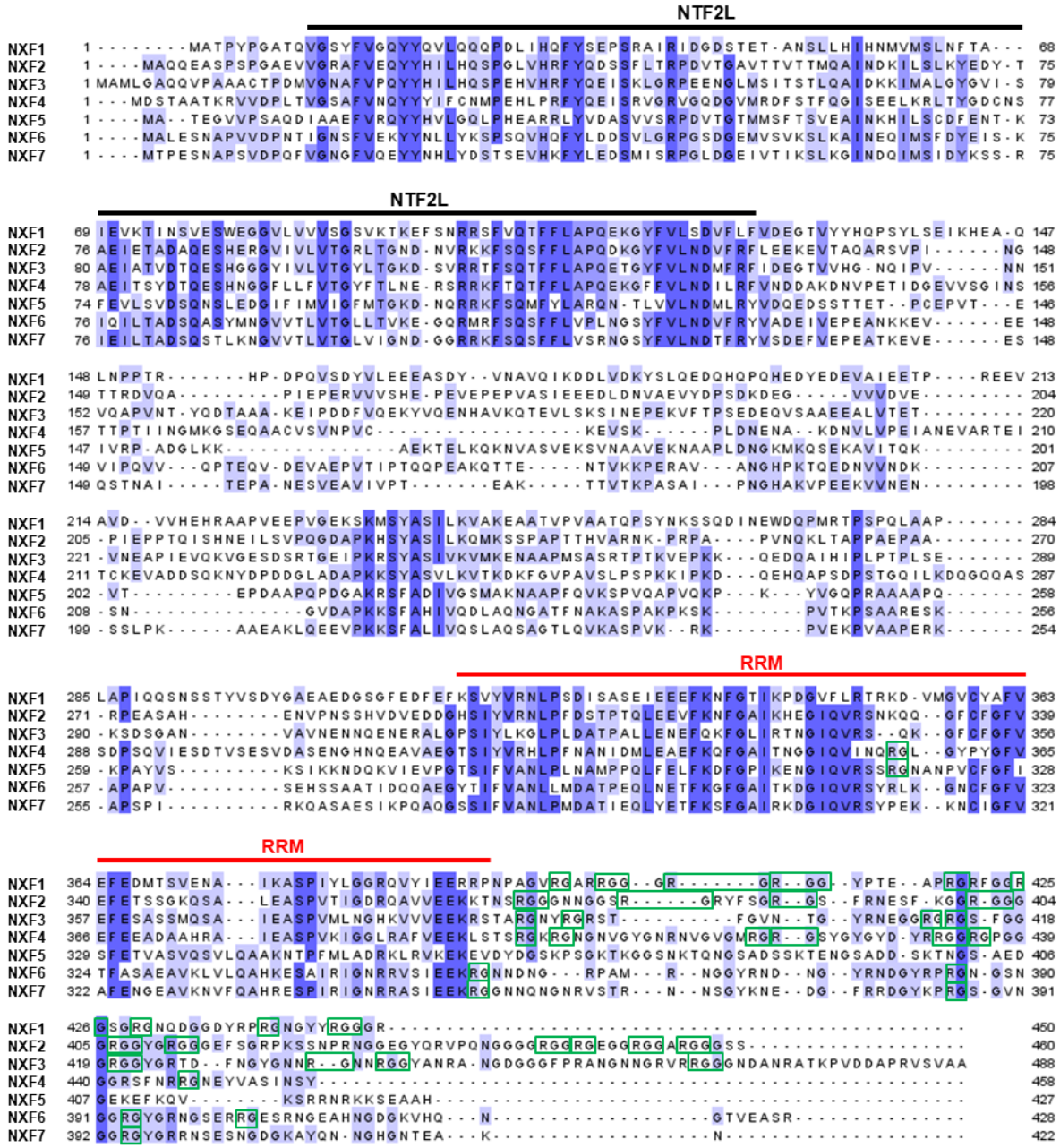

Figure 32. The seven NXF candidates show a similar modular organization. The seven NXF candidates all comprise a N-terminal NTF2-like (NTF2L) domain depicted in black. Additionally all seven candidates display a predicted RRM motif towards the C-terminus indicated in red and to different extends RG and RGG motifs at the C-terminus known to mediate binding to RNAs, highlighted in green. Multiple sequence alignment was generated using Clustal Omega (Sievers et., 2011) and the conservation of amino acid residues is highlighted in blue using JalView (Waterhouse et., al 2009).

2.3.3. NXF1-like candidates co-purify with export factors and the NPC

To further evaluate the obtained results that the seven NXF candidates co-purify with various export factors, reciprocal SG-tagging of the NXF candidates in *Arabidopsis* cell suspension cultures and affinity purification coupled to mass spectrometry was performed like described in chapter 2.3.1 (Figure 33). In other eukaryotes NXF1 or Mex67 are the factors that guide the exported transcripts through NPCs and by that should interact with nucleoporins of the NPC (Stewart, 2019). Thus, in addition to a possible interaction with mRNA export factors, it was further focused if subunits of the NPC co-purify with the NXF candidates.

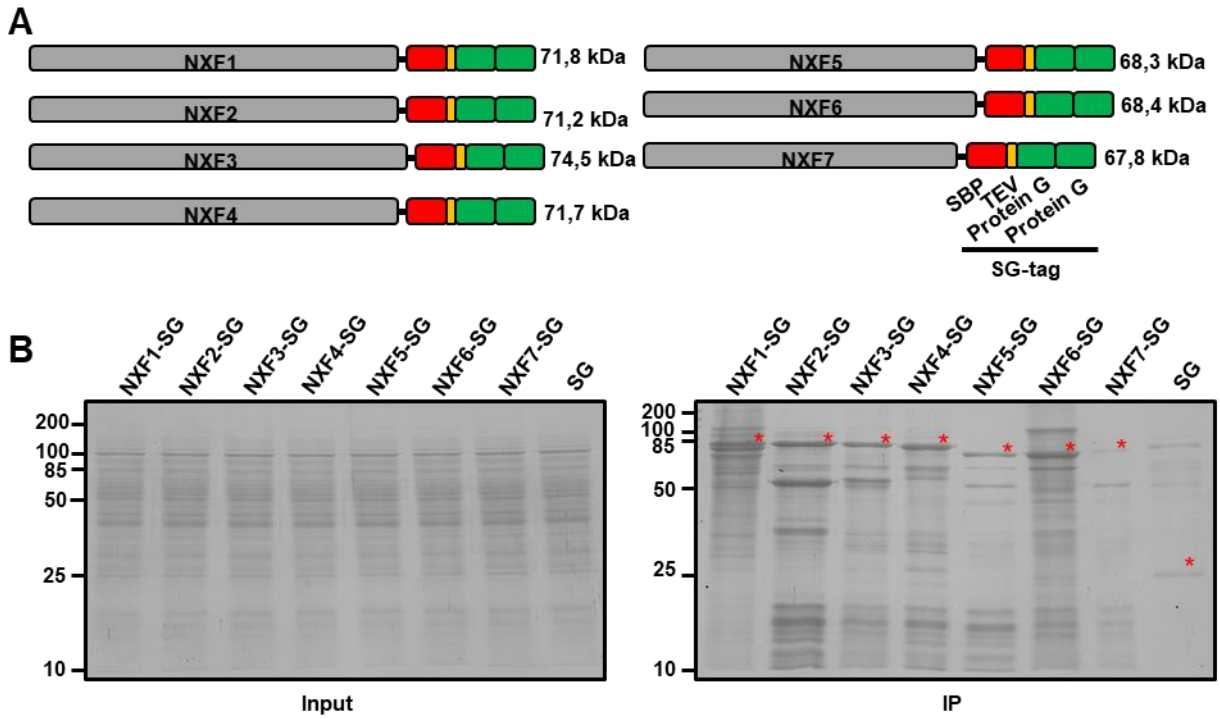

Figure 33. AP-MS analysis to screen for interactors of plant NXF1-like candidates. (A) Seven NXF1-like candidates were expressed in *Arabidopsis* cell suspension culture C-terminally fused to a SG tag composed of a streptavidin binding protein (SBP), a TEV cleavage site and two domains Protein G. Predicted molecular weights were calculated by ExPaSy pI/Mw tool. (B) Proteins were separated by SDS-PAGE and stained by Coomassie Blue. Left panel shows input used for affinity purification of the cell suspension lines transformed with the seven NXF1-like transgenes driven by a 35S promotor and the cell suspension line that was transformed with free SG driven by 35S promotor that served as a negative control. Right panel shows co-purifying proteins after affinity purification with red asterisks marking the respective SG-tagged bait protein. Molecular weights are depicted in kDa.

In total 312 proteins co-purified with NXF1-SG, 123 with NXF2-SG, 99 with NXF3-SG, 159 with NXF4-SG, 111 with NXF5-SG, 119 with NXF6-SG and 57 with NXF7-SG. AP-MS results verified a co-purification between export factors and NXF candidates. Besides ALY1, that was not detected in the NXF1-SG experiments, all other ALY proteins were detected in all experiments (Table 5). An unquestionably specific co-purification was detected between ALY3 and all seven NXF candidates as well as between UIEF1 and NXF3, NXF6 and NXF7 since

both ALY3 and UIEF1 were not detected in the unfused SG negative control. UIEF2 was not detected in any NXF AP-MS experiment.

Table 5. Components of TREX and NPC co-purify with NXF1-like candidates. (A) Seven NXF1-like candidates fused to a SG tag (highlighted in blue) were used as bait proteins for co-IP experiments. The numbers indicate the respective MASCOT score of the identified interactor and how many times the interactor was identified in three independent experiments. A protein was only considered to be a true interactor when identified in at least in two out of three experiments. In the last row interactors and corresponding MASCOT score are listed that were identified in the unfused SG negative control. Putative TREX interactors are highlighted in red and NPC components in green.

AGI		NXF1-SG	NXF2-SG	NXF3-SG	NXF4-SG	NXF5-SG	NXF6-SG	NXF7-SG	SG
AT5G43960	NXF1	6014/ 3	451/ 3		1110/ 2				
AT5G60980	NXF2	544/ 3	4553/ 3	2227/ 3	2270/ 3	2506/ 3	3111/ 3	780/ 3	137/ 2
AT3G25150	NXF3	89/ 2	712/ 3	4807/ 3	1477 3	1027/ 3	2289 3	366/ 3	
AT5G48650	NXF4	486/ 2	1474/ 3	1489/ 3	8699/ 3	561/ 3	1954/ 3		97/ 2
AT1G69250	NXF5		1342/ 3	741/ 3	559/ 3	4850/ 3	1239/ 3	2386/ 3	
AT1G13730	NXF6		294/ 3	474/ 3	511/ 3	645/ 3	3543/ 3		
AT2G03640	NXF7		104/ 2	491/ 3		4740/ 3	596/ 3	2766/ 3	167/ 3
AT5G59950	ALY1		204/ 2	435/ 3	287/ 3	151/ 2	304/ 3	267/ 3	131/ 2
AT5G02530	ALY2	272/ 3	309/ 2	249 3	262/ 3	165/ 3	267/ 3	289/ 2	185/ 2
AT1G66260	ALY3	357/ 2	288/ 3	371/ 3	333/ 3	691/ 3	493/ 3	318/ 3	
AT5G37720	ALY4	580/ 3	622/ 3	700/ 3	666/ 3	851/ 3	826/ 3	739/ 3	158/ 2
AT4G10970	UIEF1			188/ 3			104/ 3	125/2	
AT1G14850	NUP155	564/ 3			477/ 3				
AT1G33410	NUP160	252/ 3			230/ 2				
AT1G59660	NUP98b				87/ 2				
AT1G80680	NUP96	97/ 2							
AT2G05120	NUP133	187/ 3			136/ 2				
AT2G41620	NUP93a	132/ 2							
AT3G10650	NUP136	393/ 3		222/ 2	937/ 3		430/ 2		339/ 3
AT3G16310	NUP35	231/ 2	130/ 2		287/ 2		179/ 3		
AT5G05680	NUP88				252/ 3				
AT1G10390	NUP98a	326/ 2			486/ 3				
AT4G32910	NUP75	99/ 3							
AT2G30050	SEC13	295/ 2		320/ 2	162/ 2		216/ 3		415/ 2
AT5G51200	NUP205	423/ 2			408/ 2				
AT3G56900	ALADIN				216/ 3				
AT1G80670	RAE1	380/ 2	156/ 2	166/ 3	278/ 2		184/ 3		
AT5G40480	GP210	168/ 3							
AT2G39810	HOS1	259/ 3			190/ 3				

In addition to a co-purification between NXF candidates and export factors, various NXF candidates co-purified with another. Even though NXF2 and NXF4 were also detected in the unfused SG negative control, a specific co-purification of both proteins with several other NXF candidates can be assumed. NXF2 for instance was identified in the NXF3-SG, NXG4-SG, NXF5-SG and NXF6-SG AP-MS experiments with MASCOT scores more then 16-fold higher than in the negative control. Accordingly, NXF4 was detected in NXF2-SG, NXF3-SG and NXF6-SG AP-MS experiments with MASCOT scores more than 15-fold higher than in the negative control (Table 5). A putative specific co-purification could also be observed between NXF5 and NXF7 since both proteins were identified in the respective AP-MS experiments with very high MASCOT scores. An unquestionably specific co-purification was detected between NXF1 and NXF3 as well as between NXF3, NXF5 and NXF6 as these factors were not detected in the unfused SG negative control.

A possible role for the NXF candidates in mRNA export similar to the function of NXF1/Mex67 is further supported, since several subunits of the NPC co-purified with different NXF candidates. In total 17 NPC components were detected in the different AP-MS experiments with the two components NUP136 and SEC13 also being identified in the unfused SG negative control. Most NPC subunits co-purified with NXF1-SG (14) and NXF4-SG (13) whereas no Nups co-purified with NXF5 or NXF7.

The reciprocal expression of export factors and NXF candidates fused to a SG tag in *Arabidopsis* cell suspension cultures and following AP-MS experiments revealed several putative interactions between export factors and NXF candidates. Additionally, these experiments showed that several NXF candidates are potentially interconnected and that several NXF candidates, especially NXF1 and NXF4, potentially interact with the NPC.

2.3.4 NXF-eGFP fusion proteins transiently expressed in *N. benthamiana* are localized predominantly to the cytosol but are also enriched around nuclear envelopes

In yeast, Mex67 is clearly enriched around the nuclear envelope (Segref et al., 1997) whereas in human cells NXF1 proteins additionally localize to the nucleoplasm (Fribourg et al., 2001) (Tretyakova et al., 2005).

To analyse if the seven plant NXF candidates show similar localizations within plant cells and if there are differences between the NXF proteins in subcellular localization, candidates were transiently expressed by the strong viral 35S promotor in *N. benthamiana.* The localization of C-terminally fused *eGFP* fusion proteins were analysed 3 days after *A. tumefaciens* infiltration by CLSM (Figure 34). In cells expressing free eGFP fused to an NLS peptide, a green fluorescence signal was detected exclusively in the nucleoplasm of cells (Figure 34 A). In cells expressing NXF candidates on the other hand, a cytosolic signal could be detected (Figure 34 B-H). These cytosolic signals appeared to surround single tobacco cells what can be explained by the presence of comparatively large vacuoles in plant leaf mesophyll cells that fill most of the cell and displace cytosolic proteins towards the cell wall. Additionally, an enrichment of NXF fusion proteins around the nucleus could be observed.

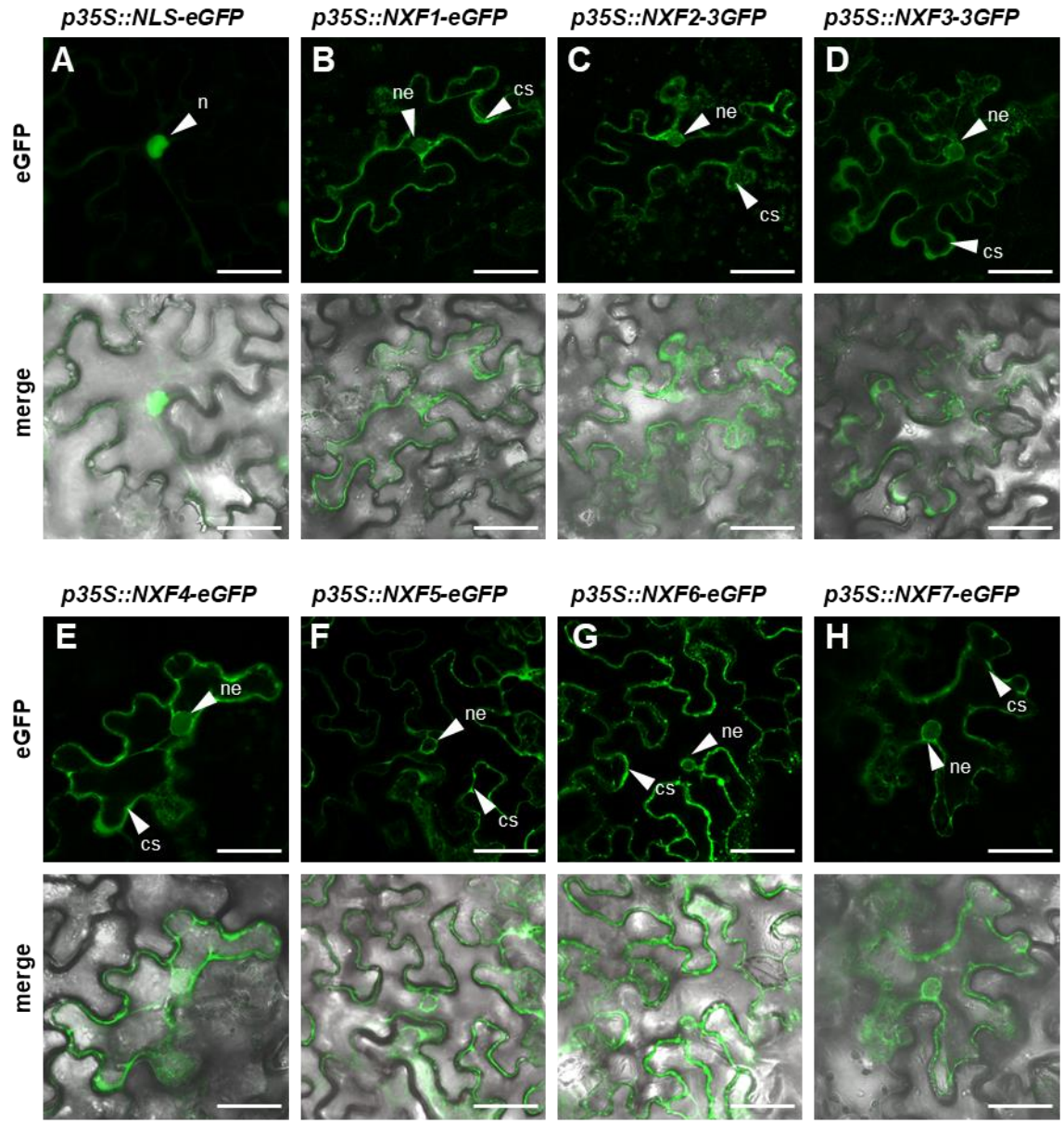

Figure 34. NXF candidates expressed in *N. benthamiana* localize predominately to the cytoplasm. NXF1-7 fused to eGFP (B-H) and NLS-eGFP (A) were transiently expressed in *N. benthamiana*. In cells expressing NLS-eGFP a green fluorescence signal is only detected in the nucleus (n). In cells expressing the seven NXF-eGFP fusion proteins a cytosolic fluorescence signal (cs) and an enrichment of green fluorescence protein at the nuclear envelopes (ne) could be detected. Size bars = 50 µm.

To unequivocally proof that NXF proteins surround nuclei, the seven NXF candidates fused to eGFP were co-expressed with a nuclear *UAP56-mCherry* marker in *N. benthamiana* leaf cells and localization of both fusion proteins was analysed by CLSM (Figure 35).

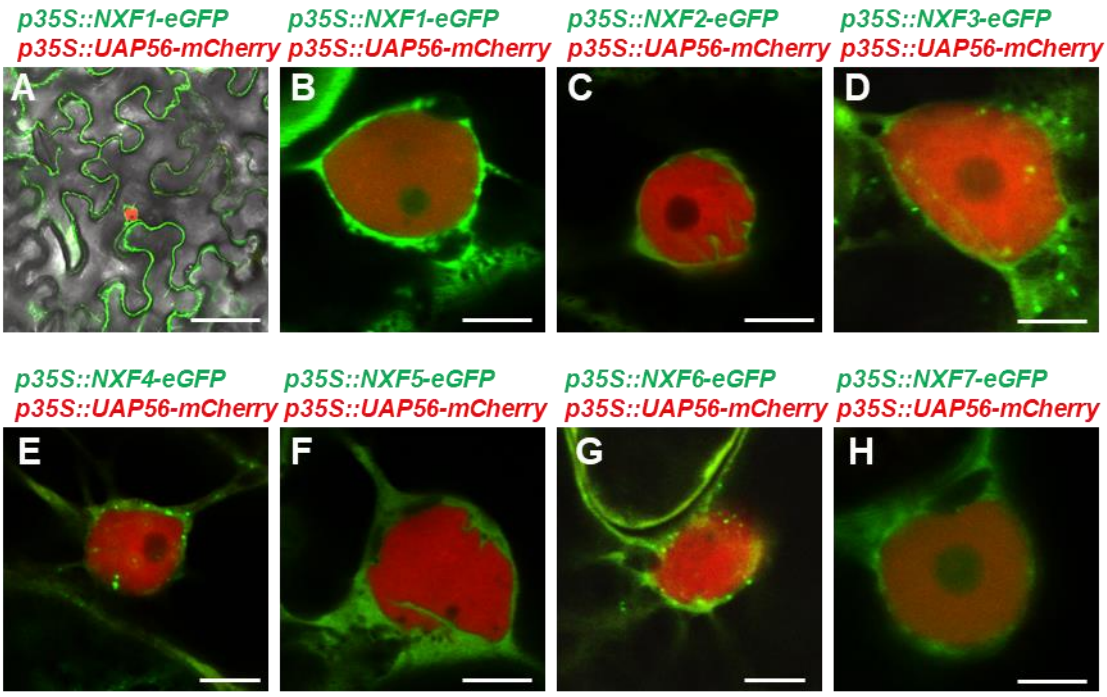

Figure 35. NXF factors expressed in *N. benthamiana* surround nuclear UAP56-mCherry proteins. *NXF1-7-3'eGFP* and *UAP56-3'mCherry* were transiently co-expressed in *N. benthamiana*.. Cells expressing both *NXF1-eGFP* and *UAP56-mCherry* show a green cytosolic NXF1 signal and a red nucleoplasmic UAP56-mCherry signal (A). (B-H) Single nuclei of cells co-expressing *NXF-eGFP* and *UAP56-mCherry* demonstrates that NXF proteins surround nuclei. Size bars (A) = 50 µm, (B-H) = 5 µm.

Co-expressing *NXF-eGFP* candidates and *UAP-mCherry* clearly showed an accumulation of NXF-eGFP signal for all seven candidates around a red nuclear UAP-mCherry signal demonstrating that *NXF* candidates expressed in tobacco cells localize to the cytosol and are enriched around nuclei of these cells (Figure 35).

2.3.5. NXF-GFP fusion proteins expressed by endogenous promotors in stable transformed *Arabidopsis* lines localize predominantly to the cytosol

Since overexpression of GFP-tagged fusion proteins can lead to GFP self-aggregation into complexes and ectopic protein localization (Gibson et al., 2013), more accurate information about the subcellular localization of *Arabidopsis* proteins can be obtained when candidates are expressed by their endogenous promotor optimally in the respective *Arabidopsis* mutant background.

Thus, homozygous *nxf* T-DNA insertion mutant plants (see 3.3.6) were analysed by CLSM that carried a respective *NXF* candidate transgene fused C-terminally to *GFP* and driven by the endogenous promotor, that was integrated into the plant genome by *A. tumefaciens* mediated transformation. Ultimately these experiments should be performed in three independent lines homozygous for the inserted transgene. Since these lines were not available yet, only one line (not always homozygous for the inserted transgene and inserted transgene not always in

mutant background) for each NXF candidate was analysed by CLSM, for what reason the following results must be considered as preliminary.

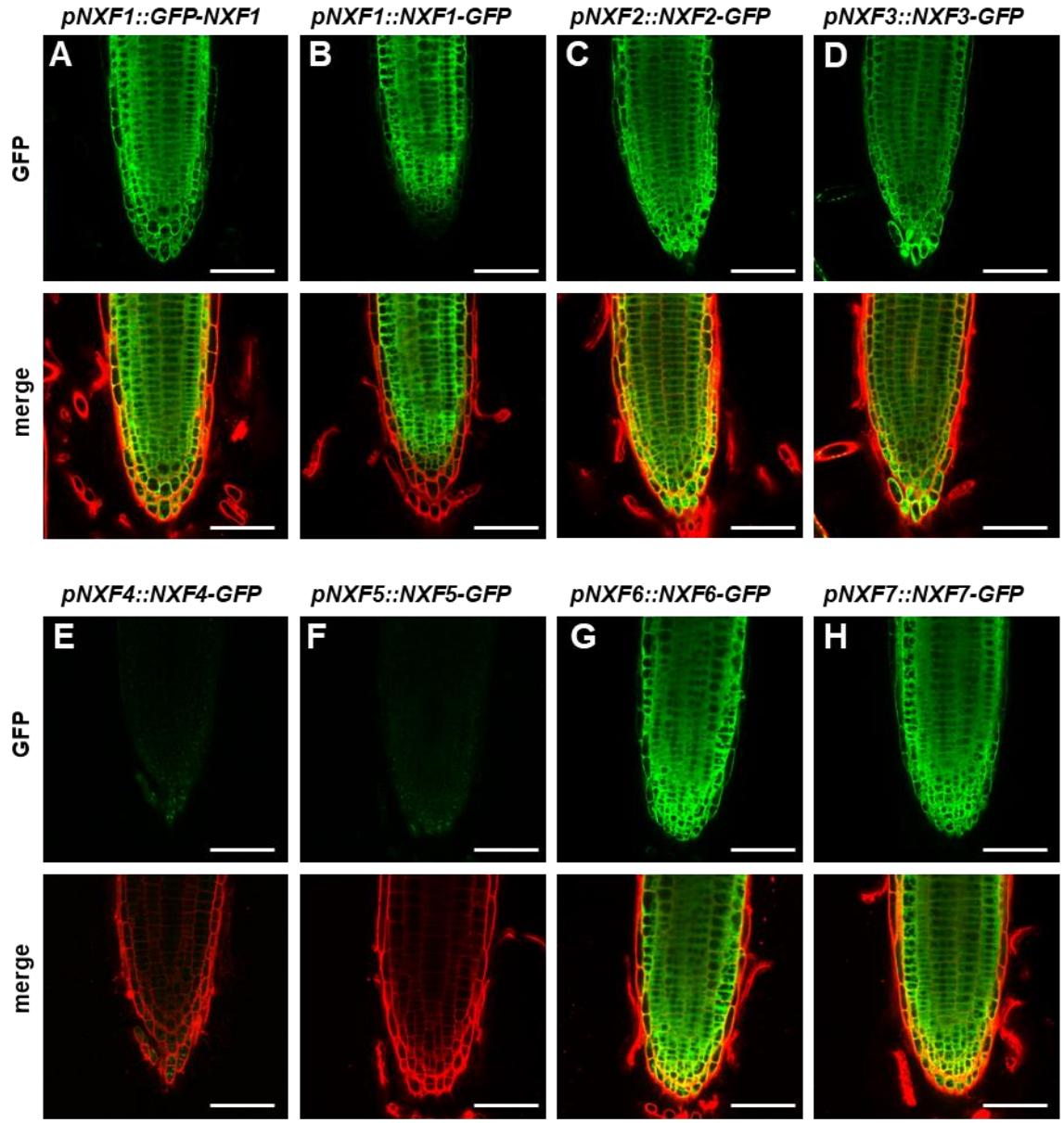

Figure 36. NXF-GFP fusion proteins localize predominantly to the cytosol in root tips . NXF-GFP localization in root tips from 8 DAS seedlings of stable transformed *Arabidopsis* transgenic lines. GFP was N-terminally fused to NXF1 (A) or C-terminally fused to NXF1-7 (B-H) driven by the respective endogenous promotor. Cell walls are counterstained with propidium iodide (red signal). Size bars = 50 µm.

In transgenic lines carrying the transgenes *pNXF4::NXF4-GFP* and *pNXF5::NXF5-GFP* a green fluorescence signal only at background levels was detected (Figure 36 E,F). This can be explained amongst other things by a low gene or protein expression, transcript or protein degradation or by an insertion of the transgene into a silenced region of the genome. To analyse the global expression profiles of *NXF* candidate genes, public available transcript

profiling data were analysed (Figure 37). The expression of *NXF4* is indeed very low in roots and in the aerial parts of plants compared to the other six NXF candidates, indicating that the absence of a GFP signal in this transgenic line is potentially caused by a low gene expression. The expression of *NXF5* in roots is also lower than the expression of the other candidates but it should still be high enough to produce proteins that can be detected by CLSM. Thus, it is more likely that the *NXF5-GFP* transgene was inserted into an unfavourable region in this transgenic line, but to verify this assumption, more independent transgenic lines, homozygous for the inserted transgene, need to be analysed in future experiments.

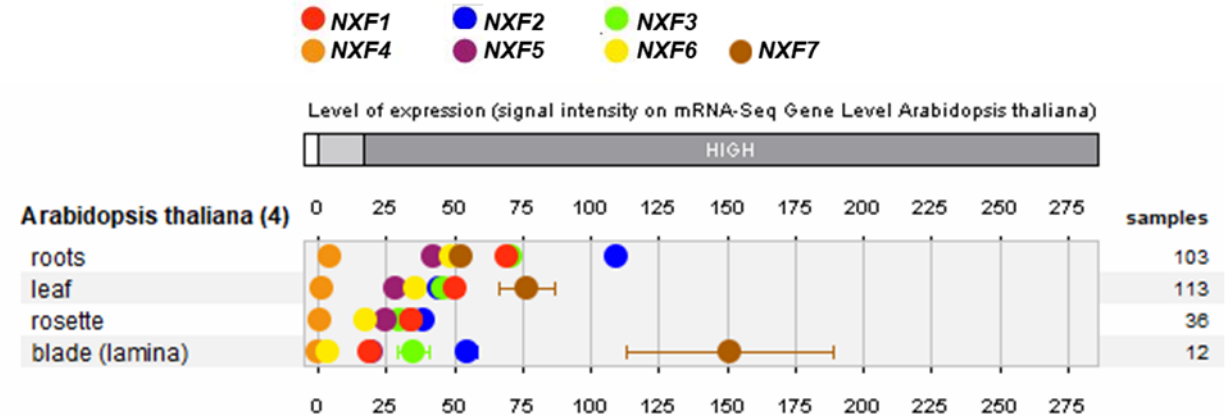

Figure 37. *NXF4* shows lowest gene expression of the seven *NXF* candidates. Gene expression of the seven *NXF* candidates in blade, roots, leaves and rosette leaves based on public transcript profiling data generated by RNAseq analysis and displayed using Genevestigator (Hruz et al., 2008).

For the other five transgenic lines tested, a distinct GFP signal could be detected. Like observed in the experiments analysing the subnuclear localization of NXF-eGFP candidates in tobacco cells (Figure 34), also in *Arabidopsis* root cells no differences regarding the localization of NXF-GFP proteins were detected in the different NXF-GFP transgenic lines. In all lines NXF-GFP was expressed in all root cells and the fusion proteins were predominantly localized to the cytosol. To exclude that this cytosolic localization was caused by an interference of a C-terminal GFP tag with protein function, a transgenic line carrying an N-terminally *GFP* tagged *NXF1* transgene was additionally analysed (Figure 36 A). In this line the same predominantly cytosolic distribution of the fusion proteins could be observed, indicating that NXF-like proteins localize predominantly to the cytosol.

2.3.6. Co-localization studies of NXF-GFP and NUP-tagRFP fusion proteins

Since in other eukaryotes the heterodimeric export receptor guides mRNAs through the NPC by a mechanism that is dependent on interactions between export receptor with FG Nups (Katahira et al., 1999; Strässer et al., 2000; Ben-Yishay et al., 2019), in the following co-localization experiments between the NXF candidate NXF1 and the FG Nup NUP54 (AT1G24310) were performed (Figure 38).

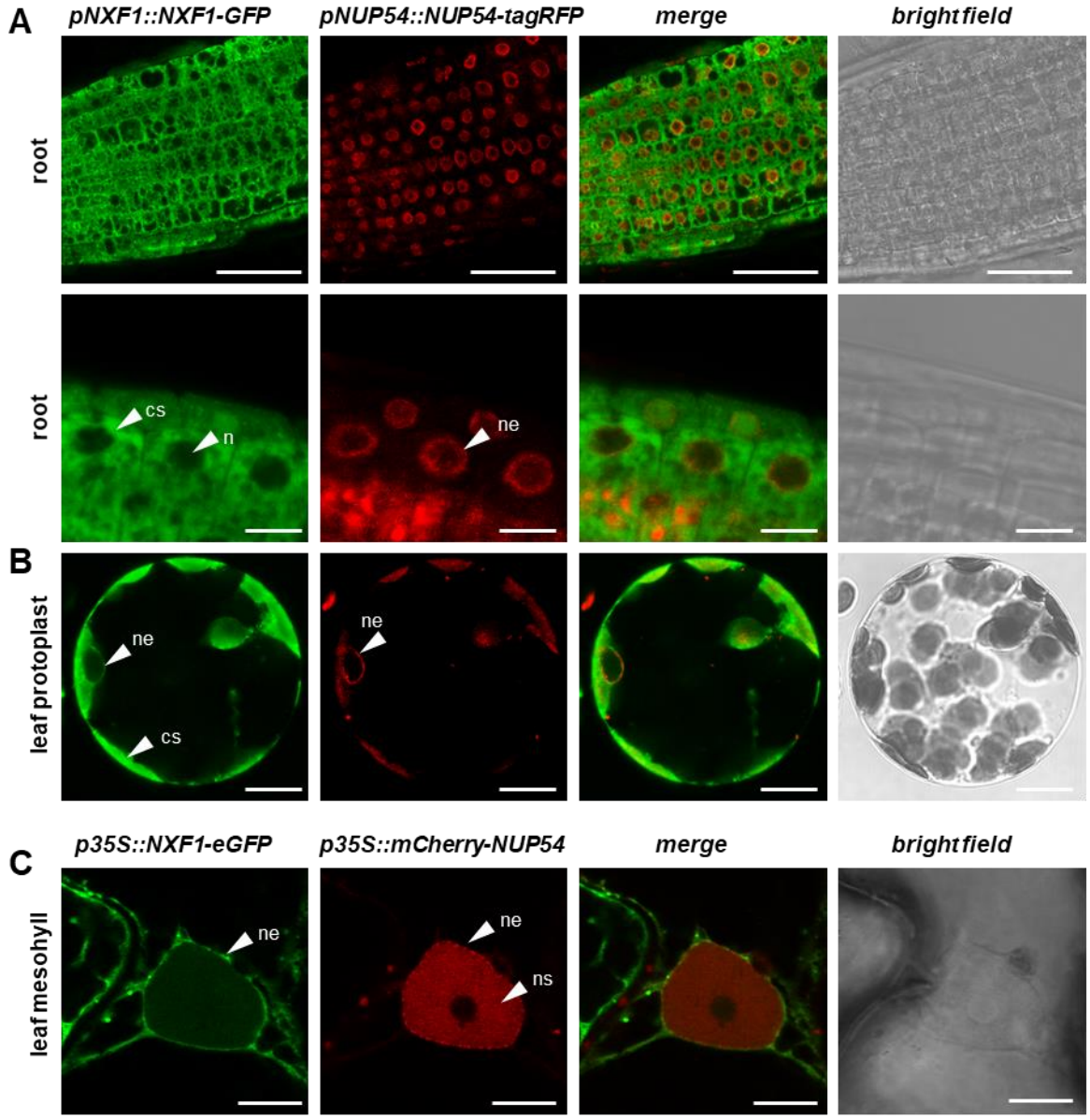

Figure 38. Co-localization of NXF1 and NUP54. (A) Root tip at 8 DAS from a stable transformed transgenic *Arabidopsis* line expressing *NXF1-GFP* and *NUP-tagRFP* under the respective endogenous promotors. NXF1-GFP shows predominately a cytosolic signal (cs) in most cells and is excluded from nuclei (n) in root tips. The NPC marker NUP54-tagRFP is detected as a ring-like structure surrounding nuclei at the nuclear envelope (ne). (B) Protoplast isolated from rosette leaves 28 DAS of transgenic plants described in (A) with NXF1-GFP showing predominately a cytosolic signal (cs) but being also enriched around the nuclear envelope (ne) and NUP54-tagRFP being detected as a ring-like structure surrounding nuclei at the nuclear envelope (ne). (C) *NXF1-eGFP* and *mCherry-NUP54* transiently overexpressed in *N. benthamiana* leaf mesophyll cells. NXF1-eGFP and mCerry-NUP54 is enriched at the nuclear envelope (ne) and mCherry-NUP54 also shows a nuclear signal (ns). Size bars = 50 µm A top row, 10 µm A bottom row, 10 µm B and 5 µm C.

The homozygous transgenic line expressing NXF1-GFP in *nxf1* mutant background described in 2.3.5 was transformed with a transgene expressing *NUP54* C-terminally fused to the fluorophore *tagRFP* from its endogenous promotor (Hachani, 2018). In the long term these co-localization experiments should be performed using T3 plants homozygous for the inserted transgene but since these plants were not available yet, segregating T2 plants were analysed by CLSM. In root cells 8 DAS, NUP54-tagRFP fusion proteins were visible as ring like structures that surrounded all nuclei of the root cells along the nuclear envelope (Figure 38 A). NXF1-GFP fusion proteins on the other hand were predominately detected in the cytosol like described in 2.3.5 and in most cells a green NXF1-GFP signal was separated from the nucleus by the red NUP54-tagRFP signal representing the nuclear envelope and no obvious co-localization could be observed (Figure 38 A).

In addition to root cells, also leaf protoplasts isolated from rosette leaves 28 DAS of the just described transgenic plants (Figure 38 B) and tobacco mesophyll cells transiently co-expressing *NXF1-eGFP* and *mCherry-NUP54* driven by the strong 35S promotor (Figure 38 C) were analysed. In both *Arabidopsis* and tobacco leaf cells, the NXF1 fusion proteins predominately localized to the cytosol but in both organisms also and enrichment of green fluorescence signals could be observed around the nuclear envelope but a clear co-localization with NUP54-tagRFP was not detectable. Similar results could be observed analysing the co-localization of the seven NXF candidates fused to eGFP with NUP35-mCherry (AT3G16310), which co-purified reproducibly with several NXF candidates in AP-MS experiments (Table 5), when NXF-eGFP and NUP35-mCherry were transiently expressed in tobacco leaf cells (Supplement S16).

In summary, the localization studies of the seven NXF candidate fusion proteins in *N. benthamiana* leaf mesophyll cells and in *Arabidopsis* root and leaf cells showed that NXF candidates mainly localize to the cytoplasm. Since NXF candidate fusion proteins were also enriched around nuclei, all seven NXF candidates can potentially function as mRNA export receptors.

2.3.7. Molecular characterization of *nxf* T-DNA insertion lines

In yeast and metazoans Mex67 and NXF1 are essential factors for bulk mRNA export and cell viability (Segref et al., 1997; Grüter et al., 1998; Katahira et al., 2009). To investigate the influence of *Arabidopsis* NXF candidates on plant growth and bulk mRNA export, T-DNA insertion mutants homozygous for the T-DNA allele were analysed. Seeds harbouring the T-DNA insertion alleles *nxf1-1*, *nxf2-1*, *nxf3-1*, *nxf4-3*, *nxf5-1*, *nxf6-1* and *nxf7-1* were obtained from the Nottingham Arabidopsis Stock Center (NASC) and homozygous mutant plants were identified by genotyping PCR. For genotyping two oligonucleotide pairs were used, one spanning the site of the T-DNA insertion and a second one targeting the T-DNA insertion site (Figure 39 A). In the seven identified homozygous T-DNA mutant plants a PCR product was only obtained when the oligonucleotides targeting the T-DNA insertion was used whereas when using genomic DNA extracted from Col-0 plants only a fragment was amplified using the oligonucleotides spanning the T-DNA insertion site, confirming that identified plants were homozygous for the respective mutant allele (Figure 39 B). The exact position of the T-DNA insertion and the presence of a premature stop codon was further confirmed by sequencing.

To verify that homozygous T-DNA mutants do not produce full-length candidate transcripts, semi quantitative RT-PCRs using oligonucleotides spanning the T-DNA insertions were performed. cDNA generated from RNA extracted from 14 DAS seedlings of Col-0 and *nxf* plants was used as templates for RT-PCR reactions. In the respective mutant lines, no PCR fragments were amplified showing that the interruption of the genomic sequences by T-DNA insertion inhibits the building of functional full-length transcripts (Figure 39 C). RT-PCR using oligonucleotides binding to *ACTIN2* demonstrated that functional cDNA was used in the RT-PCR reactions in all analysed plant lines.

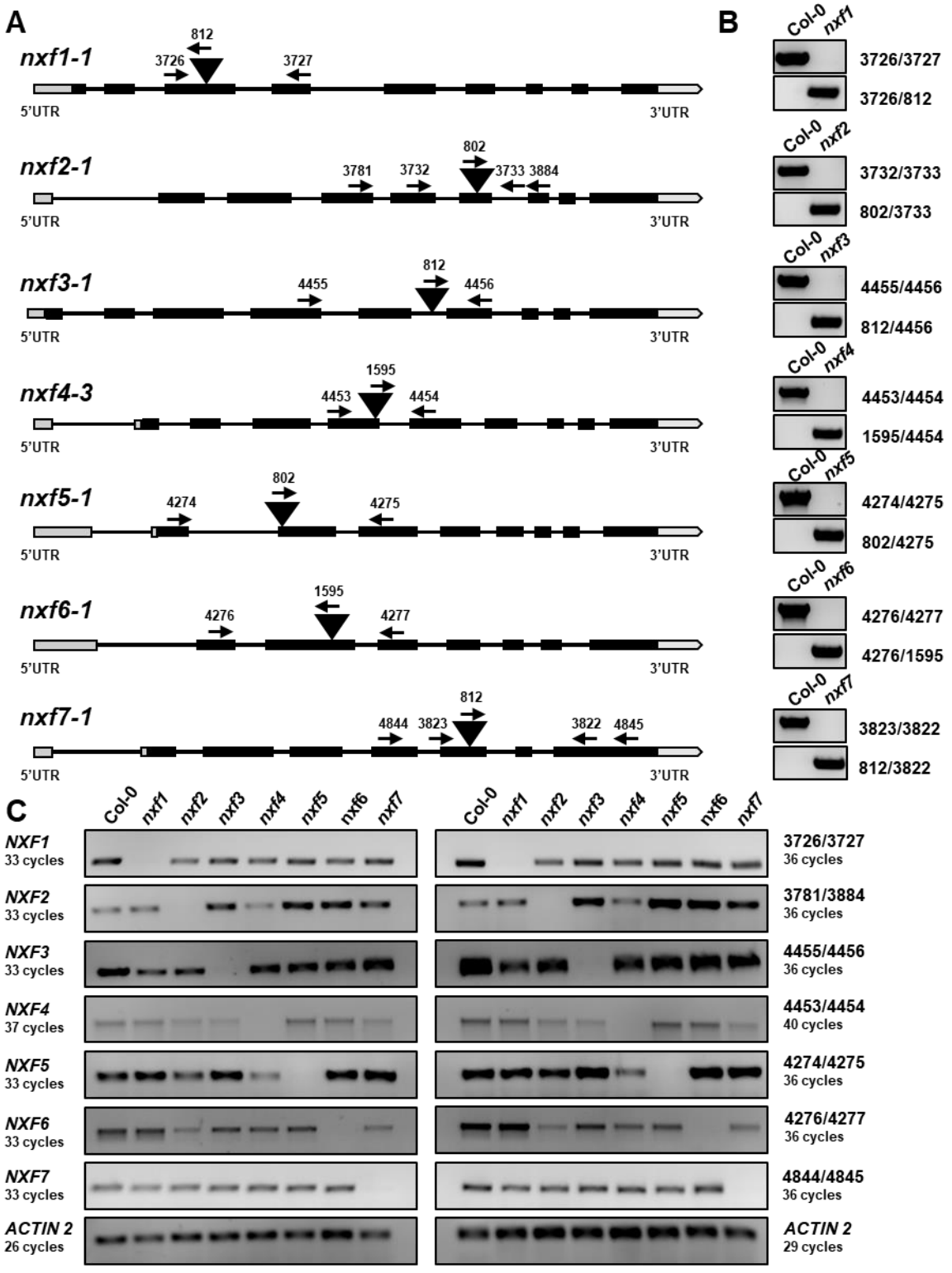

Figure 39. Molecular characterization of *nxf* T-DNA insertion lines. (A) *nxf1* - *nxf7* T-DNA insertion alleles with triangles marking the T-DNA insertion. Primers used for genotyping PCR (B) and RT-PCR (C) are highlighted with black arrows. UTRs = light grey boxes, exons = block boxes, introns = black lines. (B) Genotyping PCRs with the indicated primers in Col-0 and the homozygous *nxf1* - *nxf7* T-DNA insertion mutants. (C) RT-PCR using cDNA generated from RNA extracted from 14 DAS seedlings of Col-0 and the homozygous *nxf1* - *nxf7* T-DNA insertion mutant plants with the indicated primers spanning the T-DNA insertions. RT-PCRs were performed for various cycles to show that PCR reactions were not saturated.

2.3.8. *nxf* mutants are only mildly affected in plant growth and development

A mutant that is lacking the mRNA export receptor(s) is supposed to show a strong mRNA export block and it should be severely affected in plant growth and development when factor(s) fulfil similar functions like in other eukaryotes. Other mRNA export mutants like plants not producing the four ALY proteins for instance show a bulk mRNA export block (Figure 11) that correlates with a pleiotropic phenotype (Figure 10).

The identified single mutant plants were in the following phenotypically analysed to study the role of the seven NXF candidates during plant growth and development. Since all seven homozygous *nxf* plant lines showed no phenotypic alterations (data not shown), higher order mutants were generated. This was accomplished by first generating homozygous double mutants and in the following a quadruple mutant (*4xnxf*, *nxf1 nxf2 nxf3 nxf4)* and a triple mutant (*3xnxf*, *nxf5 nxf6 nxf7)*.

Compared to the *4xaly* mRNA export mutant (Figure 10), *4xnxf* and *3xnxf* plants showed no such major defects in plant growth or root development (Figure 40). Overall the two mutants resemble Col-0 plants apart from a severe late flowering phenotype observed in *4xnxf* plants (Figure 40 A,C,D,E,G) that is underlined by a distinct later bolting time and a reduced plant height 42 DAS. Additionally, a smaller rosette was observed in both mutant plant lines 28 DAS (Figure 40 F).

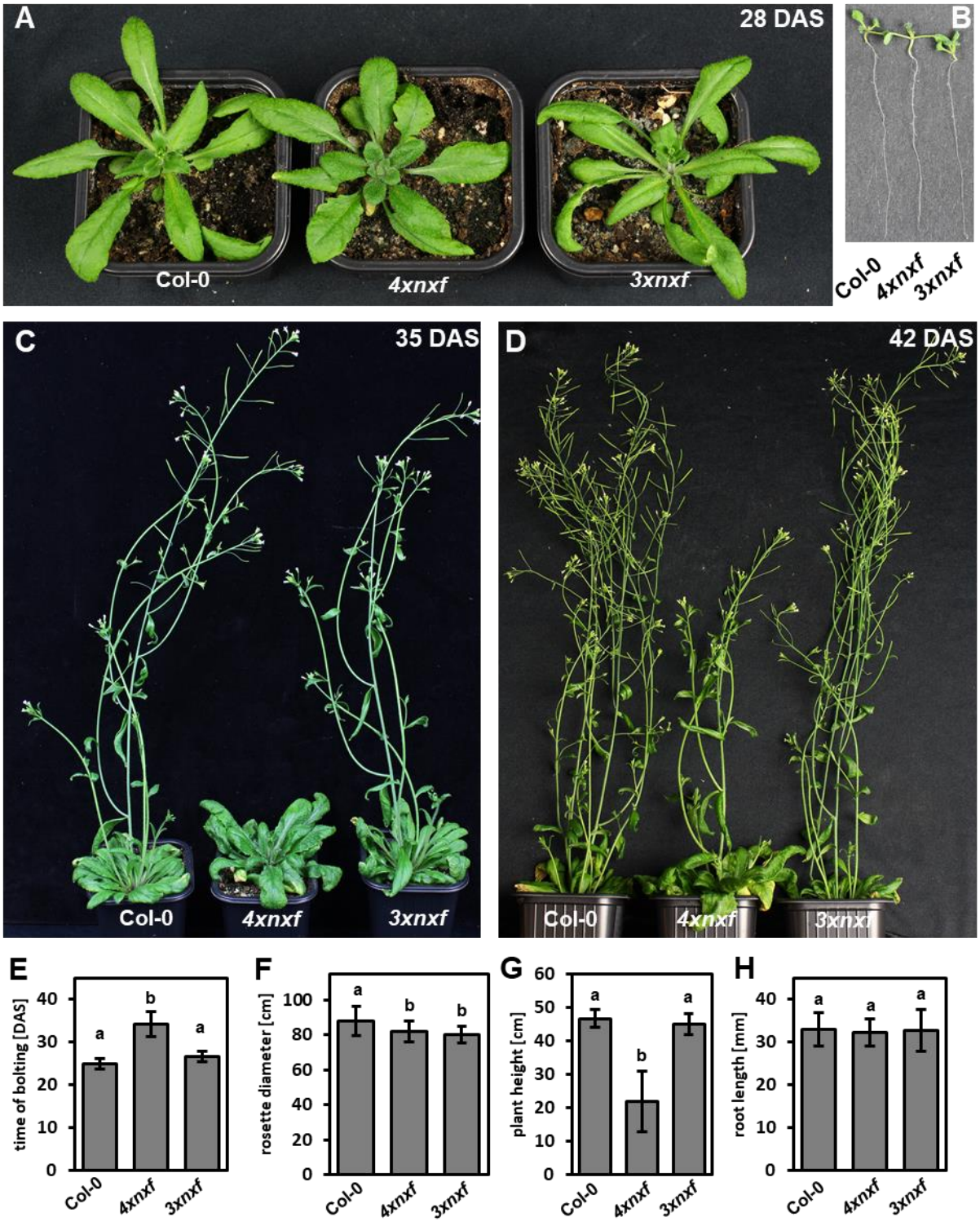

Figure 40. ***nxf*** **plants are only mildly affected in plant growth and development.** Phenotype of *4xnxf* and *3xnxf* plants compared to Col-0 at 28 DAS (A), 35 DAS (C) and 42 DAS (D). *4xnxf* and *3xnxf* plants show no differences regarding root length at 8 DAS (B). Phenotypic analysis for (E) bolting time, (F) rosette diameter 28 DAS, (G) plant height at 42 DAS and root length 8 DAS (H). Error bars indicate SD of 15 plants. Data sets marked with different letters are significantly different as assessed by a multicomparison Tukey's test ($P < 0.05$) after one-way analysis of variance.

2.3.9. *4xnxf* and *3xnxf* plants show no mRNA export block

In respect to their role as putative mRNA export receptors, the NXF mutants *4xnxf* and *3xnxf,* although not displaying a strong phenotype, were analysed for defects in the bulk export of mRNAs. Wole-mount in situ hybridization in roots was performed (Figure 41) like described in figure 11 and nuclear/cytosolic fluorescence signals were calculated in Col-0, 4x*nxf* and *3xnxf* plants. Analysis of at least 60 nuclei per genotype revealed no bulk mRNA export block in both mutant lines since the nuclear/cytosol signal ratios were not significantly different in these plants compared to Col-0 (Figure 41 B).

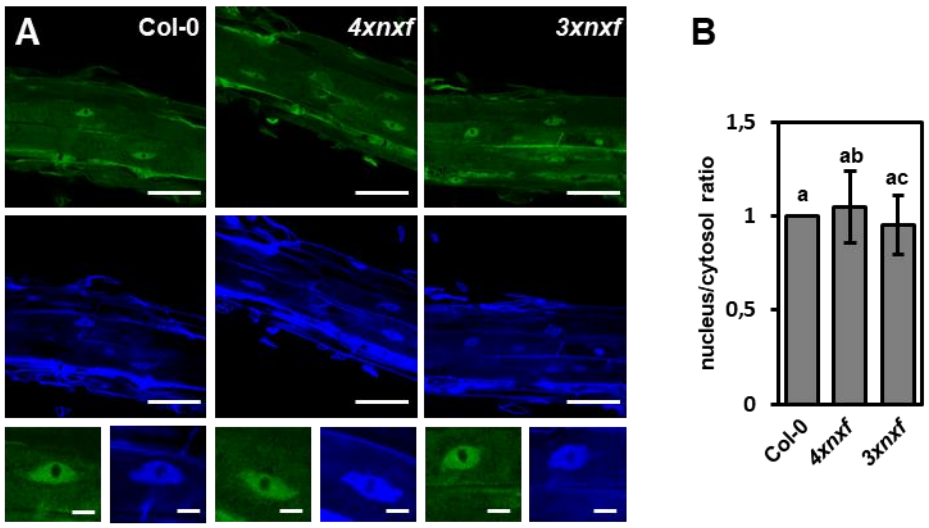

Figure 41. ***4xntf*** **and** ***3xntf*** **plants show no bulk mRNA export block.** (A) CLSM images from representative sections from roots of Col-0, *4xnxf* and *3xnxf* plants after WISH with the Alexa Fluor 488 oligo (dT) signal in green and DAPI signal in blue. Bars = 60 µm (top rows) and 10 µm (bottom row). (B) Average nuclear/cytosol signal ratio of 60 or more nuclei per genotype. The ratios are shown relative to Col-0 (ratio of 1), with error bars indicating SD. Data sets marked with different letters are significantly different as assessed by a multicomparison Tukey's test ($P < 0.05$) after one-way analysis of variance.

3. Discussion

3.1 ALY proteins function as export factors

In eukaryotes, a central role in mRNA export is played by mRNA export adaptors that are involved in the initiation of the mRNA export process. Additionally, in a later stage of mRNA export, adaptors hand mRNA over to a heterodimeric mRNA export receptor and by that are crucial for the last defining step of mRNA export, the translocation of export competent mRNPs through the NPC (Walsh et al., 2010; Heath et al., 2016).

mRNA Export adaptors are diversified in eukaryotes with only some mRNA export adaptor proteins being described in yeast whereas a variety of mRNA export adaptors and co-adaptors were identified in metazoans over the last few years (Heath et al., 2016). Although most adaptors are diversified in eukaryotes, the key mRNA export adaptor ALY (Yra1 in yeast) is conserved albeit the number of genes encoding different ALY proteins and the impact of these factors on bulk mRNA export varies in different eukaryotic systems. In yeast, the ALY orthologue Yra1 is essential for mRNA export (Strässer and Hurt, 2000; Zenklusen et al., 2001). The genome of *Caenorhabditis elegans* encodes three ALY orthologues. In contrast to yeast, a simultaneous knockdown of all three *C. elegans* ALY orthologues does not affect bulk mRNA export in these mutants significantly (Longman et al., 2003). In human and fruit fly cells, the depletion of ALY proteins results in an intermediate mRNA export block phenotype with only a modest nuclear accumulation of poly(A) RNA being detected in nuclei (Gatfield and Izaurralde, 2002; Hautbergue et al., 2009; Katahira et al., 2009). In *Arabidopsis, ALY* genes are more diversified than in other eukaryotes with the genome encoding four different ALY proteins, although their role in mRNA export has not been studied (Uhrig et al., 2004; Pendle et al., 2005).

In yeast and human cells, Yra1 and ALY can be recruited to the TRanscription and EXport (TREX) complex by a direct protein-protein interaction with the TREX subunit UAP56 (Sub2 in yeast, Luo et al., 2001; Sträßer and Hurt, 2001). A direct interaction between the *Arabidopsis* UAP56 and ALY proteins could also be demonstrated using the yeast two-hybrid (Y2H) system (Kammel et al., 2013; Pfaff et al., 2018). Since in vivo FRET experiments performed in this study could confirm these previously shown interactions in planta, the mechanism how ALY proteins are recruited to TREX is most likely conserved in *Arabidopsis*.

In yeast and metazoans it was further demonstrated that ALY orthologues bind to ssRNA, a feature supposed to be essential for factors that hand mRNA over to a mRNA receptor (Strässer and Hurt, 2000; Stutz et al., 2000; Zenklusen et al., 2001; Katahira et al., 2009). As part of our characterization of ALY proteins as possible mRNA export factors, MST experiments also demonstrated that recombinant *Arabidopsis* ALY1 preferentially binds to ssRNA *in vitro* (Pfaff et al., 2018). Additionally, we could show that the individual RRM of ALY1

interacts with ssRNA weakly and that both the N- and C- terminal domains increase the affinity of the protein for RNA (Pfaff et al., 2018). A recent RNA immunoprecipitation study further revealed that *Arabidopsis* ALY1 binds to a broad array of mRNAs *in vivo,* further supporting a possible role of *Arabidopsis* ALY proteins as mRNA export factors (Choudury et al., 2019).

A key feature of ALY mRNA export adaptors is that they are involved in several aspects of mRNA export and that they are stripped of export competent mRNPs within the nucleus before export competent mRNAs travel through the NPC (Stutz et al., 2000; Zhou et al., 2000; Rodrigues et al., 2001). CLSM analysis of *Arabidopsis* root and leaf cells using plants expressing the four *Arabidopsis* ALY proteins fused to GFP in the respective mutant background confirmed that *Arabidopsis* ALY proteins are also exclusively located in nuclei (Pfaff et al., 2018).

In yeast and metazoans, a correlation between mRNA export phenotype and defects in cell growth and development can be observed. In yeast, upon Yra1 depletion mRNA export is blocked and the loss of Yra1 is lethal (Portman et al., 1997; Strässer and Hurt, 2000). In *h. sapiens*, *C. elegans* and *D. melanogaster* the knockdown of ALY orthologues has no or only mild effects on mRNA export. In *D. melanogaster* the knockdown of the ALY ortholog leads to a decreased cell growth rate but no significant accumulation of poly(A) mRNA can be detected (Gatfield and Izaurralde, 2002). In *C. elegans* the simultaneous knockdown of the three ALY orthologs leads to a reduced mobility phenotype but also no enrichment of poly(A) mRNA in the nuclei can be observed (Longman et al., 2003). In *h. sapiens* the knockdown of ALY leads to a weak accumulation of poly(A) mRNA compared to the loss of other mRNA export factors like NXF1 and only a simultaneous knockout of more than one export adaptor results in a strong nuclear accumulation (Hautbergue et. al., 2009; Katahira et al., 2009; Viphakone et al., 2012; Chang et al., 2013). The phenotypical differences may be explained by the presence of redundant export adaptors or by an up-regulation of other export factors (Hautbergue et al., 2009; Walsh et al., 2010). In *Arabidopsis,* the loss of one ALY factor and the simultaneous knockout of the genes *aly1* and *aly2* as well as *aly3* and *aly4* has no or only minor effects on plant growth and mRNA export, suggesting that the four ALYs function redundantly (Sørensen, 2016). The severe phenotype of plants lacking all four ALY proteins supports the hypothesis that ALY proteins are functionally redundant and indicates that in *aly* single and double mutants the functional ALY proteins can compensate for the loss of one or two ALY factors, whereas in the *4xaly* mutant an additive effect on mRNA export results in a severe phenotype regarding plant growth and development.

An enrichment of poly(A) transcripts in *4xaly* nuclei detected by WISH further demonstrated a correlation of the severe growth and development phenotype with a general mRNA export defect. Phenotypic analysis and export assays showed that the loss of all four *Arabidopsis* ALY

proteins results in a strong export and growth phenotype compared to the loss of ALYs in metazoans. Additionally, the viability of *4xaly* plants showed that Yra1 plays a more prominent role in mRNA export in yeast than the ALY proteins do in *Arabidopsis* and that in plants redundant export factors exist, that can export mRNAs efficiently enough even in the absence of all ALY proteins, so plants can survive.

To address the questions what transcripts are retained in *4xaly* nuclei and by that are targets for a putative ALY mediated mRNA export, an RNAseq approach sequencing mRNAs from total cells and nuclei was performed. Using two different normalization methods, 2311 and 2205 transcripts were detected to be retained in *4xaly* nuclei. This retention of transcripts demonstrated that *4xaly* is a mRNA export mutant.

By cell fractionation followed by RNAseq of nuclei and whole cells a variety of transcripts were detected that are enriched in *4xaly* nuclei and hence exported by one or more ALY export factors. To further validate that the candidates obtained in this study are enriched in *4xaly* nuclei it would be useful to apply methods to detect single RNA molecules like single-molecule fluorescence in situ hybridization (smFISH) which was developed in the last years and which was shown to be also useful to image specific transcripts within plant cells (Raj et al., 2008, Duncan et al., 2016, Duncan and Rosa, 2018).

In human 293A-TOA cells, upon siRNA mediated ALY depletion, 3796 differentially expressed genes are significantly downregulated in a cytoplasmic fraction and 3344 differentially expressed genes are significantly upregulated in a nuclear fraction (Stubbs and Conrad, 2015). Since the *Arabidopsis* genome encodes ~27700 protein coding genes (Cheng et al., 2017) and the human genome encodes ~21300 protein coding genes (Pertea et al., 2018), in both organisms a significant portion of genes rely on ALY proteins to be properly exported out of the nucleus, but the vast majority of transcripts is not significantly affected in mRNA export upon ALY depletion. This might explain the rather mild phenotype of ALY depleted human cells und the viability of *4xaly* plants and further supports the hypothesis that also in plants the interplay of several export factors might regulate mRNA export.

Besides its role in mRNA export, human ALY is also implicated in transcriptional control. ALY interacts with two transcription factors that are involved in activation of the T cell receptor α gene (TCR α) enhancer (Bruhn et al., 1997), it associates with IWS1, a protein that interacts with the elongation factor SPT6 (Yoh et al., 2007) and the depletion of ALY results in transcription elongation defects (Domínguez-Sánchez et al., 2011). Stubbs and Conrad showed in 2015, that in human cells upon ALY depletion a variety of transcripts are downregulated in a cytoplasmic fraction and in a nuclear fraction demonstrating that the loss of ALY proteins leads to decreased transcription of particular transcripts. To verify if *Arabidopsis* ALY proteins are also involved in transcriptional control and to validate the results

obtained in this study it will be necessary to also fractionate plant cells into nuclei and cytosolic fraction and sequence both portions. Even though a clear separation of nuclei und cytosol is difficult in plants due to the presence of a rigid cell wall and a prominent vacuole, a successful separation of nuclear and cytoplasmic fraction was described in several studies (Park et al., 2005; Azevedo et al., 2019; Choudury et al., 2019).

3.2 *Arabidopsis* ALY proteins: a functional specialization?

Like mentioned above, the rather wildtype appearance of plants lacking two ALY factors and the severe phenotype of *4xaly* plants strongly suggests some kind of redundancy between ALY proteins, but the fact that plants express several ALY proteins also indicates that there might be some functional specialization among these factors. During characterization of the ALY proteins as possible export factors several findings further supported this hypothesis: Although *aly1 aly2* and *aly3 aly4* double mutants basically look like wildtype, *aly3 aly4* plants display a mild early flowering phenotype and a moderate mRNA export block suggesting that the proteins ALY1 and ALY2 have some different functions than the proteins ALY3 and ALY4 (Sørensen, 2016). A similar finding that the ALY proteins with the highest sequence identity (ALY1 and ALY2 54% amino acid sequence identity, ALY3 and ALY4 70% amino acid sequence identity) may have specific functions is indicated by a different subnuclear localization of these proteins. Although all four ALY proteins are nuclear proteins, ALY1 and ALY2 were detected primarily in the nucleoplasm of root cells whereas ALY3 and ALY4 were often strongly enriched in nucleoli (Pfaff et al., 2018). Differences between the four ALYs were also detected when analysing the expression and localization of ALY-GFP fusion proteins in the reproductive tissues. In pollen grains ALY4 was not expressed and ALY3 showed only weak expression in the nucleus of the pollen vegetative cell whereas ALY1-GFP and ALY2-GFP fusion proteins were detected in both vegetative cell and sperm cells. In ovules on the other hand, ALY2, ALY3 and ALY4 were expressed in the sporophytic tissue and ALY1 expression was restricted to the female gametophyte (Pfaff et al., 2018).

The phenotypic analysis of plants lacking three ALY proteins and expressing one ALY export factor demonstrated that different ALY proteins affect plant growth and development differently. The severe phenotype observed in *4xaly* plants is probably mainly caused by a simultaneous knockout of *ALY2, ALY3* and *ALY4* as *3xalyALY1* mutant plants show a similar phenotype like *4xaly,* which can be clearly distinguished from the other three triple mutants. The phenotypes of the different *3xaly* plants further suggest that ALY2, ALY3 and ALY4 have a similar influence on plant growth and development, different from the impact of ALY1, as *3xalyALY2*, *3xalyALY3* and *3xalyALY4* have rather comparable phenotypes clearly distinct from *3xalyALY1.* Although *3xalyALY2*, *3xalyALY3* and *3xalyALY4* have rather similar

phenotypes, differences regarding bolting time, rosette diameter and leaf morphology show that all four ALY proteins affect plant growth and development differently.

Even though there are clear phenotypic differences between the individual *aly* triple mutant plant lines, all four *aly* triple mutant plant lines exhibit significant differences compared to the Col-0 ecotype. This is different compared to the situation in the double mutants *aly1 aly2* and *aly3 aly4* which are only mildly affected (Sørensen, 2016) and what shows that the simultaneous knockout of three *ALYs* cannot be compensated by a redundant fourth ALY, resulting in defects in plant growth and development.

Since the main function of ALY proteins in eukaryotes is to act as mRNA export adaptors (Walsh et al., 2010; Heath et al., 2016), defects in plant growth and development should mainly be caused by mRNA export defects. In *4xaly* mutant plant lines the severe growth phenotype correlates with a bulk mRNA export block. Thus, the distinct phenotypes of the four *3xaly* mutants could either be caused by differences in a bulk mRNA export block or by a deficient export of specific transcripts or subsets of transcripts in the different *aly* triple mutants.

Interestingly, WISH mRNA export assays showed that the simultaneous knockout of three ALY proteins already causes a severe mRNA export defect in *Arabidopsis* similar to the export block observed in *4xaly* plants with no differences between the different *aly* triple mutants being detected. Since *aly1 aly2* and *aly3 aly4* double mutant plants show no or only a weak mRNA export defect and are not or only mildly affected in plant growth and development, a knockout of two ALY proteins can be most likely compensated by a redundant function of the remaining two functional ALY factors. The concomitant loss of three ALY proteins on the other hand results in a mRNA export block that causes defects in plant growth and development. WISH experiments further showed that the differences in *3xaly* and *4xaly* phenotypes are probably not caused by differences in a bulk mRNA export block but rather by a mRNA export-misregulation of specific genes or a subset of genes.

To gain insight into differential gene expression, the transcriptomes of *3xaly* and *4xaly* plants were compared relative to Col-0. It was further assumed that in principle if an ALY factor is necessary for the export of a transcript, 'its total levels may decrease upon ALY knockout if the transcript is more rapidly degraded when sequestered in the nucleus' (Stubbs and Conrad, 2015). To validate this hypothesis, candidate mRNAs detected in the cell fractioning experiment to be retained in *4xaly* nuclei were compared with candidates downregulated in *4xaly* mutant plants obtained by transcript profiling. The little overlap between the two experiments might be explained by plant material from different developmental stages and different experimental setups (RNA extraction method, RNAseq method) that were used for both sequencing approaches. It was assumed that a general downregulation in *3xaly* and *4xaly* mutants was primarily caused by a defect in mRNA export. In future experiments it might be

necessary to also sequence nuclei and total cells (or cytoplasm) from *3xaly* and *4xaly* mutant plants using plant material that was grown simultaneously and the same RNA extraction and sequencing methods for all tested specimen to show that a general downregulation correlates with mRNA export defects in *aly* mutants.

The most genes were downregulated in *4xaly* mutant plants what could explain the more severe phenotype of this mutant compared to the four *3xaly* plant lines. The RNAseq data also demonstrated that differences in the phenotypes of *3xaly* and *4xaly* mutant plants are likely caused by a misregulated mRNA export of specific transcripts or small subsets of mRNAs in the different mutants rather than by differences in a bulk mRNA export block. For instance, the mutant *3xalyALY4*, which shows a clear distinct phenotype compared to *4xaly*, shares around ~ 83% of reduced mRNAs with *4xaly*, whereas the mutants *3xalyALY2* and *3xalyALY3*, which display a similar phenotype like *3xalyALY4*, share much less downregulated transcripts with *4xaly*.

The bioinformatical analysis of RNAseq data revealed a subset of transcripts that might need the interplay of more than one ALY factor to be properly exported and subsets of transcripts that might be specifically exported by either ALY3 or ALY4. In contrast, only a couple of transcripts were not downregulated in *3xalyALY1* and *3xalyALY2* but downregulated in the other three *aly* triple mutants and *4xaly,* indicating that less transcripts might be specifically or preferentially exported by ALY1 or ALY2. The question if transcripts are really specifically exported or bound by one ALY or if transcripts can also be bound simultaneously by several, perhaps different ALY proteins would be interesting to answer by RNA immunoprecipitation methods. In human cells it could be shown that ALY proteins can bind to 5'end, 3'end and middle region of one transcript (Shi et al., 2017). Thus, it can be speculated that perhaps also in plants transcripts can be bound by several ALY proteins and perhaps a sophisticated interplay of several different ALY factors on one transcript regulates the nucleocytosolic transport.

Export assays, transcript profiling and qRT-PCR in the four *3xaly* and *4xaly* mutant plant lines showed, that differences in phenotypes between the different mutant plant lines are more likely caused by defective export of specific mRNAs or subsets of mRNAs in the different mutant plant lines rather than by differences regarding bulk mRNA export. RNAseq and qRT-PCR additionally revealed transcripts that might need the interplay of two or more ALY factors to be properly exported and transcripts that might be exported by specific ALY export factors. The expression and localization studies of ALY-GFP proteins and the phenotypic analysis of *3xaly* mutant plant lines showed that ALY1 may have a different function than especially ALY3 and ALY4. The observation that ALY1 may have a different function is further supported by a recent study which showed that ALY1 is the only *Arabidopsis* ALY protein that is involved in the

regulation of RNA-directed DNA methylation via export of the mRNAs *AGO6* and *DCL2* that generate proteins with known roles in RNA-directed DNA methylation (Choudury et al., 2019). RNAseq demonstrated that the differences between different *3xaly* phenotypes might be explained by a specific export of transcripts by different ALY export factors. In future experiments it will be crucial to show that the candidates that were bioinformatically identified and verified by qRT-PCR to be possibly specifically exported by ALY proteins are only properly exported in the *3xaly* mutant expressing the respective wildtype ALY protein. Besides the already mentioned RNAseq experiments of nuclei and total cells (or cytoplasm) also smFISH can be applied to validate the obtained candidates.

To globally identify transcripts that are bound by different ALY proteins, the iCLIP (individual-nucleotide resolution cross-linking and immunoprecipitation) method, that was successfully introduced for the use in plants, (Meyer et al., 2017) will be applied in future experiments. Since the protocol developed by Meyer *et al*. uses the 'GFP-trap' (Chromotek) to specifically immunoprecipitate GFP-fused RNA binding proteins after UV crosslinking, it was tested if an ALY-eGFP fusion protein is functional by expressing *ALY3-eGFP* driven by the endogenous promotor in the *4xaly* background. A limiting factor in plant affinity purification methods is often the amount of plant material that is needed for a successful immunoprecipitation (Van Leene et al., 2008). The amount of protein extract can be increased by using *Arabidopsis* cell suspension cultures. A well-established protocol uses SG-tagged bait proteins expressed in *Arabidopsis* cell suspension cultures for affinity purification (Van Leene et al., 2008; Pfab et al., 2017). Thus, it was additionally tested if *ALY3-SG* driven by the endogenous promotor in the *4xaly* background could complement the severe *4xaly* phenotype. The expression of both *ALY3-eGFP* and *ALY3-SG* clearly could complement the severe *4xaly* phenotype showing that both fusion proteins are functional and demonstrating that GFP and SG fused proteins can be used in future iCLIP experiments. ALY3-SG fusion proteins expressed in cell suspension cultures could be successfully UV-crosslinked to RNA in pilot experiments performed in this study and future RNA immunoprecipitation experiments will shed light on the RNA binding properties of different mRNA export factors.

3.3 UIEF proteins act as additional mRNA export factors

The viability of *4xaly* mutant plants showed, that in *Arabidopsis* apart from the four ALYs other proteins can act redundantly as mRNA export factors. In mammals, the TREX associated factors CHTOP, LUZP4, UIF and THOC5 can function as additional export adaptors and some functional redundancy with ALY was demonstrated since only simultaneous knockdown of ALY/THOC5, ALY/UIF and ALY/CHTOP leads to a severe mRNA export defect (Hautbergue et al., 2009; Viphakone et al., 2012; Chang et al., 2013). To identify additional mRNA export

factors in *Arabidopsis,* amino acid sequences of the human export factors LUZP4, CHTOP and UIF were used as queries to search for similar proteins in the *Arabidopsis* database (https://www.arabidopsis.org) using the BLAST algorithm. No proteins with similarity to LUZP4 and CHTOP were found but two proteins with similarities to the human UIF export adaptor were identified. In human cells UIF directly interacts with UAP56 through a N-terminal UBM and this interaction is required for UIF recruitment to mRNA (Hautbergue et al., 2009). A direct protein-protein interaction between both UIEF1, UIEF2 and UAP56 could also be detected *in planta* by FRET experiments. Like described in humans, this interaction is mediated by a conserved N-terminal UBM since mutating the UBM of UIEF1 abolished the interaction with UAP56. Since a UBM mediated protein-protein interaction between UIEFs and UAP56 was also detected by Y2H (Ehrnsberger et al., 2019b), it can be assumed that the mechanism of UIEF recruitment to mRNA is conserved in humans and *Arabidopsis*.

In human cells it was shown that UIF binds RNA *in vitro* and *in vivo* (Hautbergue et al., 2009). Although no known RNA-binding motifs are present in UIEF1 or UIEF2, *in vitro* MST analysis showed that UIEF1 preferentially binds ssRNA with the C-terminal part of the protein mainly contributing to the RNA interaction (Ehrnsberger et al., 2019b).

The nuclear localization of UIEF1-GFP and UIEF2-GFP fusion proteins in all root cells was in line with a possible function of the UIEF proteins as mRNA export factors since in other eukaryotes export adaptors remain nuclear and do not travel to the cytosol (Walsh et al., 2010).

The combined loss of both UIEF proteins has compared to the combined loss of the four ALY proteins a rather weak impact on plant growth and development. Furthermore, in contrast to ALY proteins the loss of UIEF factors does not affect the reproduction of plants what could be explained by the absence of UIEF proteins in the reproductive tissue since UIEF-GFP fusion proteins could not be detected in ovules or pollen (Ehrnsberger et al., 2019b). Although the *uief* mutants do not display a severe phenotype like *4xaly,* mild growth defects could be observed in *uief* single mutants and the respective *uief* double mutant. These defects correlated with a moderate mRNA export block in the *uief* mutant genotypes suggesting a role of UIEF proteins in mRNA export. The analysis of a mutant lacking four ALY proteins and two UIEF proteins further showed that UIEF proteins are important for efficient nucleocytosolic mRNA export. Similar to the situation in human cells where only a combined knockdown of the export adaptors ALY and UIF results in a severe mRNA export block (Hautbergue et al., 2009), a stronger mRNA export defect was detected in *4xaly 2xuief* compared to *4xaly* what correlated with more pronounced plant growth and development defects.

The transcriptomes of *2xuief*, *4xaly* and *4xaly 2xuief* plants revealed that in the quadruple and sextuple mutants about 2-times more transcripts were downregulated compared to *2xuief* what might explain the severe phenotypes of *4xaly* and *4xaly 2xuief* plants and the rather wildtype

appearance of *2xuief* plants. In *4xaly* and *4xaly 2xuief* a similar number of candidate transcripts was downregulated, and more than half of these candidates were shared in both mutants what reflects the rather similar phenotypes. qPCR validation of these candidates that were downregulated in *4xaly* and *4xaly 2xuief* but not in *2xuief* verified that there is a variety of transcripts that depend on specifically ALY-family proteins to be properly exported. Furthermore, the candidates that were selected for qRT-PCR validation were also part of the list of 950 candidate transcripts that were identified in the cell fractioning experiment to be retained in *4xaly* nuclei. The downregulation of both candidates in *4aly* and 4xaly *2xuief* mutants validated the partial overlap of candidates identified in the cell fractioning experiment to be retained in *4xaly* nuclei and candidates being downregulated in *4xaly* identified by transcriptome profiling.

Bioinformatical analysis of the RNAseq data identified only 61 candidates that were significantly downregulated in *2xuief* and *4xaly 2xuief* but not in *4xaly* indicating that only a small subset of transcripts may depend on UIEF proteins to be properly exported. RNAseq results showed that the majority of the 61 candidates that might be specifically or preferentially exported by UIEF proteins were also downregulated to some extent in *4xaly.* qRT-PCR supported the downregulation in *4xaly*, especially for the candidate AT3G06145 that showed reduced transcript levels in all mutant genotypes compared to Col-0. Thus, some mRNAs are potentially specifically or preferentially exported by UIEF proteins or these mRNAs require both ALY and UIEF factors for a successful nucleocytosolic mRNA export.

Several candidates were identified that belong to this group of transcripts that potentially depend on ALY and UIEF proteins for a successful mRNA export. A variety of transcripts were downregulated in *2xuief*, *4xaly* and *4xaly 2xuief* with the majority of these candidates showing the least downregulation in *2xuief*. It can be speculated that an additive effect of *aly* and *uief* mutations contributes to the more severe phenotype of *4xaly 2xuief* plants compared to *2xuief* and *4xaly.*

3.4 *Arabidopsis* mRNA export factors: diversified and specialized?

The results obtained in this study analysing different export factor candidates demonstrated that the four *Arabidopsis* ALY proteins function as mRNA export factors and that they are recruited to the TREX complex by a protein-protein interaction with the RNA helicase UAP56 (Figure 42 A). Some functional redundancy between ALY proteins and/or other export factors is very likely (Figure 42 B) since *aly* single and double mutants are not or only mildly affected regarding plant growth and development and show no or only a moderate mRNA export block whereas *4xaly* plants display a severe phenotype and a bulk mRNA export block. This study further indicates that the diversification of ALY proteins is accompanied by a (partial) functional

specialization since *3xaly* plants show distinct phenotypes and different ALYs might export specifically or preferentially distinct subsets of transcripts (Figure 42 C). The challenge of future investigations will be to analyse possible specific functions of different ALYs and to test if a specialization within the ALYs could be combined with tissue- and/or developmental stage-specific effects.

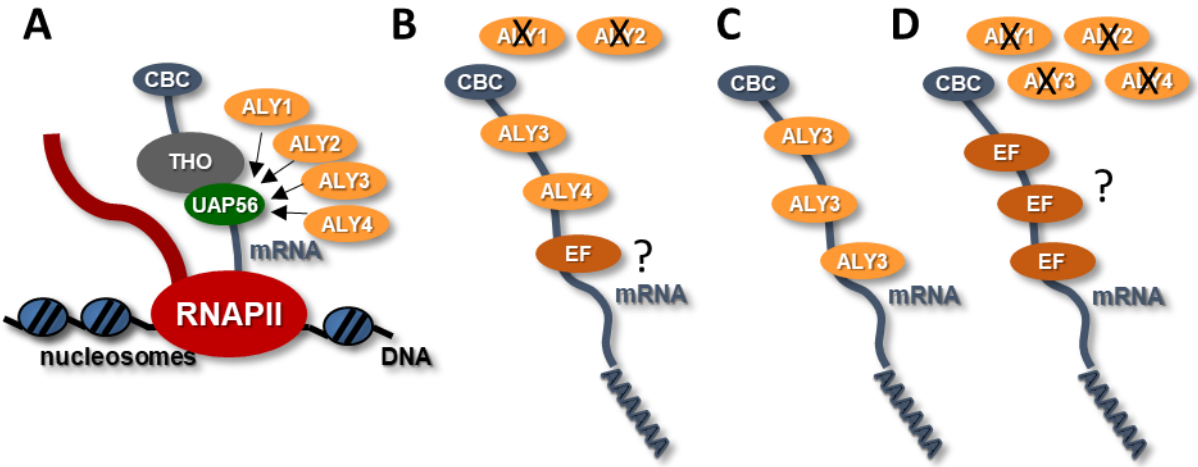

Figure 42. ***Arabidopsis*** **ALY proteins function as mRNA export factors.** (A) Four ALY proteins function as mRNA export factors and are recruited to TREX by an interaction with UAP56. (B) There is functional redundancy between ALY proteins and perhaps other export factors (EF) but (C) some transcripts are also specifically or preferentially exported by specific ALY export factors. (D) The viability of *4xaly* plants shows that similar to the situation in humans other export factors exist.

The viability of *4xaly* plants indirectly showed that additional export factors can act redundantly in the absence of the four ALY proteins (Figure 42 D) and in following experiments two UIEF proteins were characterized as additional redundant mRNA export factors that are recruited to the TREX complex by a protein-protein interaction with UAP56 (Figure 43 A). RNAseq analysis showed that a variety of transcripts use a putative specific ALY export mechanism (Figure 43 B) but it is rather unlikely that transcripts are specifically or preferentially exported by UIEF proteins. UIEF proteins are probably involved in the export of only a subset of mRNAs and it can be assumed that UIEF proteins regulate the export of these transcripts in close collaboration with ALY proteins (Figure 43 C). This is in line with findings in mammals where ALY and UIF were found to bind the same mRNA molecules (Hautbergue et al., 2009). The assumption that the mRNA export of less transcripts is regulated by UIEF proteins is also supported by a likely reduced UIEF protein expression compared to ALY proteins (Ehrnsberger et al., 2019b) what was also observed in mouse cells, where UIF is expressed at ~40-fold lower protein levels than ALY (Heath et al., 2016). Since also *4xaly 2xuief* plants are viable it seems that the situation in plants is similar to the situation in mammals where a variety of proteins can function as mRNA export adaptors. Shuttling serine/ arginine-rich (SR) proteins, that are also characterized in plants (Tillemans et al., 2005; Rausin et al., 2010) are candidates that might function as additional mRNA export factors as these proteins were characterized in other

organisms as mRNA export adaptors (Huang et al., 2003; Müller-McNicoll et al., 2016). The challenge of future studies will be to analyse to what extent mRNA factors are diversified in plants and what are the factors that in addition to the ALY and UIEF proteins regulate the nucleocytosolic mRNA export.

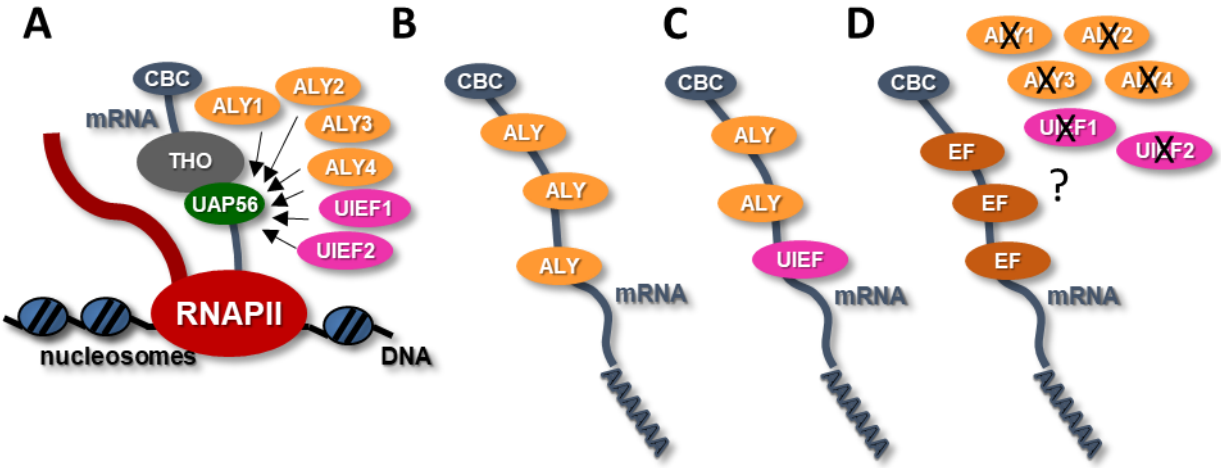

Figure 43. ***Arabidopsis*** **UIEF proteins function as mRNA export factors.** (A) Besides the four ALY proteins two UIEF proteins function as mRNA export factors and are recruited to TREX by an interaction with UAP56. (B) A variety of transcripts depends on ALY proteins only to be properly exported and (C) some transcripts need both ALY and UIEF proteins for a successful nucleocytosolic mRNA export. (D) The viability of *4xaly 2xuief* plants shows that similar to the situation in humans other export factors exist.

3.5 The interactome of *Arabidopsis* mRNA export factors

3.5.1 Export factors do not stably associate with THO

The interaction of ALY export adaptors with other components of TREX is conserved across eukaryotes. In human cells, ALY directly interacts with THO2 and THO5 *in vitro* and in both yeast and humans Yra1 and ALY associate with components of THO *in vivo* (Sträßer et al., 2002; Masuda et al., 2005; Chi et al., 2013). An interaction of both ALY (Yra1) and UIF with UAP56 (Sub2) is also well described in humans and yeast but under high salt conditions (350 - 500 mM) the interaction of THO and ALY/UAP56 is disrupted in human cells (Sträßer et al., 2002; Masuda et al., 2005; Hautbergue et al., 2009; Dufu et al., 2010; Chi et al., 2013). In *Arabidopsis,* under high-salt conditions ALY proteins do not form a stable complex with THO and UAP (Yelina et al., 2010) but under less stringent conditions ALY3 co-purified with the TREX subunit TEX1 and ALY2 and ALY4 co-purified with UAP56 (Sørensen et al., 2017). Since the same experimental setup was used in Sørensen *et al.* like applied in this study, it is surprising that no other components of TREX apart from ALY and UIEF were co-purifying with SG-tagged ALY or UIEF export factors. In *Arabidosis* cell suspension cultures used in this study, bait proteins are preferentially expressed by the strong 35S promotor because cell cultures have a high ploidy level (9n) and the expressed fusion proteins have to compete with

relatively high amounts of endogenous proteins for complex assembly (Van Leene et al., 2015). The overexpression of bait proteins might explain the results that TREX components did not co-purify with ALY-SG or UIEF-SG proteins since overexpression can also impair protein folding and complex assembly (Gibson et al., 2013) but the fact that also under stringent binding conditions ALY proteins do not associate with other TREX subunits indicates that the association of ALY and UIEF proteins with the remaining TREX is rather loose in *Arabidopsis* (Yelina et al., 2010).

3.5.2 ALY1, ALY2 and UIEF1 share a variety of interactors

Eluates of the export factor affinity purifications after SDS-PAGE and Coomassie-staining using ALY1-SG, ALY2-SG and UIEF1-SG as bait proteins showed similar results. MS analysis confirmed that ALY1, ALY2 and UIEF1 share a variety of putative interaction partners with ALY1-SG and ALY2-SG sharing around ~60% true interactors, ALY1-SG and UIEF1-SG sharing around ~52% true interactors and ALY2-SG and UIEF1-SG sharing around ~54% true interactors. AL3-SG and ALY4-SG on the other hand share less putative interactors with the other export factors and proteins co-purifying with UIEF2-SG are clearly distinct from the proteins detected by AP-MS in the other experiments (Table 6).

Table 6. Shared true interactors in ALY-SG and UIEF-SG AP-MS experiments. (A) Four ALY and two UIEF export factors fused to a SG tag were used as bait proteins for co-IP experiments. Percentage of shared interactors between different AP-MS experiments is depicted.

	ALY1-SG	ALY2-SG	ALY3-SG	ALY4-SG	UIEF1-SG	UIEF2-SG
ALY1-SG	100%	60%	32%	25%	52%	7%
ALY2-SG	60%	100%	25%	24%	54%	7%
ALY3-SG	32%	25%	100%	26%	21%	5%
ALY4-SG	25%	24%	26%	100%	22%	7%
UIEF1-SG	52%	54%	21%	22%	100%	8%
UIEF2-SG	7%	7%	5%	7%	8%	100%

Thus, the hypothesis can be proposed that the proteins ALY1 and ALY2, which share ~54% amino acid sequence identity, might not only be involved in the nucleocytosolic transport of distinct sets of mRNAs compared to ALY3 and ALY4, but they could also be involved in different regulatory processes mediated through interactions with specific factors. In human cells, ALY is also involved in transcriptional control by interaction with AML-1 and LEF-1 transcription factors, it can enhance b-ZIP transcription factor interactions and it modulates the activity of transcription factor E2F2 (Bruhn et al., 1997; Virbasius et al., 1999; Osinalde et al.,

2013). Among the four interactors with the highest scores in the ALY1-SG, ALY2-SG and UIEF1-SG experiments the proteins GBF-interacting protein 1 (GIP1, At3g13222) and GBF-interacting protein 1-like (GIP1L, AT1G55820) were detected, which function as co-activators of b-ZIP transcription factors (Sehnke et al., 2005; Lee et al., 2014; Shaikhali, 2015). Thus, it is possible that ALY1, ALY2 and UIEF1 are involved in transcriptional control by contributing to bZIP-mediated gene regulation like observed in humans and it will be challenging to investigate in future experiments if also in plants a possible connection between ALY proteins and transcriptional regulation exists.

3.5.3 An interaction between export factors?

MS results revealed a remarkable trend of export factors co-purifying with another. Apart from UIEF2, which co-purified with distinct proteins compared to the other five export factors (Table 6), a specific co-purification between ALY3 and the other four export factors as well as between UIEF1 with ALY1 and ALY2 was detected. Additionally, several export factors co-purified but since ALY1, ALY2 and ALY4 were also detected in the unfused SG negative control it is not possible to draw conclusions about the specificity of these putative interactions. However, it is possible that some of these co-purifications were specific as for instance ALY4 was detected in the ALY1-SG, ALY2-SG, ALY3-SG and UIEF1-SG experiments with more than a five-fold higher MASCOT score than in the unfused SG negative control. It is rather unlikely that the association of different export factors is mediated by direct protein-protein interactions since Y2H assays detected no or only very week reciprocal interactions between different ALY proteins (Koroleva et al., 2009). RNAseq experiments performed in this study suggested that most single mRNA molecules are not targeted by one ALY or UIEF protein or by one group of ALY proteins but rather that different ALY and UIEF factors may bind to one mRNA molecule. In addition to the possibility that ALY proteins may interact with different parts of a single mRNA molecule, the binding of several export factors to a single mRNA molecule may be important in packaging mRNPs (Heath et al., 2016; Pfaff et al., 2018). Hence tight packaging of mRNPs might prevent complete cleavage of some mRNAs by the endonuclease benzonase resulting in the co-purification of proteins that bind in close proximity to a single mRNA molecule. One of the main tasks of upcoming studies will be to analyse to what extent different ALY and/or UIEF proteins potentially bind to a single RNA molecule using RNA immunoprecipitation methods.

3.5.4 Export factors interact with proteins comprising a NTF2 domain

‘The mechanism of mRNA export in plants is still a black box, largely because no homologs of the known mRNA export receptors in yeast and mammals can be identified by sequence

similarity' (Meier, 2012). Thus, it is possible that plants use one or more factors that could share features and function with human NXF1 and yeast Mex67 or in plants a distinct mechanism of mRNA export evolved. Since in metazoans and yeast the mRNA export receptor NXF1 (Mex67) physically interacts with mRNA export adaptors such as ALY and UIF (Hautbergue et al., 2009, Heath et al., 2016), a proteomic analysis of putative interaction partners of export factors should reveal candidates that share features with human NXF1.

AP-MS experiment revealed seven putative interactors of export factors that all display a NTF2L domain and a predicted RRM motif. In yeast and metazoans it was shown that the NTF2L domain is crucial for the function of the heterodimeric export receptor since the interaction of both subunits is mediated by contact of the NTF2L domains of both proteins (Herold et al., 2001, Katahira et al., 2002, Fribourg and Conti, 2003, Valkov et al., 2012). Additionally, the NTF2L domain of NXF1 binds FG motifs present in Nups and this interaction is crucial for the transported mRNP to overcome the NPC barrier (Liker et al., 2000; Grant et al., 2003; Stewart, 2010). A co-purification of especially NXF2-NXF6 with ALY1, ALY2 and UIEF1 is supported by very high MASCOT scores whereas NXF1 might co-purify only with ALY3. NXF2, NXF4 and NXF7 were also detected in the unfused SG negative control but compared to the more likely unspecific co-purification of some export factors, a detection of especially NXF2 and NXF4 in several AP-MS experiments with very high MASCOT scores compared to the MASCOT scores of the detection in the negative control is a strong indication that the co-purification between export factors and both NXF2 and NXF4 is rather specific. NXF2 for instance was detected in all ALY1-SG, ALY2-SG and UIEF1-SG AP-MS experiments with an average MASCOT score more than 18-fold higher than the detection in the negative control. Accordingly, NXF4 was detected in all ALY1-SG, ALY2-SG and UIEF1-SG AP-MS experiments with an average MASCOT score more than 11-fold higher than in the negative control.

Reciprocal tagging, that is recommended to verify interactors when working with affinity purification in *Arabidopsis* cell culture (Dedecker et al., 2015), confirmed a possible interaction between various NXF candidates and export factors and additionally revealed possible interactions between several export receptor candidates. In yeast and metazoans, the small subunit of the heterodimeric export receptor (NXT1/Mtr2) is composed of an NTF2L domain only. In *Arabidopsis* the three NTF2L containing candidates NTF2a (AT1G27310), NTF2b (AT1G27970) and NTL (AT1G11570) consist of an NTF2L domain only but none of these factors co-purified with the seven NXF candidates. Hence it is unlikely that plants use a similar heterodimeric receptor(s) like other eukaryotes that consists of a bigger NXF-like and a smaller NXT-like subunit. But if the basic mechanism of an mRNA export receptor dimer, connected by an interaction of two NTF2L domains, is conserved, it is also possible that homo- and/or heterodimers built by NXF candidates function as mRNA receptor(s) in plants. Candidate pairs

that might form heterodimers are for instance NXF4/NXF6 and NXF5/NXF7 since for both pairs the two factors were detected in the reciprocal AP-MS experiments with very high MASCOT scores and additionally a direct protein-protein interaction of NXF4 and NXF6 was detected in a global Y2H screen (Arabidopsis Interactome Mapping Consortium, 2011). Y2H experiments analysing the seven NXF candidates further confirmed a possible heterodimerization of candidates NXF3 and NXF4 and additionally demonstrated that these two proteins might also form homodimers since a reciprocal protein-protein interaction was detected for both proteins (Hachani, 2018).

Reciprocal AP-MS experiments using export factors and export receptor candidates demonstrated that in plants it is rather unlikely that only one export receptor exists. It is possible that in plants not only export factors are diversified but also several export receptor homo- and/or heterodimers may contribute to mRNA export. It is also possible that similar to export factors these receptors function in parts redundantly what makes it challenging to proof that mRNA export receptor candidates are involved in mRNA export.

3.5.5 Export receptor candidates interact with the NPC

AP-MS showed that several receptor candidates may interact with the NPC, a feature that might also be important for a plant mRNA export receptor since in other eukaryotes export receptors interact with the NPC (Stewart, 2010). Except for NXF5 and NXF7, various Nups co-purified with the remaining five receptor candidates. In total 17 out of 30 Nups identified 2010 by Tamura et al. in a seminal proteomic study to build the plant NPC were detected at least once in the different AP-MS experiments. Over the last years some additional NPC associated factors were identified and studies on several *nup* mutants in plants revealed that specific Nup function may vary significantly between eukaryotes and that certain plant Nups are involved in diverse signalling pathways, play specific cellular roles and influence plant growth by different molecular mechanisms (Parry, 2014, Parry, 2015). Although some Nups are missing in plants or have been replaced by plant-specific proteins, the subcomplexes and Nup classes are well conserved (Meier et al., 2017). A key role in the nucleocytosolic transport of mRNPs is played in yeast and metazoans by the FG-Nup class since these factors interact with the export receptor NXF1/Mex67 and mediate the translocation through the NPC. (Bachi et al., 2000; Liker et al., 2000; Strässer et al., 2000; Stewart, 2010; Ben-Yishay et al., 2019). In *Arabidopsis* 10 Nups are rich in FG repeats (Tamura et al., 2010) and AP-MS experiment revealed that the FG-Nup NUP98b is a true interactor of NXF4 and the FG-Nup NUP98a is a true interactor of NXF1 and NXF4. Additionally, 11 Nups from other classes co-purified with NXF1 and 9 Nups from other classes co-purified with NXF4 highlighting a possible interaction of especially these two candidates with the NPC.

3.6 NTF2L containing proteins in *Arabidopsis*

Besides their function as mRNA export receptors, in other eukaryotes NTF2L domain carrying proteins are also involved in the recycling of RanGDP back to the nucleus, there are NTF2L proteins that are stimulators of export for NES-containing proteins and proteins containing one NTF2L domain and one RRM domain can act as eukaryotic Ras-GTPase-activating protein (GAP)-binding proteins (G3BP's, Nehrbass and Blobel, 1996; Smith et al., 1998; Herold et al., 2000; Tourriere et al., 2001).

The 19 plant NTF2L containing proteins can be classified into two groups. Proteins of group one contain both NTF2L and RRM domains and proteins of group two display NTF2L domains but no RRMs (Reichel et al., 2016). From the proteins that do not contain any RRM motifs only two of the three proteins that comprise an NTF2L domain only are further characterized. Besides similarities in domain structure to yeast Mtr2 and human NXT1, the three 'NTF2L domain only' factors also show significant sequence similarity to yeast and human NTF2, the protein that mediates the recycling of RanGDP back to the nucleus (Zhao et al., 2006). NTF2a (AT1G27310) and NTF2b (AT1G27970) could functionally replace NTF2 in yeast, were located at the nuclear rim, could bind Ran and were hence described as the factors that mediate Ran import in *Arabidopsis* (Zhao et al., 2006). NTL (AT1G11570) could not be described as an ortholog of NTF2 and is consequently the only candidate that might have a similar function like NXT1/Mtr2, but since NTL was not detected in any AP-MS experiment it is rather unlikely that an NXT1/Mtr2 ortholog exists in *Arabidopsis*.

A study published 2018 proposed that the eight candidates that contain both NTF2L and RRM and that comprise the seven candidates analysed in this study, are orthologs of the human RNA-binding protein Ras-GTPase activating protein SH3-domain–binding protein 1 (G3BP1, Abulfaraj et al., 2018). G3BP1 is located in stress granules (SGs) in the cytoplasm and contributes to their assembly (Tourrière et al., 2003). SGs are large macromolecular aggregates which basically contain stalled translation initiation complexes and mRNAs. (Reineke et al., 2017). Within the SGs, the phosphorylation-dependent endoribonuclease G3BP1 interacts with 40S ribosomal subunits and is tightly associated with a subset of poly(A) mRNAs (Tourriere et al., 2001; Kedersha et al., 2016). In *Arabidopsis* in the last years the candidates NXF1 and NXF4 were proposed to be G3BP1 orthologs that are located in SGs and function in virus resistance and plant immunity (Krapp et al., 2017; Abulfaraj et al., 2018). A study that used the interactome capture method to identify the portion of the proteome that binds mRNA in etiolated *Arabidopsis* seedlings further demonstrated that all seven NXF candidates analysed in this study bind mRNA *in vivo* (Reichel et al., 2016). This feature would argue for both scenarios, the NXF candidates as diversified mRNA receptors and the NXF candidates as diversified structural components of SGs.

3.7 The localization of NXF candidates

The subcellular localization of NXF-GFP fusion proteins is significantly different compared to the subcellular localization of Mex67-GFP in yeast and NXF1-GFP in human cells. Mex67-GFP reveals a typical nuclear pore labelling, with just some signal in the nucleoplasm and cytoplasm whereas NXF1-GFP is enriched at the nuclear envelope, shows a nuclear signal and just some signal in the cytoplasm (Segref et al., 1997; Fribourg et al., 2001). In contrast, the seven NXF candidates fused to eGFP and expressed in *N. benthamiana* or fused to GFP and expressed by the endogenous promotor in the respective mutant background in *Arabidopsis* showed a predominately cytosolic localization. Additionally, when expressing the fusion proteins in tobacco leaf epidermis cells, an enriched signal could be detected at the nuclear envelope what would argue for a function of the seven candidates as transporters through the NPC and against a function of NXF candidates as SG components. An enriched signal could also be observed in leaf mesophyll protoplasts where the *NXF1-GFP* expression was driven by the endogenous promotor demonstrating that the enriched signal around nuclei in tobacco cells might not be an artefact of overexpressing the candidate eGFP fusion proteins. The co-localization experiments of Nup markers and NXF candidates in tobacco cells and *Arabidopsis* leaf protoplasts showed that both proteins are enriched around the nuclear envelope, but a clear co-localization could not be observed. Since the Nup marker Nup54 is an FG-Nup that is lining the central channel and the Nup marker Nup35 is an inner ring complex Nup (Beck and Hurt, 2017) it is not surprising that no clear co-localization can be observed when NXF candidate fusion proteins are mainly cytosolic and might hence be enriched at the cytosolic site of the nuclear envelope.

The localization analysis of NXF candidate fusion proteins in combination with the localization of different Nup markers revealed a fundamental problem in describing the NXF candidates as potential export receptors, since compared to yeast or human export receptors the majority of all seven NXF candidate proteins are distributed in the cytosol and it could not be unequivocally shown that NXF candidate proteins are also found in the nucleus. Proteins containing leucin-rich export signals (NES) are exported from the nucleus by the export receptor AtXPO1 and this export can be inhibited by the cytotoxin leptomycin B (LMB, Haasen et al., 1999). When NXF candidate proteins are at any time located in the nucleus and are then exported to the cytosol by AtXPO1, it can be assumed that a treatment with LMB should result in a nuclear enrichment of NXF candidate proteins in the nucleus. Preliminary experiments treating tobacco leaves transiently expressing NXF-eGFP proteins with LMB did not reproducibly lead to an enrichment of NXF candidate fusion proteins in the nucleus (data not shown) but by improving the experimental setups in future experiments it could be possible to show that NXF candidates are not only located in the cytoplasm, but also in the nucleus. Additionally, nuclei purification from wildtype *Arabidopsis* plants or stable transformed plant lines expressing NXF-GFP fusion

proteins and detection by western blotting of either endogenous NXF proteins with antibodies that were recently produced or NXF-GFP fusion proteins with antibodies against GFP can shed light on the question if NXF proteins are also located in the nucleus. Pilot immunolocalization experiments using antibodies raised against NXF1 indicated that endogenous NXF1 is also located in the nucleus supporting the hypothesis that NXF1 may function as an mRNA export receptor.

3.8 NXF candidates: possible mRNA export receptors or SG components?

Some results obtained in this study point to a possible function of NXF candidates as structural components of SGs, but some other findings indicate that NXF candidates might act as mRNA export receptors. In mammalian cells, key SG components are eukaryotic initiation factors eIF3, eIF4E, eIF4G, the phosphorylation-dependent endoribonuclease G3BP1 and 40S ribosomal subunits (Kedersha et al., 2002; Tourrière et al., 2003; Kedersha et al., 2016). It was further shown that casein kinase 2 (CK2) is the enzyme that phosphorylates G3BP1 and regulates SG formation and that binding of G3BP1 to USP10 inhibits the assembly of SGs (Panas et al., 2015; Kedersha et al., 2016; Reineke et al., 2017).

In AP-MS experiments using the seven NXF candidates as bait proteins several SG components co-purified with the different NXF candidates. A very striking connection between especially the two candidates NXF1 and NXF4 with proteins from SGs could be detected (Table 7).

Table 7. Components of *Arabidopsis* SGs co-purifying with NXF-candidates.

TAIR	DESCRIPTION	NXF1-SG	NXF2-SG	NXF3-SG	NXF4-SG	NXF5-SG	NXF6-SG	NXF7-SG	SG
AT3G60240	eIF4G	4094/3	967/3	418/3	4427/3		364/3		117/2
AT3G50000	CKII ALPHA-2	347/ 2							
AT2G23070	CKII ALPHA-4	217/ 2							
AT3G19130	RBP47B	125/ 2							
AT1G47128	RD21A	141/ 2			135/ 2				
AT4G30890	UBP24	232/ 2	1796/ 3	1241/ 3	3127/ 3	1382/ 3	1041/ 3	576/ 3	
AT2G32060	40S PROTEIN S12	547/ 2	464/ 3	766/ 2	605/ 3	433/ 3	142/ 2		
AT4G30800	40S PROTEIN S11	384/ 2	421/ 3	333/ 3	346/ 3	361/ 2	280/ 3		
AT3G10090	40S PROTEIN S28-1	256/ 2				108/ 2			
AT5G64140	40S PROTEIN S28	126/ 2							
AT2G19750	40S PROTEIN S30				95/ 2				

Translation initiation factor eIF4G (AT3G60240) was in both NXF1-SG and NXF4-SG AP-MS experiments among the two co-purified proteins with the highest MASCOT scores. Although eIF4G was also detected in the unfused SG negative control, a detection with a MASCOT score more than 35-times higher in the NXF1-SG and NXF4-SG experiments clearly indicates

a putative interaction between both candidates and the SG component eIF4G. In the NXF1-SG AP-MS experiments, additionally two subunits of casein kinase 2 (CK2, AT3G50000, AT2G23070) and the *Arabidopsis* SG component RBP47B (AT3G19130; Weber et al., 2008) co-purified while the *Arabidopsis* SG component RD21A (AT1G47128; Bogamuwa and Jang, 2016) was identified in both NXF1-SG and NXF4-SG experiments. Proteins that were detected in the majority of the seven NXF candidate AP-MS experiments were on the one hand 40S ribosomal subunits and on the other hand UBP24 (AT4G30890), the ortholog of human USP10, which was detected with very high scores especially in the NXF2-NXF7-SG AP-MS experiment and which was also identified to directly interact with NXF1 in *Arabidopsis* (Krapp et al., 2017).

In contrast, NXF candidates co-purified reproducibly with export factors and components of the NPC what indicates a possible function as mRNA export receptors. These possible interactions were further supported by Y2H experiments performed in our lab (data not shown). But what could cause the discrepancy between an interaction with cytosolic SG components on the one hand and nuclear export factors on the other hand? Since both NXF candidates and export factors can bind mRNA *in vivo* it is possible that an interaction between both types of proteins is mediated by unspecific mRNA binding (Reichel et al., 2016; Choudury et al., 2019). A treatment with the endonuclease benzonase should prevent nucleic acid mediated protein binding but if mRNAs are bound by several export factors (what can be assumed according to the results obtained in this study) and hence tightly packed it cannot be excluded that catalytic cleavage of mRNA is perhaps partially inhibited. This would make an unspecific, mRNA mediated binding with a class of proteins that tightly bind to a subset of mRNAs (Tourriere et al., 2001) possible and could explain the co-immunoprecipitation between various export factors and NXF candidates.

Thus, in future experiments it will be crucial to further analyse protein-protein interactions between export factors, NXF candidates and SG components by for instance *in vivo* FRET and Y2H experiments or *in vitro* pulldowns to show to what class of proteins the NXF candidates can be assigned or if there are some NXF candidates that might be part of SGs and some NXF candidates that could function as mRNA export receptors. Besides the above-mentioned key experiments to show if NXF candidates are at any time located in the nucleus, a feature that would be essential for possible mRNA export receptors, studies inducing SGs in NXG-GFP expressing plants will be important to define NXF candidates as possible components of SGs. Incubation for 45 min at 37 °C to induce heat stress or treatment with potassium cyanide to cause respiratory stress resulted in the formation of stress granules in NXF1-GFP expressing plants (Krapp et al., 2017). Similar treatments of plants expressing NXF-GFP proteins will show if NXF candidates will assemble into stress granules.

Ultimately analysis of higher order *nxf* mutants will show if some NXF candidates could be involved mRNA export. Plants lacking the candidates NXF1-NXF4 and plants lacking the candidates NXF5-NXF7 show no export block and are not or only mildly affected in plant growth and development. This can have two reasons. Either plant mRNA export receptors are diversified and can function redundantly or NXF candidates have other functions, for instance as components of SGs. Currently a mutant is generated lacking all seven NXF candidates. If these plants do not show a bulk mRNA export block it is a strong indication that NXF candidates are not involved in mRNA export but if these plants show mRNA export defects it can be assumed that some of the candidates could function as possible mRNA export receptors.

4. Materials

4.1 Instruments

Table 8. Instruments used in this study.

Instrument	Model/Manufacturer
Centrifuges	Sorvall Evolution RC and Sorvall LYNX 4000 equipped with SLA1500 or SS34 rotor (Thermo Fisher Scientific), Centrifuge 5417R and 5804 R (Eppendorf)
Digital camera	EOS 600D equipped with Macro lens EF-S 60 mm 1:2.8 USM or a ETS 18-55 mm objective (Canon)
Homogenizer	TissueLyser II (Quiagen)
Hybidization Oven	Hybridisierungsöfen (Uniequip)
Imager	BioDocAnalyze System (Biometra), Intas Gel iX 20 plus (Intas)
Microscope	TCS SP8 (Leica), SMZ645 stereo microscope (Nikon) with KL 1500 LCD (Schott), Discovery V8 stereo with Axiocam MRc5 and KL1500 LCD (Zeiss)
Plant incubator	Plant incubator (Percival Scientific)
Quantum Meter	Quantum Flux ML-200 (Apogee Instruments)
RT-qPCR Cycler	Mastercycler® ep RealPlex (Eppendorf)
Shaking Incubator	Multitron Standart, Pro, Ecotron, Minitron (Infors HT)
Sonicator	UW2070 MS73 (Bandelin electronic)
Spektrophotometer	NanoDrop ND-1000 (PEQLAB)
Thermocycler	T3000 Thermocycler and T Gradient (Biometra)

4.2 Chemicals and enzymes

Chemicals and reagents were purchased from Applichem (Germany), Carl Roth (Germany), Clonetech, Duchefa (Netherlands), Fluka (Switzerland), Life Technologies (UK), Merck (Germany), Sigma Aldrich (Germany), USBiologcal (USA), and VWR (USA). Enzymes were purchased from Thermo Fisher Scientific (USA), PEQLAB/VWR (USA) and New England Biolabs (USA).

4.3 Oligonucleotides

Table 9. List of oligonucleotides used in the cell fractioning experiment. Oligonucleotides were obtained from MWG eurofins genomics. No = lab ID

Sequence 5'- 3'	Description	No.
AGGCGCGCAAATTACCCAATC	qRT-PCR normalization 18S rRNA	5028
CAGACTCGAAAGAGCCCGGTATTG	qRT-PCR normalization 18S rRNA	5029
AACAAAGCGTCCGGTGAGAACC	qRT-PCR normalization u12 snRNA	5034
AGTAAGCAGCGTCAACACATCGG	qRT-PCR normalization u12 snRNA	5035
TGGGAAAGTGTTGCCATCC	qRT-PCR normalization GAP (AT1G13440)	4973
CTTCATTTTGCCTTCAGATTCCTC	qRT-PCR normalization GAP (AT1G13440)	4974
AACGTGGCCAAAATGATGC	qRT-PCR normalization PP2AA (AT1G13320)	4977
CACATTGTCAATAGATTGGAGAGC	qRT-PCR normalization PP2AA (AT1G13320)	4978
CGTACAACCGGTATTGTGC	qRT-PCR normalization ACT2 (AT3G18780)	3384
GTCCAGCAAGGTCAAGACG	qRT-PCR normalization ACT2 (AT3G18780)	3385
AGGCATTGCATTGACTTCACCAG	qRT-PCR (AT1G73480)	4949
GCCATGATTGGAGCAAGAACAGC	qRT-PCR (AT1G73480)	4950
TCAGATGCAGCCGATGGAGATG	qRT-PCR (AT2G43010)	4959
CGACGGTTGTTGACTTTGCTGTC	qRT-PCR (AT2G43010)	4960
CCTTCACTCACACCATCAAAGCAC	qRT-PCR (AT5G46110)	4963
TGAATTGAGAAGCAGCCGCATTG	qRT-PCR (AT5G46110)	4964
GATGTGGGAGAGGAATGGTGAATG	qRT-PCR (AT4G24350)	4965
GGGATGCTCACATCTCCTATGGAC	qRT-PCR (AT4G24350)	4966
TCAGCAAATGCGGCTCATACTCG	qRT-PCR (AT1G25400)	4971
TTCCAAGCCGTCGGATCCTTTC	qRT-PCR (AT1G25400)	4972
CCAATGCTGTTGCACCTAATGTTG	qRT-PCR (AT2G29310)	5036
ACCGACGTCCTCGAGATAAGATTG	qRT-PCR (AT2G29310)	5037
GGGATATCTCTCCGGTCGAT	qPCR MOS11 (AT5G02770)	4532
TCAATTTCACCGAAACACCA	qPCR MOS11 (AT5G02770)	4533
ACAGGTGGAAAATGCACACA	qPCR TEX1 (AT5G56130)	4536
TGTGTCCCGTCAGGTTTGTA	qPCR TEX1 (AT5G56130)	4537
TTCGAACTCTTTCAGCAGCA	qPCR SSRP1 (AT3G28730)	4542
TTCGATGACGAAGCCTCTTT	qPCR SSRP1 (AT3G28730)	4543

Table 10. List of oligonucleotides used in the transcript profiling experiment. Oligonucleotides were obtained from MWG eurofins genomics. No = lab ID

Sequence 5'- 3'	Description	No.
TGGGAAAGTGTTGCCATCC	qRT-PCR normalization GAP (AT1G13440)	4973
CTTCATTTTGCCTTCAGATTCCTC	qRT-PCR normalization GAP (AT1G13440)	4974
AACGTGGCCAAAATGATGC	qRT-PCR normalization PP2AA (AT1G13320)	4977
CACATTGTCAATAGATTGGAGAGC	qRT-PCR normalization PP2AA (AT1G13320)	4978
CGTACAACCGGTATTGTGC	qRT-PCR normalization ACT2 (AT3G18780)	3384
GTCCAGCAAGGTCAAGACG	qRT-PCR normalization ACT2 (AT3G18780)	3385
CCAATGCTGTTGCACCTAATGTTG	qRT-PCR (AT2G29310)	5036
ACCGACGTCCTCGAGATAAGATTG	qRT-PCR (AT2G29310)	5037
ATCACCAAGATGCTGACCCAGAC	qRT-PCR (AT1G60140)	5038
CAAGCCCTTTGCTTACTCCCTGAG	qRT-PCR (AT1G60140)	5039
AAACCTGGCCGTTCCAAGAAGC	qRT-PCR (AT3G06145)	5040
ACGTCCTTCCTGGTCATCAACG	qRT-PCR (AT3G06145)	5041
TTCAGAACCGTAGGGCAAGGAC	qRT-PCR (AT2G44910)	5042
AGACAACTTCAACGCCCTCAGC	qRT-PCR (AT2G44910)	5043
CCAAGCTCACAATGAACACTTCCC	qRT-PCR (AT4G04840)	5044
ATAGAACCGTACGCCACTCCTC	qRT-PCR (AT4G04840)	5045
ATAAGGTTGTTGACTCCGTCGTTG	qRT-PCR (AT5G51720)	5046
ACCTCCAACACCTGCAATAGGG	qRT-PCR (AT5G51720)	5047
TGGCATGACTCAGGCAGAGTTG	qRT-PCR (AT5G48490)	5048
TGGGCTCGTCGGGTTATTCTTG	qRT-PCR (AT5G48490)	5049
CCTCTGTTTGCGGTGCTTTAACC	qRT-PCR (AT1G66100)	5050
CATTCACGATTTCACTTGCATCGG	qRT-PCR (AT1G66100)	5051
TCACGTGCCATTCCCTGACTAC	qRT-PCR (AT2G21650)	5052
TGCAGCTTCATGCTTCTCATCCTC	qRT-PCR (AT2G21650)	5053
TGCTCTTAGCTCACACCACTTCC	qRT-PCR (AT5G03350)	5054
AGCGTCTCCAAGGAAGACCAAC	qRT-PCR (AT5G03350)	5055
CAGCCTGATTACTACACGGATGTG	qRT-PCR (AT3G28740)	5058
AGTCCCGGCAAGTATCATAACAAG	qRT-PCR (AT3G28740)	5059
TCCCTCTCTGCAGGCAATTTAGG	qRT-PCR (AT3G48360)	5060
CACCAGAAGCTTCCACTTGGTG	qRT-PCR (AT3G48360)	5061
TGCTGCTACAGAGGCTACTACG	qRT-PCR (AT2G05540)	5062
ACAGCCTGACCAGCATAAGCAC	qRT-PCR (AT2G05540)	5063
ATCTCCTTGCGCCAGATGACAC	qRT-PCR (AT3G22740)	5064
TTCAGACCGTCGTAGACTTCCC	qRT-PCR (AT3G22740)	5065
TGTTGTCGACGCAAGAGGAAGG	qRT-PCR (AT4G20820)	5066
GCCCAGAAGAAATCTTCACCCATC	qRT-PCR (AT4G20820)	5067

Table 11. List of oligonucleotides used for genotyping, RT-PCR and colony PCR. Oligonucleotides were obtained from MWG eurofins genomics. No = lab ID

Sequence 5'- 3'	Description	No.
CACTGCGATTGAAGTGAAGACGATTAATTC	genotyping, RT-PCR nxf1-1 (AT5G43960)	3726
CTCTACTGGTGCAGCCCGATG	genotyping RT-PCR nxf1-1 (AT5G43960)	3727
TGAGCCTGCAGCAAGACCC	genotyping nxf2-1 (AT5G60980)	3732
AAATACGTGTAAGGGACCAATAAGCAAAGG	genotyping nxf2-1 (AT5G60980)	3733
CCTCAAGGAGATGCTCCTAAGCA	RT-PCR nxf2-1 (AT5G60980)	3781
CTCGAGGGCACTTTGCTTTCCG	RT-PCR nxf2-1 (AT5G60980)	3884
GCGAAATTCCAAAGAGATCTTATG	genotyping, RT-PCR nxf3-1 (AT3G25150)	4455
CTTCTGGCTTCTCACTTGAATTC	genotyping, RT-PCR nxf3-1 (AT3G25150)	4456
GCATGAAGGGTTCGGAGCAAG	genotyping, RT-PCR nxf4-3 (AT5G48650)	4453
CTGTATCAGATTCTATCACTTGAG	genotyping, RT-PCR nxf4-3 (AT5G48650)	4454
GTGAGACAGTACTATCATGTTTTAGGACAGC	genotyping, RT-PCR nxf5-1 (AT1G69250)	4274
CGTTTTTCTGTTTCAGCTCAGTCTTCTC	genotyping, RT-PCR nxf5-1 (AT1G69250)	4275
ACCTCTTGTATAAGTCACCATCGCAAGT	genotyping, RT-PCR nxf6-1 (AT1G13730)	4276
GCTCTGGTGTAGCGTCCATGAG	genotyping, RT-PCR nxf6-1 (AT1G13730)	4277
ACAATGCCTTTCAGAAACTTGCCTC	genotyping nxf7-1 (AT2G03640)	3822
CACGTATCAGCTCAGGGTAGTTCC	genotyping nxf7-1 (AT2G03640)	3823
CCCAATTCGTAAACAGGCTTC	RT-PCR nxf7-1 (AT2G03640)	4844
CTTGTAGAGACTCTGTTGCC	RT-PCR nxf7-1 (AT2G03640)	4845
TGATCGGAAACGTTTTGACTC	genotyping uief1-1 (AT4G10970)	2357
TTCCTTGGAAATTAGACCTCTTCTTAGCAAAAGC	genotyping, RT-PCR uief1-1 (AT4G10970)	2783
GACTGAGAAACCGATTACTACGGAGA	RT-PCR uief1-1 (AT4G10970)	2733
AATGAAATTAGGCCACGTGTG	genotyping uief2-1 (AT4G23910)	2352
TACCAACAGCACCCTGAAAAG	genotyping uief2-1 (AT4G23910)	2353
CTGGAACACCACTTATAGCGGAGA	RT-PCR uief2-1 (AT4G23910)	2741
TTGGGAAAATCTTCTGGCTCTAACCC	RT-PCR uief2-1 (AT4G23910)	2625
GTTCAGGTCCTTCTGGGAGAC	colony PCR pGreen0179:ALY3::ALY3-3'SG/eGFP	2349
AGACCCTCCACAACGTGGCC	colony PCR pGreen0179:ALY3::ALY3-3'SG	2313
AACTTCAGGGTCAGCTTGCCGTAG	colony PCR pGreen0179:ALY3::ALY3-3'eGFP	4073
GCCTTTTCAGAAATGGATAAATAGCCTTGCTTCC	genotyping SAIL T-DNA insertion lines	802
GTTGCCCGTCTCACTGGTGA	genotyping SALK T-DNA insertion lines	812
ATATTGACCATCATACTCATTGC	genotyping GK T-DNA insertion lines	1595

Table 12. List of oligonucleotides used for cloning. Oligonucleotides were obtained from MWG eurofins genomics. No = lab ID

Sequence 5'- 3'	Description	No.
GCTCTAGAATGGCGACTCCTTATCCTG	Insertion NXF1 CDS in pCambia2300:35S::3'SG/eGFP	4078
ATAGGATCCGCGACCACCACC	Insertion NXF1 CDS in pCambia2300:35S::3'SG/eGFP	3680
GCTCTAGAATGGCACAGCAGGAAG	Insertion NXF2 CDS in pCambia2300:35S::3'SG/eGFP	4079
GCGGGATCCAGATGAACCACCA	Insertion NXF2 CDS in pCambia2300:35S::3'SG/eGFP	3682
GCTCTAGAATGAATTTCTCTGTATTACTTTATATAAACTC	Insertion NXF3 CDS in pCambia2300:35S::3'SG/eGFP	4074
AGCGGATCCCGCAGCAAC	Insertion NXF3 CDS in pCambia2300:35S::3'SG/eGFP	4075
CGTCTAGAATGGATTCTACTGCTGCAAC	Insertion NXF4 CDS in pCambia2300:35S::3'SG/eGFP	4076
AGCGGATCCGTACGAGTTGATG	Insertion NXF4 CDS in pCambia2300:35S::3'SG/eGFP	4077
AGTTCTAGAATGGCTACCGAGGGAGT	Insertion NXF5 CDS in pCambia2300:35S::3'SG/eGFP	4790
ATCGGATCCATGTGCGGCTTCA	Insertion NXF5 CDS in pCambia2300:35S::3'SG/eGFP	4791
GTCTAGAATGGCACTTGAATCAAATGCTCC	Insertion NXF6 CDS in pCambia2300:35S::3'SG/eGFP	4337
AGCGGATCCACGGCTAGCT	Insertion NXF6 CDS in pCambia2300:35S::3'SG/eGFP	4338
CTCTAGAATGACACCTGAATCAAACGCTC	Insertion NXF7 CDS in pCambia2300:35S::3'SG/eGFP	4339
AGCGGATCCGTTTTTGGCCTC	Insertion NXF7 CDS in pCambia2300:35S::3'SG/eGFP	4340
GCTCTAGAATGTCGACTGGATTAGATATGTCTCTCGAC	Insertion ALY1 CDS in pCambia2300:35S::3'SG	2640
TTTTCTAGAGTTTGTCTCCATATCTCCAGAATGGTA	Insertion ALY1 CDS in pCambia2300:35S::3'SG	2884
GCTCTAGAATGTCAGGTGGCTTAGATATGTC	Insertion ALY2 CDS in pCambia2300:35S::3'SG	4096
GCAGGATCCACTTGTTTCCATTGCC	Insertion ALY2 CDS in pCambia2300:35S::3'SG	4097
GCTCTAGAATGTCAGACGCTTTGAATATGACTCTTGATG	Insertion ALY3 CDS in pCambia2300:35S::3'SG	2642
TTTGGATCCAGAGATGTTCATAGCTTCAGC	Insertion ALY3 CDS in pCambia2300:35S::3'SG	2888
GCTCTAGAATGTCTGGAGCATTGAATATGACT	Insertion ALY4 CDS in pCambia2300:35S::3'SG	4094
CGAGGATCCAGAGGTGTTCATGGC	Insertion ALY4 CDS in pCambia2300:35S::3'SG	4095
GCTCTAGAATGGACATGTCTTTAGATGAGATTATCAAG	Insertion UIEF1 CDS in pCambia2300:35S::3'SG	4098
GCAGGATCCGTTGGGGAATCTTG	Insertion UIEF1 CDS in pCambia2300:35S::3'SG	4099
GCTCTAGAATGGAGACTGGAACACCAC	Insertion UIEF2 CDS in pCambia2300:35S::3'SG	4100
GCAGGATCCTTGGGAAAATCTTCTGG	Insertion UIEF2 CDS in pCambia2300:35S::3'SG	4101
AAAGGATCCGATATGTGAGTGAGTGAACTAGA	Insertion of gen. ALY3 in pGreen0179:ALY3::3'eGFP	2887
TTTGGATCCAGAGATGTTCATAGCTTCAGC	Insertion of gen. ALY3 in pGreen0179:ALY3::3'eGFP	2888

4.4 Plasmids

Table 13. List of plasmids used in this study. * = generated in this study, L = Lab collection, K = Kanamycin resistance, B = Basta resistance, H = Hygromycin B resistance, R. site = Restriction site, S = Source, R = Plant resistance marker, No = Lab ID, Exp = Experiment

Plasmid	Exp.	Description (Insert in plasmid, primers)	R. Sites	S	R	No
pCambia2300:35S::ALY1-3'SG	AP-MS	ALY1 CDS in P728, 2640+2884	XbaI	*	K	1178
pCambia2300:35S::ALY2-3'SG	AP-MS	ALY2 CDS in P728, 4096+4097	XbaI/BamHI	*	K	1179
pCambia2300:35S::ALY3-3'SG	AP-MS	ALY3 CDS in P728, 2642+2888	XbaI/BamHI	*	K	1180
pCambia2300:35S::ALY4-3'SG	AP-MS	ALY4 CDS in P728, 2642+2888	XbaI/BamHI	*	K	1181
pCambia2300:35S::UIEF1-3'SG	AP-MS	UIEF1 CDS in P728, 4072+4073	XbaI/BamHI	*	K	1182
pCambia2300:35S::UIEF2-3'SG	AP-MS	UIEF2 CDS in P728, 4100+4001	XbaI/BamHI	*	K	1183
pCambia2300:35S::SG	AP-MS	negative control		L	K	728
pCambia2300:35S::ALY1-3'eGFP	FRET	ALY1 CDS in P1121, 2640+2884	XbaI	L	K	1251
pCambia2300:35S::ALY3-3'eGFP	FRET	ALY3 CDS in P1121, 2642+2888	XbaI/BamHI	L	K	1253
pCambia2300:35S::UIEF1-3'eGFP	FRET	UIEF1 CDS in P1121, 4072+4073	XbaI/BamHI	L	K	1244
pCambia2300:35S::UIEF2-3'eGFP	FRET	UIEF2 CDS in P1121, 4100+4001	XbaI/BamHI	L	K	1245
pCambia2300:35S::UIEF1mut-3'eGFP	FRET	UIEF1mut CDS in P1121, 4072+4073	XbaI/BamHI	L	K	1298
pCambia2300:35S::eGFP-NLS-mCherry	FRET	positive control		L	K	966
pCambia2300:35S::mCherry-NLS	FRET	negative control		L	K	921
pcambia2300:35S::UAP56-3'mCherry	FRET	UAP56 CDS in P1141, 2174+2819	XbaI/XmaI	L	K	1254
pGreen0229:UIEF1::UIEF1-3'GFP	CLSM	genomic UIEF1 in 638, 2745+2747	BamHI	L	B	1036
pGreen0229:UIEF2::UIEF2-3'GFP	CLSM	genomic UIEF2 in 638, 4145+ 4146	BamHI	L	B	1159
pGreen0179:ALY3::ALY3-3'SG	Compl.	genomic ALY3 in 834, 2887+2888	BamHI	L	H	1016
pGreen0179:ALY3::ALY3-3'eGFP	Compl.	genomic ALY3 in 1199, 2887+2888	BamHI	*	H	1403
pCambia2300:35S::NXF1-3'SG	AP-MS	NXF1 CDS in P728, 4078+3680	XbaI/BamHI	*	K	1168
pCambia2300:35S::NXF2-3'SG	AP-MS	NXF2 CDS in P728, 4079+3682	XbaI/BamHI	*	K	1169
pCambia2300:35S::NXF3-3'SG	AP-MS	NXF3 CDS in P728, 4074+4075	XbaI/BamHI	*	K	1170
pCambia2300:35S::NXF4-3'SG	AP-MS	NXF4 CDS in P728, 4076+4077	XbaI/BamHI	*	K	1171
pCambia2300:35S::NXF5-3'SG	AP-MS	NXF5 CDS in P728, 4790+4791	XbaI/BamHI	*	K	1311
pCambia2300:35S::NXF6-3'SG	AP-MS	NXF6 CDS in P728, 4337+4338	XbaI/BamHI	*	K	1172
pCambia2300:35S::NXF7-3'SG	AP-MS	NXF7 CDS in P728, 4339+4340	XbaI/BamHI	*	K	1173
pCambia2300:35S::NXF1-3'eGFP	CLSM	NXF1 CDS in P1121, 4078+3680	XbaI/BamHI	*	K	1174
pCambia2300:35S::NXF2-3'eGFP	CLSM	NXF2 CDS in P1121, 4079+3682	XbaI/BamHI	*	K	1175
pCambia2300:35S::NXF3-3'eGFP	CLSM	NXF3 CDS in P1121, 4074+4075	XbaI/BamHI	*	K	1176
pCambia2300:35S::NXF4-3'eGFP	CLSM	NXF4 CDS in P1121, 4076+4077	XbaI/BamHI	*	K	1177
pCambia2300:35S::NXF5-3'eGFP	CLSM	NXF5 CDS in P1121, 4790+4791	XbaI/BamHI	*	K	1310
pCambia2300:35S::NXF6-3'eGFP	CLSM	NXF6 CDS in P1121, 4337+4338	XbaI/BamHI	*	K	1401
pCambia2300:35S::NXF7-3'eGFP	CLSM	NXF7 CDS in P1121, 4339+4340	XbaI/BamHI	*	K	1402
pCambia2300:NXF1::5'eGFP-NXF1	CLSM	genomic NXF1 in 983, 4050+4051	NruI/BamHI	L	K	987
pGreen0229:NXF1::NXF1-3'GFP	CLSM	genomic NXF1 in 638, 4127+4128	SmaI	L	B	988
pCambia2300:NXF2::NXF2-3'eGFP	CLSM	genomic NXF2 in 1121, 4057+4058	SmaI/ BamHI	L	K	986
pGreen0229:NXF3::NXF3-3'GFP	CLSM	genomic NXF3 in 638, 4136+4137	SmaI/BamHI	L	B	1004
pGreen0229:NXF4::NXF4-3'GFP	CLSM	genomic NXF4 in 638, 4138+4139	XbaI/SmaI	L	B	991
pGreen0229:NXF5::NXF5-3'GFP	CLSM	genomic NXF5 in 638, 4198+4199	SmaI/BamHI	L	B	998
pGreen0229:NXF6::NXF6-3'GFP	CLSM	genomic NXF6 in 638, 4196+4197	SmaI/BamHI	L	B	999
pGreen0229:NXF7::NXF7-3'GFP	CLSM	genomic NXF7 in 638, 4200+4201	XbaI/SmaI	L	B	995
pGreen0179:NUP54::NUP54-3'tagRFP	CLSM	genomic NUP54 in 1094,4404+4346	XbaI/BamHI	L	K	1229
pGreen0229:35S:5'mcherry-NUP54	CLSM	NUP54 CDS in 1211, 4723+4724	BamHI	L	B	1306
pCambia2300:35S::NUP35-3'mCherry	CLSM	NUP35 CDS in 1141, 4793+4795	XbaI/BamHI	L	K	1312

4.5 Organisms

Table 14. List of T-DNA lines analysed in this study.

Name	T-DNA insertion	AGI	Source
aly1-1	SAIL_381E08	AT5G59950	NASC
aly2-1	wiscDsLox461-464N10	AT5G02530	NASC
aly3-1	SALK_063320	AT1G66260	NASC
aly4-1	GK-497B06	AT5G37720	NASC
uief1-1	SALK_129143	AT4G10970	NASC
uief2-1	SALK_059956	AT4G23910	NASC
nxf1-1	SALK_011708	AT5G43960	NASC
nxf2-1	SAIL_87G09	AT5G60980	NASC
nxf3-1	SALK_144662	AT3G25150	NASC
nxf4-3	GK-797C02	AT5G48650	NASC
nxf5-1	SAIL_750A08	AT1G69250	NASC
nxf6-1	GK-685A10	AT1G13730	NASC
nxf7-1	SALK_058330	AT2G03640	NASC

Table 15. List of bacteria strains used in this study.

Organism	Name	Resistance	Purpose	Company
A. tumefciens	GV::pMP90 + pSoup	Gentamycin, Rifampicin,Tetracyclin	Plant transformation	DSMZ
E. coli	XL1 blue	Tetracyclin	Plasmid amplification	Stratagene

4.6 Databases, Online Tools, Software

Table 16. List of databases, Online Tools, Software used in this study.

Databases, Online Tools, Software	https://
Geneinvestigator	(https://genevestigator.com/gv/)
ImageJ 1.49	(https://imagej.nih.gov/ij/)
Leica Application Suite X	(https://www.leica-microsystems.com)
Mendeley	(https://www.mendeley.com/)
Microsoft Excel 2016	(https://www.microsoft.com/)
Needle (EMBOSS)	(https://www.ebi.ac.uk/Tools/psa/emboss_needle/)
PANTHER 14.0	(http://www.pantherdb.org/geneListAnalysis.do)
Past 3.26	(https://folk.uio.no/ohammer/past/)
Primer3 v 0.4.0	(http://bioinfo.ut.ee/primer3-0.4.0/primer3/input.htm)
QuantPrime	(http://quantprime.mpimp-golm.mpg.de/)
SnapGene v2.3.2	(http://www.snapgene.com/)
The Arabidopsis Information Resource v10	(https://www.arabidopsis.org/)
UniProt	(http://www.uniprot.org/)

5. Methods

5.1 Nucleic acid based methods

5.1.1 Isolation of genomic DNA from *Arabidopsis* leaves

One *Arabidopsis* leaf was frozen in liquid nitrogen in a 1.5 mL tube with two glass beads and was homogenized using the Tissue Lyser II (Qiagene) with a frequency of 30 Hz for 30 sec. 400 µL Edward buffer (200 mM Tris pH 7.5, 250 mM NaCl, 25 mM EDTA, 0.5 % (w/v) SDS) was added to the ground tissue. The sample was mixed by vortexing and centrifuged for 5 min at 12000 g and RT. To precipitate the DNA, 300 µL of the supernatant were mixed with 300 µL of 100 %(v/v) isopropanol and incubated at RT for 2 min. After centrifugation for 5 min at 12000 g and RT the DNA pellet was washed once with 70 % (v/v) ethanol, air dried and resuspended in 50 µL H_2O.

5.1.2 Isolation of RNA (for semi-quantitative RT-PCR)

Aerial parts from 10 DAS *Arabidopsis* seedlings were homogenized using the Tissue Lyser II (Qiagene) with a frequency 30 Hz for 60 sec. 50-100 mg of homogenized material was used to extract RNA using the TRIzol™ reagent (Invitrogen) according to the manufacturer's instructions. The purified RNA was dissolved in 30 µL H_2O. To remove DNA contaminations, 4 µg extracted RNA was incubated with 2 U of DNaseI (NEB) for 80 minutes at 37 °C according to the manufacturer's instructions.

5.1.3 Isolation of RNA and genomic DNA (cell fractioning)

Aerial parts from 14 DAS *Arabidopsis* seedlings were homogenized using the Tissue Lyser II (Qiagene) with a frequency of 30 Hz for 60 sec. 50 mg of homogenized material was used to simultaneously extract RNA and genomic DNA using the TRIzol™ reagent (Invitrogen) according to the manufacturer's instructions. 400 mg of homogenized material was used to extract nuclei. Homogenized plant material was mixed with 30 mL Extraction Buffer 1 (0.4 M Sucrose, 10 mM HEPES pH 8, 5 mM β-mercaptoethanol) in a 50 mL Falcon tube and incubated on a rotating wheel at 4 °C for 15 min. Solution was filtered through a double layer of Miracloth into a new 50 mL Falcon tube and centrifuged at 3000 g and 4 °C for 20 min. Pellet was resuspended in 1 mL Extraction Buffer 2 (0.25 M Sucrose, 10 mM HEPES pH 8, 1 % (v/v) Triton X-100, 10 mM $MgCl_2$, 5 mM β-mercaptoethanol) and centrifuged at 12000 g and 4 °C for 10 min. Washing was repeated 2 - 3 times. Pellet was resuspended in 400 µL Extraction Buffer 3 (1.7 M Sucrose, 10 mM HEPES pH 8, 0.15 % (v/v) Triton X-100, 2 mM $MgCl_2$, 5 mM β-mercaptoethanol) and another 400 µL of Extraction Buffer 3 was added to a new 1.5 mL tube and overlaid with the pellet from the previous step. Following centrifugation at 16000 g

and 4 °C for 60 min pellet was resuspended in 200 µL Nuclei Lysis Buffer (50 mM HEPES pH 8, 10 mM EDTA, 0.1 % (w/v) SDS). RNA and genomic DNA was simultaneously extracted from lysed nuclei using the TRIzol™ reagent (Invitrogen) according to the manufacturer's instructions. The purified RNAs from total cells and nuclei were dissolved in 30 µL H_2O. To remove DNA contaminations, up to 3 µg extracted RNA was incubated with 2 U of DNaseI (NEB) for 80 minutes at 37 °C according to the manufacturer's instructions. To remove DNAseI, RNA was filled up with water to a final volume of 200 µL and was mixed with 200 µL Roti® - Aqua - P/C/I (Roth). After centrifugation at 20000 g for 10 min and RT, 200 µL of the upper phase were transferred to a new 1.5 mL tube and were mixed with 20 µL 3 M KAc pH 4.8 and 500 µL 100 % (v/v) ethanol and frozen in liquid nitrogen. After thawing at -20 °C and centrifugation at 20000 g and 4 °C for 10 min, RNA pellet was washed once with 70 % (v/v) ethanol, air dried and resuspended in 30 µL H_2O.

5.1.4 Isolation of RNA (transcriptome profiling)

Aerial parts from 10 DAS Arabidopsis seedlings were homogenized using the Tissue Lyser II (Qiagene) with a frequency of 30 Hz for 60 sec. 50-100 mg of homogenized material was used to extract RNA using RNeasy® Mini Plant kit (Qiagen) according to the manufacturer's instructions. The purified RNA was dissolved in 30 µL H_2O. To remove DNA contaminations, 4 µg extracted RNA was incubated with 2 U of DNaseI (NEB) for 80 minutes at 37 °C according to the manufacturer's instructions. To remove DNAseI, RNA was filled up with water to a final volume of 200 µL and was mixed with 200 µL Roti® - Aqua - P/C/I (Roth). After centrifugation at 20000 g and RT, 200 µL of the upper phase were transferred to a new 1.5 mL tube and were mixed with 20 µL 3 M KAc pH 4.8 and 500 µL 100 % ethanol (v/v) and frozen in liquid nitrogen. After thawing at -20 °C and centrifugation at 20000 g and 4 °C for 10 min, RNA pellet was washed once with 70 % ethanol (v/v), air dried and resuspended in 30 µL H_2O.

5.1.5 Reverse transcription (cDNA synthesis)

RNA was transcribed into cDNA using RevertAid™H Minus M-MuLV Reverse Transcriptase (Thermo Fisher Scientific). In a total volume of 11 µL, 2 µg of DNaseI-treated RNA were mixed with 0.5 µg oligo-dT primers or 0.2 µg random hexamer primers for 5 min at 70 °C and cooled down to 4 °C. Reaction buffer (1x), dNTP (1 mM) and 20 U RNase Inhibitor (Thermo Fisher Scientific) were added to a final volume of 19 µL and the mixture was incubated for 5 min at 37 °C (5 min at 25 °C when random hexamer primers were used). To synthesize cDNA, 200 U of RevertAid™H Minus M-MulV Reverse Transcriptase were added and the sample was incubated for 60 min at 42 °C (10 min at 25 °C followed by 60 min at 42 °C when random

hexamer primers were used). The reaction was stopped by heating the samples at 70 °C for 10 min. For cDNA library preparation used for validation of transcriptome profiling results oligo-dT primers were used. For cDNA library preparation used for validation of deep sequencing results of total cells and nuclei random hexamer primers were used.

5.1.6 Polymerase chain reaction (PCR)

Taq DNA Polymerase (Peqlab) was used for genotyping, semi-quantitative RT-PCR and colony PCR. Herculase II Fusion DNA Polymerase (Agilent) DNA Polymerase was used for cloning due to its proofreading activity. PCR cycle programs and PCR reaction mixes are displayed in Table 16 and Table 17, respectively. Amplified fragments were analysed on 1 – 2 % agarose gels depending on fragment size.

Table 17. Cycling conditions for PCR reactions using Taq and Herculase II Fusion DNA Polymerase.

	Taq			Herculase		
	Temperature	Time	Cycles	Temperature	Time	Cycles
Initial denaturation	95 °C	5 min	1	95 °C	2 min	1
Denaturation	95 °C	30 sec	26 - 40	95 °C	20 sec	34
Annealing	Primer Tm -5 °C	30 sec	26 - 40	Primer Tm -5 °C	20 sec	34
Extension	72 °C	1 min/1 kbp	26 - 40	68 °C[A]/72 °C[B]	30 sec[A],1 min[B]/1 kbp	34
Final extension	72 °C	5 min	1	68 °C[A]/72 °C[B]	5 min	1

Table 18. PCR reaction mixes using Taq and Herculase II Fusion DNA Polymerase. A) Settings to amplify genomic or plasmid targets B) Settings to amplify cDNA targets.

Reagent	Taq	Herculase
Buffer	1x Taq reaction buffer (Peqlab)	1x Herculase reaction buffer (Agilent)
dNTP	0.2 mM each dNTP	0.3 mM each dNTP
Forward primer	0.5 µM	0.2 µM
Reverse primer	0.5 µM	0.2 µM
Polymerase	0.5 U Taq DNA polymerase (Peqlab)	0.5 U Herculase DNA polymerase (Agilent)
H_2O	Up to 25 µL	Up to 50 µL

5.1.7 Real time quantitative PCR (qRT-PCR)

The qPCR reactions were performed in a total volume of 10 µL using KAPA™ SYBR® FAST QPCR MasterMix Universal (PEQLAB), G003-SF stripes (Kisker Biotech GmbH and Co KG) and the Mastercycler epgradient S realplex^2 with realplex software v2.2 (Eppendorf AG) according to the manufacturer's instructions. Targets were amplified with specific primer pairs (Table 7, 8) that were design with the web applications quantprime (Arvidsson et al., 2008) or primer3 (Untergasser et al., 2007). The following cycling program was used: 1) Initial Denaturation (2 sec at 98 °C), 2) Two step cycling (40 x 5 sec at 98 °C followed by 15 sec at

60 °C) and 3) Melting curve for quality control. The normalised relative quantities (NRQ) were calculated according to Hellemans et al., 2007 using the three mRNA references genes *GAP*, *PP2AA3* and *ACT2* or the non-mRNA reference genes 18S rRNA and U12 snRNA (Kwok et al., 2013, Kudo et al., 2016). Primer efficiencies for the specific primer pairs were calculated using a three-step dilution of the cDNA templates.

5.1.8 Agarose gel electrophoresis

1 - 2% (w/v) agarose gels (40 mM Tris pH 8, 20 mM acetic acid, 1 mM EDTA) supplemented with 0.005 % (v/v) ethidium bromide were used to separate DNA/RNA fragments. DNA/RNA samples were mixed with 6x loading dye (250 mM Tris pH 7.5, 10% (w/v) SDS, 30% (v/v) glycerol, 0.5 M DTT, 0.1% (w/v) bromophenol blue) and gels were run at 150 V. DNA/RNA fragments were visualized by excitation at 256 nm with a BioDoc Analyser (Biometra GmbH, Göttingen).

5.1.9 PCR clean up and DNA extraction from agarose gels

For the clean-up of PCR samples and DNA fragments from agarose gels, the NucleoSpin® Gel and PCR Clean-up kit (Macherey-Nagel) was used according to the manufacturer's instructions.

5.1.10 Restriction digest and dephosphorylation

Plasmids and PCR fragments were digested with restriction enzymes (NEB) according to the manufacturer's instructions. Digestions were performed o/n. To prevent self-ligation, 5' - phosphate groups from digested plasmids were removed by incubation with 5 U of Antarctic Phosphatase (NEB) in 1 x Antarctic Phosphatase buffer (NEB) for 60 min at 37 °C.

5.1.11 Ligation

Digested inserts and plasmids were mixed in a 4:1 molar ratio with the addition of 5U T4 DNA ligase (Thermo Scientific) and 1x T4 Ligase buffer in a total volume of 20 µL. Ligation was performed o/n at 4 °C:

5.1.12 Isolation of plasmid DNA from *E. coli*

For minipreparation of plasmid DNA, 2 mL selective LB-medium were inoculated with a positive transformed *E. coli* colony and incubated o/n at 37 °C and 200 rpm. Cells from1.5 ml liquid cultures were harvested by centrifugation for 3 min at 1800 g. Cell pellet was resuspended in 200 µL P1 buffer (50 mM Tris-HCl pH 8, 10 mM EDTA, 100 µg/mL RNase A). For cell lysis, 300 µL of P2 buffer (0.2 M NaOH, 1 % (w/v) SDS) were added and the mixture was incubated for 5 min at RT. To stop the cell lysis, 300 µL of P3 buffer (3 M potassium acetate, pH 4.8) were added and the sample was incubated for 10 min on ice before centrifugation at 12000 g for 10 min and RT. The supernatant was transferred to a new 1.5 mL tube and an equal amount of 100 % (v/v) isopropanol was added. After incubation for 5 min at RT to precipitate the plasmid DNA, sample was spun down at 12000 g for 10 min at RT and the pellet was washed with 70 % (v/v) ethanol, air dried and re-dissolved in 50 µL H_2O.

Midipreparation of plasmid DNA was performed using the NucleoBond® Xtra Midi Kit (Macherey Nagel) according to the manufacturer's instructions.

5.1.13 Sequencing of plasmid DNA

Sequencing of purified plasmid DNA was performed by the TubeSeq Service of Eurofins MWG Operon (Ebersberg). DNA samples and sequencing primers were prepared according to instructions of the provider (https://www.eurofinsgenomics.eu).

5.1.14 RNA sequencing

Library preparation and RNAseq were performed at the service facility "KFB - Center of Excellence for Fluorescent Bioanalytics" (Regensburg, Germany; www.kfb-regensburg.de). Library preparation and RNAseq were carried out as described in the Illumina TruSeq Stranded mRNA Sample Preparation Guide, the Illumina HiSeq 1000 System User Guide (Illumina, Inc., San Diego, CA, USA), and the KAPA Library Quantification Kit - Illumina/ABI Prism User Guide (Kapa Biosystems, Inc., Woburn, MA, USA).

In brief, 250 ng total or nuclear RNA was used for purifying the poly-A containing mRNA molecules using poly-T oligo-attached magnetic beads. Following purification, the mRNA was fragmented to an average insert size of 200-400 bases using divalent cations under elevated temperature (94 °C for 4 minutes). Next, the cleaved RNA fragments were reverse transcribed into first strand cDNA using reverse transcriptase and random hexamer primers. Actinomycin D was added to improve strand specificity by preventing spurious DNA-dependent synthesis. Blunt-ended second strand cDNA was synthesized using DNA Polymerase I, RNase H and dUTP nucleotides. The incorporation of dUTP, in place of dTTP, quenched the second strand

during the later PCR amplification, because the polymerase does not incorporate past this nucleotide. The resulting cDNA fragments were adenylated at the 3' ends, the indexing adapters were ligated, and subsequently specific cDNA libraries were created by PCR enrichment. A column based size selection with a ≥200 bp cutoff was applied to the nuclear samples (Select-a-Size DNA Clean & Concentrator, Zymo Research). The libraries were quantified using the KAPA SYBR FAST ABI Prism Library Quantification Kit. Equimolar amounts of each library were used for cluster generation on the cBot with the Illumina TruSeq PE Cluster Kit v3. The sequencing run was performed on an HiSeq 1000 instrument using the indexed, 2x100 cycles paired end (PE) protocol for RNA sequencing of total cells and nuclei in the cell fractioning experiment (7.1.3) and the 50 cycles single-read (SR) protocol for the transcript profiling experiment (7.1.4) with the TruSeq SBS v3 Reagents according to the Illumina HiSeq 1000 System User Guide. Image analysis and base calling resulted in .bcl files, which were converted into .fastq files with the bcl2fastq v2.18 software.

The analysis of RNA-seq data was performed by Dr. Julia Engelmann (Royal Netherlands Institute for Sea Research).

5.2 Protein based methods

5.2.1 Affinity purification of SG-tagged proteins

Affinity purifications of SG-tagged proteins expressed in suspension cultured cells were performed as described in Pfab et al., 2017. Briefly, 15 g of transformed PSB-D cells were frozen in liquid nitrogen and ground to a fine powder using mortar and pestle. The ground cells were mixed with 20 mL prechilled extraction Buffer (25 mM HEPES-KOH pH 7.4, 100 mM NaCl, 0.05 % (v/v) IGEPALCA-630, 1 mM DTT, 2 mM $MgCl_2$, 5 mM EGTA, 10 % (w/v) glycerol, cOmplete™EDTA free proteinase inhibitor tablets (Sigma-Aldrich), 1 mM PMSF dissolved in 2-propanol). To disrupt the cells and shear the nucleic acids defrosted cells were sonicated five times for 30- seconds at 30 % intensity followed by 60-seconds intervals for cooling using a UW2070 MS73 (Bandelin) Sonicator. $MgCl_2$ (to a final concentration of 5 mM) and 50 U/mL Benzonase were added to the mixture to degrade RNA and DNA. The sample was incubated for 30 minutes at 4 °C on a rotating wheel. Cell debris was spun down at 40000 x g and 4 °C for 60 min and the supernatant was filtered through a 0.45 µm syringe filter. The protein concentration of the cell extract was determined by Bradford protein assay. 10 µL protein mix was filled up with H_2O to a total volume of 200 µL and mixed with 1 mL Bradford reagent (0.01 % (w/v) Coomassie Blue G-250, 5 % (v/v) ethanol, 10 % (v/v) phosphoric acid) in a polystyrol cuvette (Sarstedt AG & Co, Germany). After incubation of 10 minutes, the absorbance was measured at 595 nm with the BioPhotometer® (Eppendorf AG, Hamburg) and the protein concentration was estimated by comparison with a BSA calibration curve. 150

mg of total proteins were adjusted with extraction buffer to a final volume of 30 mL. 100 µL magnetic beads were washed four times with extraction buffer and added to the protein extract. Proteins were incubated with magnetic beads for 60 min at 4 °C on a rotating wheel. After centrifugation at 2000 g and 4 °C for 10 min the beads were transferred into a 1.5 mL tube and washed three times with 1 mL extraction buffer using a magnetic rack. Proteins were eluted from beads with 300 µL elution buffer (0.1 M glycine-HCl, pH 2.7) for 5 minutes at RT and 700 rpm. Beads were separated from eluted proteins with a magnetic rack and the protein containing supernatant was transferred to a 1.5 mL tube.

5.2.2 Acetone precipitation

To precipitate proteins eluted from magnetic beads (6.2.1), the sample was mixed with ice-cold acetone to a final concentration of 20 % (v/v). Eluted proteins and acetone were mixed, and proteins were precipitated o/n at -20 °C. After centrifugation at 20000 g and 4 °C for 20 min the precipitated proteins were washed twice with 500 µL ice cold acetone. After washing, the protein pellet was resuspended in 25 µL 1x PBS.

5.2.3 SDS-PAGE

The SDS polyacrylamide gel electrophoresis (SDS-PAGE) was performed with polyacrylamide gels containing a resolving gel (9 % acrylamide: bisacrylamide (30:0.15), 0.75 M Tris pH 8.8, 0.2 % (w/v) SDS, 0.1 % (w/v) ammonium persulfate (APS) and 0.02 % (v/v) TEMED) and a stacking gel (5 % (v/v) acrylamide mix Gel 30 (5:1), 140 mM Tris pH 6.8, 0.23 % (w/v) SDS, 0.11 % (w/v) APS and 0.06 % (v/v) TEMED). Gels were cast using a Bio-RAD Mini- Protean® 3 Multicaster system (Bio-Rad). Analysed samples were mixed with 6 x SDS loading buffer (50 mM Tris pH 6.8, 0.002 % (w/v) bromophenol blue, 2.5 % (w/v) glycerol, 1 % (w/v) SDS and 143 mM -mercaptoethanol) to a final concentration of 1x and heated at 95 °C for 10 min. SDS polyacrylamide gel electrophoresis (SDS-PAGE) was performed in a Bio-RAD Mini-Protean® 3 running chamber using Laemmli running buffer (0.1% SDS (w/v), 3.03 g/L Tris, and 14.41 g/L glycine). Gels were run at 200 V and sizes of proteins were estimated using PageRuler™ unstained protein ladder (Thermo Scientific).

5.2.4 Coomassie Brilliant Blue (CBB) staining

Proteins were visualized by incubation of SDS polyacrylamide gels in Coomassie Brilliant Blue (CBB) solution (0.2 % (w/v) CBB G-250, 30 % (v/v) ethanol and 10 % (v/v) acetic acid) for 30 min and destaining with 7.5 % (v/v) ethanol and 5 % (v/v) acetic acid o/n.

5.2.5 Trypsin in-gel digestion

Proteins that were purified (5.2.1), separated by SDS-PAGE electrophoresis (5.2.3) and stained with Coomassie Brilliant Blue (5.2.4) were cut out of the gel using a scalpel. One gel lane was divided into 6 gel pieces and each piece was cut into 1mm fragments. Fragments were transferred into a 2 mL tube and washed four times while gently shaking. 1x 60 min (50 mM NH_4HCO_3), 1x 60 min (Mix 50 mM NH_4HCO_3 and acetonitrile in the ratio 3:1), 1x 30 min (Mix 50 mM NH4HCO3 and acetonitrile in the ratio 1:1) and 1x 10 min (200 µL acetonitrile). Gel fragments were subsequently lyophilised for 60 min. To reduce cysteines, 200 µL of 1 mg/ml DTT dissolved in 50 mM NH_4HCO_3 were added to the samples and incubated for 35 min at 56 °C. For carbamidomethylation of the cysteines, supernatant was removed and 200 µL of 5 mg/ml iodoacetamide dissolved in 50 mM NH_4HCO_3 was added to the samples. Samples were incubated at RT in the dark for 35 min. The four washing steps as described above were repeated and gel fragments were lyophilised. Dry gel fragments were incubated with 10-20 µL of trypsin mix (0.04 µg/µL trypsin in 50 mM NH_4HCO_3), covered with 40 µL 50 mM NH_4HCO_3 and incubate o/n at 37 °C. The supernatant that contains the extracted peptides was transferred to a 0.5 mL collection tube. 40 µL 100 mM NH_4HCO_3 was added to each tube and the samples were incubated for 60 min at 39 °C while gently shaking. The supernatant was transferred to the collection tube and extraction step was repeated once with 100 mM NH_4HCO_3 at 39 °C and once with a mix of 100 mM NH_4HCO_3 and acetonitrile in the ratio 1:1 at 30 °C. The collection tube with the pooled peptides of all three extraction steps was lyophilize o/n.

5.2.6 Mass spectrometry

Mass spectrometry was performed in the lab of Dr. Astrid Bruckmann (Department of Biochemistry I, University of Regensburg) as described in Antosz et al., 2017. Briefly, the peptides obtained by trypsin digestion were separated by reverse-phase chromatography on an UltiMate 3000 RSLCnano System (Thermo Scientific) using a Reprosil-Pur Basic C18 nano column. A linear gradient of 4 to 40% acetonitrile in 0.1% formic acid was applied for 90 min. The HPLC system was coupled to a maXis plus UHR-QTOF system (Bruker Daltonics) via a nanoflow electrospray source (Bruker Daltonics). Data-dependent acquisition of tandem mass spectrometry (MS/MS) spectra by CID fragmentation was performed utilizing a dynamic method with a fixed cycle time of 3 s (Compass 1.7; Bruker Daltonics). Protein Scape 3.1.3 (Bruker Daltonics) in connection with Mascot 2.5.1 (Matrix Science) facilitated database searching of the NCBI database. Mascot peptide ion score cut-off was set to 25. A protein score of minimum 80 was considered as criteria for reliable protein identification.

5.3 Microbial work

5.3.1 Cultivation of bacteria

Luria Bertani (LB) medium (5 g/L Yeast extract, 10 g/L NaCl, 10 g/L tryptone) was used as standard growth medium for all bacterial strains used in this study. Medium to cast LB plates was obtained by adding 1.5 % (w/v) agar prior to autoclaving. For bacterial selection, the LB medium was supplemented with sterile-filtered antibiotics leading to the following final concentrations: 50 µg/ml gentamycin, 50 µg/ml (*E. coli*) or 25 µg/ml (*A. tumefaciens*) kanamycin, 50 µg/ml rifampicin and 12 µg/ml tetracyclin. *E. coli* and *A. tumefaciens* bacteria strains were grown at 37 °C or 28 °C, respectively. Bacteria in liquid LB media were grown under agitation at 200 rpm.

5.3.2 Preparation of chemically competent cells

10 mL LB medium with appropriate antibiotics was inoculated with a single *E. coli* or *A. tumefaciens* bacteria starter colony and incubated o/n at 37 °C or 28 °C and 200 rpm, respectively. The starter culture was used to inoculate 100 mL selective LB media to an OD600 of 0.1. After the cells were grown to an OD600 of 0.75 they were harvested by centrifugation for 10 min at 4000 g and 4 °C. The cell pellet was re-suspended in 30 mL sterile filtered cold TBF1 buffer (100 mM RbCl, 10 mM $CaCl_2$, 50mM $MnCl_2$, 30mM NaOAc; adjusted to pH 5.8 with acetic acid) and incubated on ice for 90 min. The cells were harvested for 10 min at 3000 g and 4 °C and re-suspended in 4 mL of sterile filtered cold TBF2 buffer (10 mM MOPS, 10 mM RbCl, 75 mM $CaCl_2$ and 15% (w/v) glycerol). Chemically competent cells were stored in 50 µL aliquots at -80 °C.

5.3.3 Transformation of chemically competent *E. coli* cells

50 µL chemically competent *E. coli* cells (5.3.2) thawed on ice were mixed with 200 ng plasmid DNA or 10 µL ligation product (5.1.11). After incubation for 20 min on ice a heat shock at 42 °C was applied for 2 min. After 10 min incubation on ice the sample was mixed with 1 mL LB medium without selection and incubated for 60 min at 37 °C and 200 rpm. Transformed cells were spread on LB plates with the appropriate selection and incubated o/n at 37 °C.

5.3.4 Transformation of chemically competent *A. tumefaciens* cells

50 µL chemically competent *A. tumefaciens* cells (5.3.2) thawed on ice were mixed with 200 ng plasmid DNA. After incubation for 5 min on ice and 5 min in liquid nitrogen a heat shock at 37 °C was applied for 5 min. After heat shock the sample was mixed with 1 mL LB medium

without selection and incubated for 120 min at 28 °C and 200 rpm. Transformed cells were spread on LB plates with the appropriate selection and incubated for 2-3 days at 28 °C.

5.4 Plant work

5.4.1 Cultivation of *Arabidopsis* plants

Arabidopsis seeds were sown on soil (80% (v/v) Einheitserde Typ ED 73, 10% (v/v) sand and 10% Isoself® from Knauf Perlite). Soil was pre-soaked in water containing 0.03% (v/v) confidor WG70 (Bayer) and 3 g/L fertiliser Osmocote Start (The Scotts Company). After sowing out, the pots were stratified for 2-3 days at 4 °C in the dark before plants were grown under long-day conditions (LD; 16 hour light) at 22 °C and 100 µmol m^{-2} s^{-1} light.

For plant growth under sterile conditions, *Arabidopsis* seeds were sterilized using chloric gas (40 mL 12.5% hypochloric acid (w/v) and 2 mL 37% HCl (v/v)). *Arabidopsis* seeds were sown on solid 0.5x MS plates (2.15 g/L Murashige and Skoog media, 1% (w/v) sucrose, 0.7% or 1% (w/v) phyto agar adjusted to pH 5.8). After stratification (2-3 days at 4 °C in the dark), plants were grown in a plant incubator (Percival Scientific) under LD conditions at 22 °C and 100 µmol m^{-2} s^{-1}.

Transgenic *Arabidopsis* plants carrying a hygromycin B resistance were selected on solid 0.5x MS plates (2.15 g/L Murashige and Skoog media, 1% (w/v) sucrose, 0.7% phyto agar (w/v); adjusted to pH 5.8) supplemented with hygromycin B to a final concentration of 30 µg/ml.

5.4.2 Transformation of *Arabidopsis* plants by floral dipping

Arabidopsis plants were stably transformed using the ‘Floral Dip’ method described in Clough and Bent, 1998. Briefly, approximately 10-30 *Arabidopsis* plants grown in one pot with 10-15 cm inflorescences were used for each transformation. *A. tumefaciens* GV3101 + pSoup carrying cells transformed by heat shock (7.3.4) with pGreen-derived plasmids were used for transformation. Selected bacteria colonies were tested by colony PCR for insertion of the plasmid. Colonies carrying the pGreen-derived plasmids were grown o/n in 5 mL selective LB at 28 °C and 200 rpm. 500 mL selective LB were inoculated with 500 µL of the starter culture and incubated o/n at 28 °C and 200 rpm. The cells were harvested by centrifugation for 15 min at 5000 g and were re-suspended in 500 mL infiltration medium (5% (w/v) sucrose, 10 mM MgCl2, 0.02% (v/v) Silvet L77 and 0.01 mM acetosyringone dissolved in ethanol). The inflorescences of the plants were dipped into the infiltration medium for 1 min and were left o/n covered with plastic foil. Plants were grown to maturity in the plant growth chamber and plants of the next generation were selected for transformation with the transgene.

5.4.3 Crossing of *Arabidopsis* plants

For crossing of *Arabidopsis* plants with different genotypes, 3-5 unopened flower buds from genotype A were emasculated by removing all anthers, sepals and petals with a crossing tweezer. Pollen from genotype B was subsequently transferred to stigmas from genotype A. Plants were grown for 14-21 days in the plant growth chamber and the siliques with the hybrid seeds were harvested.

5.4.4 Phenotyping of *Arabidopsis* plants

For soil based phenotypic analysis, the plants were grown under LD conditions. The plant trays were rotated every 2 days to avoid that position of plants affects plant phenotypes. The morphology and development of *Arabidopsis* plants were monitored by documenting specific plant traits at several defined developmental stages as described in Boyes et al., 2001. Siliques were bleached by o/n incubation in 75 % ethanol and 25 % acetic acid. All pictures were taken with a Zeiss Discovery V8 stereo microscope or a Canon EOS 600D equipped with a Macro lens EF-S 60 mm 1:2.8 USM (Canon) or an ETS 18-55 mm objective (Canon).

For MS based phenotypic analysis of *Arabidopsis* roots, seeds were sown on 0.5x MS plates (2.15 g/L Murashige and Skoog, 1% (w/v) sucrose, 1% phyto agar (w/v); adjusted to pH 5.8) and plants were grown upright under LD conditions. All phenotypic analyses were performed at least twice.

5.4.5 Isolation of protoplasts from *Arabidopsis* rosette leaves

The isolation of *Arabidopsis* mesophyll protoplasts was performed like described in Wu et al., 2009. Briefly, the epidermis from leaves from 3-5-week-old plants was removed using a Tesafilm (Tesa) and peeled leaves (8-10) were transferred to a Petri dish containing 10 mL enzyme solution (1% cellulase Onozuka R10 (Duchefa), 0.25% macerozyme R10 (Duchefa), 0.4 M mannitol, 10 mM $CaCl_2$, 20 mM KCl, 0.1% BSA and 20 mM MES, pH 5.7). The leaves were gently shaken at 40 rpm for 120 min until the protoplasts were released into the solution.

5.4.6 Whole mount in situ hybridization (WISH) of *Arabidopsis* seedlings

WISH was performed as described in Gong et al., 2005. Briefly, seedlings (6 DAS) were fixed for 30 min in a 1:1 solution of heptane and fixation buffer (120 mM NaCl, 7 mM Na_2HPO_4, 3 mM NaH_2PO_4, 2.7mM KCl, 0.1% (v/v) Tween20, 80 mM EGTA, 10% (v/v) DMSO and 5% formaldehyde) and washed 2x in 100% ethanol and 3x with 100% methanol for five minutes. The seedlings were then incubated for 30 min in a 1:1 100% ethanol/xylene solution and washed 2x in 100% ethanol, 2x in 100% methanol and 1x in 1:1 100% methanol/fixation buffer without formaldehyde solution. Post fixation was conducted for 30 min in fixation buffer with

formaldehyde. The fixed seedlings were washed 2x for 5 min in fixation buffer without formaldehyde and 1x for 5min in Perfect Hyb™plus (Sigma) hybridization buffer. Seedlings were incubated in fresh Perfect Hyb™plus hybridization buffer for 60 min at 50 °C in a hybridization oven before 25 pmol of a 48mer of poly(dT) probe labelled at the 5'end with Alexa Fluor® 488 dye was added, and seedlings were incubated o/n at 50 °C. The seedlings were washed 1x for 60 min with 2x SCC (0.15 M NaCl, 0.015 M sodium citrate) supplemented with 0.1% (w/v) SDS, and 1x 20 min with 0.2x SCC supplemented with 0.1% (w/v) SDS. The seedlings were mounted on an object slide in DAPI solution and the roots were examined by CLSM using a Leica SP8 microscope. Intensities of the Alexa Fluor 488 signals in cytoplasm and nucleoplasm were measured in ImageJ software version 1.49m. WISH experiments were performed at least twice.

5.4.7 Cultivation of *Arabidopsis* PSB-D cells

The *Arabidopsis* landsberg erecta PSB-D suspension cells (Arabidopsis Biological Resource Center) were cultured and transformed under sterile conditions according to Van Leene et al., 2011. The cells were grown in darkness at 25 °C while shaking at 130 rpm. Once a week, the cells were diluted by transferring 7 mL cells into a 100 mL Erlenmeyer flask containing 43 mL MSMO medium (0.443 % Murashige and Skoog Salt mixture (US Biological), 3 % (w/v) sucrose, 0.5 mg/L NAA dissolved in 100 mM NaOH, 100 mg/L myo-inositol, 0.05 mg/L kinetin dissolved in DMSO, 0.4 mg/L thiamine, adjusted to pH 5.7 with 1 M KOH). For selection, MSMO medium was supplemented with kanamycin or hygromycin B to a final concentration of 50 µg/mL or 20 µg/mL, respectively.

5.4.8 Transformation of *Arabidopsis* PSB-D cells

The *Arabidopsis* suspension cells were transformed by *A. tumefaciens* mediated cell transformation. An *A. tumefaciens* colony carrying a plant expression vector (5.3.4) was grown as a starter culture in 2 mL LB medium supplemented with kanamycin o/n at 28 °C and 200 rpm. The starter culture was transferred into 20 mL selective LB medium and was grown o/n at 28 °C and 200 rpm. The cells were harvested by centrifugation for 15 min at 3000 g and re-suspended in 40 mL sterile MSMO medium. This washing step was repeated once and the OD600 of the cell suspension was adjusted to 1.0. For transformation, 3 mL of 3-days old *Arabidopsis* suspension cells (OD600: 1.2 - 1.3) were co-cultivated with 200 µl of the *A. tumefaciens*/MSMO solution and 6 µL 100 mM acetosyringone in one well of a 6-well plate. The 6-well plate was taped with Micropore surgical tape and cells were incubated for 3 days in a shaking incubator at 130 rpm and 25 °C in the dark.

For selection in liquid medium, the 3 mL transformed cells were transferred into a 25 mL Erlenmayer flask containing 8 mL MSMO medium supplemented with 50 µL/mL kanamycin or 20 µg/mL hygromycin B (for plasmid selection), 500 µL/mL vancomycin and 500 µL/mL carbenicillin (to kill *A. tumefaciens* cells). After cultivation for 8 days in a shaking incubator at 130 rpm and 25 °C the 10 mL cell suspension were transferred into a 100 mL Erlenmayer flask containing 25 mL MSMO supplemented with kanamycin or hygromycin, vancomycin and carbenicillin and the suspension culture was incubated for 7 days. In the following suspension cultures were diluted once a week like described in 5.4.7.

For selection on solid medium, the 3 mL transformed cells were washed with 40 mL MSMO medium. Cells were harvested by centrifugation for 5 min at 500 g and 2-3 mL of cells were spread on MSMO plates supplemented with 50 µL/mL kanamycin or 20 µg/mL hygromycin B, 500 µL/mL vancomycin and 500 µL/mL carbenicillin. The MSMO plates were incubated for 2-5 weeks at 25 °C in the dark. Using a scarpel, the grown callus was scraped off the plates and transferred into a 100 mL Erlenmayer flask containing 30 mL MSMO supplemented with 50 µL/mL kanamycin or 20 µg/mL hygromycin B, 500 µL/mL vancomycin and 500 µL/mL carbenicillin. After one week of incubation at 25 °C in a shaking incubator at 130 rpm, cells were diluted once a week like described in 5.4.7.

After 4-8 weeks growth in liquid MSMO medium, the transformed *Arabidopsis* suspension cells were gradually upscaled to a final volume of 5 L per transformed cell suspension culture and cells were harvested in 15 g aliquots and stored at -80 °C.

5.4.9 Tobacco infiltration

For transient expression of transgenic fusion proteins in *Nicotiana benthamiana,* 10 mL selective LB medium were inoculated with an *A. tumefaciens* colony carrying a plant expression vector (6.3.4) and grown o/n at 28 °C and 200 rpm. The bacteria were harvested by centrifugation for 10 min at 4000 g and re-suspending the bacteria pellet in 10 mL infiltration medium (10 mM MES-KOH pH 5.7, 10 mM $MgCl_2$, 0.1 mM acetosyringone dissolved in ethanol). *A. tumefaciens* cells in infiltration medium were infiltrated in the abaxial side of leaves from 2-4 weeks old *N. benthamiana* plants using a syringe. After 2-3 days, infiltrated leaves were mounted on objective slides and analysed by CLSM (5.5.1).

5.5 Microscopy

5.5.1 Confocal Laser Scanning Microscopy (CLSM)

Confocal laser scanning microscopy (CLSM) was performed using a Leica SP8 microscope, equipped with a 10X NA 0,3, 40X Oil NA 1,3 or 63X Glycerol NA 1.3 objective. DAPI was

excited with a 405 nm laser, GFP/Alexa Fluor® 488 were excited using an Argon laser at 488 nm and tagRFP/mCherry/PI were exited using an DPSS laser at 561 nm. The emission of GFP/ Alexa Fluor® 488 and tagRFP/mCherry were detected with Hybrid detectors at 500-550 nm or 570-620 nm, respectively. The emissions of DAPI or PI were detected with PMTs at 410-495 nm or 570-620 nm, respectively.

5.5.2 Förster resonance energy transfer (FRET)

For FRET acceptor photobleaching (FRET-APB), eGFP and mCherry fusion proteins acting as donor/acceptor pairs were expressed in *N. benthamiana* leaves (5.4.9) and FRET efficiencies were measured and calculated as described in Weidtkamp-peters and Stahl, 2017. Briefly, square pieces (0.5 x 0.5 cm) of infiltrated *N. benthamiana* leaves were mounted in H_2O on an objective slide with the abaxial side facing up. Images were acquired using a SP8 (Leica,Wetzlar, Germany) confocal laser scanning microscope (CLSM) equipped with a 63X Glycerol NA 1.3 objective (5.5.1). For bleaching, a circular area was bleached at 100% laser power for 80 iterations. 15 pre-bleach and 15 post-bleach images were analysed by ImageJ software version 1.49m. The mean FRET efficiencies were calculated by the following formula: ([IPOST – IPRE] / IPRE) x 100 with IPOST = mean fluorescence intensity of 15 postbleached frames and IPRE = mean fluorescence intensity of 15 prebleached frames.

5.5.3 DAPI staining

After WISH (5.4.6) and before CLSM analysis (5.5.1), *Arabidopsis* roots were mounted in DAPI solution (1x PBS pH 7.5, 0.2 µg/mL 4’,6-diamidino-2-phenylindole (DAPI), 0.1 % Triton X-100) and incubated for 10 min at RT.

5.5.4 Propidium iodide (PI) staining

Arabidopsis roots were mounted in 15 µM propidium iodide on an objective slide with a cover slip and were incubated for 10 min at RT before CLSM analysis.

6. Supplements

Table S1. Phenotypic evaluation of *4xaly* plants compared to Col-0 plants. All data are means ± SD. n = 15 for number of leaves, rosette diameter at bolting, bolting, primary inflorescences and n = 30 for root length and hypocotyl length

Genotype	No. of leaves at bolting	Rosette diameter at bolting [mm]	Bolting [DAS]	Pr. Infl. [42 DAS]	Root length 8 DAS [cm]	Hypocotyl length 8 DAS [mm]
Col-0	13.4 ± 0.63	57.2 ± 5.00	27.6 ± 1.76	4.73 ± 0.68	3.14 ± 0.30	1.96 ± 0.32
4xaly	9.13 ± 0.99	34.67 ± 7.70	30.6 ± 1.5	2.73 ± 0.44	1.95 ± 0.38	4.52 ± 0.50

Table S2. Phenotypic evaluation of *3xaly* plants compared to Col-0 plants. All data are means ± SD. n = 15

Genotype	Bolting [DAS]	Rosette diameter 28 DAS [mm]	Plant height 42 DAS [cm]	Root length 8 DAS [cm]
Col-0	26.26 ± 1.27	92.66 ± 8.20	39.53 ± 3.44	2.66 ± 0.38
3xalyALY1	28.13 ± 1.30	49.66 ± 4.62	28.13 ± 3.39	1.69 ± 0.18
3xalyALY2	23.13 ± 1.72	93.53 ± 6.66	40.4 ± 6.31	2.44 ± 0.40
3xalyALY3	21.33 ± 1.44	98.46 ± 10.76	38.53 ± 5.01	2.76 ± 0.32
3xalyALY4	21.13 ± 0.91	77.13 ± 6.18	38.46 ± 3.04	2.55 ± 0.38
4xaly	30 ± 2.17	45.53 ± 6.67	19.53 ± 10.76	1.4 ± 0.24

Table S3 . Phenotypic evaluation of *4xaly* plants expressing *ALY3-SG* compared to Col-0, *3xalyALY3* and *4xaly* plants. All data are means ± SD. n = 15

Genotype	Bolting [DAS]	Rosette diameter 28 DAS [mm]	Plant height 28 DAS [cm]
Col-0	27.4 ± 0.61	78 ± 7.15	0.26 ± 0.24
4xaly	30.8 ± 1.55	49.86 ± 9.35	0.03 ± 0.12
3xalyALY3	19.73 ± 1.18	82.8 ± 4.73	9.6 ± 2.17
# 1.3	20 ± 0.96	84.33 ± 8.15	11.1 ± 2.53
# 2.1	20.66 ± 0.86	91.73 ± 8.88	9.2 ± 2.85
# 4.8	21.2 ± 0.65	96.66 ± 8.88	8.23 ± 2.66

Table S4. Phenotypic evaluation of *4xaly* plants expressing *ALY3-eGFP* compared to Col-0, *3xalyALY3* and *4xaly* plants. All data are means ± SD. n = 15

Genotype	Bolting [DAS]	Rosette diameter 28 DAS [mm]	Plant height 28 DAS [cm]
Col-0	27.4 ± 0.61	78 ± 7.15	0.26 ± 0.24
4xaly	30.8 ± 1.55	49.86 ± 9.35	0.03 ± 0.12
3xalyALY3	19.73 ± 1.18	82.8 ± 4.73	9.6 ± 2.17
# 4.11	20.06 ± 0.92	81 ± 8.23	9.7 ± 2.95
# 5.10	21.13 ± 1.74	88.4 ± 8.22	9.13 ± 3.92
# 7.9	19.66 ± 0.86	87.66 ± 8.73	12.46 ± 2.67

Table S5. Phenotypic evaluation of *uief* mutant plants compared to Col-0 plants. All data are means ± SD. n = 15

Genotype	Bolting [DAS]	Rosette diameter 28 DAS [cm]	Plant height 42 DAS [cm]	Root length 8 DAS [mm]
Col-0	25 ± 0.63	10.68 ± 0.37	37.66 ± 2.29	32.06 ± 5.40
uief1	25.8 ± 1.22	9.28 ± 0.78	32.53 ± 2.91	33.13 ± 3.46
uief2	25.2 ± 0.74	9.53 ± 0.64	32.4 ± 1.78	33.06 ± 3.73
2xuief	25.73 ± 1.23	8.64 ± 0.91	30.53 ± 1.70	33.86 ± 3.68

Table S6. Phenotypic evaluation of 2x*uief*, *4xaly* and *4xaly2xuief* mutant plants compared to Col-0 plants. All data are means ± SD. n = 15

Genotype	Bolting [DAS]	Rosette diameter 28 DAS [cm]	Plant height 42 DAS [cm]	Root length 8 DAS [mm]
Col-0	27.2 ± 1.46	6.99 ± 0.72	31.06 ± 2.51	34.06 ± 5.00
2xuief	27.86 ± 1.02	5.14 ± 0.58	24.73 ± 1.87	34.15 ± 3.72
4xaly	30.93 ± 3.92	4.08 ± 0.68	13.93 ± 7.53	18.48 ± 3.41
4xaly 2xuief	30.4 ± 3.89	3.32 ± 0.44	10.46 ± 5.31	18.68 ± 3.21

Table S7. Phenotypic evaluation of *uief* mutant plants compared to Col-0 plants. All data are means ± SD. n = 15

Genotype	Bolting [DAS]	Rosette diameter 28 DAS [mm]	Plant height 42 DAS [cm]	Root length 8 DAS [mm]
Col-0	24.93 ± 1.28	88 ± 8.57	46.6 ± 2.65	33.06 ± 3.91
4xnxf	34.2 ± 2.97	81.86 ± 5.82	22 ± 9.05	32.2 ± 3.14
3xnxf	26.6 ± 1.25	80.33 ± 4.64	44.93 ± 3.19	32.73 ± 4.94

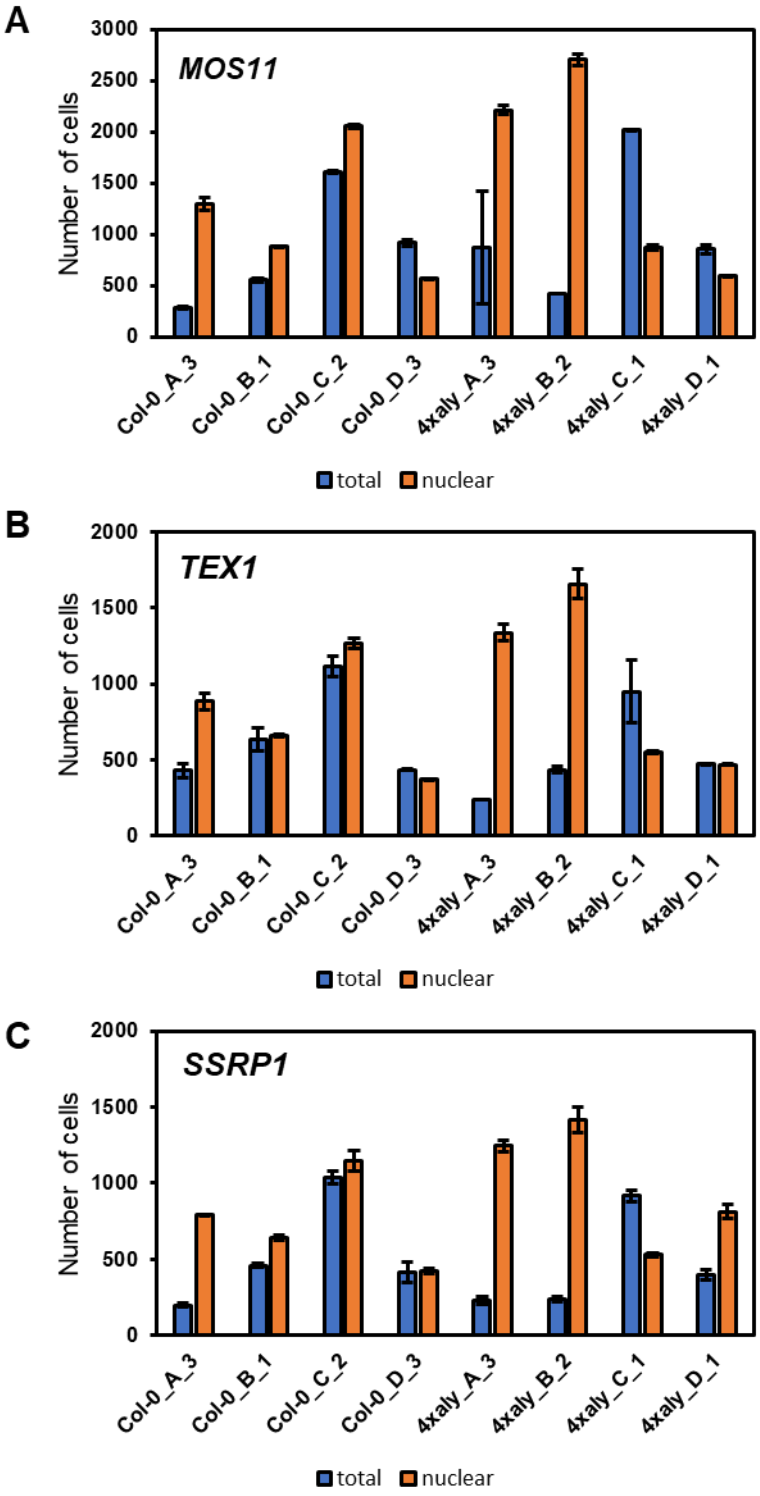

Figure S8. Number of cells determined by qPCR that were used to extract RNA for RNA sequencing. Genomic DNA isolated from a total fraction (0.05 g plant material) and a nuclear fraction (0.5 g plant material) from four biological replicates of Col-0 and *4xaly* plants was used to amplify regions from the three single copy genes (A) *MOS11*, (B) *TEX1* and (C) *SSRP1* by qPCR. Number of cells were determined by standard curves that were made based on qPCR results using known number of plasmids carrying genomic *MOS11*, *TEX1* or *SSRP1* as templates.

Table S9. List of 70 candidates identified to use a putative ALY dependent mRNA export pathway. 70 candidates were identified by transcriptomic profiling to be downregulated in 4xaly log2 < -1 (*4xaly* downregulated) and by cell fractioning followed by RNAseq to display an mRNA export block in *4xaly* EB log2 > 1 and a nuclear enrichment in *4xaly* NE log2 >1.

TAIR	DESCRIPTION	*4xaly* downregulated	*4xaly* EB	*4xaly* NE
AT1G75380	BIFUNCTIONAL NUCLEASE 1	-1.35	25.94	25.37
AT5G57655	XYLOSE ISOMERASE	-1.29	4.15	1.48
AT2G27150	ABSCISIC-ALDEHYDE OXIDASE-RELATED	-1.07	24.5	22.26
AT5G56870	BETA-GALACTOSIDASE 4	-2.32	24.07	25.53
AT2G19800	INOSITOL OXYGENASE 2	-1.57	23.27	24.5
AT5G18630	ALPHA/BETA-HYDROLASES SUPERFAMILY PROTEIN	-1.26	23.06	23.09
AT5G14120	Major facilitator superfamily protein	-1.51	1.6	1.55
AT3G19720	DYNAMIN-LIKE PROTEIN B	-1.38	11.61	8.63
AT5G36700	PHOSPHOGLYCOLATE PHOSPHATASE 1A	-1.05	11.37	9.34
AT5G41240	GLUTATHIONE S-TRANSFERASE T1-RELATED	-1.04	9.35	9.06
AT4G00750	METHYLTRANSFERASE PMT15-RELATED	-1.19	9.32	25.19
AT1G63860	DISEASE RESISTANCE PROTEIN	-1.03	9.07	8.52
AT1G07745	DNA REPAIR PROTEIN RAD51 HOMOLOG 4	-1.01	8.68	8.66
AT4G09760	CHOLINE KINASE 3-RELATED	-1.1	8.58	6.24
AT1G07135	Glycine-rich protein	-1.47	7.94	1.3
AT5G37360	LOW protein: ammonium transporter 1-like protein	-1.07	7.72	9.73
AT5G67480	BTB/POZ AND TAZ DOMAIN-CONTAINING PROTEIN 4	-1.31	7.39	8.12
AT1G15125	S-adenosyl-L-methionine-dependent methyltransferases	-1.45	7.27	25.42
AT3G53830	REGULATOR OF CHROMOSOME CONDENSATION	-1.32	6.09	7.84
AT4G19530	DISEASE RESISTANCE PROTEIN	-1.7	5.81	4.4
AT2G26560	PATATIN-LIKE PROTEIN 2	-2.05	5.2	1.87
AT3G26840	ESTERASE/LIPASE/THIOESTERASE FAMILY PROTEIN	-1.02	5.16	5.7
AT1G72930	TOLL/INTERLEUKIN-1 RECEPTOR-LIKE PROTEIN	-1.42	5.14	1.85
AT5G47040	LON PROTEASE HOMOLOG 2	-1.07	5.02	3.47
AT4G26555	PEPTIDYL-PROLYL CIS-TRANS ISOMERASE FKBP16-1	-1.84	4.92	6.7
AT3G50560	NAD(P)-binding Rossmann-fold superfamily protein	-1.06	4.69	4.97
AT4G19500	NUCLEOSIDE-TRIPHOSPHATASE/TRANSMEMBRANE RECEPTOR	-1.16	4.38	2.38
AT4G27710	CYTOCHROME P450 709B3	-1.18	4.11	3.92
AT3G26510	OCTICOSAPEPTIDE/PHOX/BEM1P FAMILY PROTEIN	-1.08	3.6	6.68
AT1G76650	CALCIUM-BINDING PROTEIN CML38	-2.59	3.56	1.42
AT2G41290	PROTEIN STRICTOSIDINE SYNTHASE-LIKE 2	-1.01	3.55	1.44
AT5G49730	SUPEROXIDE-GENERATING NADPH OXIDASE HEAVY CHAIN SUBUNIT B	-1.02	3.39	3.7
AT1G73480	MONOGLYCERIDE LIPASE	-1.27	3.39	1.65
AT1G18020	12-OXOPHYTODIENOATE REDUCTASE-LIKE PROTEIN 2A-RELATED	-1.43	2.89	2.43
AT4G23300	CYSTEINE-RICH RECEPTOR-LIKE PROTEIN KINASE 11-RELATED	-1.01	1.03	1.25
AT3G44860	ATPP-LIKE PROTEIN-RELATED	-1.5	2.5	1.94
AT2G20725	CAAX AMINO TERMINAL PROTEASE FAMILY PROTEIN	-1.01	2.46	1.21
AT5G46110	GLUCOSE-6-PHOSPHATE/PHOSPHATE TRANSLOCATOR-LIKE	-1.17	2.4	1.58
AT4G02520	GLUTATHIONE S-TRANSFERASE F2	-1.38	2.38	3.29
AT1G60140	Enzyme putatively involved in trehalose biosynthesis	-1.54	2.3	2.62
AT3G15356	LECTIN-LIKE PROTEIN-RELATED	-1.67	2.24	1.89
AT4G36690	SPLICING FACTOR U2AF LARGE SUBUNIT A	-1.21	2.18	3.57
AT1G18730	PHOTOSYNTHETIC NDH SUBUNIT OF SUBCOMPLEX B 4	-1.4	2.15	1.32
AT4G24350	PHOSPHORYLASE SUPERFAMILY PROTEIN	-1.38	2.03	2.07
AT2G29310	Tropinone reductase homolog	-1.63	1.98	1.03
AT2G23600	METHYLESTERASE 2-RELATED	-1.08	1.91	1.32
AT4G25835	AAA-ATPase	-1.21	1.84	3.6
AT2G43010	TRANSCRIPTION FACTOR PIF4	-1.07	1.81	1.22
AT1G72450	PROTEIN TIFY 11B	-1.02	1.77	1.12
AT1G21100	INDOLE GLUCOSINOLATE O-METHYLTRANSFERASE 1-RELATED	-1.59	1.71	1.49
AT4G31550	WRKY TRANSCRIPTION FACTOR 11-RELATED	-1.55	1.67	1.51
AT5G25240	STRESS INDUCED PROTEIN	-1.65	1.63	1.92
AT5G03350	LECTIN-LIKE PROTEIN-RELATED	-1.31	1.62	1.7
AT2G28120	DEUBIQUITILATING ENZYME 1	-1.5	1.62	1.41
AT1G61100	CSL1	1.06	1.55	1.03
AT4G13495	Full length noncoding primary transcript	-1.22	1.49	1.18
AT2G30990	N-METHYLTRANSFERASE	-1.35	1.46	1.19
AT3G26210	CYTOCHROME P450 71B23	-1.03	1.35	1.4
AT2G40100	CHLOROPHYLL A-B BINDING PROTEIN CP29.3	-1.24	1.29	1.35
AT1G23090	SULFATE TRANSPORTER 3.3-RELATED	-1.07	1.28	8.35
AT5G64572	Natural antisense transcript	-1.14	1.27	1.19
AT3G14930	UROPORPHYRINOGEN DECARBOXYLASE 1	-1.36	1.24	1.47
AT5G24470	TWO-COMPONENT RESPONSE REGULATOR-LIKE APRR5	-1.48	1.16	1.12
AT4G16860	DISEASE RESISTANCE PROTEIN	-1.07	1.15	1.6
AT2G47060	Probable receptor-like protein kinase	-1.1	1.15	1.21
AT1G02840	SERINE/ARGININE-RICH SPLICING FACTOR SR34B-RELATED	-1.19	1.14	1.04
AT1G25400	Transmembrane protein	-1.96	1.12	1.09
AT3G19680	Uncharacterized protein	-1.34	1.05	1.17
AT5G44568	Transmembrane protein	-1.37	1.03	1.63
AT1G27450	ADENINE PHOSPHORIBOSYLTRANSFERASE 1	-1.03	1.01	1.39

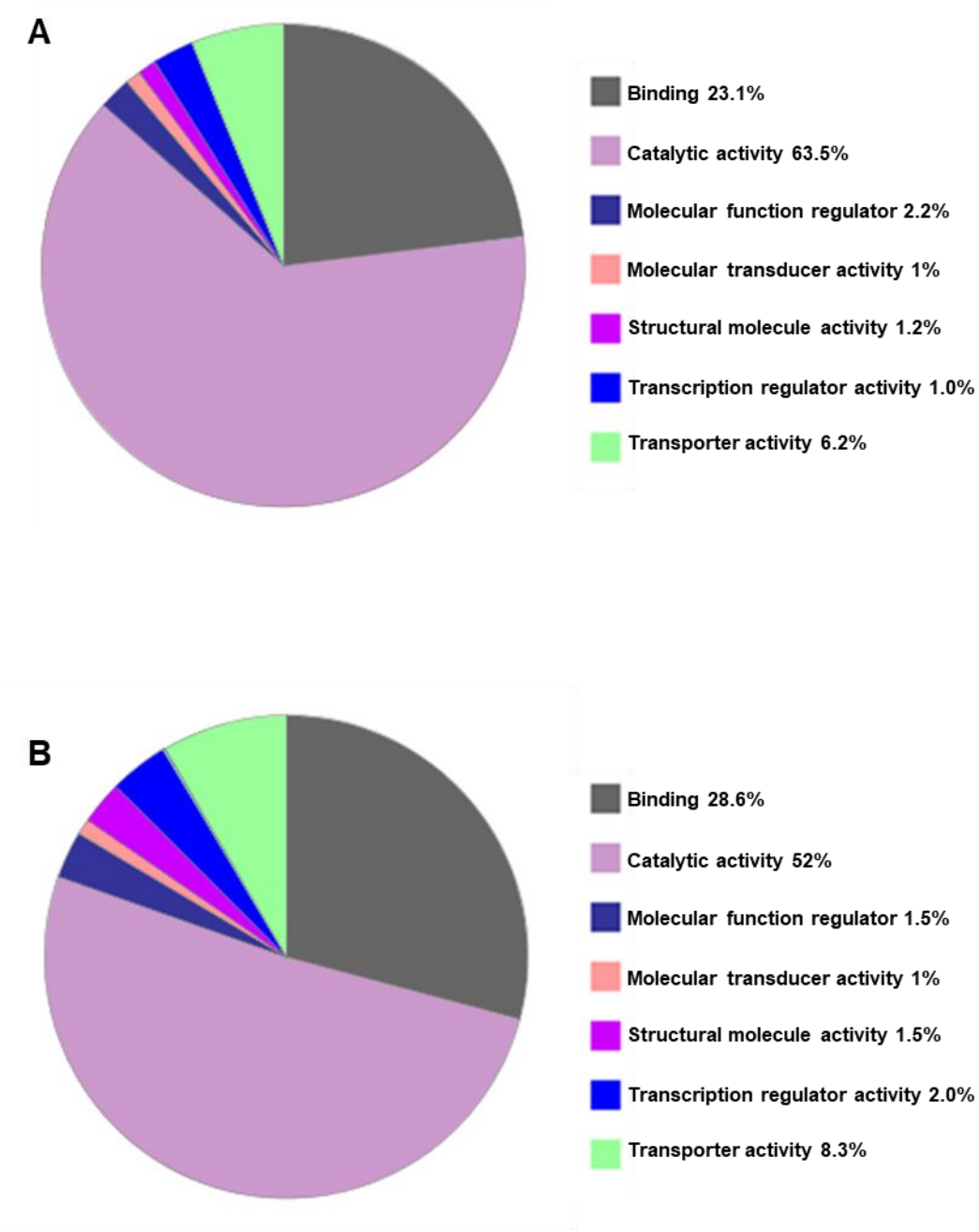

Figure S10. GO-term analysis of candidates identified to use a putative ALY dependent mRNA export pathway. (A) GO term analysis for molecular function of 403 function hits identified from 1085 candidate genes detected by transcript profiling to be downregulated in 4xaly log2 < -1 (*4xaly* downregulated). (B) GO term analysis for molecular function of 480 function hits identified from 964 candidate genes detected in the cell fractioning experiment with *4xaly* EB log2 > 1 and *4xaly* NE log2 > 1. Analysis was done using http://www.pantherdb.org.

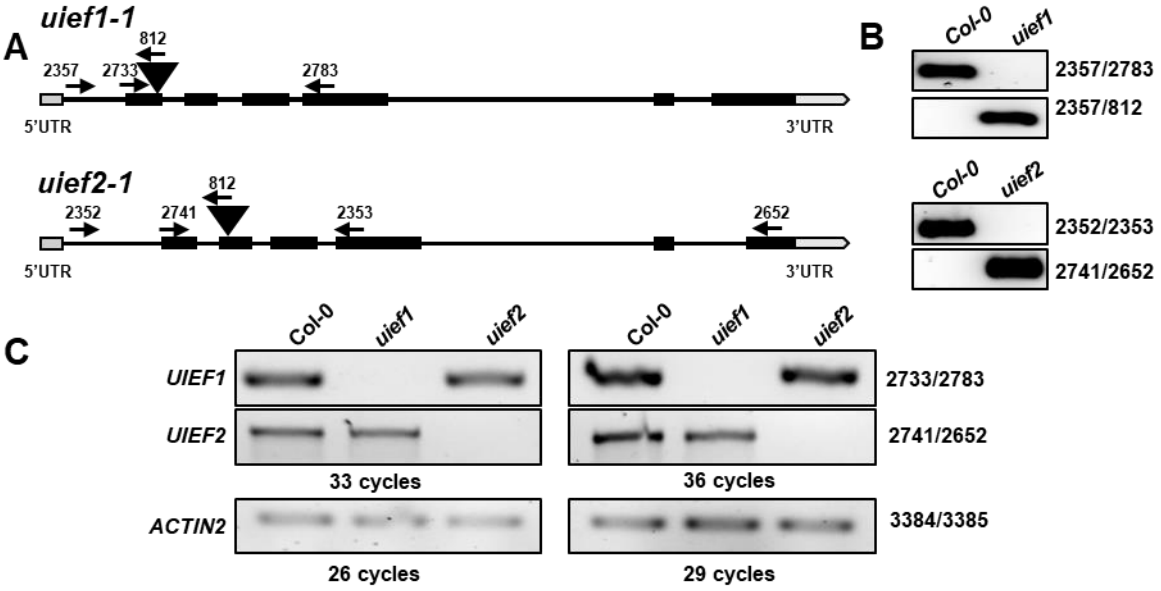

Figure S11. Molecular characterization of *uief1-1* and *uief2-1* T-DNA insertion lines. (A) *uief1-1* and *uief2-1* T-DNA insertion alleles with triangles marking the T-DNA insertion. Primers used for genotyping PCR (B) and RT-PCR (C) are highlighted with black arrows. UTRs = light grey boxes, exons = block boxes, introns = black lines. (B) Genotyping PCRs with the indicated primers in the homozygous *uief1-1* and *uief2-1* T-DNA insertion mutants. (C) RT-PCR using cDNA generated from RNA extracted from 14 DAS seedlings of Col-0 and the homozygous *uief1-1* and *uief2-1* T-DNA insertion mutant plants with the indicated primers spanning the T-DNA insertions. RT-PCRs were performed for various cycles to show that PCR reactions were not saturated.

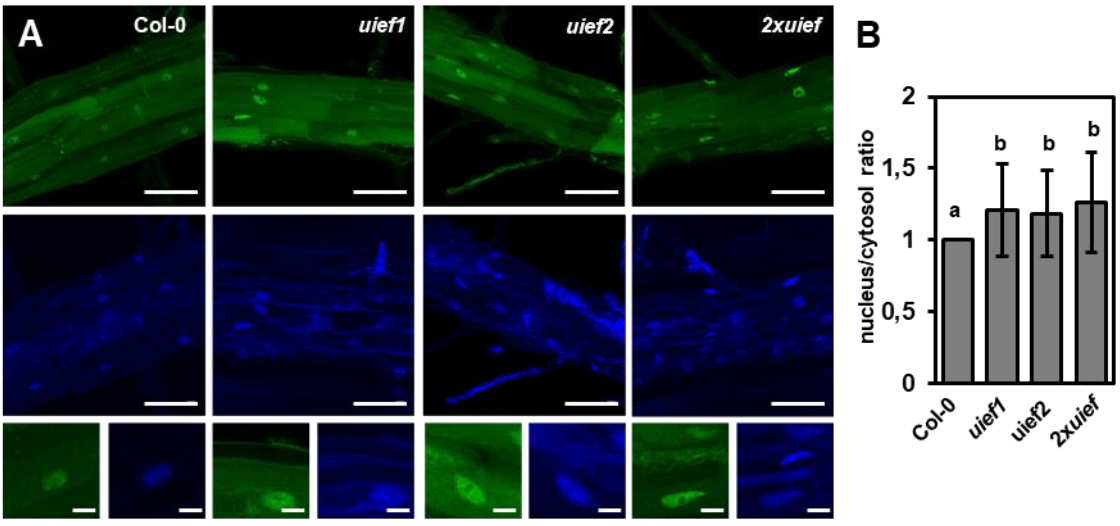

Figure S12. *uief* single and double mutants show moderate mRNA export block. (A) CLSM images from representative sections from roots of Col-0, *uief1, uief2* and *2xuief plants* after WISH with the Alexa Fluor 488 oligo (dT) signal in green and DAPI signal in blue. Bars = 60 µm (top rows) and 10 µm (bottom row). (B) Average nuclear/cytosol signal ratio of 75 or more nuclei per genotype. The ratios are shown relative to Col-0 (ratio of 1), with error bars indicating SD. Data sets marked with different letters are significantly different as assessed by a multicomparison Tukey's test ($P < 0{,}001$) after one-way analysis of variance.

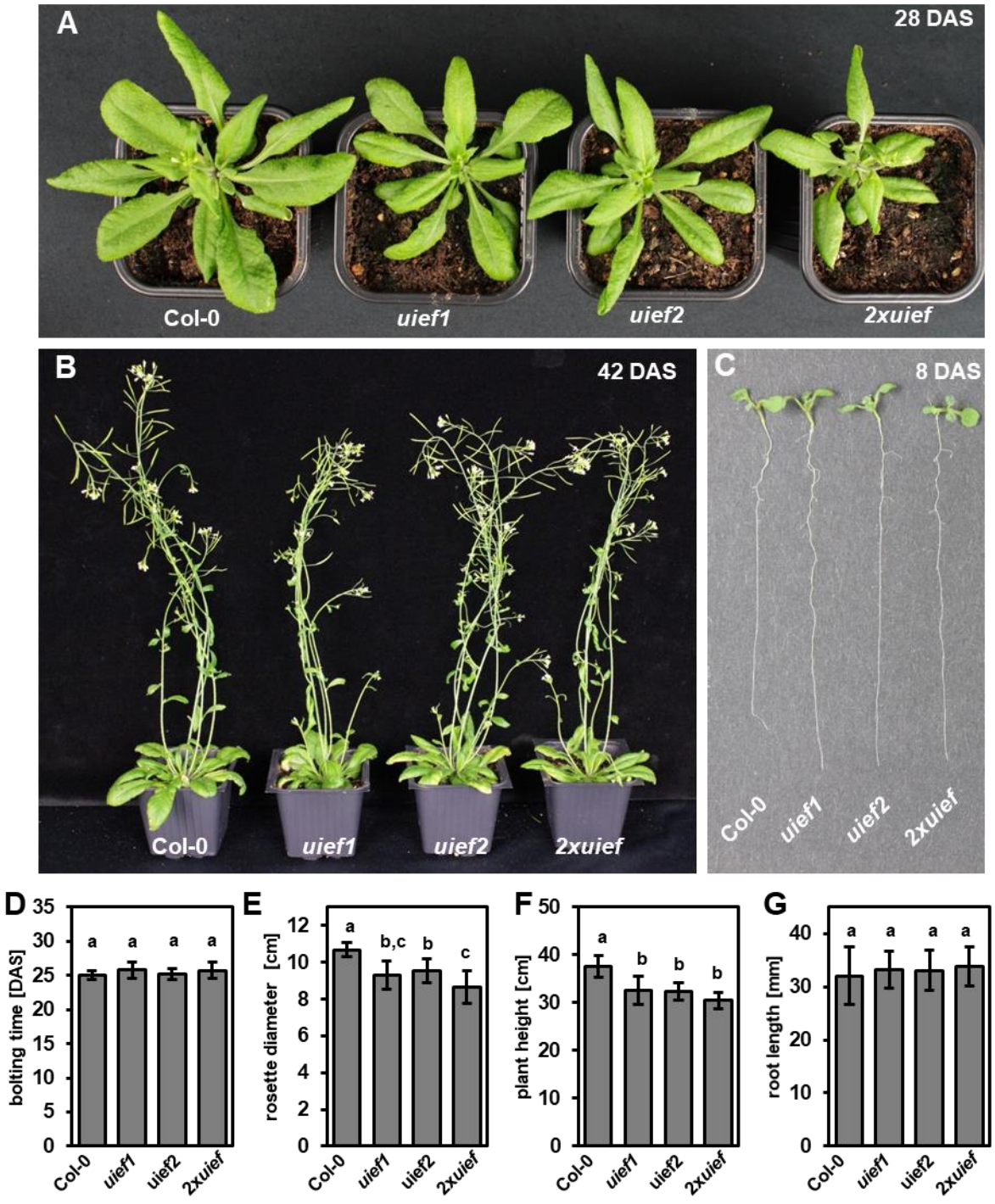

Figure S13. ***uief*** **single and double plants are only mildly affected regarding plant growth and development.** Phenotype of *uief1*, *uief2* and *2xuief* plants compared to Col-0 at 28 DAS (A) and 42 DAS (B). *uief* plants show no altered root length at 8 DAS (C). (D-G) Phenotypic analysis for (D) bolting time, (E) rosette diameter at bolting, (F) plant height 42 DAS and (G) root length 8 DAS. Error bars indicate SD of 15 plants Data sets marked with different letters are significantly different as assessed by a multicomparison Tukey's test ($P < 0.05$) after one-way analysis of variance.

Table S14a. List of expected interactors of mRNA export factors. Proteins that co-purified with ALY1-SG, ALY2-SG, ALY3-SG, ALY4-SG, UIEF1-SG and UIEF2-SG. Proteins that co-purified with unfused SG were removed from the list. The average MASCOT score is shown and how many times the protein was detected in out three independent experiments.

TAIR	DESCRIPTION	ALY1	ALY2	ALY3	ALY4	UIEF1	UIEF2
AT3G13990	UBQ3 – polyubiquitin 3	4772/ 3	3437/ 3	290/ 3		3969/ 3	
AT1G55820	GBF-INTERACTING PROTEIN 1-RELATED	3929/ 3	3447/ 3		198/ 2	3459/ 3	148/ 2
AT3G13222	GBF-INTERACTING PROTEIN 1-RELATED	3344/ 3	2175/ 3			2845/ 3	
AT1G13730	NUCLEAR TRANSPORT FACTOR 2	2840/ 3	2584/ 3			3307/ 3	147/ 2
AT1G29350	RNA POLYMERASE II DEGRADATION FACTOR-LIKE PROTEIN	1836/ 3	1344/ 3			1525/ 3	
AT5G03740	HISTONE DEACETYLASE HDT3	1368/ 3	1113/ 3			1395/ 3	
AT3G25150	NUCLEAR TRANSPORT FACTOR 2	1121/ 3	1346/ 3			1388/ 3	
AT5G13850	HMR-RELATED	1093/ 3	1048/ 3	423/ 2	267/ 2	887/ 3	176/ 2
AT2G27840	HISTONE DEACETYLASE HDT4	1130/ 3	929/ 3			1135/ 3	
AT1G69250	NUCLEAR TRANSPORT FACTOR 2	1153/ 3	1293/ 3	248/ 2		1531/ 3	
AT3G12390	NASCENT POLYPEPTIDE-ASSOCIATED COMPLEX SUBUNIT	805/ 3	836/ 3	226/ 2	206/ 2	841/ 2	
AT2G43030	50S RIBOSOMAL PROTEIN L3-1	642/ 3	747/ 3	394/ 3	406/ 3	790/ 3	208/ 2
AT4G17520	RGG REPEATS NUCLEAR RNA BINDING PROTEIN B	1007/ 3	715/ 3	336/ 2		1106/ 3	
AT5G47210	AT19571P-RELATED	779/ 3	836/ 3	362/ 2		1454/ 3	202/ 2
AT2G20060	39S RIBOSOMAL PROTEIN L4	424/ 3	484/ 3	351/ 3	512/ 3	627/ 3	
AT4G01310	54S RIBOSOMAL PROTEIN L7	729/ 3	1022/ 3	568/ 3	724/ 3	946/ 3	
AT5G44780	MULTIPLE ORGANELLAR RNA EDITING FACTOR 4	606/ 3	574/ 3	162/ 2		582/ 3	180/ 3
AT2G42710	MITOCHONDRIAL RIBOSOMAL PROTEIN	748/ 3	808/ 3	531/ 2	500/ 3	987/ 3	
AT1G70180	Sterile alpha motif (SAM) domain-containing protein	583/ 3	1461/ 3	1272/ 3	373/ 3	290/ 3	
AT3G25920	54S RIBOSOMAL PROTEIN L10	724/ 3	1021/ 3	1005/ 3	792/ 3	832/ 3	
AT4G30890	UBIQUITIN CARBOXYL-TERMINAL HYDROLASE 10	555/ 3	601/ 3			693/ 3	
AT3G27925	PROTEASE DO-LIKE 1	506/ 3	597/ 3			776/ 3	
AT1G66260	THO COMPLEX SUBUNIT 4C	499/ 3	463/ 3	2749/ 3	177/ 3	420/ 3	
AT1G07310	CALCIUM-DEPENDENT LIPID-BINDING	474/ 3	455/ 3			388/ 3	
AT1G76940	NUCLEAR SPECKLE RNA-BINDING PROTEIN A	541/ 3	521/ 3			471/ 3	257/ 2
AT5G66860	RIBOSOMAL PROTEIN L25/GLN-TRNA SYNTHETASE	537/ 3	637/ 3	644/ 3	583/ 3	699/ 3	157/ 2
AT1G07320	50S RIBOSOMAL PROTEIN L4	367/ 3	538/ 3	333/ 3	455/ 3	589/ 3	128/ 2
AT1G48620	HIGH MOBILITY GROUP A5	449/ 3	400/ 3	331/ 3	213/ 3	424/ 3	
AT3G52150	30S RIBOSOMAL PROTEIN 2	429/ 3	393/ 3	572/ 3	317/ 3	438/ 3	
AT3G51800	PROLIFERATION-ASSOCIATED PROTEIN 2G4	374/ 3	289/ 3			417/ 3	
AT5G55210	Hypothetical protein	383/ 3	329/ 3			377/ 3	
AT4G05400	39S RIBOSOMAL PROTEIN L40	241/ 3	430/ 3	855/ 3	626/ 3	337/ 3	107/ 2
AT1G52370	Ribosomal protein L22p/L17e family protein	365/ 3	389/ 3	414/ 3	301/ 3	386/ 3	
AT4G38150	Pentatricopeptide repeat-containing protein	285/ 3	380/ 3			220/ 3	
AT5G23900	60S RIBOSOMAL PROTEIN L13-3	238/ 3	263/ 3			295/ 3	
AT4G28360	Ribosomal protein L22p/L17e family protein	289/ 3	315/ 3	309/ 2	245/ 3	262/ 3	
AT5G52380	VASCULAR-RELATED NAC-DOMAIN 6	188/ 3	245/ 2	207/ 2		182/ 3	
AT5G59870	HISTONE H2A	180/ 3	347/ 2			268/ 2	
AT2G33845	EXPRESSED PROTEIN	169/ 3	131/ 2				
AT3G61820	EUKARYOTIC ASPARTYL PROTEASE FAMILY PROTEIN	162/ 3	358/ 3	548/ 2	274/ 2	386/ 3	
AT5G46020	28 KDA HEAT/ACID-STABLE PHOSPHOPROTEIN-LIKE PROTEIN	139/ 3	183/ 2			245/ 3	
AT3G44750	HISTONE DEACETYLASE HDT1	123/ 3	113/ 3			166/ 2	
AT1G32990	50S RIBOSOMAL PROTEIN L11	1148/ 2	995/ 3	1230/ 3	642/ 3		
AT2G32060	40S RIBOSOMAL PROTEIN S12	705/ 2		370/ 3		146/ 2	
AT1G17880	TRANSCRIPTION FACTOR BTF3	639/ 2	545/ 3				
AT3G15190	30S RIBOSOMAL PROTEIN S20	533/ 2	601/ 3	289/ 2	194/ 3		
AT3G49470	NASCENT POLYPEPTIDE-ASSOCIATED COMPLEX SUBUNIT	374/ 2	393/ 3			227/ 3	
AT4G30800	40S RIBOSOMAL PROTEIN S11	425/ 2	410/ 3				
AT3G55620	EUKARYOTIC TRANSLATION INITIATION FACTOR 6-1-RELATED	352/ 2	220/ 3			442/ 2	
AT5G17510	GLUTAMINE-RICH PROTEIN-RELATED	256/ 2	216/ 2			215/ 2	
AT1G31817	RIBOSOMAL PROTEIN S11	246/ 2	200/ 3	565/ 3	262/ 3	303/ 3	
AT1G78630	50S RIBOSOMAL PROTEIN L13	326/ 2	295/ 3	294/ 2	137 2	296/ 2	
AT1G03230	EUKARYOTIC ASPARTYL PROTEASE FAMILY PROTEIN	260/ 2	380/ 3	144/ 2	112/ 3	156/ 3	
AT1G62850	CLASS I PEPTIDE CHAIN RELEASE FACTOR	281/ 2	230/ 3			299/ 2	
AT1G24240	39S RIBOSOMAL PROTEIN L19	274/ 2	391/ 3	380/ 3	309/ 2		
AT5G23535	39S RIBOSOMAL PROTEIN L24	321/ 2	348/ 3	483/ 3	328/ 3		
AT4G10480	NASCENT POLYPEPTIDE-ASSOCIATED COMPLEX SUBUNIT	315/ 2	332/ 3			276/ 2	
AT3G03920	H/ACA RIBONUCLEOPROTEIN COMPLEX SUBUNIT 1	225/ 2	131/ 2			249/ 2	
ATCG00900	28S RIBOSOMAL PROTEIN S7	250/ 2	245/ 3	130/ 2			
AT2G22780	MALATE DEHYDROGENASE	204/ 2	136/ 3			250/ 2	
AT5G64260	PROTEIN EXORDIUM-LIKE 2	296/ 2	237/ 3	263/ 3		260/ 3	
ATCG00750	28S RIBOSOMAL PROTEIN S11	196/ 2		372/ 2			
AT2G05920	SUBTILISIN-LIKE PROTEASE SBT1.8	250/ 2	279/ 2		828/ 2	323/ 3	
AT5G65220	50S RIBOSOMAL PROTEIN L29	198/ 2		293/ 2			
AT4G16830	RGG REPEATS NUCLEAR RNA BINDING PROTEIN A	252/ 2	183/ 2			369/ 2	
AT3G48800	STERILE ALPHA MOTIF	180/ 2	245/ 3	168/ 2		208/ 3	84/ 2
AT5G30510	30S RIBOSOMAL PROTEIN S1	221/ 2	279/ 3	128/ 2		226/ 3	
AT5G54600	50S RIBOSOMAL PROTEIN L24	218/ 2	278/ 3	467/ 3	167/ 2		
AT5G18550	ZINC FINGER CCCH DOMAIN-CONTAINING PROTEIN 58	170/ 2					
ATCG00830	39S RIBOSOMAL PROTEIN L2	185/ 2	175/ 2			114 2	
AT1G69530	EXPANSIN-A1	171/ 2	183/ 3	127/ 2			
AT5G40950	39S RIBOSOMAL PROTEIN L27	163/ 2		321/ 2			
AT2G44210	carboxyl-terminal peptidase	141/ 2	152/ 3			227/ 2	
AT5G42960	OUTER ENVELOPE PORE PROTEIN 24A	150/ 2	203/ 2			191/ 2	
AT3G09480	HISTONE H2B.5-RELATED	172/ 2					
AT3G07170	LD21067P	153/ 2	120/ 2	94/ 2			
AT1G76460	RNA-BINDING	136/ 2					
AT2G42680	MULTIPROTEIN-BRIDGING FACTOR 1A	141/ 2					
AT2G44525	NADH dehydrogenase ubiquinone 1 alpha subcomplex	133/ 2	173/ 3				
AT3G55605	Mitochondrial glycoprotein	119/ 2	131/ 3				
AT4G10970	RIBOSOME MATURATION FACTOR	120/ 2	87/ 2			1448/ 3	
AT3G63190	RIBOSOME-RECYCLING FACTOR	145/ 2	163/ 3				
AT5G07310	ETHYLENE-RESPONSIVE TRANSCRIPTION FACTOR ERF115	112/ 2				98/ 2	
AT4G28440	Nucleic acid-binding, OB-fold-like protein	114/ 2					
AT1G69410	EUKARYOTIC TRANSLATION INITIATION FACTOR 5A-3	112/ 2	147/ 2				
AT1G47420	SUCCINATE DEHYDROGENASE SUBUNIT 5	113/ 2	242/ 2				
AT5G62200	EMBRYO-SPECIFIC PROTEIN ATS3B	120/ 2				110/ 2	
AT3G56910	50S RIBOSOMAL PROTEIN 5	122/ 2	136/ 3	159/ 2			
AT5G27670	HISTONE H2A.5-RELATED	126/ 2	152/ 3				

Table S14b. List of expected interactors of mRNA export factors. Proteins that co-purified with ALY1-SG, ALY2-SG, ALY3-SG, ALY4-SG, UIEF1-SG and UIEF2-SG. Proteins that co-purified with unfused SG were removed from the list. The average MASCOT score is shown and how many times the protein was detected in out three independent experiments.

TAIR	DESCRIPTION	ALY1	ALY2	ALY3	ALY4	UIEF1	UIEF2
AT5G09440	PROTEIN EXORDIUM-LIKE 4	102/ 2		162/ 2			
AT1G01300	ASPARTYL PROTEASE FAMILY PROTEIN 2	120/ 2	408/ 3			248/ 3	
AT2G22720	SPT2 CHROMATIN PROTEIN	104/ 2					
AT4G22745	METHYL-CPG-BINDING DOMAIN-CONTAINING PROTEIN 1-RELATED	94/ 2	123/ 2			309/ 2	
AT2G19750	40S RIBOSOMAL PROTEIN S30	92/ 2					
AT3G53650	HISTONE H2B.8		1452/ 3				
AT1G20220	ALBA DNA/RNA-BINDING PROTEIN		230/ 3			209/ 3	
AT4G12080	AT-HOOK MOTIF NUCLEAR-LOCALIZED PROTEIN 1		157/ 3		192/ 2	275/ 3	
AT2G45850	AT-HOOK MOTIF NUCLEAR-LOCALIZED PROTEIN 9		191/ 3				
AT4G33250	EUKARYOTIC TRANSLATION INITIATION FACTOR 3 SUBUNIT K		245/ 3			309/ 2	
AT1G21690	REPLICATION FACTOR C SUBUNIT 4		198/ 3			107/ 2	
AT1G64510	30S RIBOSOMAL PROTEIN S6 ALPHA		162/ 3	314/ 2			
AT3G18580	NUCLEIC ACID-BINDING		160/ 3				
AT5G53070	RIBOSOMAL PROTEIN L9/RNASE H1		141/ 3		269/ 2	216/ 2	
AT1G60640	STRESS RESPONSE PROTEIN		135/ 3			306/ 3	
AT4G27380	Hypothetical protein		132/ 3				
AT1G52740	HISTONE H2A VARIANT 3-RELATED		118/ 3	104/ 2		99/ 2	
AT5G67510	60S RIBOSOMAL PROTEIN L26-1-RELATED		113/ 3				
AT3G51010	Protein translocase subunit		112/ 3				
AT3G13120	37S RIBOSOMAL PROTEIN S10		113/ 3				
AT5G23680	Sterile alpha motif (SAM) domain-containing protein		92/ 3			99/ 3	
AT5G64670	39S RIBOSOMAL PROTEIN L15		99/ 3			123/ 2	
AT4G31810	3-HYDROXYISOBUTYRYL-COA HYDROLASE-LIKE PROTEIN 2		339/ 2			187/ 2	
AT5G51590	AT-HOOK MOTIF NUCLEAR-LOCALIZED PROTEIN 4		260/ 2		203 3	253/ 3	
AT2G47680	DEXH-BOX ATP-DEPENDENT RNA HELICASE DEXH8		260/ 2				
AT1G28110	SERINE CARBOXYPEPTIDASE-LIKE 45		197/ 2				
AT3G12700	ASPARTIC PROTEINASE NANA		194/ 2				
AT1G64350	NUCLEOPORIN SEH1		196/ 2				
AT2G41040	S-adenosyl-L-methionine-dependent methyltransferases superfamily protein		190/ 2				387/ 2
AT5G09770	39S RIBOSOMAL PROTEIN L17		218/ 2		132/ 2		
AT5G64650	39S RIBOSOMAL PROTEIN L17		207/ 2				
AT1G26770	EXPANSIN-A10		151/ 2				
AT1G76010	ALBA DNA/RNA-BINDING PROTEIN		129/ 2				
AT3G61310	AT-HOOK MOTIF NUCLEAR-LOCALIZED PROTEIN 11		129/ 2				
AT2G44065	60S RIBOSOMAL PROTEIN L2		117/ 2	293/ 2			
AT4G03120	U1 SMALL NUCLEAR RIBONUCLEOPROTEIN C		111/ 2			102/ 2	
AT2G42610	PROTEIN LIGHT-DEPENDENT SHORT HYPOCOTYLS 10		127/ 2				
AT1G68560	ALPHA-XYLOSIDASE 1-RELATED		102/ 2				
AT2G21440	EXPRESSED PROTEIN		99/ 2				
AT3G20740	POLYCOMB PROTEIN EED		105/ 2				
AT3G27010	TRANSCRIPTION FACTOR TCP11-RELATED		98/ 2				
AT5G13510	39S RIBOSOMAL PROTEIN L10		86/ 2				
AT3G13230	RNA-BINDING PROTEIN PNO1		83/ 2			126/ 2	
AT1G75350	50S RIBOSOMAL PROTEIN L31			371/ 3			
AT1G73940	umor necrosis factor receptor family protein			356/ 3			
AT4G34620	30S RIBOSOMAL PROTEIN S16-1			294/ 3			
AT5G40040	60S ACIDIC RIBOSOMAL PROTEIN P2			293/ 3			
AT5G39600	39S RIBOSOMAL PROTEIN L53			235/ 3			
AT1G79850	30S RIBOSOMAL PROTEIN S17			228/ 3			
AT5G40080	39S RIBOSOMAL PROTEIN L41			279/ 3			
AT5G27820	Ribosomal L18p/L5e family protein			222/ 3			
AT4G37660	Ribosomal protein L12/ ATP-dependent Clp protease adaptor protein			200/ 3			
AT3G01740	39S RIBOSOMAL PROTEIN L54			198/ 3			
AT5G43960	GB|AAD20086.1			1491/ 2			
ATCG00680	PHOTOSYSTEM II CP47 REACTION CENTER PROTEIN			397/ 2	257/ 2		
AT4G35490	39S RIBOSOMAL PROTEIN L11			425/ 2			
AT5G55140	39S RIBOSOMAL PROTEIN L30			503/ 2			
AT1G07830	39S RIBOSOMAL PROTEIN L47			412/ 2			
AT5G39800	39S RIBOSOMAL PROTEIN L41			369/ 2			
AT1G48350	39S RIBOSOMAL PROTEIN L18			371/ 2			
AT3G59650	39S RIBOSOMAL PROTEIN L43			331/ 2			
AT1G49400	37S RIBOSOMAL PROTEIN S17			319/ 2			
AT5G50600	11-BETA-HYDROXYSTEROID DEHYDROGENASE 1A-RELATED			301/ 2			
AT4G21280	OXYGEN-EVOLVING ENHANCER PROTEIN 3-1			200/ 2			
AT5G14910	Heavy metal transport/detoxification superfamily protein			252/ 2			
AT1G70190	50S RIBOSOMAL PROTEIN L7/L12-RELATED			209/ 2		106/ 2	
ATCG00020	PHOTOSYSTEM II PROTEIN D1			167/ 2			
AT1G74970	30S RIBOSOMAL PROTEIN S9			163/ 2			
AT1G27435	hypothetical protein			183 2			
AT1G77750	SMALL RIBOSOMAL SUBUNIT PROTEIN S13			205/ 2			
AT2G33450	50S RIBOSOMAL PROTEIN L28			168/ 2			
AT5G52370	28S RIBOSOMAL S34 PROTEIN			150/ 2			
ATCG00905	28S RIBOSOMAL PROTEIN S12			143/ 2			
AT5G02050	MITOCHONDRIAL GLYCOPROTEIN FAMILY PROTEIN			144/ 2			
AT1G17560	50S RIBOSOMAL PROTEIN HLL			145/ 2			
AT1G03890	12S SEED STORAGE PROTEIN CRD			122/ 2			
AT1G68590	30S RIBOSOMAL PROTEIN 3-1			114/ 2			
AT3G27850	50S RIBOSOMAL PROTEIN L12-1			119/ 2			
AT1G54870	GLUCOSE AND RIBITOL DEHYDROGENASE HOMOLOG 2-RELATED			108/ 2			
ATCG00820	37S RIBOSOMAL PROTEIN S19			122/ 2			
AT5G15760	30S RIBOSOMAL PROTEIN 3-2			97/ 2			
AT1G69620	60S RIBOSOMAL PROTEIN L34-1-RELATED			92/ 2			
AT3G12370	50S RIBOSOMAL PROTEIN L10				166/ 3		
AT3G50820	OXYGEN-EVOLVING ENHANCER PROTEIN 1-2				108/ 3		
AT2G37230	Pentatricopeptide repeat-containing protein				476/ 2		192/ 2
ATCG00280	PHOTOSYSTEM II CP43 REACTION CENTER PROTEIN				229/ 2		
AT5G14740	BETA CARBONIC ANHYDRASE 2				204/ 2		
AT3G01500	BETA CARBONIC ANHYDRASE 1				191/ 2		
AT4G38970	FRUCTOSE-BISPHOSPHATE ALDOLASE 2				153/ 2		

Table S14c. List of expected interactors of mRNA export factors. Proteins that co-purified with ALY1-SG, ALY2-SG, ALY3-SG, ALY4-SG, UIEF1-SG and UIEF2-SG. Proteins that co-purified with unfused SG were removed from the list. The average MASCOT score is shown and how many times the protein was detected in out three independent experiments.

TAIR	DESCRIPTION	ALY1	ALY2	ALY3	ALY4	UIEF1	UIEF2
AT3G06040	RIBOSOMAL PROTEIN L12/ ATP-DEPENDENT CLP PROTEASE				125/ 2		
AT4G39880	39S RIBOSOMAL PROTEIN L23				111/ 2		
AT5G09500	40S RIBOSOMAL PROTEIN S15-3-RELATED				105/ 2		
AT3G04590	AT-HOOK MOTIF NUCLEAR-LOCALIZED PROTEIN 14					201/ 3	
AT2G33620	AT-HOOK MOTIF NUCLEAR-LOCALIZED PROTEIN 10					107/ 3	
AT3G63030	METHYL-CPG-BINDING DOMAIN-CONTAINING PROTEIN 1-RELATED					327/ 2	
AT1G54770	DEOXYNUCLEOTIDYLTRANSFERASE INTERACTING PROTEIN 2					175/ 2	
AT4G32605	Mitochondrial glycoprotein family protein					212/ 2	
AT5G43310	COP1-INTERACTING PROTEIN-LIKE PROTEIN					152/ 2	108/ 2
AT1G32730	ELECTRON CARRIER/IRON ION-BINDING PROTEIN					163/ 2	
AT2G22090	UBP1-ASSOCIATED PROTEINS 1A-RELATED					172/ 2	
AT1G33780	TRANSPORTER					156/ 2	
AT1G74000	PROTEIN STRICTOSIDINE SYNTHASE-LIKE 11					161/ 2	
AT5G11900	TRANSLATION MACHINERY-ASSOCIATED PROTEIN 22					149/ 2	
AT1G61150	GLUCOSE-INDUCED DEGRADATION PROTEIN 8 HOMOLOG					136/ 2	
AT5G23400	DISEASE RESISTANCE PROTEIN-LIKE					139/ 2	
AT5G47390	TRANSCRIPTION FACTOR KUA1					125/ 2	
AT3G01160	ESF1 HOMOLOG					109/ 2	
AT1G35140	PROTEIN EXORDIUM-RELATED					96/ 2	
AT2G43650	SOMETHING ABOUT SILENCING PROTEIN 10					92/ 2	
AT2G39700	EXPANSIN-A4					86/ 2	
AT4G23910	UAP56-INTERACTING EXPORT FACTOR 2						1335/ 3
AT3G06850	LIPOAMIDE ACYLTRANSFERASE COMPONENT						319/ 3
AT2G44530	RIBOSE-PHOSPHATE PYROPHOSPHOKINASE 5						202/ 3
AT5G08420	KRR1 SMALL SUBUNIT PROCESSOME COMPONENT HOMOLOG						231/ 3
AT1G76810	EUKARYOTIC TRANSLATION INITIATION FACTOR 5B						662/ 2
AT5G13530	E3 UBIQUITIN-PROTEIN LIGASE KEG						385/ 2
AT1G73720	WD40 REPEAT-CONTAINING PROTEIN SMU1						349/ 2
AT5G65770	PROTEIN CROWDED NUCLEI 4						346/ 2
AT3G48170	BETAINE ALDEHYDE DEHYDROGENASE 2						383/ 2
AT1G44910	PRP40 PRE-MRNA PROCESSING FACTOR 40 HOMOLOG A						347/ 2
AT1G14850	NUCLEAR PORE COMPLEX PROTEIN NUP155						211/ 2
AT5G64840	ABC TRANSPORTER F FAMILY MEMBER 5						200/ 2
AT2G05120	NUCLEAR PORE COMPLEX PROTEIN NUP133						231/ 2
AT2G22300	CALMODULIN-BINDING TRANSCRIPTION ACTIVATOR						227/ 2
AT4G36690	SPLICING FACTOR U2AF LARGE SUBUNIT A						223/ 2
AT3G19960	MYOSIN-1-RELATED						223/ 2
AT5G22040	ubiquitin carboxyl-terminal hydrolase						190/ 2
AT3G18165	PRE-MRNA-SPLICING FACTOR SPF27						212/ 2
AT1G32380	RIBOSE-PHOSPHATE PYROPHOSPHOKINASE 2						181/ 2
AT2G20760	CLATHRIN LIGHT CHAIN						170/ 2
AT5G53440	LOW PROTEIN: ZINC FINGER CCCH DOMAIN PROTEIN						170 2
AT1G33410	NUCLEAR PORE COMPLEX PROTEIN NUP160						170/ 2
AT1G73960	TRANSCRIPTION INITIATION FACTOR TFIID SUBUNIT 2						190/ 2
AT1G14650	SPLICING FACTOR 3A SUBUNIT 1						188/ 2
AT4G10840	PROTEIN KINESIN LIGHT CHAIN-RELATED 1						180/ 2
AT2G16485	ZINC FINGER CCCH DOMAIN-CONTAINING PROTEIN 19						202/ 2
AT3G27670	FOCADHESIN						226/ 2
AT5G06160	SPLICING FACTOR 3A SUBUNIT 3						165/ 2
AT2G44200	PRE-MRNA-SPLICING FACTOR CWC25 HOMOLOG						193/ 2
AT5G15120	PLANT CYSTEINE OXIDASE 1						214/ 2
AT1G65260	MEMBRANE-ASSOCIATED PROTEIN VIPP1						175/ 2
AT2G32600	SPLICING FACTOR 3A SUBUNIT 2						149/ 2
AT5G15020	PAIRED AMPHIPATHIC HELIX						166/ 2
AT3G55340	PHRAGMOPLASTIN INTERACTING PROTEIN 1						192/ 2
AT5G16930	AAA-TYPE ATPASE FAMILY PROTEIN						137/ 2
AT5G54770	THIAMINE THIAZOLE SYNTHASE						156/ 2
AT3G23300	METHYLTRANSFERASE PMT1-RELATED						131/ 2
AT1G60900	RNA-BINDING						136/ 2
AT2G18330	ATPASE FAMILY AAA DOMAIN-CONTAINING PROTEIN 3						143/ 2
AT2G20810	GALACTURONOSYLTRANSFERASE 10-RELATED						137/ 2
AT3G56510	ACTIVATOR OF BASAL TRANSCRIPTION 1						139/ 2
AT5G56630	ATP-DEPENDENT 6-PHOSPHOFRUCTOKINASE 7						127/ 2
AT1G01510	C-TERMINAL BINDING PROTEIN AN						138/ 2
AT3G46960	DEXH-BOX ATP-DEPENDENT RNA HELICASE DEXH11						114/ 2
AT2G18465	CHAPERONE DNAJ-DOMAIN SUPERFAMILY PROTEIN						110/ 2
AT1G64880	37S RIBOSOMAL PROTEIN S5						134/ 2
AT5G61150	RNA POLYMERASE-ASSOCIATED PROTEIN LEO1						135/ 2
AT2G31410	COILED-COIL DOMAIN-CONTAINING PROTEIN 86						108/ 2
AT5G14460	TRNA PSEUDOURIDINE SYNTHASE 1-RELATED						122/ 2
AT4G32610	COPPER ION BINDING PROTEIN						128/ 2
AT2G15270	PRKR-INTERACTING PROTEIN 1 HOMOLOG						105/ 2
AT4G32840	ATP-DEPENDENT 6-PHOSPHOFRUCTOKINASE 6						118/ 2
AT4G21710	DNA-DIRECTED RNA POLYMERASE II SUBUNIT RPB2						100/ 2
AT4G31180	ASPARTATE--TRNA LIGASE						95/ 2
AT2G04842	THREONINE--TRNA LIGASE						93/ 2
AT5G02310	E3 UBIQUITIN-PROTEIN LIGASE UBR1						97/ 2
AT1G04170	EUKARYOTIC TRANSLATION INITIATION FACTOR 2 SUBUNIT 3						91/ 2

Table S15a. List of expected interactors of mRNA export receptor candidates. Proteins that co-purified with NXF-SG candidates. Proteins that co-purified with unfused SG were removed from the list. The average MASCOT score is shown and how many times the protein was detected in out three independent experiments.

TAIR	DESCRIPTION	NXF1	NXF2	NXF3	NXF4	NXF5	NXF6	NXF7
AT5G43960	NUCLEAR TRANSPORT FACTOR 2	6014/ 3	451/ 3		1110/ 2			
AT1G29350	RNA POLYMERASE II DEGRADATION FACTOR-LIKE PROTEIN	4178/ 3	250/ 3	2594/ 3	506/ 3	245/ 3	1748/ 3	
AT3G13990	UBQ3 – polyubiquitin 3	3653/ 3	2366/ 3	1270/ 3	1662/ 3	575/ 3	3470/ 3	479/ 3
AT3G22430	RNA RECOGNITION MOTIF XS DOMAIN PROTEIN	1259/ 3			150/ 3			
AT1G76940	NUCLEAR SPECKLE RNA-BINDING PROTEIN A	1126/ 3	242/ 2	178/ 3	245/ 3		174/ 3	
AT5G44780	MULTIPLE ORGANELLAR RNA EDITING FACTOR 4	1206/ 3	433/ 2	167/ 2	396/ 3		245/ 3	
AT1G07310	CALCIUM-DEPENDENT LIPID-BINDING	674/ 3			549/ 3		511/ 3	
AT5G15540	NIPPED-B-LIKE PROTEIN	787/ 3						
AT1G36990	C-JUN-AMINO-TERMINAL KINASE-INTERACTING PROTEIN	734/ 3						
AT2G31320	POLY [ADP-RIBOSE] POLYMERASE 1	811/ 3						
AT1G14850	NUCLEAR PORE COMPLEX PROTEIN NUP155	564/ 3			477/ 3			
AT3G61690	NUCLEOTIDYLTRANSFERASE	744/ 3						
AT1G22060	SPORULATION-SPECIFIC PROTEIN	808/ 3						
AT1G55820	GBF-INTERACTING PROTEIN 1-RELATED	794/ 3	494/ 3	752/ 3	1365/ 3	365/ 3	3467/ 3	568/ 3
AT3G13222	GBF-INTERACTING PROTEIN 1-RELATED	581/ 3	229/ 2	1613/ 3	1111/ 3	268/ 3	2430/ 3	353/ 3
AT1G48650	DEXH-BOX ATP-DEPENDENT RNA HELICASE DEXH3	563/ 3			258/ 2			
AT2G03150	CCAR1 HOMOLOG	560/ 3						
AT3G49490	Hypothetical protein	406/ 3						
AT3G48800	STERILE ALPHA MOTIF	408/ 3						
AT1G70180	Sterile alpha motif (SAM) domain-containing protein	383/ 3	126/ 2	199/ 2	172/ 3		202/ 3	
AT5G59710	NOT TRANSCRIPTION COMPLEX SUBUNIT VIP2-RELATED	418/ 3						
AT1G28110	SERINE CARBOXYPEPTIDASE-LIKE 45	324/ 3			204/ 2			
AT5G65540	BASIC PROLINE-RICH PROTEIN 1, BPP1	402/ 3						
AT3G08850	REGULATORY-ASSOCIATED PROTEIN OF MTOR	365/ 3						
AT2G40070	Flocculation FLO11-like protein	462/ 3						
AT5G13530	E3 UBIQUITIN-PROTEIN LIGASE KEG	359/ 3			113/ 2			
AT3G18110	PENTATRICOPEPTIDE REPEAT	371/ 3						
AT2G17970	2-OXOGLUTARATE	453/ 3			267/ 2			
AT2G46340	PROTEIN SUPPRESSOR OF PHYA-105 1	477/ 3						
AT3G04590	AT-HOOK MOTIF NUCLEAR-LOCALIZED PROTEIN 14	401/ 3	241/ 3	205/ 2	356/ 3		193/ 2	
AT5G22040	ubiquitin carboxyl-terminal hydrolase	337/ 3						
AT1G79490	Pentatricopeptide repeat-containing protein	336/ 3						
AT5G53440	LOW PROTEIN: ZINC FINGER CCCH DOMAIN PROTEIN	323/ 3						
AT2G44710	RNA-binding (RRM/RBD/RNP motifs) family protein	334/ 3						
AT1G48410	ARGONAUTE-1	336/ 3						
AT2G16485	ZINC FINGER CCCH DOMAIN-CONTAINING PROTEIN 19	388/ 3			104/ 2			
AT3G06920	Tetratricopeptide repeat (TPR)-like superfamily protein	340/ 3						
AT2G32950	E3 UBIQUITIN-PROTEIN LIGASE COP1	405/ 3						
AT1G14840	MICROTUBULE-ASSOCIATED PROTEIN 70-4	348/ 3						
AT4G02390	POLY [ADP-RIBOSE] POLYMERASE 2	375/ 3						
AT3G54230	SUPPRESSOR OF ABI3-5	354/ 3						
AT1G62930	RNA PROCESSING FACTOR 3, RPF3	293/ 3						
AT2G39810	E3 UBIQUITIN-PROTEIN LIGASE HOS1	259/ 3			190/ 3			
AT5G15020	PAIRED AMPHIPATHIC HELIX	319/ 3						
AT2G25320	TRAF-LIKE FAMILY PROTEIN	316/ 3						
AT4G08510	C-JUN-AMINO-TERMINAL KINASE-INTERACTING PROTEIN	223/ 3						
AT3G07030	ALBA DNA/RNA-BINDING PROTEIN	315/ 3			129/ 2			
AT5G51590	AT-HOOK MOTIF NUCLEAR-LOCALIZED PROTEIN 4	216/ 3			263/ 3		147/ 2	
AT1G33410	NUCLEAR PORE COMPLEX PROTEIN NUP160	252/ 3			230/ 2			
AT2G26920	Ubiquitin-associated/translation elongation factor EF1B protein	221/ 3						
AT2G40240	Tetratricopeptide repeat (TPR)-like superfamily protein	222/ 3						
AT5G27030	TOPLESS-RELATED PROTEIN 3	294/ 3						
AT1G64880	37S RIBOSOMAL PROTEIN S5	198/ 3						
AT3G48150	CELL DIVISION CYCLE PROTEIN 23 HOMOLOG	284/ 3						
AT3G45630	RNA BINDING	204/ 3						
AT1G24290	ATPASE WRNIP1	208/ 3						
AT5G04280	SRA STEM-LOOP-INTERACTING RNA-BINDING PROTEIN	287/ 3						
AT5G13260	MYOSIN	256/ 3						
AT5G51340	MAU2 CHROMATID COHESION FACTOR HOMOLOG	238/ 3						
AT2G41040	S-adenosyl-L-methionine-dependent methyltransferases superfamily protein	206/ 3		117/ 2				
AT5G22450	SPECTRIN BETA CHAIN	239/ 3						
AT3G62120	BIFUNCTIONAL GLUTAMATE/PROLINE--TRNA LIGASE	210/ 3						
AT2G43030	50S RIBOSOMAL PROTEIN L3-1	176/ 3	383/ 3	389/ 3	255/ 3	397/ 3	414/ 3	318/ 3
AT3G21810	ZINC FINGER CCCH DOMAIN-CONTAINING PROTEIN 40	220/ 3						
AT2G46610	SERINE/ARGININE-RICH SPLICING FACTOR RS31-RELATED	174/ 3						
AT3G13460	METHYLATED RNA-BINDING PROTEIN 1	209/ 3					136/ 2	
AT1G60650	GLYCINE-RICH RNA-BINDING PROTEIN RZ1B	208/ 3						
AT2G15690	Pentatricopeptide repeat-containing protein	181/ 3						
AT5G40480	GP210 ORTHOLOG	168/ 3						
AT2G05120	NUCLEAR PORE COMPLEX PROTEIN NUP133	187/ 3			136/ 2			
AT2G18330	ATPASE FAMILY AAA DOMAIN-CONTAINING PROTEIN 3	188/ 3						
AT4G21710	DNA-DIRECTED RNA POLYMERASE II SUBUNIT RPB2	190/ 3						
AT3G20250	PUMILIO HOMOLOG 5	184/ 3						
AT2G22910	AMINO-ACID ACETYLTRANSFERASE NAGS1	150/ 3						
AT5G10960	POP2	147/ 3						
AT2G42590	14-3-3-LIKE PROTEIN GF14 MU-RELATED	161/ 3						
AT4G23650	CALCIUM-DEPENDENT PROTEIN KINASE 3	160/ 3						
AT3G55340	PHRAGMOPLASTIN INTERACTING PROTEIN 1	135/ 3						
AT3G53930	SERINE/THREONINE-PROTEIN KINASE ATG1B	131/ 3						
AT4G32050	NEUROCHONDRIN	146/ 3						
AT3G27670	FOCADHESIN	138/ 3						
AT4G24550	AP-4 COMPLEX SUBUNIT MU-1	102/ 3						
AT5G08550	GC-RICH SEQUENCE DNA-BINDING FACTOR-LIKE PROTEIN	137/ 3						
AT1G13980	GUANINE NUCLEOTIDE EXCHANGE FACTOR 1	130/ 3						
AT2G34680	187-KDA MICROTUBULE-ASSOCIATED PROTEIN AIR9	120/ 3						
AT4G01050	RHODANESE-LIKE DOMAIN-CONTAINING PROTEIN 4	112/ 3						
AT5G05670	SIGNAL RECOGNITION PARTICLE RECEPTOR SUBUNIT BETA	96/ 3						
AT4G32910	NUCLEAR PORE COMPLEX PROTEIN NUP85	99/ 3						
AT1G67170	PROTEIN FLX-LIKE 2	785/ 2						

Table S15b. List of expected interactors of mRNA export receptor candidates. Proteins that co-purified with NXF-SG candidates. Proteins that co-purified with unfused SG were removed from the list. The average MASCOT score is shown and how many times the protein was detected in out three independent experiments.

TAIR	DESCRIPTION	NXF1	NXF2	NXF3	NXF4	NXF5	NXF6	NXF7
AT3G14750	PROTEIN FLX-LIKE 1	834/ 2						
AT2G22780	MALATE DEHYDROGENASE	701/ 2		190/ 2		139/ 2		
AT3G58580	CARBON CATABOLITE REPRESSOR PROTEIN 4 HOMOLOG 2	684/ 2						
AT5G03740	HISTONE DEACETYLASE HDT3	529/ 2	733/ 2	832/ 3	795/ 2	1283/ 3	1186/ 3	884/ 3
AT1G01300	ASPARTYL PROTEASE FAMILY PROTEIN 2	628/ 2	172/ 2	487/ 3	332/ 2	104 2	411/ 3	
AT4G12080	AT-HOOK MOTIF NUCLEAR-LOCALIZED PROTEIN 1	509/ 2	429/ 2		243/ 2		248/ 3	
AT5G23680	Sterile alpha motif (SAM) domain-containing protein	560/ 2						
AT3G27400	PECTATE LYASE 11-RELATED	366/ 2						
AT2G47250	PRE-MRNA-SPLICING FACTOR	367/ 2						
AT4G20020	MULTIPLE ORGANELLAR RNA EDITING FACTOR 1	455/ 2						
AT4G15840	BTB/POZ DOMAIN-CONTAINING PROTEIN	375/ 2						
AT3G21215	RNA-binding (RRM/RBD/RNP motifs) family protein	482/ 2	304/ 3	440/ 2	278/ 2		338/ 2	
AT2G33620	AT-HOOK MOTIF NUCLEAR-LOCALIZED PROTEIN 10	380/ 2	188/ 2				199/ 2	
AT5G24520	PROTEIN TRANSPARENT TESTA GLABRA 1	527/ 2			117/ 2			
AT5G57250	Pentatricopeptide repeat-containing protein	514/ 2			305/ 3			
AT5G15680	PROTEIN FURRY	508/ 2						
AT5G61960	PROTEIN MEI2-LIKE 1-RELATED	443/ 2						
AT2G38550	PROTEIN FATTY ACID EXPORT 3	431/ 2						
AT5G12330	PROTEIN LATERAL ROOT PRIMORDIUM 1	429/ 2						
AT1G66260	THO COMPLEX SUBUNIT 4C	357/ 2	288/ 3	371/ 3	333/ 3	691/ 3	493/ 3	318/ 3
AT2G42710	MITOCHONDRIAL RIBOSOMAL PROTEIN	437/ 2	689/ 3	793/ 3	570/ 3	293/ 3	735/ 3	254/ 3
AT5G17510	GLUTAMINE-RICH PROTEIN-RELATED	320/ 2						
AT3G62330	Zinc knuckle (CCHC-type) family protein	362/ 2						
AT5G26710	GLUTAMATE--TRNA LIGASE	278/ 2						
AT5G61910	NICOTINIC RECEPTOR-ASSOCIATED PROTEIN 1	290/ 2						
AT4G02570	CULLIN-1-RELATED	303/ 2						
AT2G45140	AT11025P-RELATED	380/ 2						
AT1G32380	RIBOSE-PHOSPHATE PYROPHOSPHOKINASE 2	347/ 2						
AT5G51200	NUCLEAR PORE COMPLEX PROTEIN NUP205	423/ 2			408/ 2			
AT2G44530	RIBOSE-PHOSPHATE PYROPHOSPHOKINASE 5	371/ 2						
AT1G71210	Pentatricopeptide repeat (PPR) superfamily protein	287/ 2			273/ 2			
AT2G47940	PROTEASE DO-LIKE 2	328/ 2						
AT2G22360	CHAPERONE PROTEIN DNAJ A6	412/ 2						
AT1G43850	TRANSCRIPTIONAL COREPRESSOR SEUSS	292/ 2						
AT5G13850	HMR-RELATED	361/ 2	596/ 2	655/ 2	642/ 3	875/ 3	821/ 3	811/ 3
AT3G22590	PARAFIBROMIN	265/ 2						
AT3G54610	GH11602P	357/ 2						
AT3G63470	SERINE CARBOXYPEPTIDASE-LIKE 36-RELATED	384/ 2						
AT2G35390	RIBOSE-PHOSPHATE PYROPHOSPHOKINASE 2-RELATED	313/ 2						
AT3G27925	PROTEASE DO-LIKE 1	237/ 2					372/ 3	
AT5G49220	Hypothetical protein	288/ 2						
AT2G02880	MUCIN-LIKE PROTEIN	249/ 2						
AT1G31817	RIBOSOMAL PROTEIN S11	230/ 2	352/ 3	197/ 2	372/ 2	146/ 2	176/ 3	140/ 2
AT1G54360	TAF6-LIKE RNA POLYMERASE II P300	253/ 2						
AT2G29140	PUMILIO HOMOLOG 1-RELATED	303/ 2						
AT5G16930	AAA-TYPE ATPASE FAMILY PROTEIN	243/ 2						
AT3G12590	Hypothetical protein	252/ 2						
AT4G16340	Guanine nucleotide exchange factor SPIKE 1	234/ 2						
AT4G22770	AT-HOOK MOTIF NUCLEAR-LOCALIZED PROTEIN 2	229/ 2						
AT2G32070	CCR4-ASSOCIATED FACTOR 1 HOMOLOG 2-RELATED	357/ 2						
AT3G50000	CASEIN KINASE II SUBUNIT ALPHA-2-RELATED	347/ 2						
AT1G04400	SI:CH1073-390K14.1	253/ 2						
AT5G41770	CROOKED NECK-LIKE PROTEIN 1	295/ 2						
AT3G61670	G-LIKE PROTEIN	303/ 2						
AT1G10390	NUCLEAR PORE COMPLEX PROTEIN NUP98A	326/ 2			486/ 3			
AT3G16060	KINESIN-LIKE PROTEIN KIN-13B	232/ 2						
AT4G00660	DEAD-BOX ATP-DEPENDENT RNA HELICASE 8	273/ 2						
AT5G66100	LARP	257/ 2						
AT1G69840	HYPERSENSITIVE-INDUCED RESPONSE PROTEIN 2	248/ 2						
AT1G15920	CCR4-ASSOCIATED FACTOR 1 HOMOLOG 2-RELATED	256/ 2						
AT1G79090	PROTEIN ASSOCIATED WITH TOPO II RELATED-1	244/ 2						
AT2G43950	OUTER ENVELOPE PORE PROTEIN 37	237/ 2					140/ 2	
AT5G64260	PROTEIN EXORDIUM-LIKE 2	226/ 2	237/ 2	286/ 3	163/ 3	230/ 2	259/ 3	149/ 2
AT3G16310	NUCLEOPORIN NUP35	231/ 2	130/ 2		287/ 2		179/ 3	
AT2G32700	TRANSCRIPTIONAL COREPRESSOR LEUNIG_HOMOLOG	231/ 2						
AT1G21700	SWI/SNF COMPLEX SUBUNIT SWI3C	208/ 2						
AT3G61820	EUKARYOTIC ASPARTYL PROTEASE FAMILY PROTEIN	211/ 2	591/ 3	508/ 3	619/ 3	227/ 3	262/ 3	229/ 3
AT5G35980	HOMEODOMAIN INTERACTING PROTEIN KINASE	204/ 2						
AT4G25880	PUMILIO HOMOLOG 6	221/ 2						
AT5G64320	MITOCHONDRIAL TRANSLATION FACTOR 1	287/ 2			164/ 2			
AT2G22300	CALMODULIN-BINDING TRANSCRIPTION ACTIVATOR	246/ 2						
AT5G63610	CYCLIN-DEPENDENT KINASE 8	213/ 2						
AT1G55040	ZINC FINGER	264/ 2						
ATCG00830	39S RIBOSOMAL PROTEIN L2	190/ 2		242/ 2				
AT1G09630	RAS-RELATED PROTEIN RABA2A	205/ 2						
AT3G12410	POLYNUCLEOTIDYL TRANSFERASE	199/ 2						
AT4G31120	PROTEIN ARGININE N-METHYLTRANSFERASE 5	225/ 2						
AT1G62914	Pentatricopeptide repeat-containing protein	234/ 2						
AT3G62240	E3 UBIQUITIN-PROTEIN LIGASE ZNF598	193/ 2	167/ 2	156/ 2	220/ 2		166/ 2	
AT1G58100	TRANSCRIPTION FACTOR TCP23-RELATED	195/ 2						
AT3G15010	HETEROGENEOUS NUCLEAR RIBONUCLEOPROTEIN A0	207/ 2		166/ 2			196/ 2	
AT1G33780	TRANSPORTER	204/ 2			220/ 3			
AT5G15120	PLANT CYSTEINE OXIDASE 1	194/ 2						
AT4G31810	3-HYDROXYISOBUTYRYL-COA HYDROLASE-LIKE PROTEIN 2	218/ 2	110/ 2	186/ 2	290/ 3		124/ 2	
AT4G31180	ASPARTATE--TRNA LIGASE	214/ 2						
AT1G62670	Pentatricopeptide repeat-containing protein	228/ 2						
AT3G58640	Mitogen activated protein kinase kinase kinase-like protein	184/ 2						
AT2G06000	Pentatricopeptide repeat-containing protein	235/ 2						
AT1G78810	Hypothetical protein	185/ 2						

Table S15c. List of expected interactors of mRNA export receptor candidates. Proteins that co-purified with NXF-SG candidates. Proteins that co-purified with unfused SG were removed from the list. The average MASCOT score is shown and how many times the protein was detected in out three independent experiments.

TAIR	DESCRIPTION	NXF1	NXF2	NXF3	NXF4	NXF5	NXF6	NXF7
AT1G55460	DNA/RNA-BINDING PROTEIN KIN17	165/ 2						
AT1G73720	WD40 REPEAT-CONTAINING PROTEIN SMU1	242/ 2						
AT2G23070	CASEIN KINASE II SUBUNIT ALPHA-4	217/ 2						
AT2G45850	AT-HOOK MOTIF NUCLEAR-LOCALIZED PROTEIN 9	234/ 2	211/ 2	191/ 2			122/ 2	
AT4G29010	PEROXISOMAL FATTY ACID BETA-OXIDATION PROTEIN AIM1	164/ 2						
AT5G13480	PRE-MRNA 3' END PROCESSING PROTEIN WDR33	223/ 2						
AT4G28990	GH13594P-RELATED	185/ 2						
AT5G16310	UBIQUITIN CARBOXYL-TERMINAL HYDROLASE ISOZYME L5	203/ 2						
AT4G27880	E3 UBIQUITIN-PROTEIN LIGASE SINAT4	173/ 2						
AT3G06850	LIPOAMIDE ACYLTRANSFERASE COMPONENT	235/ 2						
AT4G05020	EXTERNAL ALTERNATIVE NAD	175/ 2						
AT5G35590	PROTEASOME SUBUNIT ALPHA TYPE-6	159/ 2						
AT2G03510	ERLIN	224/ 2		148/ 2	122/ 3			
AT2G18960	ATPASE 1	221/ 2						
AT4G30890	UBIQUITIN CARBOXYL-TERMINAL HYDROLASE 10	232/ 2	1796/ 3	1241/ 3	3127/ 3	1382/ 3	1041/ 3	576/ 3
AT3G46830	RAS-RELATED PROTEIN RABA2C-RELATED	213/ 2						
AT2G37230	RIBOSOMAL PENTATRICOPEPTIDE REPEAT PROTEIN 5	185/ 2						
AT2G44020	EXPRESSED PROTEIN	196/ 2						
AT4G17330	G2484-1 PROTEIN	169/ 2						
AT2G18465	CHAPERONE DNAJ-DOMAIN SUPERFAMILY PROTEIN	195/ 2						
AT3G16830	TOPLESS-RELATED PROTEIN 2	216/ 2						
AT5G01400	SYMPLEKIN	161/ 2						
AT5G18660	DIVINYL CHLOROPHYLLIDE A 8-VINYL-REDUCTASE	149/ 2						
AT3G03060	P-LOOP CONTAINING NUCLEOSIDE TRIPHOSPHATE HYDROLASES	191/ 2						
AT5G57870	EUKARYOTIC TRANSLATION INITIATION FACTOR ISOFORM 4G-1	181/ 2						
AT3G63410	2-METHYL-6-PHYTYL-1	199/ 2						
AT5G45750	RAS-RELATED PROTEIN RABA1C	206/ 2						
AT1G60070	ADAPTOR PROTEIN COMPLEX 1	152/ 2						
AT1G12775	Pentatricopeptide repeat-containing protein	204/ 2						
AT4G38150	Pentatricopeptide repeat-containing protein	195/ 2			155/ 2		141/ 2	
AT5G47210	rbp	188/ 2	983/ 3	902/ 3	745/ 3	1120/ 3	1206/ 3	886/ 3
AT1G07320	50S RIBOSOMAL PROTEIN L4	197/ 2	188/ 3	311/ 3	174/ 3	300/ 3	286/ 3	260/ 3
AT3G49080	28S RIBOSOMAL PROTEIN S9	173/ 2						
AT5G66930	AUTOPHAGY-RELATED PROTEIN 101	148/ 2						
AT3G18165	PRE-MRNA-SPLICING FACTOR SPF27	165/ 2						
AT4G14790	DEXH-BOX ATP-DEPENDENT RNA HELICASE DEXH16	155/ 2						
AT2G20760	CLATHRIN LIGHT CHAIN	159/ 2					87/ 2	
AT1G80030	MOLECULAR CHAPERONE HSP40/DNAJ FAMILY PROTEIN	159/ 2						
AT1G67360	REF/SRPP-like protein	170/ 2						
AT3G61310	AT-HOOK MOTIF NUCLEAR-LOCALIZED PROTEIN 11	140/ 2	158/ 2	111/ 3	230/ 2		141/ 2	
AT3G46220	E3 UFM1-PROTEIN LIGASE 1	133/ 2						
AT1G47128	CYSTEINE PROTEINASE RD21A	141/ 2			135/ 2			
AT1G79730	PAF1 HOMOLOG	143/ 2						
AT2G26890	DNAJ HOMOLOG SUBFAMILY C MEMBER 13	148/ 2						
AT1G80780	CCR4-ASSOCIATED FACTOR 1 HOMOLOG 6-RELATED	165/ 2						
AT5G42960	OUTER ENVELOPE PORE PROTEIN 24A	134/ 2						
AT1G51965	Pentatricopeptide repeat-containing protein	157/ 2						
AT5G20950	GLYCOSYL HYDROLASE FAMILY PROTEIN	134/ 2		168/ 3	259/ 2		150/ 2	
AT1G32220	NAD(P)-binding Rossmann-fold superfamily protein	176/ 2						
AT3G53110	DEAD-BOX HELICASE DBP80	140/ 2						
AT5G58040	FIP1[III]-LIKE PROTEIN-RELATED	138/ 2						
AT5G24650	CHLOROPLASTIC TRANSLOCASE SUBUNIT HP30-2	158/ 2						
AT1G53720	PEPTIDYL-PROLYL CIS-TRANS ISOMERASE-LIKE 4	129/ 2						
AT3G58210	TRAF-LIKE FAMILY PROTEIN-RELATED	130/ 2						
AT5G01160	E3 UBIQUITIN-PROTEIN LIGASE HAKAI	164/ 2						
AT5G04895	ATP-DEPENDENT RNA HELICASE A-LIKE PROTEIN	165/ 2						
AT5G23900	60S RIBOSOMAL PROTEIN L13-3	140/ 2	209/ 3	219/ 3	179/ 3	211/ 3	208/ 3	242/ 3
AT3G62200	ENDONUCLEASE OR GLYCOSYL HYDROLASE-RELATED	130/ 2						
AT1G04870	PROTEIN ARGININE N-METHYLTRANSFERASE PRMT10	149/ 2			304/ 3			
AT1G61010	CLEAVAGE AND POLYADENYLATION SPECIFICITY FACTOR 3	133/ 2						
AT2G22370	MEDIATOR OF RNA POLYMERASE II TRANSCRIPTION SUBUNIT 18	142/ 2						
AT5G06320	NDR1/HIN1-LIKE PROTEIN 3	142/ 2						
AT5G18900	PROLYL 4-HYDROXYLASE SUBUNIT ALPHA-3	125/ 2						
AT4G26780	GRPE PROTEIN HOMOLOG	124/ 2						
AT5G18620	ISWI CHROMATIN-REMODELING COMPLEX ATPASE CHR17	123/ 2						
AT2G26280	POLYADENYLATE-BINDING PROTEIN-INTERACTING PROTEIN 7	154/ 2						
AT5G50600	11-BETA-HYDROXYSTEROID DEHYDROGENASE 1A-RELATED	146/ 2	200/ 2		423/ 2			
AT1G05890	E3 UBIQUITIN-PROTEIN LIGASE ARI5-RELATED	143/ 2						
AT5G12110	ELONGATION FACTOR 1-BETA 1	142/ 2						
AT5G46920	NUCLEAR INTRON MATURASE 2	133/ 2						
AT5G41360	TRANSCRIPTION AND DNA REPAIR FACTOR IIH HELICASE XPB	152/ 2						
AT2G41620	NUCLEAR PORE COMPLEX PROTEIN NUP93A	132/ 2						
AT5G39960	GTP-BINDING PROTEIN	131/ 2						
AT2G20060	39S RIBOSOMAL PROTEIN L4	146/ 2	211/ 3	262/ 3	237/ 2	216/ 3	291/ 3	274/ 3
AT3G19130	POLYADENYLATE-BINDING PROTEIN RBP47B	125/ 2						
AT5G35910	PROTEIN RRP6-LIKE 2	131/ 2						
AT1G55170	PROTEIN FLX-LIKE 3	150/ 2						
AT1G02930	GLUTATHIONE S-TRANSFERASE F6-RELATED	120/ 2						
AT2G36480	PRE-MRNA CLEAVAGE COMPLEX 2 PCF11-LIKE PROTEIN	137/ 2						
AT1G53140	DYNAMIN-RELATED PROTEIN 5A	124/ 2						
AT5G12120	Ubiquitin-associated/translation elongation factor EF1B protein	134/ 2						
AT4G35850	Pentatricopeptide repeat (PPR) superfamily protein	132/ 2						
AT1G01510	C-TERMINAL BINDING PROTEIN AN	131/ 2						
AT1G31780	CONSERVED OLIGOMERIC GOLGI COMPLEX SUBUNIT 6	129/ 2						
AT1G22730	MA3 DOMAIN-CONTAINING PROTEIN	125/ 2						
AT4G16420	TRANSCRIPTIONAL ADAPTER 2-BETA	120/ 2						
AT4G16100	heat shock protein	130/ 2						
AT4G35800	DNA-DIRECTED RNA POLYMERASE II SUBUNIT 1	108/ 2						
AT4G27750	BINDING PROTEIN	113/ 2						

Table S15d. List of expected interactors of mRNA export receptor candidates. Proteins that co-purified with NXF-SG candidates. Proteins that co-purified with unfused SG were removed from the list. The average MASCOT score is shown and how many times the protein was detected in out three independent experiments.

TAIR	DESCRIPTION	NXF1	NXF2	NXF3	NXF4	NXF5	NXF6	NXF7
AT3G06650	ATP-CITRATE SYNTHASE	111/ 2						
AT4G36690	SPLICING FACTOR U2AF LARGE SUBUNIT A	119/ 2						
AT5G62270	GB|AAC32909.1	124/ 2						
AT5G28370	F21B23.6 PROTEIN	125/ 2			145/ 2			
AT1G12470	VACUOLAR PROTEIN SORTING-ASSOCIATED PROTEIN 18 HOMOLOG	123/ 2						
AT5G60960	PENTATRICOPEPTIDE REPEAT-CONTAINING PROTEIN PNM1	123/ 2						
AT1G65440	TRANSCRIPTION ELONGATION FACTOR SPT6	109/ 2						
AT3G54980	Pentatricopeptide repeat (PPR) superfamily protein	107/ 2						
AT1G04690	HYPERKINETIC	114/ 2						
AT1G73460	PROTEIN KINASE SUPERFAMILY PROTEIN	111/ 2						
AT3G58040	E3 UBIQUITIN-PROTEIN LIGASE SINAT2	112/ 2						
AT2G01970	TRANSMEMBRANE 9 SUPERFAMILY MEMBER 3	100/ 2						
AT4G00800	VACUOLAR PROTEIN SORTING 8 HOMOLOG	110/ 2						
AT5G19320	RAN GTPASE-ACTIVATING PROTEIN 2	110/ 2						
AT1G47200	WPP DOMAIN-CONTAINING PROTEIN 1-RELATED	112/ 2			178/ 2			
AT3G17040	PROTEIN HIGH CHLOROPHYLL FLUORESCENT 107	106/ 2						
AT1G51590	MANNOSYL-OLIGOSACCHARIDE 1	109/ 2						
AT3G48560	ACETOLACTATE SYNTHASE	100/ 2						
AT3G45900	Ribonuclease P protein subunit P38-like protein	104/ 2						
AT5G43310	COP1-INTERACTING PROTEIN-LIKE PROTEIN	103/ 2						144/ 2
AT1G09070	PROTEIN SRC2 HOMOLOG	113/ 2						
AT1G80680	NUCLEAR PORE COMPLEX PROTEIN NUP96	97/ 2						
AT5G20610	PROTEIN PLASTID MOVEMENT IMPAIRED 1-RELATED 1	106/ 2						
AT4G32285	Probable clathrin assembly protein	102/ 2						
AT3G61520	F21B23.6 PROTEIN	102/ 2						
AT3G63150	MITOCHONDRIAL RHO GTPASE 2	98/ 2						
AT5G26210	PHD FINGER PROTEIN ALFIN-LIKE 4	96/ 2						
AT1G51560	PYRIDOXAMINE 5'-PHOSPHATE OXIDASE FAMILY PROTEIN	101/ 2						
AT2G39260	REGULATOR OF NONSENSE TRANSCRIPTS 2	94/ 2						
AT1G07990	SIT4 phosphatase-associated family protein	94/ 2						
AT3G63250	HOMOCYSTEINE S-METHYLTRANSFERASE 2	93/ 2						
AT2G39050	RICIN B-LIKE LECTIN EULS3	102/ 2						
AT1G48570	T1N15.19	90/ 2						
AT5G14460	TRNA PSEUDOURIDINE SYNTHASE 1-RELATED	97/ 2						
AT2G20190	CLIP-ASSOCIATED PROTEIN	96/ 2						
AT1G75210	CYTOSOLIC PURINE 5'-NUCLEOTIDASE	91/ 2						
AT3G25150	NUCLEAR TRANSPORT FACTOR 2	89/ 2	712/ 3	4807/ 3	1477 3	1027/ 3	2289/ 3	366/ 3
AT3G13060	EVOLUTIONARILY CONSERVED C-TERMINAL REGION 5	91/ 2						
AT2G36900	GOLGI SNAP RECEPTOR COMPLEX MEMBER 2	94/ 2						
AT1G64550	ATP-BINDING CASSETTE SUB-FAMILY F MEMBER 3	94/ 2						
AT4G12790	GPN-LOOP GTPASE 3	88/ 2						
AT2G43130	RAS-RELATED PROTEIN RABA5C	87/ 2						
AT1G31800	PROTEIN LUTEIN DEFICIENT 5	90/ 2						
AT4G10610	POLYADENYLATE-BINDING PROTEIN-INTERACTING PROTEIN 12	86/ 2						
AT5G15550	RIBOSOME BIOGENESIS PROTEIN WDR12	86/ 2			204/ 3			
AT2G22660	GLYCINE-RICH DOMAIN-CONTAINING PROTEIN 1	80/ 2						
AT1G69250	NUCLEAR TRANSPORT FACTOR 2		1342/ 3	741/ 3	559/ 3	4850/ 3	1239/ 3	2386/ 3
AT4G17520	RGG REPEATS NUCLEAR RNA BINDING PROTEIN B		853/ 3	929/ 3	561/ 3	947/ 3	1247/ 3	771/ 3
AT3G25920	54S RIBOSOMAL PROTEIN L10		535/ 3	609/ 3	455/ 2	420/ 3	729/ 3	518/ 3
AT4G01310	54S RIBOSOMAL PROTEIN L7		585/ 3	605/ 3	799/ 2	299/ 3	719/ 3	339/ 3
AT4G05400	39S RIBOSOMAL PROTEIN L40		408/ 3	240/ 3	228/ 2	196/ 3	295/ 3	279/ 3
AT3G52150	30S RIBOSOMAL PROTEIN 2		397/ 3	256/ 2	322/ 2	256/ 3	276/ 3	246/ 2
AT1G13730	NUCLEAR TRANSPORT FACTOR 2		294/ 3	474/ 3	511/ 3	645/ 3	3543/ 3	
AT1G48620	HON5		340/ 3	606/ 3	606/ 3	882/ 3	649/ 3	437/ 3
AT5G66860	RIBOSOMAL PROTEIN L25/GLN-TRNA SYNTHETASE		357/ 3	458/ 3	291/ 3	248/ 3	549/ 3	312/ 3
AT3G12390	NASCENT POLYPEPTIDE-ASSOCIATED COMPLEX SUBUNIT		285/ 3	343/ 3	426/ 3	635/ 2	589/ 3	764/ 2
ATCG00280	PHOTOSYSTEM II CP43 REACTION CENTER PROTEIN		190/ 3			393/ 3		
AT5G09440	PROTEIN EXORDIUM-LIKE 4		156/ 3		114/ 2			
AT1G32990	50S RIBOSOMAL PROTEIN L11		684/ 2	368/ 3	532/ 2	763/ 3	731/ 2	
AT2G32060	40S RIBOSOMAL PROTEIN S12		547/ 2	464/ 3	766/ 2	605/ 3	433/ 3	142/ 2
AT3G03740	BTB/POZ AND MATH DOMAIN-CONTAINING PROTEIN 4		649/ 2					
ATCG00270	PHOTOSYSTEM II D2 PROTEIN		440/ 2			385/ 3		
AT5G40040	60S ACIDIC RIBOSOMAL PROTEIN P2		508/ 2		624/ 3	154/ 2		
AT4G30800	40S RIBOSOMAL PROTEIN S11		384/ 2	421/ 3	333/ 3	346/ 3	361/ 2	280/ 3
AT3G59650	39S RIBOSOMAL PROTEIN L43		483/ 2		392/ 3		274/ 2	
ATCG00750	28S RIBOSOMAL PROTEIN S11		296/ 2		247/ 2			
AT4G16830	RGG REPEATS NUCLEAR RNA BINDING PROTEIN A		297/ 2	226/ 3	254/ 2	275/ 3	347/ 3	269/ 3
AT5G30510	30S RIBOSOMAL PROTEIN S1		408/ 2		159/ 2		159/ 2	
AT1G52370	Ribosomal protein L22p/L17e family protein		382/ 2	402/ 3	364/ 3	253/ 3	385/ 3	267/ 3
AT1G75350	50S RIBOSOMAL PROTEIN L31		312/ 2		338/ 2			
AT5G23535	39S RIBOSOMAL PROTEIN L24		311/ 2	243/ 3	182/ 2	230/ 3	334/ 2	168/ 3
AT2G34160	NVOLVED IN RRNA PROCESSING 7		279/ 2		346/ 2			
AT1G07830	39S RIBOSOMAL PROTEIN L47		379/ 2		285/ 3	177/ 2		
AT5G55140	39S RIBOSOMAL PROTEIN L30		413/ 2		305/ 3			
AT2G27840	HISTONE DEACETYLASE HDT4		319/ 2	787/ 3	336/ 2	468/ 3	1037/ 3	920/ 2
AT1G17880	TRANSCRIPTION FACTOR BTF3		266/ 2	230/ 2	179/ 3	296/ 2	296/ 2	255/ 2
AT1G48350	39S RIBOSOMAL PROTEIN L18		275/ 2		202/ 2	94/ 2	148/ 2	
AT4G34620	30S RIBOSOMAL PROTEIN S16-1		346/ 2		200/ 2			
AT5G54600	50S RIBOSOMAL PROTEIN L24		268/ 2		246/ 2	209/ 2	168/ 2	
AT1G03230	EUKARYOTIC ASPARTYL PROTEASE FAMILY PROTEIN		243/ 2	171/ 3			268/ 2	
AT3G10090	40S RIBOSOMAL PROTEIN S28-1		256/ 2				108/ 2	
AT3G15190	30S RIBOSOMAL PROTEIN S20		266/ 2	255/ 2	411/ 2	235/ 3	278/ 2	
AT3G51800	PROLIFERATION-ASSOCIATED PROTEIN 2G4		280/ 2	226/ 3	372/ 2		426/ 3	
ATCG00820	37S RIBOSOMAL PROTEIN S19		245/ 2		222/ 2			
AT5G27700	40S RIBOSOMAL PROTEIN S21		226/ 2		193/ 3			
AT1G78630	50S RIBOSOMAL PROTEIN L13		249/ 2	192/ 3	91 2	176/ 2	149/ 3	120/ 2
AT4G21280	OXYGEN-EVOLVING ENHANCER PROTEIN 3-1		203/ 2			330/ 3		
AT5G14320	37S RIBOSOMAL PROTEIN SWS2		284/ 2		390/ 2			
AT4G05180	OXYGEN-EVOLVING ENHANCER PROTEIN 3-2		201/ 2			160/ 3		

Table S15e. List of expected interactors of mRNA export receptor candidates. Proteins that co-purified with NXF-SG candidates. Proteins that co-purified with unfused SG were removed from the list. The average MASCOT score is shown and how many times the protein was detected in out three independent experiments.

TAIR	DESCRIPTION	NXF1	NXF2	NXF3	NXF4	NXF5	NXF6	NXF7
AT5G21010	BTB/POZ AND MATH DOMAIN-CONTAINING PROTEIN 5-RELATED		281/ 2					
AT5G27820	Ribosomal L18p/L5e family protein		186/ 2					
AT1G24240	39S RIBOSOMAL PROTEIN L19		258/ 2		184/ 3	122/ 2	279/ 2	108/ 2
AT1G73940	tumor necrosis factor receptor family protein		179/ 2		111/ 2	87/ 2	153/ 2	
AT1G62850	CLASS I PEPTIDE CHAIN RELEASE FACTOR		198/ 2	256/ 2	216/ 3	224/ 2	264/ 3	262/ 2
AT2G05920	SUBTILISIN-LIKE PROTEASE SBT1.8		185/ 2	635/ 3	589/ 2		343/ 2	
AT5G39600	39S RIBOSOMAL PROTEIN L53		213/ 2					
AT5G40950	39S RIBOSOMAL PROTEIN L27		235/ 2		209/ 2	178/ 3	154/ 2	
AT1G79850	30S RIBOSOMAL PROTEIN S17		173/ 2		133/ 2	101/ 3	144/ 2	
AT2G05070	CHLOROPHYLL A-B BINDING PROTEIN 2.1		169/ 2			233/ 3		
AT1G76300	SMALL NUCLEAR RIBONUCLEOPROTEIN SM D3		222/ 2		162/ 3			
ATCG00900	28S RIBOSOMAL PROTEIN S7		162/ 2		173/ 2			
AT1G53645	hydroxyproline-rich glycoprotein family protein		160/ 2		228/ 2			
AT5G65220	50S RIBOSOMAL PROTEIN L29		209/ 2		247/ 2			
AT2G47680	DEXH-BOX ATP-DEPENDENT RNA HELICASE DEXH8		161/ 2	528/ 2	376/ 3			
AT5G19000	BTB/POZ AND MATH DOMAIN-CONTAINING PROTEIN 1		175/ 2					
AT3G12700	ASPARTIC PROTEINASE NANA		167/ 2	237/ 3	354/ 3		266/ 2	
AT4G38970	FRUCTOSE-BISPHOSPHATE ALDOLASE 2		203/ 2			344/ 3		
AT5G47700	60S ACIDIC RIBOSOMAL PROTEIN P1-1-RELATED		143/ 2			115/ 2	109 2	
AT5G46020	28 KDA HEAT/ACID-STABLE PHOSPHOPROTEIN-LIKE PROTEIN		188/ 2	122/ 2	142/ 2	265/ 3		
AT1G52740	HISTONE H2A VARIANT 3-RELATED		169/ 2		136/ 3			
AT3G27850	50S RIBOSOMAL PROTEIN L12-1		149/ 2		101 2	125/ 2		
AT5G06860	POLYGALACTURONASE INHIBITOR 1		149/ 2					
AT1G15820	CHLOROPHYLL A-B BINDING PROTEIN		146/ 2			171/ 2		
AT5G64140	40S RIBOSOMAL PROTEIN S28		126/ 2					
AT1G64510	30S RIBOSOMAL PROTEIN S6 ALPHA		139/ 2		106/ 2			
AT1G06680	OXYGEN-EVOLVING ENHANCER PROTEIN 2-1		139/ 2			261/ 2		
AT4G32605	Mitochondrial glycoprotein family protein		132/ 2	121/ 2	225/ 2			
AT5G14910	Heavy metal transport/detoxification superfamily protein		154/ 2		135/ 2		133/ 2	
AT5G53070	RIBOSOMAL PROTEIN L9/RNASE H1		145/ 2	202/ 2			159/ 3	
AT1G20220	ALBA DNA/RNA-BINDING PROTEIN		148/ 2	303/ 3	253/ 2	138/ 3	191/ 3	149/ 3
AT2G22720	SPT2 CHROMATIN PROTEIN		135/ 2					
AT3G03920	H/ACA RIBONUCLEOPROTEIN COMPLEX SUBUNIT 1		122/ 2	279/ 2	172/ 2		266/ 3	152/ 3
AT3G56910	50S RIBOSOMAL PROTEIN 5		120/ 2		130/ 2	113/ 3	102/ 2	
AT5G01530	CHLOROPHYLL A-B BINDING PROTEIN CP29.1		139/ 2			179/ 3		
AT4G39880	39S RIBOSOMAL PROTEIN L23		114/ 2	147/ 2	107/ 2		149/ 3	
AT1G69620	60S RIBOSOMAL PROTEIN L34-1-RELATED		113/ 2		114 2	100/ 2		
AT4G37660	Ribosomal protein L12/ ATP-dependent Clp protease adaptor protein		123/ 2				108/ 2	
AT1G44575	PHOTOSYSTEM II 22 KDA PROTEIN		108/ 2			138/ 2		
AT4G17720	SI:CH211-195B21.5		126/ 2				201/ 2	
AT5G57290	60S ACIDIC RIBOSOMAL PROTEIN P3-1-RELATED		113/ 2		112/ 2		128/ 2	
AT3G01740	39S RIBOSOMAL PROTEIN L54		106/ 2					
AT3G09480	HISTONE H2B.5-RELATED		106/ 2					
AT3G44300	NITRILASE 1-RELATED		103/ 2					
AT2G41730	CALCIUM-BINDING SITE PROTEIN-RELATED		91/ 2		120/ 2			
AT1G15280	CASC3/BARENTSZ EIF4AIII BINDING PROTEIN		93/ 2				127/ 2	
AT4G01150	PROTEIN CURVATURE THYLAKOID 1A		94/ 2					
AT4G10970	RIBOSOME MATURATION FACTOR			188/ 3			104/ 3	125/ 2
AT5G55210	Hypothetical protein			251/ 3	220/ 3	167/ 3	225/ 3	207/ 3
AT4G28360	Ribosomal protein L22p/L17e family protein			258/ 3	262/ 3	161/ 2	265/ 3	234/ 2
AT1G42440	PRE-RRNA-PROCESSING PROTEIN TSR1 HOMOLOG			146/ 3	131/ 2			
AT3G01790	39S RIBOSOMAL PROTEIN L13			164/ 3	100/ 3			
AT1G60640	STRESS RESPONSE PROTEIN			155/ 3				147/ 2
AT5G22010	REPLICATION FACTOR C SUBUNIT 1			108/ 3				
AT5G21105	FI03373P-RELATED			525/ 2	428/ 2	1278/ 3	398/ 3	182/ 3
AT5G18550	ZINC FINGER CCCH DOMAIN-CONTAINING PROTEIN 58			332/ 2		108/ 3	307/ 2	
AT1G06670	DEXH-BOX ATP-DEPENDENT RNA HELICASE DEXH2-RELATED			288/ 2				
AT4G10710	FACT COMPLEX SUBUNIT SPT16-RELATED			207/ 2				
AT4G36020	COLD SHOCK DOMAIN-CONTAINING PROTEIN 3-RELATED			213/ 2			170/ 2	
AT1G76010	ALBA DNA/RNA-BINDING PROTEIN			180/ 2	203/ 2			
AT3G45960	EXPANSIN-LIKE A1-RELATED			170/ 2				
AT1G68560	ALPHA-XYLOSIDASE 1-RELATED			158/ 2	178/ 2			
AT4G32330	PROTEIN WVD2-LIKE 5-RELATED			211/ 2				
AT5G59460	M-PHASE PHOSPHOPROTEIN 6			194/ 2				131/ 2
AT3G52120	SURP AND G PATCH DOMAIN-CONTAINING 1			147/ 2	111/ 2			
AT3G01160	ESF1 HOMOLOG			155/ 2		98/ 2		118 2
AT5G52380	VASCULAR-RELATED NAC-DOMAIN 6			147/ 2		223/ 2	215/ 3	156/ 2
AT3G13230	RNA-BINDING PROTEIN PNO1			146/ 2				
AT1G74000	PROTEIN STRICTOSIDINE SYNTHASE-LIKE 11			173/ 2			167/ 2	
AT2G42610	PROTEIN LIGHT-DEPENDENT SHORT HYPOCOTYLS 10			148/ 2	185/ 2	110/ 2	198/ 3	
AT3G55620	EUKARYOTIC TRANSLATION INITIATION FACTOR 6-1-RELATED			150/ 2		137/ 2	227/ 2	
AT5G27670	HISTONE H2A.5-RELATED			134/ 2		210/ 3	137/ 2	
AT2G39795	Mitochondrial glycoprotein family protein			120/ 2				
AT3G44750	HISTONE DEACETYLASE HDT1			104/ 2			204/ 2	
AT2G44525	NADH dehydrogenase ubiquinone 1 alpha subcomplex assembly factor-like			101/ 2				
AT5G10950	Tudor/PWWP/MBT superfamily protein			104/ 2			154 2	
AT3G51010	Protein translocase subunit			97/ 2				
AT3G02220	CHROMOSOME 9 OPEN READING FRAME 85			93/ 2	85/ 2			
AT4G34980	SUBTILISIN-LIKE PROTEASE SBT1.6			89/ 2	255/ 2			
AT3G55560	AT-HOOK MOTIF NUCLEAR-LOCALIZED PROTEIN 15			88/ 2				
AT1G06190	RHO-N DOMAIN-CONTAINING PROTEIN 1			84/ 2				
AT5G02240	Protein is tyrosine-phosphorylated				307/ 3			
AT3G56900	ALADIN				216/ 3			
AT5G05680	NUCLEAR PORE COMPLEX PROTEIN NUP88				252/ 3			
AT3G52960	PEROXIREDOXIN-5				150/ 3			
AT3G43810	CALMODULIN-7-RELATED				153/ 3	104/ 2		
AT1G20580	SMALL NUCLEAR RIBONUCLEOPROTEIN SM D3				123/ 3			
AT5G12190	Splicing factor 3B subunit 6-like protein				120/ 3			
AT3G53650	HISTONE H2B.8				1088/ 2			

Table S15f. List of expected interactors of mRNA export receptor candidates. Proteins that co-purified with NXF-SG candidates. Proteins that co-purified with unfused SG were removed from the list. The average MASCOT score is shown and how many times the protein was detected in out three independent experiments.

TAIR	DESCRIPTION	NXF1	NXF2	NXF3	NXF4	NXF5	NXF6	NXF7
AT1G35660	ERYTHROID DIFFERENTIATION-RELATED FACTOR 1				760/ 2			
AT4G29510	ARGININE METHYLTRANSFERASE 1-RELATED				292/ 2			
AT1G10200	LIM DOMAIN-CONTAINING PROTEIN WLIM1				213/ 2			
AT3G46960	DEXH-BOX ATP-DEPENDENT RNA HELICASE DEXH11				200/ 2			
AT1G47420	SUCCINATE DEHYDROGENASE SUBUNIT 5				185/ 2			
AT3G18580	NUCLEIC ACID-BINDING				153/ 2			
AT5G04440	RAP release 2, galactose-binding-like domain protein				146/ 2			
AT1G20110	PROTEIN FREE1				137/ 2			
AT1G49400	37S RIBOSOMAL PROTEIN S17				138/ 2			
AT1G80230	CYTOCHROME C OXIDASE SUBUNIT 5B				114/ 2			
AT1G77750	SMALL RIBOSOMAL SUBUNIT PROTEIN S13				141/ 2			
AT3G22640	Cupin family protein				127/ 2			
AT5G09770	39S RIBOSOMAL PROTEIN L17				122/ 2			
AT5G11900	TRANSLATION MACHINERY-ASSOCIATED PROTEIN 22				92/ 2			
AT5G16140	CHLOROPLASTIC GROUP IIB INTRON SPLICING FACILITATOR CRS2-B				93/ 2			
AT2G39740	POLY HESO1				86/ 2			
AT3G59410	EIF-2-ALPHA KINASE GCN2				88/ 2			
AT1G59660	NUCLEAR PORE COMPLEX PROTEIN NUP98-NUP96				87/ 2			
AT2G07675	Ribosomal protein S12/S23 family protein				82/ 2			
AT1G51760	IAA-AMINO ACID HYDROLASE ILR1-LIKE 4-RELATED				81/ 2			
ATCG00680	PHOTOSYSTEM II CP47 REACTION CENTER PROTEIN					486/ 3		
AT3G50820	OXYGEN-EVOLVING ENHANCER PROTEIN 1-2					323/ 3		
AT5G59870	HISTONE H2A					273/ 3	194/ 2	
AT4G03280	CYTOCHROME B6-F COMPLEX IRON-SULFUR SUBUNIT					221/ 3		
AT4G28750	PHOTOSYSTEM I REACTION CENTER SUBUNIT IV A					185/ 3		
AT5G26000	MYROSINASE 1-RELATED					153/ 3		
ATCG00020	PHOTOSYSTEM II PROTEIN D1					185/ 3		
AT1G69530	EXPANSIN-A1					151/ 3		
AT3G01500	BETA CARBONIC ANHYDRASE 1					602/ 2		
AT5G14740	BETA CARBONIC ANHYDRASE 2					398/ 2		
AT3G14420	(S)-2-HYDROXY-ACID OXIDASE GLO1					319/ 2		
AT5G38430	RIBULOSE BISPHOSPHATE CARBOXYLASE SMALL CHAIN 1A					239/ 2		
AT1G61520	PHOTOSYSTEM I CHLOROPHYLL A/B-BINDING PROTEIN 3-1					277/ 2		
AT3G14415	(S)-2-hydroxy-acid oxidase GLO2					267/ 2		
AT2G20260	PHOTOSYSTEM I REACTION CENTER SUBUNIT IV A					211/ 2		
AT4G00810	60S ACIDIC RIBOSOMAL PROTEIN P1-2					204/ 2		
AT1G11860	AMINOMETHYLTRANSFERASE-RELATED					178/ 2		
ATCG00340	PHOTOSYSTEM I P700 CHLOROPHYLL A APOPROTEIN A2					154/ 2		
AT3G08940	CHLOROPHYLL A-B BINDING PROTEIN CP29.2					175/ 2		
AT1G31330	PHOTOSYSTEM I REACTION CENTER SUBUNIT III					135/ 2		
AT3G49470	NASCENT POLYPEPTIDE-ASSOCIATED COMPLEX SUBUNIT					147/ 2	221/ 2	241/ 2
AT1G23310	GLUTAMATE--GLYOXYLATE AMINOTRANSFERASE 1					126/ 2		
AT1G78830	EP1-LIKE GLYCOPROTEIN 1-RELATED					122/ 2		
AT1G03130	PHOTOSYSTEM I REACTION CENTER SUBUNIT II-1					113/ 2		
AT1G32060	PHOSPHORIBULOKINASE					139 2		
AT5G04140	FERREDOXIN-DEPENDENT GLUTAMATE SYNTHASE 1					117/ 2		
AT4G10480	NASCENT POLYPEPTIDE-ASSOCIATED COMPLEX SUBUNIT					119/ 2	215/ 3	346/ 2
AT1G63940	MONODEHYDROASCORBATE REDUCTASE					119 2		
AT1G54770	DEOXYNUCLEOTIDYLTRANSFERASE TERMINAL-INTERACTING					107/ 2	103/ 2	89/ 2
AT2G42680	MULTIPROTEIN-BRIDGING FACTOR 1A					121/ 2		
AT1G08580	Hypothetical protein					110/ 2	136/ 2	
AT2G21170	TRIOSEPHOSPHATE ISOMERASE					113/ 2		
AT2G30870	GLUTATHIONE S-TRANSFERASE F10					101/ 2		
AT3G44320	NITRILASE 1-RELATED					104/ 2		
AT3G46940	DEOXYURIDINE TRIPHOSPHATASE					97/ 2		
AT2G19750	40S RIBOSOMAL PROTEIN S30					95/ 2		
AT4G25100	SUPEROXIDE DISMUTASE [FE] 1					86/ 2		
AT4G22745	METHYL-CPG-BINDING DOMAIN-CONTAINING PROTEIN 1-RELATED						131/ 3	141/ 2
AT1G53830	PECTINESTERASE 2						116/ 3	
AT2G33845	EXPRESSED PROTEIN						141/ 3	
AT4G27380	Hypothetical protein						129/ 3	
AT2G43210	PLANT UBX DOMAIN-CONTAINING PROTEIN 11						327/ 2	
AT1G77510	PROTEIN DISULFIDE ISOMERASE-LIKE 1-2						235/ 2	
AT4G35890	LARP						193/ 2	
AT1G21750	PROTEIN DISULFIDE ISOMERASE-LIKE 1-1						179/ 2	
AT2G22090	UBP1-ASSOCIATED PROTEINS 1A-RELATED						199/ 2	
AT5G63510	GAMMA CARBONIC ANHYDRASE-LIKE 1						142/ 2	
AT1G63470	AT-HOOK MOTIF NUCLEAR-LOCALIZED PROTEIN 12-RELATED						131/ 2	
AT1G69410	EUKARYOTIC TRANSLATION INITIATION FACTOR 5A-3						123/ 2	
AT5G08420	KRR1 SMALL SUBUNIT PROCESSOME COMPONENT HOMOLOG						110/ 2	
AT3G13120	37S RIBOSOMAL PROTEIN S10						103/ 2	
AT1G66070	EUKARYOTIC TRANSLATION INITIATION FACTOR 3 SUBUNIT J						102/ 2	
AT3G22850	ALUMINUM INDUCED PROTEIN WITH YGL AND LRDR MOTIFS						103/ 2	
AT2G44065	60S RIBOSOMAL PROTEIN L2						92/ 2	157/ 2
AT1G48610	PUTATIVE DNA-BINDING PROTEIN							124/ 2
AT5G17710	GRPE PROTEIN HOMOLOG							112/ 2
AT3G63030	METHYL-CPG-BINDING DOMAIN-CONTAINING PROTEIN 1-RELATED							107/ 2
AT1G16810	PROTEIN FAM32A							98/ 2
AT2G21160	TRANSLOCON-ASSOCIATED PROTEIN SUBUNIT ALPHA							99/ 2

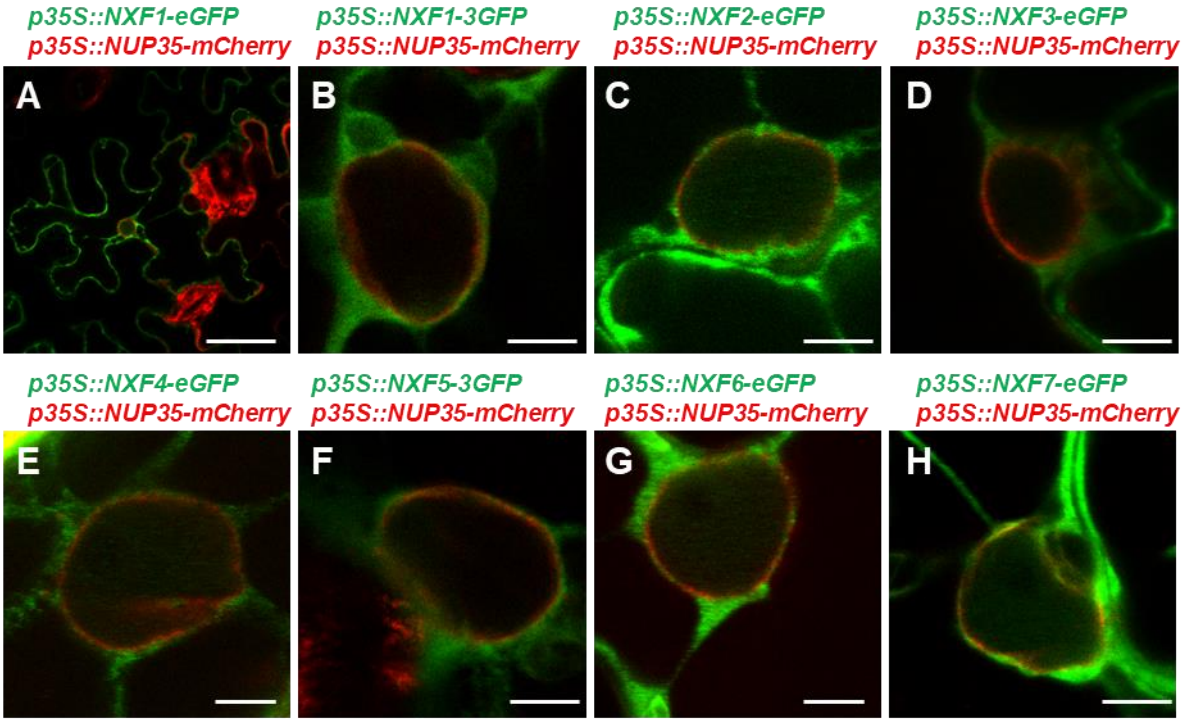

Figure S16. Co-expression of NXF-eGFP candidates and NUP35-mCherry in *N. benthamiana*. *NXF1-7-3'eGFP* and *NUP35-3'mCherry* were transiently co-expressed in *N. benthamiana*. Cells expressing both *NXF1-eGFP* and *NUP35-mCherry* show a green cytosolic NXF1 signal and a red NUP35-mCherry signal enriched at the nuclear envelope (A). (B-H) Single nuclei of cells co-expressing *NXF-eGFP* and *UAP56-mCherry* demonstrates that NXF proteins and NUP35 proteins are enriched around the nuclear envelope. Size bars (A) = 50 µm, (B-H) = 5 µm.

Publications

Publications related to this work:

Pfaff C, Ehrnsberger HF, Flores-Tornero M, Soerensen BB, Schubert T, Längst G, Griesenbeck J, Sprunck S, Grasser M, Grasser KD (2018) ALY RNA-binding proteins are required for nucleo-cytosolic mRNA transport and modulate plant growth and development. Plant Physiol **177**: pp.00173.2018

Ehrnsberger HF, Pfaff C, Hachani I, Flores-Tornero M, Sørensen BB, Längst G, Sprunck S, Grasser M, Grasser KD (2019) The UAP56-Interacting Export Factors UIEF1 and UIEF2 Function in mRNA Export. Plant Physiol **179**: 1525–1536

Ehrnsberger HF, Grasser M, Grasser KD (2019) Nucleocytosolic mRNA transport in plants: export factors and their influence on growth and development. J Exp Bot **70**: 3757–3763

Sørensen BB, Ehrnsberger HF, Esposito S, Pfab A, Bruckmann A, Hauptmann J, Meister G, Merkl R, Schubert T, Längst G, et al (2017) The Arabidopsis THO/TREX component TEX1 functionally interacts with MOS11 and modulates mRNA export and alternative splicing events. Plant Mol Biol **93**: 283–298

Other publications:

Antosz W, Pfab A, Ehrnsberger HF, Holzinger P, Köllen K, Mortensen SA, Bruckmann A, Schubert T, Längst G, Griesenbeck J, et al (2017) The Composition of the Arabidopsis RNA Polymerase II Transcript Elongation Complex Reveals the Interplay between Elongation and mRNA Processing Factors. Plant Cell **29**: 854–870

Acknowledgements

Zunächst möchte ich mich bei Prof. Dr. Klaus D. Grasser bedanken, dass du mir es ermöglicht hast in deiner Arbeitsgruppe zu promovieren. Danke für die Begutachtung meiner Arbeit, die Unterstützung durch Ratschläge und Diskussionen und die Geduld die du in den Jahren aufbringen musstest.

Ein weiterer Dank gilt Prof. Dr. Gunter Meister, Prof. Dr. Wolfgang Frank, Dr. Jan Medenbach, Prof. Dr. Herbert Tschochner und Prof. Dr. Thomas Dresselhaus für die Betreuung als Mentor, die Zweitbegutachtung meiner Arbeit und die die Bereitschaft als Drittprüfer beziehungsweise als Prüfungsvorsitzender zu fungieren.

Ein besonderer Dank geht auch an Dr. Julia Engelmann und Simon Obermeyer für eure tatkräftige Hilfe bei der Auswertung der Sequenzierungsdaten.

Ich möchte mich außerdem bei allen aktuellen und ehemaligen Studenten und Mitarbeitern der AG Grasser für die Unterstützung und die freundschaftliche und entspannte Atmosphäre bedanken, die in all den Jahren hier vorzufinden war. Ein spezieller Dank geht hierbei an Marion, für deine Hilfsbereitschaft und Freundlichkeit, die du hier allen entgegenbringst.

Außerdem möchte ich mich ganz besonders bei den ‘old good KDGs‘ bedanken, die mich die längste Zeit hier begleitet haben. Allen voran bei den guten Seelen dieses Teams Silvia and Alex, dem besten Bench Nachbar Wojtey, meinem alten Betreuerfreund Brian und unserem Küken und Meisterbetreuer Philipp.

Ich möchte mich darüber hinaus bei allen ehemaligen und aktuellen Mitgliedern des Lehrstuhls für euere Hilfestellungen und für eine tolle Arbeitsatmosphäre bedanken.

Ein großes Dankeschön geht auch an meine Party-Biologen-Freunde Phil, Tom, Karin und Tina für all die schönen Momente, die wir miteinander erleben durften. Einen speziellen Applaus möchte ich hierbei an meine beste Co-Pilotin Tini richten, weil es mit dir einfach immer Spaß macht.

Ich möchte mich auch bei meiner Familie bedanken, da ohne euch das alles nicht möglich gewesen wäre.

Zu guter Letzt geht ein herzlicher Dank an meine allerbeste Kathy: Für deine Unterstützung und weil das Leben mit dir einfach viel schöner ist.

Bibliography

Abulfaraj AA, Mariappan K, Bigeard J, Manickam P, Blilou I, Guo X, Al-Babili S, Pflieger D, Hirt H, Rayapuram N (2018) The Arabidopsis homolog of human G3BP1 is a key regulator of stomatal and apoplastic immunity. Life Sci Alliance **1**: 1–13

Adams RL, Wente SR (2013) Uncovering Nuclear Pore Complexity with Innovation. Cell **152**: 1218–1221

Aibara S, Katahira J, Valkov E, Stewart M (2015) The principal mRNA nuclear export factor NXF1:NXT1 forms a symmetric binding platform that facilitates export of retroviral CTE-RNA. Nucleic Acids Res **43**: 1883–1893

Aitchison JD, Blobel G, Rout MP (1996) Kap104p: A Karyopherin Involved in the Nuclear Transport of Messenger RNA Binding Proteins. Science (80-) **274**: 624–627

Aitchison JD, Rout MP (2012) The Yeast Nuclear Pore Complex and Transport Through It. Genetics **190**: 855–883

Allen NPC, Huang L, Burlingame A, Rexach M (2001) Proteomic Analysis of Nucleoporin Interacting Proteins. J Biol Chem **276**: 29268–29274

Antosz W, Pfab A, Ehrnsberger HF, Holzinger P, Köllen K, Mortensen SA, Bruckmann A, Schubert T, Längst G, Griesenbeck J, et al (2017) The Composition of the Arabidopsis RNA Polymerase II Transcript Elongation Complex Reveals the Interplay between Elongation and mRNA Processing Factors. Plant Cell **29**: 854–870

Arabidopsis Interactome Mapping Consortium (2011) Evidence for network evolution in an Arabidopsis interactome map. Science **333**: 601–7

Arvidsson S, Kwasniewski M, Riano-Pachon DM, Mueller-Roeber B (2008) QuantPrime - a flexible tool for reliable high-throughput primer design for quantitative PCR. BMC Bioinformatics **9**: 465

Azevedo J, Picart C, Dureau L, Pontier D, Jaquinod-Kieffer S, Hakimi M, Lagrange T (2019) UAP56 associates with DRM2 and is localized to chromatin in Arabidopsis. FEBS Open Bio **9**: 973–985

Bachi A, Braun IC, Rodrigues JP, Panté N, Ribbeck K, von Kobbe C, Kutay U, Wilm M, Görlich D, Carmo-Fonseca M, et al (2000) The C-terminal domain of TAP interacts with the nuclear pore complex and promotes export of specific CTE-bearing RNA substrates. RNA **6**: 136–58

Beck M, Hurt E (2017) The nuclear pore complex: Understanding its function through structural insight. Nat Rev Mol Cell Biol **18**: 73–89

Ben-Yishay R, Ashkenazy AJ, Shav-Tal Y (2016) Dynamic Encounters of Genes and Transcripts with the Nuclear Pore. Trends Genet **32**: 419–431

Ben-Yishay R, Mor A, Shraga A, Ashkenazy-Titelman A, Kinor N, Schwed-Gross A, Jacob A, Kozer N, Kumar P, Garini Y, et al (2019) Imaging within single NPCs reveals NXF1's role in mRNA export on the cytoplasmic side of the pore. J Cell Biol jcb.201901127

Blobel G (1985) Gene gating: a hypothesis. Proc Natl Acad Sci **82**: 8527–8529

Bogamuwa S, Jang J-C (2016) Plant Tandem CCCH Zinc Finger Proteins Interact with ABA, Drought, and Stress Response Regulators in Processing-Bodies and Stress Granules. PLoS One **11**: e0151574

Bortvin A, Winston F (1996) Evidence That Spt6p Controls Chromatin Structure by a Direct Interaction with Histones. Science (80-) **272**: 1473–1476

Boyes DC, Zayed AM, Ascenzi R, McCaskill AJ, Hoffman NE, Davis KR, Görlach J (2001) Growth stage-based phenotypic analysis of Arabidopsis: a model for high throughput functional genomics in plants. Plant Cell **13**: 1499–510

Bruhn L, Munnerlyn A, Grosschedl R (1997) ALY, a context-dependent coactivator of LEF-1 and AML-1, is required for TCRalpha enhancer function. Genes Dev **11**: 640–653

Canto T, Uhrig JF, Swanson M, Wright KM, MacFarlane SA (2006) Translocation of Tomato Bushy Stunt Virus P19 Protein into the Nucleus by ALY Proteins Compromises Its Silencing Suppressor Activity. J Virol **80**: 9064–9072

Chang C-T, Hautbergue GM, Walsh MJ, Viphakone N, van Dijk TB, Philipsen S, Wilson SA (2013) Chtop is a component of the dynamic TREX mRNA export complex. EMBO J **32**: 473–486

Cheng C-Y, Krishnakumar V, Chan AP, Thibaud-Nissen F, Schobel S, Town CD (2017) Araport11: a complete reannotation of the Arabidopsis thaliana reference genome. Plant J **89**: 789–804

Cheng H, Dufu K, Lee C-S, Hsu JL, Dias A, Reed R (2006) Human mRNA Export Machinery Recruited to the 5′ End of mRNA. Cell **127**: 1389–1400

Chi B, Wang Q, Wu G, Tan M, Wang L, Shi M, Chang X, Cheng H (2013) Aly and THO are required for assembly of the human TREX complex and association of TREX components with the spliced mRNA. Nucleic Acids Res **41**: 1294–1306

Chinnusamy V, Gong Z, Zhu J-K (2008) Nuclear RNA export and its importance in abiotic

stress responses of plants. Curr Top Microbiol Immunol **326**: 235–55

Choudury SG, Shahid S, Cuerda-Gil D, Panda K, Cullen A, Ashraf Q, Sigman MJ, McCue AD, Slotkin RK (2019) The RNA Export Factor ALY1 Enables Genome-Wide RNA-Directed DNA Methylation. Plant Cell **31**: 759–774

Clough SJ, Bent AF (1998) Floral dip: a simplified method for Agrobacterium-mediated transformation of Arabidopsis thaliana. Plant J **16**: 735–43

Damelin M, Silver PA (2000) Mapping Interactions between Nuclear Transport Factors in Living Cells Reveals Pathways through the Nuclear Pore Complex. Mol Cell **5**: 133–140

Dedecker M, Van Leene J, De Jaeger G (2015) Unravelling plant molecular machineries through affinity purification coupled to mass spectrometry. Curr Opin Plant Biol **24**: 1–9

Dimitrova L, Valkov E, Aibara S, Flemming D, McLaughlin SH, Hurt E, Stewart M (2015) Structural Characterization of the Chaetomium thermophilum TREX-2 Complex and its Interaction with the mRNA Nuclear Export Factor Mex67:Mtr2. Structure **23**: 1246–1257

Domínguez-Sánchez MS, Barroso S, Gómez-González B, Luna R, Aguilera A (2011) Genome Instability and Transcription Elongation Impairment in Human Cells Depleted of THO/TREX. PLoS Genet **7**: e1002386

Dufu K, Livingstone MJ, Seebacher J, Gygi SP, Wilson SA, Reed R (2010) ATP is required for interactions between UAP56 and two conserved mRNA export proteins, Aly and CIP29, to assemble the TREX complex. Genes Dev **24**: 2043–2053

Duncan S, Olsson TSG, Hartley M, Dean C, Rosa S (2016) A method for detecting single mRNA molecules in Arabidopsis thaliana. Plant Methods **12**: 13

Duncan S, Rosa S (2018) Gaining insight into plant gene transcription using smFISH. Transcription **9**: 166–170

Ehrnsberger HF, Grasser M, Grasser KD (2019a) Nucleocytosolic mRNA transport in plants: export factors and their influence on growth and development. J Exp Bot **70**: 3757–3763

Ehrnsberger HF, Pfaff C, Hachani I, Flores-Tornero M, Sørensen BB, Längst G, Sprunck S, Grasser M, Grasser KD (2019b) The UAP56-Interacting Export Factors UIEF1 and UIEF2 Function in mRNA Export. Plant Physiol **179**: 1525–1536

Fan J, Kuai B, Wang K, Wang L, Wang Y, Wu X, Chi B, Li G, Cheng H (2018) mRNAs are sorted for export or degradation before passing through nuclear speckles. Nucleic Acids Res **46**: 8404–8416

Fan J, Kuai B, Wu G, Wu X, Chi B, Wang L, Wang K, Shi Z, Zhang H, Chen S, et al (2017)

Exosome cofactor hMTR4 competes with export adaptor ALYREF to ensure balanced nuclear RNA pools for degradation and export. EMBO J **36**: 2870–2886

Fica SM, Nagai K (2017) Cryo-electron microscopy snapshots of the spliceosome: structural insights into a dynamic ribonucleoprotein machine. Nat Struct Mol Biol **24**: 791–799

Fischer T, Rodríguez-Navarro S, Pereira G, Rácz A, Schiebel E, Hurt E (2004) Yeast centrin Cdc31 is linked to the nuclear mRNA export machinery. Nat Cell Biol **6**: 840–848

Folkmann AW, Noble KN, Cole CN, Wente SR (2011) Dbp5, Gle1-IP 6 and Nup159. Nucleus **2**: 540–548

Francisco-Mangilet AG, Karlsson P, Kim M-H, Eo HJ, Oh SA, Kim JH, Kulcheski FR, Park SK, Manavella PA (2015) THO2, a core member of the THO/TREX complex, is required for microRNA production in Arabidopsis. Plant J **82**: 1018–1029

Fribourg S, Braun IC, Izaurralde E, Conti E (2001) Structural basis for the recognition of a nucleoporin FG repeat by the NTF2-like domain of the TAP/p15 mRNA nuclear export factor. Mol Cell **8**: 645–656

Fribourg S, Conti E (2003) Structural similarity in the absence of sequence homology of the messenger RNA export factors Mtr2 and p15. EMBO Rep **4**: 699–703

Furumizu C, Tsukaya H, Komeda Y (2010) Characterization of EMU, the Arabidopsis homolog of the yeast THO complex member HPR1. RNA **16**: 1809–1817

Gaouar O, Germain H (2013) mRNA export: threading the needle. Front Plant Sci **4**: 59

Gatfield D, Izaurralde E (2002) REF1/Aly and the additional exon junction complex proteins are dispensable for nuclear mRNA export. J Cell Biol **159**: 579–588

Germain H, Qu N, Cheng YT, Lee E, Huang Y, Dong OX, Gannon P, Huang S, Ding P, Li Y, et al (2010) MOS11: A New Component in the mRNA Export Pathway. PLoS Genet **6**: e1001250

Gibson TJ, Seiler M, Veitia RA (2013) The transience of transient overexpression. Nat Methods **10**: 715–21

Golovanov AP, Hautbergue GM, Tintaru AM, Lian L-Y, Wilson SA (2006) The solution structure of REF2-I reveals interdomain interactions and regions involved in binding mRNA export factors and RNA. RNA **12**: 1933–1948

Gong Z, Dong C-H, Lee H, Zhu J, Xiong L, Gong D, Stevenson B, Zhu J-K (2005) A DEAD box RNA helicase is essential for mRNA export and important for development and stress responses in Arabidopsis. Plant Cell **17**: 256–67

Grant RP, Neuhaus D, Stewart M (2003) Structural basis for the interaction between the Tap/NXF1 UBA domain and FG nucleoporins at 1A resolution. J Mol Biol **326**: 849–58

Gromadzka AM, Steckelberg A-L, Singh KK, Hofmann K, Gehring NH (2016) A short conserved motif in ALYREF directs cap- and EJC-dependent assembly of export complexes on spliced mRNAs. Nucleic Acids Res **44**: 2348–2361

Grünwald D, Singer RH (2010) In vivo imaging of labelled endogenous β-actin mRNA during nucleocytoplasmic transport. Nature **467**: 604–607

Grüter P, Tabernero C, von Kobbe C, Schmitt C, Saavedra C, Bachi A, Wilm M, Felber BK, Izaurralde E (1998a) TAP, the Human Homolog of Mex67p, Mediates CTE-Dependent RNA Export from the Nucleus. Mol Cell **1**: 649–659

Grüter P, Tabernero C, Von Kobbe C, Schmitt C, Saavedra C, Bachi A, Wilm M, Felber BK, Izaurralde E (1998b) TAP, the human homolog of Mex67p, mediates CTE-dependent RNA export from the nucleus. Mol Cell **1**: 649–659

Haasen D, Kohler C, Neuhaus G, Merkle T (1999) Nuclear export of proteins in plants: AtXPO1 is the export receptor for leucine-rich nuclear export signals in Arabidopsis thaliana. Plant J **20**: 695–705

Hachani I (2018) Functional characterization of proteins involved in mRNA export in Arabidopsis thaliana. Master thesis University of Regensburg

Hautbergue GM, Hung M-L, Golovanov AP, Lian L-Y, Wilson SA (2008) Mutually exclusive interactions drive handover of mRNA from export adaptors to TAP. Proc Natl Acad Sci **105**: 5154–5159

Hautbergue GM, Hung M-L, Walsh MJ, Snijders APL, Chang C-T, Jones R, Ponting CP, Dickman MJ, Wilson SA (2009) UIF, a New mRNA Export Adaptor that Works Together with REF/ALY, Requires FACT for Recruitment to mRNA. Curr Biol **19**: 1918–1924

Heath CG, Viphakone N, Wilson SA (2016) The role of TREX in gene expression and disease. Biochem J **473**: 2911–2935

Hellemans J, Mortier G, De Paepe A, Speleman F, Vandesompele J (2007) qBase relative quantification framework and software for management and automated analysis of real-time quantitative PCR data. Genome Biol **8**: R19

Herold A, Klymenko T, Izaurralde E (2001) NXF1/p15 heterodimers are essential for mRNA nuclear export in Drosophila. RNA **7**: 1768–80

Herold A, Suyama M, Rodrigues JP, Braun IC, Kutay U, Carmo-Fonseca M, Bork P,

Izaurralde E (2000) TAP (NXF1) Belongs to a Multigene Family of Putative RNA Export Factors with a Conserved Modular Architecture. Mol Cell Biol **20**: 8996–9008

Le Hir H (2001) The exon-exon junction complex provides a binding platform for factors involved in mRNA export and nonsense-mediated mRNA decay. EMBO J **20**: 4987–4997

Hodge CA, Tran EJ, Noble KN, Alcazar-Roman AR, Ben-Yishay R, Scarcelli JJ, Folkmann AW, Shav-Tal Y, Wente SR, Cole CN (2011) The Dbp5 cycle at the nuclear pore complex during mRNA export I: dbp5 mutants with defects in RNA binding and ATP hydrolysis define key steps for Nup159 and Gle1. Genes Dev **25**: 1052–1064

Hruz T, Laule O, Szabo G, Wessendorp F, Bleuler S, Oertle L, Widmayer P, Gruissem W, Zimmermann P (2008) Genevestigator v3: a reference expression database for the meta-analysis of transcriptomes. Adv Bioinformatics **2008**: 420747

Huang Y, Gattoni R, Stévenin J, Steitz JA (2003) SR Splicing Factors Serve as Adapter Proteins for TAP-Dependent mRNA Export. Mol Cell **11**: 837–843

Hülsmann BB, Labokha AA, Görlich D (2012) The Permeability of Reconstituted Nuclear Pores Provides Direct Evidence for the Selective Phase Model. Cell **150**: 738–751

Hung M-L, Hautbergue GM, Snijders APL, Dickman MJ, Wilson SA (2010) Arginine methylation of REF/ALY promotes efficient handover of mRNA to TAP/NXF1. Nucleic Acids Res **38**: 3351–3361

Jauvion V, Elmayan T, Vaucheret H (2010) The Conserved RNA Trafficking Proteins HPR1 and TEX1 Are Involved in the Production of Endogenous and Exogenous Small Interfering RNA in Arabidopsis. Plant Cell **22**: 2697–2709

Johnson SA, Cubberley G, Bentley DL (2009) Cotranscriptional recruitment of the mRNA export factor Yra1 by direct interaction with the 3' end processing factor Pcf11. Mol Cell **33**: 215–26

Kabachinski G, Schwartz TU (2015) The nuclear pore complex - structure and function at a glance. J Cell Sci **128**: 423–429

Kammel C, Thomaier M, Sørensen BB, Schubert T, Längst G, Grasser M, Grasser KD (2013) Arabidopsis DEAD-Box RNA Helicase UAP56 Interacts with Both RNA and DNA as well as with mRNA Export Factors. PLoS One **8**: e60644

Katahira J (2015) Nuclear Export of Messenger RNA. Genes (Basel) **6**: 163–184

Katahira J, Inoue H, Hurt E, Yoneda Y (2009) Adaptor Aly and co-adaptor Thoc5 function in the Tap-p15-mediated nuclear export of HSP70 mRNA. EMBO J **28**: 556–567

Katahira J, Okuzaki D, Inoue H, Yoneda Y, Maehara K, Ohkawa Y (2013) Human TREX component Thoc5 affects alternative polyadenylation site choice by recruiting mammalian cleavage factor I. Nucleic Acids Res **41**: 7060–7072

Katahira J, Straesser K, Saiwaki T, Yoneda Y, Hurt E (2002) Complex Formation between Tap and p15 Affects Binding to FG-repeat Nucleoporins and Nucleocytoplasmic Shuttling. J Biol Chem **277**: 9242–9246

Katahira J, Strässer K, Podtelejnikov A, Mann M, Jung JU, Hurt E (1999) The Mex67p-mediated nuclear mRNA export pathway is conserved from yeast to human. EMBO J **18**: 2593–609

Kedersha N, Chen S, Gilks N, Li W, Miller IJ, Stahl J, Anderson P (2002) Evidence that ternary complex (eIF2-GTP-tRNA(i)(Met))-deficient preinitiation complexes are core constituents of mammalian stress granules. Mol Biol Cell **13**: 195–210

Kedersha N, Panas MD, Achorn CA, Lyons S, Tisdale S, Hickman T, Thomas M, Lieberman J, McInerney GM, Ivanov P, et al (2016) G3BP–Caprin1–USP10 complexes mediate stress granule condensation and associate with 40S subunits. J Cell Biol **212**: 845–860

Kilchert C, Wittmann S, Vasiljeva L (2016) The regulation and functions of the nuclear RNA exosome complex. Nat Rev Mol Cell Biol **17**: 227–239

Kim SJ, Fernandez-Martinez J, Nudelman I, Shi Y, Zhang W, Raveh B, Herricks T, Slaughter BD, Hogan JA, Upla P, et al (2018) Integrative structure and functional anatomy of a nuclear pore complex. Nature **555**: 475–482

Koroleva OA, Calder G, Pendle AF, Kim SH, Lewandowska D, Simpson CG, Jones IM, Brown JWS, Shaw PJ (2009) Dynamic Behavior of Arabidopsis eIF4A-III, Putative Core Protein of Exon Junction Complex: Fast Relocation to Nucleolus and Splicing Speckles under Hypoxia. Plant Cell **21**: 1592–1606

Krapp S, Greiner E, Amin B, Sonnewald U, Krenz B (2017) The stress granule component G3BP is a novel interaction partner for the nuclear shuttle proteins of the nanovirus pea necrotic yellow dwarf virus and geminivirus abutilon mosaic virus. Virus Res **227**: 6–14

Kudo T, Sasaki Y, Terashima S, Matsuda-Imai N, Takano T, Saito M, Kanno M, Ozaki S, Suwabe K, Suzuki G, et al (2016) Identification of reference genes for quantitative expression analysis using large-scale RNA-seq data of *Arabidopsis thaliana* and model crop plants. Genes Genet Syst **91**: 111–125

Kwok CK, Ding Y, Tang Y, Assmann SM, Bevilacqua PC (2013) Determination of in vivo

RNA structure in low-abundance transcripts. Nat Commun **4**: 2971

Lee H-S, Lee D-H, Cho HK, Kim SH, Auh JH, Pai H-S (2015) InsP 6 -Sensitive Variants of the Gle1 mRNA Export Factor Rescue Growth and Fertility Defects of the ipk1 Low-Phytic-Acid Mutation in Arabidopsis. Plant Cell **27**: 417–431

Lee HW, Park JH, Park MY, Kim J (2014) GIP1 may act as a coactivator that enhances transcriptional activity of LBD18 in Arabidopsis. J Plant Physiol **171**: 14–18

Van Leene J, Eeckhout D, Cannoot B, De Winne N, Persiau G, Van De Slijke E, Vercruysse L, Dedecker M, Verkest A, Vandepoele K, et al (2015) An improved toolbox to unravel the plant cellular machinery by tandem affinity purification of Arabidopsis protein complexes. Nat Protoc **10**: 169–87

Van Leene J, Eeckhout D, Persiau G, Van De Slijke E, Geerinck J, Van Isterdael G, Witters E, De Jaeger G (2011) Isolation of transcription factor complexes from Arabidopsis cell suspension cultures by tandem affinity purification. Methods Mol Biol **754**: 195–218

Van Leene J, Witters E, Inzé D, De Jaeger G (2008) Boosting tandem affinity purification of plant protein complexes. Trends Plant Sci **13**: 517–20

Liker E (2000) The structure of the mRNA export factor TAP reveals a cis arrangement of a non-canonical RNP domain and an LRR domain. EMBO J **19**: 5587–5598

Liker E, Fernandez E, Izaurralde E, Conti E (2000) The structure of the mRNA export factor TAP reveals a cis arrangement of a non-canonical RNP domain and an LRR domain. EMBO J **19**: 5587–98

Longman D, Johnstone IL, Cáceres JF (2003) The Ref/Aly proteins are dispensable for mRNA export and development in Caenorhabditis elegans. RNA **9**: 881–91

Lu Q, Tang X, Tian G, Wang F, Liu K, Nguyen V, Kohalmi SE, Keller WA, Tsang EWT, Harada JJ, et al (2010) Arabidopsis homolog of the yeast TREX-2 mRNA export complex: components and anchoring nucleoporin. Plant J **61**: 259–70

Lund MK, Guthrie C (2005) The DEAD-Box Protein Dbp5p Is Required to Dissociate Mex67p from Exported mRNPs at the Nuclear Rim. Mol Cell **20**: 645–651

Luo M-J, Zhou Z, Magni K, Christoforides C, Rappsilber J, Mann M, Reed R (2001a) Pre-mRNA splicing and mRNA export linked by direct interactions between UAP56 and Aly. Nature **413**: 644–647

Luo M -j., Reed R (1999) Splicing is required for rapid and efficient mRNA export in

metazoans. Proc Natl Acad Sci **96**: 14937–14942

Luo MJ, Zhou Z, Magni K, Christoforides C, Rappsilber J, Mann M, Reed R (2001b) Pre-mrna splicing and mRNA export linked by direct interactions between UAP56 and aly. Nature **413**: 644–647

Ma J, Liu Z, Michelotti N, Pitchiaya S, Veerapaneni R, Androsavich JR, Walter NG, Yang W (2013) High-resolution three-dimensional mapping of mRNA export through the nuclear pore. Nat Commun **4**: 2414

Masuda S, Das R, Cheng H, Hurt E, Dorman N, Reed R (2005) Recruitment of the human TREX complex to mRNA during splicing. Genes Dev **19**: 1512–7

Meier I (2012) mRNA export and sumoylation—Lessons from plants. Biochim Biophys Acta - Gene Regul Mech **1819**: 531–537

Meier I, Richards EJ, Evans DE (2017) Cell Biology of the Plant Nucleus. Annu Rev Plant Biol **68**: 139–172

Meinel DM, Burkert-Kautzsch C, Kieser A, O'Duibhir E, Siebert M, Mayer A, Cramer P, Söding J, Holstege FCP, Sträßer K (2013) Recruitment of TREX to the Transcription Machinery by Its Direct Binding to the Phospho-CTD of RNA Polymerase II. PLoS Genet **9**: e1003914

Meyer K, Köster T, Nolte C, Weinholdt C, Lewinski M, Grosse I, Staiger D (2017) Adaptation of iCLIP to plants determines the binding landscape of the clock-regulated RNA-binding protein AtGRP7. Genome Biol **18**: 204

Moore MJ, Proudfoot NJ (2009) Pre-mRNA Processing Reaches Back toTranscription and Ahead to Translation. Cell **136**: 688–700

Mor A, Suliman S, Ben-Yishay R, Yunger S, Brody Y, Shav-Tal Y (2010) Dynamics of single mRNP nucleocytoplasmic transport and export through the nuclear pore in living cells. Nat Cell Biol **12**: 543–552

Müller-McNicoll M, Botti V, de Jesus Domingues AM, Brandl H, Schwich OD, Steiner MC, Curk T, Poser I, Zarnack K, Neugebauer KM (2016) SR proteins are NXF1 adaptors that link alternative RNA processing to mRNA export. Genes Dev **30**: 553–566

Nehrbass U, Blobel G (1996) Role of the Nuclear Transport Factor p10 in Nuclear Import. Science (80-) **272**: 120–122

Okamura M, Inose H, Masuda S (2015) RNA export through the NPC in eukaryotes. Genes (Basel) **6**: 124–149

Orphanides G, Wu W-H, Lane WS, Hampsey M, Reinberg D (1999) The chromatin-specific transcription elongation factor FACT comprises human SPT16 and SSRP1 proteins. Nature **400**: 284–288

Osinalde N, Olea M, Mitxelena J, Aloria K, Rodriguez JA, Fullaondo A, Arizmendi JM, Zubiaga AM (2013) The nuclear protein ALY binds to and modulates the activity of transcription factor E2F2. Mol Cell Proteomics **12**: 1087–98

Pan H, Liu S, Tang D (2012) HPR1, a component of the THO/TREX complex, plays an important role in disease resistance and senescence in Arabidopsis. Plant J **69**: 831–843

Panas MD, Schulte T, Thaa B, Sandalova T, Kedersha N, Achour A, McInerney GM (2015) Viral and cellular proteins containing FGDF motifs bind G3BP to block stress granule formation. PLoS Pathog **11**: e1004659

Park MY, Wu G, Gonzalez-Sulser A, Vaucheret H, Poethig RS (2005) Nuclear processing and export of microRNAs in Arabidopsis. Proc Natl Acad Sci **102**: 3691–3696

Parry G (2015a) The plant nuclear envelope and regulation of gene expression. J Exp Bot **66**: 1673–1685

Parry G (2015b) The plant nuclear envelope and regulation of gene expression. J Exp Bot **66**: 1673–1685

Parry G (2014) Components of the Arabidopsis nuclear pore complex play multiple diverse roles in control of plant growth. J Exp Bot **65**: 6057–67

Pendle AF, Clark GP, Boon R, Lewandowska D, Lam YW, Andersen J, Mann M, Lamond AI, Brown JWS, Shaw PJ (2005) Proteomic analysis of the Arabidopsis nucleolus suggests novel nucleolar functions. Mol Biol Cell **16**: 260–9

Pertea M, Shumate A, Pertea G, Varabyou A, Breitwieser FP, Chang Y, Madugundu AK, Pandey A, Salzberg SL (2018) CHESS: a new human gene catalog curated from thousands of large-scale RNA sequencing experiments reveals extensive transcriptional noise. Genome Biol **19**: 208

Pfab A, Antosz W, Holzinger P, Bruckmann A, Griesenbeck J, Grasser KD (2017) Analysis of In Vivo Chromatin and Protein Interactions of Arabidopsis Transcript Elongation Factors. Methods Mol Biol **1629**: 105–122

Pfab A, Bruckmann A, Nazet J, Merkl R, Grasser KD (2018) The Adaptor Protein ENY2 Is a Component of the Deubiquitination Module of the Arabidopsis SAGA Transcriptional Co-activator Complex but not of the TREX-2 Complex. J Mol Biol **430**: 1479–1494

Pfaff C (2017) Genetic and cytological characterization of mRNA export adaptors in Arabidopsis thaliana, Master thesis University of Regensburg

Pfaff C, Ehrnsberger HF, Flores-Tornero M, Soerensen BB, Schubert T, Längst G, Griesenbeck J, Sprunck S, Grasser M, Grasser KD (2018) ALY RNA-binding proteins are required for nucleo-cytosolic mRNA transport and modulate plant growth and development. Plant Physiol **177**: pp.00173.2018

Portman DS, O'Connor JP, Dreyfuss G (1997) YRA1, an essential Saccharomyces cerevisiae gene, encodes a novel nuclear protein with RNA annealing activity. RNA **3**: 527–37

Preker PJ, Kim KS, Guthrie C (2002) Expression of the essential mRNA export factor Yra1p is autoregulated by a splicing-dependent mechanism. RNA **8**: 969–80

Raj A, van den Bogaard P, Rifkin SA, van Oudenaarden A, Tyagi S (2008) Imaging individual mRNA molecules using multiple singly labeled probes. Nat Methods **5**: 877–879

Rajoo S, Vallotton P, Onischenko E, Weis K (2018) Stoichiometry and compositional plasticity of the yeast nuclear pore complex revealed by quantitative fluorescence microscopy. Proc Natl Acad Sci **115**: E3969–E3977

Rausin G, Tillemans V, Stankovic N, Hanikenne M, Motte P (2010) Dynamic Nucleocytoplasmic Shuttling of an Arabidopsis SR Splicing Factor: Role of the RNA-Binding Domains. Plant Physiol **153**: 273–284

Rehwinkel J, Herold A, Gari K, Köcher T, Rode M, Ciccarelli FL, Wilm M, Izaurralde E (2004) Genome-wide analysis of mRNAs regulated by the THO complex in Drosophila melanogaster. Nat Struct Mol Biol **11**: 558–566

Reichel M, Liao Y, Rettel M, Ragan C, Evers M, Alleaume A-M, Horos R, Hentze MW, Preiss T, Millar AA (2016) In Planta Determination of the mRNA-Binding Proteome of Arabidopsis Etiolated Seedlings. Plant Cell **28**: 2435–2452

Reineke LC, Tsai W-C, Jain A, Kaelber JT, Jung SY, Lloyd RE (2017) Casein Kinase 2 Is Linked to Stress Granule Dynamics through Phosphorylation of the Stress Granule Nucleating Protein G3BP1. Mol Cell Biol **37**: 1–19

Ribbeck K, Görlich D (2001) Kinetic analysis of translocation through nuclear pore complexes. EMBO J **20**: 1320–30

Rodrigues JP, Rode M, Gatfield D, Blencowe BJ, Carmo-Fonseca M, Izaurralde E (2001a) REF proteins mediate the export of spliced and unspliced mRNAs from the nucleus. Proc

Natl Acad Sci **98**: 1030–1035

Rodrigues JP, Rode M, Gatfield D, Blencowe BJ, Carmo-Fonseca M, Izaurralde E (2001b) REF proteins mediate the export of spliced and unspliced mRNAs from the nucleus. Proc Natl Acad Sci **98**: 1030–1035

Romanowski A, Yanovsky MJ (2015) Circadian rhythms and post-transcriptional regulation in higher plants. Front Plant Sci **6**: 1–11

Rout MP, Aitchison JD, Magnasco MO, Chait BT (2003) Virtual gating and nuclear transport: the hole picture. Trends Cell Biol **13**: 622–8

Saroufim M-A, Bensidoun P, Raymond P, Rahman S, Krause MR, Oeffinger M, Zenklusen D (2015) The nuclear basket mediates perinuclear mRNA scanning in budding yeast. J Cell Biol **211**: 1131–1140

Schmidt HB, Görlich D (2016) Transport Selectivity of Nuclear Pores, Phase Separation, and Membraneless Organelles. Trends Biochem Sci **41**: 46–61

Segref A, Sharma K, Doye V, Hellwig A, Huber J, Lührmann R, Hurt E (1997) Mex67p, a novel factor for nuclear mRNA export, binds to both poly(A)+ RNA and nuclear pores. EMBO J **16**: 3256–71

Sehnke PC, Laughner BJ, Lyerly Linebarger CR, Gurley WB, Ferl RJ (2005) Identification and characterization of GIP1, an Arabidopsis thaliana protein that enhances the DNA binding affinity and reduces the oligomeric state of G-box binding factors. Cell Res **15**: 567–75

Shaikhali J (2015) GIP1 protein is a novel cofactor that regulates DNA-binding affinity of redox-regulated members of bZIP transcription factors involved in the early stages of Arabidopsis development. Protoplasma **252**: 867–83

Shav-Tal Y, Tripathi T (2018) Yeast and Human Nuclear Pore Complexes: Not So Similar After All. Trends Cell Biol **28**: 589–591

Shi M, Zhang H, Wu X, He Z, Wang L, Yin S, Tian B, Li G, Cheng H (2017) ALYREF mainly binds to the 5′ and the 3′ regions of the mRNA in vivo. Nucleic Acids Res **45**: 9640–9653

Siebrasse JP, Kaminski T, Kubitscheck U (2012) Nuclear export of single native mRNA molecules observed by light sheet fluorescence microscopy. Proc Natl Acad Sci **109**: 9426–9431

Sievers F, Wilm A, Dineen D, Gibson TJ, Karplus K, Li W, Lopez R, McWilliam H, Remmert M, Söding J, et al (2011) Fast, scalable generation of high-quality protein

multiple sequence alignments using Clustal Omega. Mol Syst Biol **7**: 539

Silla T, Karadoulama E, Mąkosa D, Lubas M, Jensen TH (2018) The RNA Exosome Adaptor ZFC3H1 Functionally Competes with Nuclear Export Activity to Retain Target Transcripts. Cell Rep **23**: 2199–2210

Singh G, Kucukural A, Cenik C, Leszyk JD, Shaffer SA, Weng Z, Moore MJ (2012) The Cellular EJC Interactome Reveals Higher-Order mRNP Structure and an EJC-SR Protein Nexus. Cell **151**: 750–764

Smith A, Brownawell A, Macara IG (1998) Nuclear import of Ran is mediated by the transport factor NTF2. Curr Biol **8**: 1403-S1

Sørensen BB, Ehrnsberger HF, Esposito S, Pfab A, Bruckmann A, Hauptmann J, Meister G, Merkl R, Schubert T, Längst G, et al (2017) The Arabidopsis THO/TREX component TEX1 functionally interacts with MOS11 and modulates mRNA export and alternative splicing events. Plant Mol Biol **93**: 283–298

Sørensen BB (2016) Molecular and functional characterization of the THO/TREX complex in Arabidopsis thaliana. PhD thesis University of Regensburg

Staiger D, Korneli C, Lummer M, Navarro L (2013) Emerging role for RNA-based regulation in plant immunity. New Phytol **197**: 394–404

Stewart M (2019) Polyadenylation and nuclear export of mRNAs. J Biol Chem **294**: 2977–2987

Stewart M (2010) Nuclear export of mRNA. Trends Biochem Sci **35**: 609–617

Strässer K, Bassler J, Hurt E (2000) Binding of the Mex67p/Mtr2p heterodimer to FXFG, GLFG, and FG repeat nucleoporins is essential for nuclear mRNA export. J Cell Biol **150**: 695–706

Strässer K, Hurt E (2000) Yra1p, a conserved nuclear RNA-binding protein, interacts directly with Mex67p and is required for mRNA export. EMBO J **19**: 410–420

Sträßer K, Hurt E (2001) Splicing factor Sub2p is required for nuclear mRNA export through its interaction with Yra1p. Nature **413**: 648–652

Sträßer K, Masuda S, Mason P, Pfannstiel J, Oppizzi M, Rodriguez-Navarro S, Rondón AG, Aguilera A, Struhl K, Reed R, et al (2002) TREX is a conserved complex coupling transcription with messenger RNA export. Nature **417**: 304–308

Stubbs SH, Conrad NK (2015) Depletion of REF/Aly alters gene expression and reduces RNA polymerase II occupancy. Nucleic Acids Res **43**: 504–519

Stutz F, Bachi A, Doerks T, Braun IC, Séraphin B, Wilm M, Bork P, Izaurralde E (2000) REF, an evolutionary conserved family of hnRNP-like proteins, interacts with TAP/Mex67p and participates in mRNA nuclear export. RNA **6**: 638–50

Tamura K, Fukao Y, Iwamoto M, Haraguchi T, Hara-Nishimura I (2010) Identification and Characterization of Nuclear Pore Complex Components in Arabidopsis thaliana. Plant Cell **22**: 4084–4097

Teplova M, Wohlbold L, Khin NW, Izaurralde E, Patel DJ (2011) Structure-function studies of nucleocytoplasmic transport of retroviral genomic RNA by mRNA export factor TAP. Nat Struct Mol Biol **18**: 990–998

Thandapani P, O'Connor TR, Bailey TL, Richard S (2013) Defining the RGG/RG Motif. Mol Cell **50**: 613–623

Tillemans V, Dispa L, Remacle C, Collinge M, Motte P (2005) Functional distribution and dynamics of Arabidopsis SR splicing factors in living plant cells. Plant J **41**: 567–582

Tourrière H, Chebli K, Zekri L, Courselaud B, Blanchard JM, Bertrand E, Tazi J (2003) The RasGAP-associated endoribonuclease G3BP assembles stress granules. J Cell Biol **160**: 823–31

Tourriere H, Gallouzi I -e., Chebli K, Capony JP, Mouaikel J, van der Geer P, Tazi J (2001) RasGAP-Associated Endoribonuclease G3BP: Selective RNA Degradation and Phosphorylation-Dependent Localization. Mol Cell Biol **21**: 7747–7760

Tran DDH, Saran S, Williamson AJK, Pierce A, Dittrich-Breiholz O, Wiehlmann L, Koch A, Whetton AD, Tamura T (2014) THOC5 controls 3′end-processing of immediate early genes via interaction with polyadenylation specific factor 100 (CPSF100). Nucleic Acids Res **42**: 12249–12260

Tretyakova I, Zolotukhin AS, Tan W, Bear J, Propst F, Ruthel G, Felber BK (2005) Nuclear Export Factor Family Protein Participates in Cytoplasmic mRNA Trafficking. J Biol Chem **280**: 31981–31990

Uhrig JF, Canto T, Marshall D, MacFarlane SA (2004) Relocalization of Nuclear ALY Proteins to the Cytoplasm by the Tomato Bushy Stunt Virus P19 Pathogenicity Protein. Plant Physiol **135**: 2411–2423

Untergasser A, Nijveen H, Rao X, Bisseling T, Geurts R, Leunissen JAM (2007) Primer3Plus, an enhanced web interface to Primer3. Nucleic Acids Res **35**: W71–W74

Valkov E, Dean JC, Jani D, Kuhlmann SI, Stewart M (2012) Structural basis for the assembly and disassembly of mRNA nuclear export complexes. Biochim Biophys Acta - Gene

Regul Mech **1819**: 578–592

Viphakone N, Cumberbatch MG, Livingstone MJ, Heath PR, Dickman MJ, Catto JW, Wilson SA (2015) Luzp4 defines a new mRNA export pathway in cancer cells. Nucleic Acids Res **43**: 2353–2366

Viphakone N, Hautbergue GM, Walsh M, Chang C-T, Holland A, Folco EG, Reed R, Wilson SA (2012) TREX exposes the RNA-binding domain of Nxf1 to enable mRNA export. Nat Commun **3**: 1006

Viphakone N, Sudbery I, Griffith L, Heath CG, Sims D, Wilson SA (2019) Co-transcriptional Loading of RNA Export Factors Shapes the Human Transcriptome. Mol Cell 1–14

Virbasius C-MA, Wagner S, Green MR (1999) A Human Nuclear-Localized Chaperone that Regulates Dimerization, DNA Binding, and Transcriptional Activity of bZIP Proteins. Mol Cell **4**: 219–228

Walsh MJ, Hautbergue GM, Wilson SA (2010) Structure and function of mRNA export adaptors. Biochem Soc Trans **38**: 232–236

Waterhouse AM, Procter JB, Martin DMA, Clamp M, Barton GJ (2009) Jalview Version 2--a multiple sequence alignment editor and analysis workbench. Bioinformatics **25**: 1189–91

Weber C, Nover L, Fauth M (2008) Plant stress granules and mRNA processing bodies are distinct from heat stress granules. Plant J **56**: 517–30

Weidtkamp-peters S, Stahl Y (2017) Plant Receptor Kinases. doi: 10.1007/978-1-4939-7063-6

Weirich CS, Erzberger JP, Flick JS, Berger JM, Thorner J, Weis K (2006) Activation of the DExD/H-box protein Dbp5 by the nuclear-pore protein Gle1 and its coactivator InsP6 is required for mRNA export. Nat Cell Biol **8**: 668–676

Wickramasinghe VO, Andrews R, Ellis P, Langford C, Gurdon JB, Stewart M, Venkitaraman AR, Laskey RA (2014) Selective nuclear export of specific classes of mRNA from mammalian nuclei is promoted by GANP. Nucleic Acids Res **42**: 5059–5071

Wickramasinghe VO, McMurtrie PIA, Mills AD, Takei Y, Penrhyn-Lowe S, Amagase Y, Main S, Marr J, Stewart M, Laskey RA (2010) mRNA Export from Mammalian Cell Nuclei Is Dependent on GANP. Curr Biol **20**: 25–31

Wiegand HL, Coburn GA, Zeng Y, Kang Y, Bogerd HP, Cullen BR (2002) Formation of Tap/NXT1 Heterodimers Activates Tap-Dependent Nuclear mRNA Export by Enhancing

Recruitment to Nuclear Pore Complexes. Mol Cell Biol **22**: 245–256

Wu F-H, Shen S-C, Lee L-Y, Lee S-H, Chan M-T, Lin C-S (2009) Tape-Arabidopsis Sandwich - a simpler Arabidopsis protoplast isolation method. Plant Methods **5**: 16

Xu C, Zhou X, Wen C-K (2015) HYPER RECOMBINATION1 of the THO/TREX Complex Plays a Role in Controlling Transcription of the REVERSION-TO-ETHYLENE SENSITIVITY1 Gene in Arabidopsis. PLOS Genet **11**: e1004956

Yelina NE, Smith LM, Jones AME, Patel K, Kelly KA, Baulcombe DC (2010) Putative Arabidopsis THO/TREX mRNA export complex is involved in transgene and endogenous siRNA biosynthesis. Proc Natl Acad Sci **107**: 13948–13953

Yoh SM, Cho H, Pickle L, Evans RM, Jones KA (2007) The Spt6 SH2 domain binds Ser2-P RNAPII to direct Iws1-dependent mRNA splicing and export. Genes Dev **21**: 160–174

Zenklusen D, Vinciguerra P, Strahm Y, Stutz F (2001) The Yeast hnRNP-Like Proteins Yra1p and Yra2p Participate in mRNA Export through Interaction with Mex67p. Mol Cell Biol **21**: 4219–4232

Zhao Q, Leung S, Corbett AH, Meier I (2006) Identification and characterization of the Arabidopsis orthologs of nuclear transport factor 2, the nuclear import factor of ran. Plant Physiol **140**: 869–78

Zhou Z, Luo M, Straesser K, Katahira J, Hurt E, Reed R (2000) The protein Aly links pre-messenger-RNA splicing to nuclear export in metazoans. Nature **407**: 401–405